Predictions For Composite Higgs Models Using Gauge/Gravity Duality

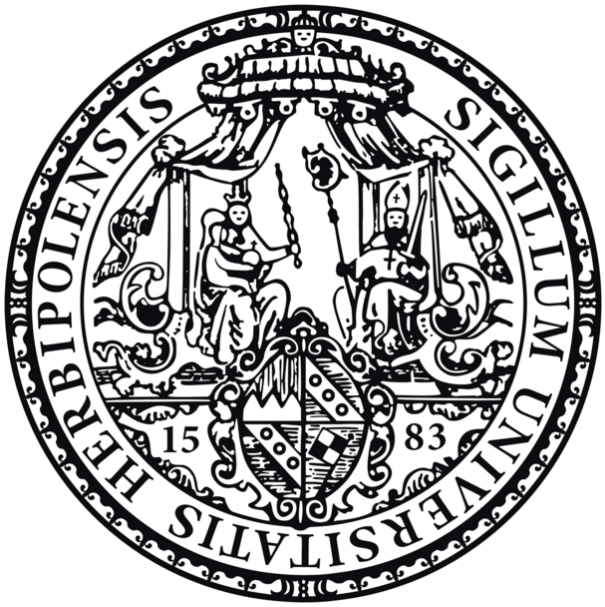

Dissertation zur Erlangung des naturwissenschaftlichen Doktorgrades
an der Fakultät für Physik und Astronomie
der Julius-Maximilians-Universität Würzburg

vorgelegt

von

Yang Liu

aus Shandong, China

Würzburg, im Juni 2024

Eingereicht bei der Fakultät für Physik und Astronomie am _____

Gutachter der Dissertation

1. Gutachter: Prof. Dr. Werner Porod

2. Gutachter: Prof. Dr. Johanna Erdmenger

Prüfer des öffentlichen Promotionskolloquiums

1. Prüfer: Prof. Dr. Werner Porod

2. Prüfer: Prof. Dr. Johanna Erdmenger

3. Prüfer:

Tag des öffentlichen Promotionskolloquiums:

_____

Doktorurkunde ausgehändigt am

_____

Contents

Abstract

This thesis is dedicated to construct a non-abelian holographic dynamical minimal composite Higgs model. We first build a non-abelian bottom-up AdS/YM model that can explain the QCD meson spectrum well. The model is made non-abelian by considering non-abelian DBI action in the top-down model. We then change the dual theory from the QCD to the minimal composite Higgs model $U(4)/Sp(4)$. By adding a second explicit $U(4) \to Sp(4)$ breaking through the NJL interaction at the boundary, we managed to construct a composite Higgs phase and a technicolor phase in this model. The transition between the two phases is also realized, which is controlled by the NJL coupling. This thesis is based on the works [1, 2].

Zusammenfassung

Diese Arbeit konstruiert ein nicht-abelsches holographisches dynamisches minimales Composite-Higgs-Modell. Wir erstellen zunächst ein nicht-abelsches Bottom-up-AdS/YM-Modell, das das QCD-Mesonenspektrum gut erklären kann. Das Modell ist nicht-abelsch, da die nicht-abelsche DBI-Wirkung im Top-Down-Modell berücksichtigt wird. Anschließend ändern wir die duale Theorie von der QCD auf das minimale Composite-Higgs-Modell $U(4)/Sp(4)$. Durch das Hinzufügen einer zweiten expliziten Brechung $U(4) \to Sp(4)$, das die NJL-Wechselwirkung an der Grenze durchbricht, konstruierten wir in diesem Modell eine Composite-Higgs-Phase und eine Technicolor-Phase. Auch der Übergang zwischen den beiden Phasen wird realisiert, welcher durch die NJL-Kopplung gesteuert wird. Diese Arbeit basiert auf den Arbeiten [1, 2].

Acknowledgment

The story can be date back to 12 years ago. I somehow started learning German as a hobby. Back then I was still in my early bachelor, had only a vague clue about what I will do in the future. I thought maybe I could do my PhD in Germany, of course, if I could ever make it to the PhD level. It was just a thought that I didn't even expect to realize. Then things start to change. Two years later I decided to start my master study in Germany. I was hardworking and lucky enough to pass the language test within one year and got the Zulassung. It seems like everything was on the right track.

Then my study started in Germany. My life was suddenly switched to the hard mode. It was obstacles after obstacles on top of obstacles that are marinated in other obstacles...

I'm glad that I conquered all of them and made it to write this acknowledgment. I'm very grateful for the times I spend in Germany while climbing the way up in physics. (There's a certain interference between the two that made life harder, but it never crossed the threshold). If I hadn't gone through these difficulties, I probably would, by chance, become a person that takes things for granted, who couldn't empathize with the people that are currently going through their hard times just because they are not lucky enough. I really appreciate the hard times that direct me to the right track.

Having written so much about the background story behind this thesis, it's time to get on with the real business. I would like to thank first my parents who paid for my master study in Germany (and of course everything before) and made all these happen. Without their supports I wouldn't be able to learn and experience so much.

Of course, this thesis couldn't be finished without the supervision of Prof. Dr. Johanna Erdmenger, Prof. Dr. Nick Evans and Prof. Dr. Werner Porod. I'm grateful for each of the help Johanna offered, given that she is buried under her very intensive schedule as a Lehrstuhlinhalberin, and as a scholar who is very active in organizing various workshops/conferences to

provide opportunities for young physicists and to stimulate collaborations in this field. I would also like to say a sincerely “Thank You” to Prof. Nick Evans. Nick is the leading force of our project. Whenever I have physics related questions (a lot of times stupid questions), he was always kind and patient to answer them. Without him, we couldn’t have published the papers.

My special thanks go to Prof. Werner Porod. Werner was my supervisor for my master thesis. Not surprisingly, I continued my PhD study with him. It was a tough time when I started my PhD. Back then the government cut down their budget for researches, and it was also at the beginning of the Pandemic. Werner had tried a lot to help me get the funding, but things didn’t work out as we expected. Werner was also willing to offer his students opportunities to collaborate with researchers from aboard, which I’m very grateful too. I guess simply saying “thank you” to Werner is far from enough comparing to what he did for me. I would like to express my gratitude to Werner with a little conversation I had with Johanna and Nick.

It was last year when Nick was invited over for an academic stay for one week here in Würzburg. We went to the Nachsitzung after his talk. It was only Nick, Johanna and I. As we were chatting, Johanna mentioned that she was finding the Southern Cross on her flight back but she couldn’t see that. Then I said “ I might have seen that, but I’m not sure...” — I was on the flight from Peru to Germany back from a six-week academic stay supported by DAAD. I happen to seat next to a window and woke up in the middle of the flight when it was dark and clear. I looked out, there were tones of shinny stars floating around the plane as if I was sitting in the cradle made of stars. There were some major ones that are far more larger and brighter than the ones I’ve seen in the Northern Hemisphere. I’m not sure whether they are the Southern Cross or not, but at that moment when I told them about this, I realized “Oh damn, this is some once-in-my-life experience, I must be really lucky to even have seen that. Weren’t it because of Werner, none of this would even happen”.

In the end I would like to thank all the people that had helped me during my stay in Germany. Specially my former landlord Mark Elswick, who really warmed my heart with his generosity. I would also like to thank Studienstiftung des deutschen Volkes, who supported my first three-year PhD study during the Pandemic, and Prof. Dr. Robert Harlander from RWTH Aachen, who passed my interview from Studienstiftung which is a cornerstone of my PhD study. And I would like to thank Mr. Jan Hadlik for correcting the Zusammenfassung.

Chapter 1

Introduction

The discovery of the Higgs boson at the LHC in 2012 [3, 4] found the last missing piece of the standard model (SM). Even though the standard model has provided an elegant mathematical tool that could explain most of the experimental data, it is known that the standard model alone is not the end of the story. The SM fails to provide a candidate(s) for the dark matter (DM). The neutrinos are predicted to be massless in the SM, where it has been found and verified by the experiments [5, 6] that the neutrinos are massive. The quarks' flavor hierarchy is also not explained, where it is unnatural that the lightest quark is only a couple of MeV where the heaviest one is 173 GeV [7]. Not to mention that the standard model only describes three fundamental forces, where the gravitational interaction that we see and feel in everyday life is not contained.

The most infamous problem the SM fails to explain in particle physics is the hierarchy problem. The electroweak symmetry breaking (EWSB) is well explained by the then discovered Higgs. But the Higgs model is more of a parametrization than a defining theory of the EWSB, since the origin that generates the EWSB dynamically is still unknown. Aside from that, being an elementary particle, the Higgs boson is not protected by any symmetry. The consequence follows is that the Higgs mass receives a radiative correction that is a function of the energy scale. This is then unbounded if the energy is set arbitrarily high. How would the EWSB scale be stable comparing to much larger scales is not explained.

There has been attempts to resolve the hierarchy problem. The proposals usually modify the symmetry that the theory describes. The most famous attempt in the past decades is the supersymmetry (SUSY), which includes symmetry between the bosons and fermions. Due to

this extra symmetry, the cancellation of the contributions from the fermions and the bosons protects the Higgs mass and makes it naturally light. Even though it's a mathematically elegant theory, the searches for SUSY particles at the colliders haven't been succeeded. This sets bounds on the SUSY particles' masses higher and higher, making SUSY gradually less attractive for physicists in the past decade.

Aside from the SUSY, all the other attempts assume certain compositeness of the Higgs boson [8], whether it's QCD (quantum chromodynamics) pion inspired composite state or in the sense of string theory. The extension that is analog to the QCD pion is the technicolor (TC) model [9, 10]. It considers EWSB to be a scaled-up QCD theory which is a simple and elegant extension of the SM. However, the drawback of the TC is the absence of the scalar field, the Higgs. The technicolor models also suffer from producing FCNC (flavor changing neutral currents) processes that are not observed in the experiment. An economical way to resolve these problems from both the Higgs model and the TC is to combine them together. The Higgs boson in this frame is no more elementary, but a composite state made of fermions from an extended strongly interacting sector. This is the so-called composite Higgs (CH) model, which is the main topic of this thesis.

The composite Higgs models, also the technicolor models, utilize an extra strongly coupled sector. This sector introduces extra fermions, the so-called hyperquarks, that are charged under certain symmetry group assumed in this sector. Given that the new particles are strongly coupled, for low-energy effective theory the perturbative calculations are not viable. An old alternative theory of the strongly interacting theory — the string theory — provides answers to this problem.

String theory was born in the 1960s as a theory to explain the strong interactions in particle physics where the strings are initially postulated as "flux tubes". Later as the QCD theory was developed and became the theory for strong interactions in particle physics, the study on string theory in explaining strong dynamics cooled down for about two decades. Physicists' interests on this subject boost again after the famous paper by Maldacena [11] in 1998. In that paper, dualities between strongly (conformal field theory, CFT) and weakly coupled theory (gravity) are postulated, by identifying the theories on the two limits of the D3-branes. The most intensively studied version of the duality is the AdS_5/CFT_4, which states the IIB supergravity living in the $AdS_5 \times S^5$ space is dual to the $\mathcal{N} = 4$ super Yang-Mills theory (SYM), i.e. a four-dimensional CFT, living on the boundary of the AdS_5, which is a flat 4D Minkowski spacetime. Other variants of the AdS/CFT (anti de-Sitter, AdS) correspondence are Ad_7/CFT_6, Ad_4/CFT_3, Ad_3/CFT_2 and Ad_2/CFT_1 [11, 12].

This soon stimulated researches in various fields. The AdS/CFT correspondence is generalized to the gauge/gravity duality, where the dual field theory becomes a general gauge theory, which is not necessarily conformal. It is widely applied in condensed matter physics which later becomes the AdS/CMT (condensed matter theory) correspondence. This is a very active research field, where such correspondence are used in studying high-temperature superconductors [13, 14], strange metal [15], superfluid [16] etc., see also [17, 18]. It also leads to the birth of the SYK (Sachdev-Ye-Kitaev) model [19, 20], which is involved in studying non-Fermi liquid [21] and even realizing traversable wormhole on tabletop [22, 23].

One of the active research field of the AdS/CFT correspondence, or more precisely the gauge/gravity duality, is the particle physics. It brings the string theory back to the origin, i.e. to explain the strongly coupled sector of the SM, and generally a strongly coupled sector in beyond standard model (BSM) models. Initially the precise form of the duality is used in model building, i.e. the dual field theory is conformal. The open string modes living in the world volume of coincident N Dp-branes transform in the adjoint representation of the $U(N)$ gauge theory. To implement matter fields in the fundamental representation, extra Dq-branes are needed [24]. The open strings between the Dp- and Dq-branes transform in the fundamental representation of the $U(N)$ gauge group. Adding just the fundamental matter is not enough. To reproduce the special features — confinement and chiral symmetry breaking, different geometries are constructed on the gravity side, for example [25–28], and more references see section 3.4. Such models involves the D3-stack/D7-probe set up based on the IIB superstring theory [24, 29–31] and the Sakai-Sugimoto model (D4-D8-$\overline{\text{D8}}$) [32–38] based on the IIA superstring theory. These models originate from supersymmetry theories, therefore contain more states than the QCD.

Another approach is from the bottom-up. The so-called AdS/QCD model was first proposed in [39]. This model takes the common property of the top-down models, constructed the dual gravity theory of QCD on the AdS_5. It assumes a chiral symmetry that is spontaneously broken, the vector fields in the bulk are implemented in a hidden-local symmetry way [40], such that they are dynamical fields in the bulk and dual to the vector mesons in the QCD. This model takes only three free parameters, but is able to make a rough prediction of the meson spectrum which makes it a powerful alternative of lattice QCD.

The bottom-up model is much easier to apply on model building, since one no more needs to consider complicated brane architectures to get the dual gauge theory right. The cost is that the result is only an approximation. For AdS/QCD model, the error is usually at 10-15% level [39], which is already a good estimation. Thus bottom-up models are actively used in BSM

model building, such as technicolor [41–47], composite Higgs [48–53], neutrino physics [54, 55], dark matter and dark energy [56], see also [57] and references therein.

This thesis aims to construct a holographic composite Higgs model, which contains two phases — the composite Higgs phase and the technicolor phase — and the transition between the two. In that, we first constructed a non-abelian AdS/YM (Yang-Mills) theory, non-abelian in the sense that the flavor symmetry of the dual field theory is made explicitly by considering the non-abelian Dirac-Born-Infeld action (DBI action) and imposing different boundary conditions for the flavor branes in the gravity dual. As a first test, we compared the meson spectrum predicted by our model with the QCD data, which shows a good agreement. The same technique is them applied to the construction of the holographic composite Higgs model mentioned above. Both of the two phases and their transition is realized. The symmetry breaking pattern is $U(4) \to Sp(4) \to SU(2) \times SU(2)$. This involves two different $U(4) \to Sp(4)$ breakings, the first one comes with the holographic model, realized in the similar way as the AdS/QCD. The second is introduced by inserting the NJL (Nambu-Jona-Lasino) interactions at the boundary. After a unitary transformation, such a construction finds itself to be simply a non-abelian holographic model that we constructed in the first place. We computed the bound states' spectra and decay constants. The results show that the transition between the two phases are highly fine-tuned.

The structure of this thesis is organized as follows. It contains two parts. The first part is the theory part. In this part we review the necessary theory backgrounds that will be used in the research part. Our research involves mainly two theories — the composite Higgs models and the gauge/gravity duality. Both of them cover a vast range of topics. We will only review the basics and focus more on the related topics that are relevant to our research. The fundamentals of the composite Higgs models are reviewed in chapter 2, especially we review the 4D field theory composite Higgs model that we made holographic in the research part in section 2.3. Other holographic composite Higgs models are also briefly discussed. In chapter 3 we review the AdS/CFT correspondence and more generally gauge/gravity duality when applied to the particle physics. We discuss both the abelian top-down and bottom-up holographic models and set our conventions for later parts. Especially we discuss realizing confinement, chiral symmetry breaking and inserting NJL interaction terms on the boundary in the holographic models in this chapter.

The second part is the research part. It contains also two chapters. In chapter 4 we introduce our work that published in [1]. In that we first reviewed a non-abelian top-down D3/D7 model, and constructed a bottom-up model along this line and tested it against the QCD data. We

developed the numerical tool that could cope with the coupled equations of motion that appear frequently in the non-abelian holographic models. We show at the end of this part that we have constructed a non-abelian dynamical AdS/YM model. In chapter 5 we apply this AdS/YM model to a $U(4) \to Sp(4)$ global symmetry breaking composite Higgs model that we reviewed in chapter 2. This chapter introduces the work that we published in [2]. We first look at the degenerate case, which corresponds to a $U(4) \to Sp(4)$ composite Higgs model. Then we look into the case where the flavors are no more degenerated. It's role becomes clear when we add a second $U(4) \to Sp(4)$ symmetry breaking through inserting the NJL interactions at the boundary. In the end, we are able to realize a holographic model which manifests a transition between a composite Higgs and a technicolor model. In chapter 6 we make our conclusions and discuss the outlook of our work.

We put the supplementary materials in the appendices. In appendix A we show explicitly the calculations in the non-abelian top-down model. Similar calculations are performed in the bottom-up model and automatized with `Mathematica`. Therefore we only show the calculation once and list the equations directly in the later parts. In appendix B we review the implementation of the dynamical running introduced in section 3.6. In appendix C we derive the equations of motion for a general parametrization in the non-abelian bottom-up model, to motivate the parametrizaiton we adopted in the main text. The resulting equations of motion using the adopted parametrization is shown in appendix D and appendix E for two- and three-flavor QCD, respectively. In appendix F we work out explicitly the relation between the Δm^2 and A that show up in the holographic composite Higgs model we constructed in chapter 5. In appendix G we list the equations of motion when adding the NJL interaction in the holographic composite Higgs model.

Chapter 2

Composite Higgs Models

In this chapter we review some fundamentals of the composite Higgs models. Topics like CCWZ construction [58, 59] that is important in building a CH model from possible symmetry breaking patterns, possible modifications to resolve certain model dependent problems, current bounds on specific BSM particles will not be discussed. We will start from its origin in the technicolor, introduce the basic idea of CH in section 2.1, and move to a minimal composite Higgs model in section 2.2 to see how the physical quantities are calculated. Then we will introduce another minimal and viable composite Higgs model in section 2.3 that is made holographic in the later research part in chapter 5. At the end of this chapter, we will mention briefly the holographic extensions of the composite Higgs models in section 2.4. Some of the content in section is based on [60–62]. Further reviews see also [63].

2.1 General Idea

The Higgs model is an economical way to explain the EWSB by just adding a weakly interaction scalar singlet under the EW (electroweak) gauge group. At leading order the Higgs is a light scalar, this makes the theory calculable and compatible with the electroweak precision test. However, it's mass is not protected by any symmetry, in that the Higgs boson's potential is sensitive to BSM physics. This hierarchy problem is a long-time puzzle that is not solved until now in the standard model.

Before the Higgs was discovered, another type of model also provides interesting explaination to the EWSB. It's the so-called technicolor model [9, 10], for systematic reviews on this topic, see

[64–66]. This type of model assumes that the EWSB could be a scaled-up QCD. The starting point is in the chiral limit, to let the QCD vacuum break the EWSB at a scale $F_\pi = v = 246$ GeV through the interaction of the EW gauge bosons with the hyperquarks. The constant F_π is analog to the pion decay constant $f_\pi = 93$ MeV. Also the Higgs boson is removed from the model. However, the EW gauge bosons W and Z are not massless, since due to the Higgs mechanism, the massless QCD pions are eaten and become the longitudinal components of the gauge fields. The QCD pions are composite states of the elementary quarks. In this way, the W boson receives a mass of about 29 MeV. This is of course too few comparing to the measured W mass. In general one considers an extended technicolor sector with a global symmetry $SU(2)_L \times SU(2)_R$ with the gauge group $SU(N_{TC})$. Then the Goldstone bosons (GBs) that becomes the longitudinal parts of the gauge bosons are linear combinations of the pion and the techni-pion from the new sector, with the mixing angle $\tan\alpha = f_\pi/F_\pi$. The gauge bosons W and Z will get much more massive since the mixing is dominated by the TC-pion, since $F_\pi \gg f_\pi$.

Technicolor theories solve the hierarchy problem by giving a dynamical origin of the EWSB, in the same way as the QCD scale is generated. But it has several drawbacks. The technicolor models fail to keep the Peskin-Takeuchi S parameter [67, 68] in the correct range constraint by the EW precision tests. The Peskin-Takeuchi S parameter is defined to be [68]

$$S = -4\pi \left(\Pi'_{VV}(0) - \Pi'_{AA}(0)\right), \tag{2.1.1}$$

where Π_{VV} and Π_{AA} are the vector-vector and axial-axial (axial-vector) correlators, respectively. The TC predicts an S parameter about 1 where the current bound is [7]

$$S < 0.14 \quad @ \quad 95\% \text{ CL.} \tag{2.1.2}$$

Another failure is related to the generation of fermions in the TC models. Different families of fermions are embedded in the same extended technicolor group, this violates the CP and leads to FCNC processes that set constraints on the energy scales[1]. The walking technicolor model was proposed to resolve this problem, but this idea leads to problems like the anomalous dimension of the fermion mass operator isn't large enough [71].

[1]The problem with FCNC processes is typical in the one family model with extended techni-color (ETC) group [69]. Additional terms contribute first to the $K_L - K_S$ mass difference that is accurately measured and second, to the $\mu \to e\bar{e}e, e\gamma$, which is not observed. Having the FCNC processes suppressed requires an ETC scale $\sim 10^3$ TeV [70]. This will in turn lead to a mismatch of the top quark mass. Review see for example [71]. Adding scalar to TC models see [72–75]

Both of the attempts face different challenges when trying to explain the origin of the electroweak symmetry breaking. The Higgs model is confirmed by the discovery of the Higgs boson at the LHC, but it suffers from the naturalness problem. In the meanwhile the technicolor models can't find a balance between the solving the naturalness problem and having FCNC processes under control. Also it does not contain a light scalar that can be identified as the already found Higgs boson. A new type of model must be constructed that contains a naturally light Higgs boson while can explain the dynamical origin of the EWSB.

Clearly, combining the two ideas of the Higgs model and the technicolor is a natural and economical candidate of such a model. If the Higgs is a pseudo Nambu-Goldstone boson (pNGB) of a broken symmetry, then it's mass can be naturally light. This is the idea behind the composite Higgs model. First brought up by Kaplan and Georgi [76–78], the CH model considers an extra strongly interacting sector, like in the technicolor models. This new strong sector has an global symmetry G. This global symmetry group is sponatenously broken down to a subgroup H at the energy scale f. The degrees of freedom (dof) from the coset G/H give rise to the Higgs and longitudinal components of the W and Z bosons. At this stage the Higgs is still an NGB. The standard model particles are considered to be external of this strong sector. If gauge the subgroup $H_0 \subset G$ with the SM EW gauge group and the composite operators are in the complete representation of the global group, the interactions between the SM gauge bosons and the extended quarks from the new strong sector will break the global symmetry G explicitly. This generates a Higgs potential at 1-loop that triggers an EWSB at the energy scale $v = 246$ GeV.

The spontaneous and explicit breaking happen at different energy scales f and v, their ratio $\xi = \sin^2 f/v$ characterizes the vacuum misalignment. Unlike the TC, these two scales are separated in the CH models. In the limit $\xi \to 0$, the CH model becomes the Higgs model. In the other limit $\xi \to 1$, the CH model is a technicolor model plus a light scalar field. Usually the realistic CH is defined with a small $\xi \ll 1$.

The choice of the global group is constraint by the experimental data. To protect the Peskin-Takeuchi S and T parameters, the invariant subgroup H must contain the custodial symmetry $SU(2)_{cus}$ [2][79]. Also the invariant subgroup must contain the SM EW group $SU(2)_L \times U(1)_Y$ as a subgroup. The coset must contain one $SU(2)_L$ to allow a Higgs doublet in the model. For

[2]This symmetry is an unbroken global symmetry in the Higgs sector which relates the charged current interaction with the neutral current interaction in the weak interacting sector. The four components of a Higgs doublet has a $SO(4)$ symmetry before spontaneous symmetry breaking. When the Higgs acquires a vev, this $SO(4)$ is broken down to an $SO(3) \sim SU(2)$. This $SU(2)$ is the custodial symmetry.

a general non-abelian global flavor symmetry with any gauge group having Dirac fermions, the symmetry breaking pattern is limited by the reality of the representation of the Dirac fermion [80]. If the fermions are in the real or pseudoreal representation, then the global symmetry is bound to be $SU(2N_f)$ with N_f the number of flavors. One can rewrite the Dirac fermions as $2N_f$ Weyl fermions ψ_c^f, $f = 1, ..., 2N_f$, and the simplest condensation is $\psi_c^f \psi_{c'}^{f\prime}$. If the fermions are in the real representation, then the global symmetry is broken down to the $SO(2N_f)$ subgroup. In this case, the invariant product is in the symmetric 2-index representation of $SU(2N_f)$. If the fermions are in the pseudoreal representation, the symmetry breaking pattern is $SU(2N_f) \to Sp(2N_f)$, with condensates in the anti-symmetric 2-index representation. If the fermions are in the complex representation, the global flavor symmetry can only be $SU(N_f) \times SU(N_f)$.

Based on this discussion, one of the minimal composite Higgs model would have the direct global symmetry breaking as $SU(4) \to SO(4)$. However this breaking doesn't provide a GB Higgs which makes it not favored for constructing composite pNGB Higgs model. But it's still interesting for technicolor models and lattice studies. The other minimal model will be $SU(4) \to Sp(4)$. This model contains a composite pNGB Higgs and is the minimal model that we used in the later research. We will review its model construction in section 2.3. Aside from these models, one can also have $SU(5) \to SO(5)$[3] and $SU(6) \to Sp(6)$, where both models provide 14 GBs. For complex representation, the minimal construction would be $SU(4) \times SU(4)$, which has 15 GBs in the coset, provides two Higgs doublets, one triplet and four singlets.

We have only listed the minimal composite Higgs models that have fermions in the fundamental representation of the gauge group. If the fermion masses are explained through the partial compositeness, then the models are further classified depending on the gauge symmetry of the strong sector and different representations of fermions that can form invariants. These models are named with $\mathrm{M}_1 - \mathrm{M}_{12}$ in [86]. They are particularly interesting for phenomenological searches. We will not list them here given that the focus of this thesis is to construct a holographic version of the minimal model. For a thorough discussion see the original paper [86] and review [62].

The initial minimal CH model is $SO(5) \to SO(4)$ proposed in [87]. It couldn't be realized according to the former discussion, but it still serves as a good toy model to explain all the essential and general discussions on the composite Higgs models. We will review this model in the next section and justify the introduction of the essential concepts like vacuum misalignment

[3]Note that for flavor symmetry of the form $SU(2N_f + 1)$, the discussion in the last paragraph doesn't apply, see also [81]. In this case the symmetry is realized using just Weyl fermions instead of Dirac fermions. Model constructions see [82–85].

and partial compositeness.

2.2 A Minimal Example

This section summarizes the results of the minimal $SO(5)/SO(4)$ composite Higgs model published in the early papers by Contino et.al. [87, 88]. We review the basic construction of the composite Higgs model in solving the naturalness problem and the fast FCNC problem of the technicolor while providing a naturally light Higgs. For details the readers are recommended to consult the original papers and the reviews [60, 61]. Related topics on this model see also [58, 59, 89–92].

The global group of the composite sector is $SU(3)_c \times SO(5) \times U(1)_X$. The $SU(3)_c$ doesn't involve in the discussion, so we omit it and considers the global symmetry $SO(5) \times U(1)_X$. This is spontaneously broken down to $SO(4) \times U(1)_X$. Since Lie algebra of the $SO(4)$ is isomorphic to the ones of $SU(2)_L \times SU(2)_R$, this model contains the SM EW group $SU(2)_L \times U(1)_Y$ as an unbroken subgroup, $Y = T^{3R} + X$. The custodial group is identified with the invariant $SU(2)_V$, this will protect the Peskin-Takeuchi T parameter from receiving large corrections in this model. The standard model field contents without the Higgs boson are the elementary particles in this model and are taken to be external to the composite sector. The coset $SO(5)/SO(4)$ contains 4 real degrees of freedom. Before gauging the composite sector with the EW gauge symmetry, these dofs are NGBs. These four NGBs transform as the fundamental representation of the $SO(4)$, or a complex doublet of $SU(2)_L$. Together with it's charge conjugation, (H, H^c) transforms as bidoublet under the $SU(2)_L \times SU(2)_R$.

Mathematically the spontaneous symmetry breaking are formulated using the effective theory similar to the chiral symmetry breaking. The GBs are expressed in the Goldstone matrix using the CCWZ construction

$$\Sigma = \Sigma_0 e^{\frac{-i\sqrt{2}}{f} h^{\hat{a}}(x) T^{\hat{a}}}, \quad \Sigma_0 = (0, 0, 0, 0, 1), \tag{2.2.1}$$

where $\hat{a}$ represents the broken generators of the SO(5). f is like the pion decay constant f_π, and it represents the typical scale of the symmetry breaking. The most general Lagrangian of the relevant part we are interest in that respects the $SO(5) \times U(1)_X$ symmetry to the quadratic order is

$$\mathcal{L} = \frac{1}{2}(P_T)^{\mu\nu} \left[\Pi_0^X(q^2) X_\mu X_\nu + \Pi_0(q^2) \mathrm{Tr}(A_\mu A_\mu) + \Pi_1(q^2) \Sigma A_\mu A_\nu \Sigma^t \right], \tag{2.2.2}$$

where P_T is the transverse projector $(P_T)^{\mu\nu} = \eta^{\mu\nu} - \frac{q^\mu q^\nu}{q^2}$, q is the momentum. X_μ and A_μ are the $U(1)_X$ and $SO(5)$ gauge fields, Π_0^X, Π_1 are form factors. To get the effective action that contains only the mass and the Higgs interaction terms, the heavy states are integrated out and only the EW fields are considered. To further simplify the calculations, we take large N limit of the form factors and expand around small q^2. The Higgs doublet is defined and rotated to align the vacuum expectation value (vev) along the h^3 direction

$$\hat{H} \equiv \frac{1}{h} H = \frac{1}{h} \begin{pmatrix} h^1 - ih^2 \\ h^3 - ih^4 \end{pmatrix} \to (h^1, h^2, h^3, h^4) = (0, 0, 1, 0). \tag{2.2.3}$$

The final effective Lagrangian that considers only the composite sector and the EW contributions is

$$\begin{aligned} \mathcal{L}_{eff} =& (P_T)^{\mu\nu} \Bigg\{ \frac{1}{2} \left(\frac{f^2 \sin^2(\langle h \rangle / f)}{4} \left(B_\mu B_\nu + W_\mu^3 W_\nu^3 - 2 W_\mu^3 B_\nu \right) + \left(\frac{f^2 \sin^2(\langle h \rangle / f)}{4} \right) W_\mu^+ W_\nu^- \right) \\ &+ \frac{q^2}{2} \left[\Pi_0'(0) W_\mu^{a_L} W_\nu^{a_L} + (\Pi_0'(0) + \Pi_0^{X\prime}(0)) B_\mu B_\nu \right] + ... \Bigg\}, \end{aligned} \tag{2.2.4}$$

where $\Pi' = d\Pi / dq^2$. Identifying the factors with the EW coefficients, one see that the EW scale is

$$v = f \sin \frac{\langle h \rangle}{f}. \tag{2.2.5}$$

One can define a parameter ξ to better describe the ratio of the EW and strong dynamics' scale

$$\xi \equiv \frac{v^2}{f^2} = \sin^2 \frac{\langle h \rangle}{f}. \tag{2.2.6}$$

Expanding the Higgs field around the vev

$$h^{\hat{a}} = \begin{pmatrix} 0 \\ 0 \\ \langle h \rangle + h \\ 0 \end{pmatrix}, \tag{2.2.7}$$

one can get the vector to Higgs couplings modified with the parameter ξ

$$g_{VVh} = \sqrt{1 - \xi} g_{VVh}^{SM}, \quad g_{VVhh} = (1 - 2\xi) g_{VVhh}^{SM}. \tag{2.2.8}$$

The interaction of the SM gauge fields with the composite sector induces a Coleman-Weinberg potential at 1-loop level. Summing up all the diagrams in fig. 2.1, the Coleman-Weinberg

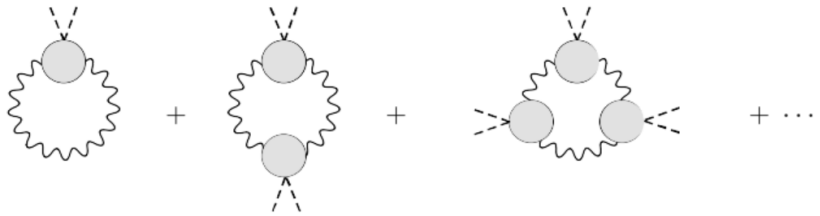

Figure 2.1: The 1-loop diagrams of the gauge bosons that contribute to the Coleman-Weinberg potential [60]. The grey blob encodes the strong dynamics represented by the form factor Π_1.

potential from the gauge boson loops is

$$V(h) = \frac{9}{2}\int \frac{d^4Q}{(2\pi)^4}\log\left[1+\frac{1}{4}\frac{\Pi_1(Q^2)}{\Pi_0(Q^2)}\sin^2\left(\frac{h}{f}\right)\right]. \tag{2.2.9}$$

The form factors are associated to different currents at large Euclidean momentum Q^2. Π_0 is related to the products of conserved currents J^a_μ where Π_1 is related to the difference between the conserved and the broken ones

$$\langle J^a_\mu(q)J^a_\nu(-q)\rangle = \Pi_0(q^2)(P_T)_{\mu\nu}, \quad \langle J^a_\mu(q)J^a_\nu(-q)\rangle - \langle J^{\hat{a}}_\mu(q)J^{\hat{a}}_\nu(-q)\rangle = -\frac{1}{2}\Pi_1(q^2)(P_T)_{\mu\nu}. \tag{2.2.10}$$

Thus the Π_1 is an order parameter that characterizes the transition from the symmetry broken phase to the unbroken phase, and it should vanish in the higher energy scales. If Π_1 vanishes fast enough in the higher energy, the integral in the potential will be convergent and positive. However, as pointed out by Witten [93], like in the QCD, the gauge boson loop induced Coleman-Weinberg potential of the pions tends to align the vacuum along the direction that preserves the gauge symmetry. This also happens in the minimal composite Higgs model. Where one can show that after including the Higgs potential generated by the gauge boson loops, the vacuum is aligned with the $SU(2)_L$ preserving direction, i.e. $\xi = 0$.

Several proposals are brought up to misalign the vacuum, such as introducing additional elementary scalar that mixes with the composite Higgs [76][4], exchange of heavy vectors at higher scale to break the global symmetry explicitly [77], extend the composite sector global symmetry to include an extra $U(1)_A$ such that the EW is preserved while the global symmetry is broken [78, 82, 94, 95]. An very interesting solution among them is the partial compositeness, which we will discuss next.

[4]This is done by introducing an extra fundamental scalar (not Higgs), which in turn introduces a Yukawa coupling that forces the misalignment.

2.2.1 Partial Compositeness

So far the discussion is restricted to the gauge bosons' contributions. The effective Lagrangian eq. (2.2.4) doesn't contain the terms that explain the fermion mass. This issue is also related to the hierarchy of the quark masses. Why do the quarks have the observed flavor families where different families are separated by mass gaps. Especially the heavies quark, the top quark, is about 10^5 times heavier than the lightest quark — the up quark. This could be explained, together with the fermion mass generation and vacuum misalignment, by the partial compositeness of the physical quark. Since the top quark is the heaviest, it suffices to restrict the discussion on the partial compositeness of the top quark.

The idea of partial compositeness is to inlcude a linear coupling of the elementary fermions with the strong sector fermionic operator [8, 87, 96]

$$\Delta\mathcal{L} = \lambda\bar{q}O + h.c., \tag{2.2.11}$$

where λ is the linear coupling, q is the elementary fermion. O is the composite fermionic operator that has the same quantum number as the SM fermions under the SM group. It is analog to the QCD baryon[5]. This interaction adds an additional contribution to the Coleman-Weinberg potential and thus misalign the vacuum. The different quark mass hierarchies are controlled by the coupling strength of different quark families, if such interactions are added for all three quark families. This mechanism gives in this way a natural explanation of the flavor hierarchy — the heavier quarks have stronger couplings. To see that including such a contribution to the Coleman-Weinberg potential misaligns the vacuum, it suffices to include just the top quark generation.

Suppose the global symmetry is still $SO(5) \times U(1)_X$. The elementary particles are the SM ones. The composite fermionic operators transform as a complete representation of the global symmetry group, but the elementary fermions don't. The Lagrangian will in addition contain the terms

$$\mathcal{L} = \lambda_q\bar{q}_L O_q + \lambda_u\bar{u}_L O_u + \lambda_d\bar{d}_L O_d + h.c.. \tag{2.2.12}$$

For simplicity the coupling matrices $\lambda_{q,u,d}$ are assumed to be diagonal. The fermion fields are

[5] If realize this holographically, the operator $\mathcal{O}$ will be a fermionic operator in the field theory, which is realized in the bulk (gravitational theory) as a fermionic bulk field. This is however beyond the scope of this these, we will not discuss the further details.

embedded in the full $SO(5)$ spinorial representation as

$$\Psi_q = \begin{pmatrix} q_L \\ Q_L \end{pmatrix}, \quad \Psi_u = \begin{pmatrix} q_R^u \\ \begin{pmatrix} u_R \\ d'_R \end{pmatrix} \end{pmatrix}, \quad \Psi_d = \begin{pmatrix} q_R^d \\ \begin{pmatrix} u'_R \\ d_R, \end{pmatrix} \end{pmatrix}, \tag{2.2.13}$$

where Q_L, $q_R^{u,d}$, u'_R and d'_R are spurions. They are external non-physical sources. Consider the most general Lagrangian that is invariant under $SO(5) \times U(1)_X$, keeping only the top quark generation as physical fields while setting all the other quarks to zero[6], one arrives at the effective Lagrangian

$$\begin{aligned} \mathcal{L}_{eff,t} =& \bar{q}_L \not{p} \left(\Pi_0^q(p) + \Pi_1^q(p)\cos(h/f)\right) q_L + \bar{t}_R \not{p} \left(\Pi_0^u(p) - \Pi_1^u(p)\cos(h/f)\right) t_R \\ &+ \sin(h/f) M_1^u(p) \bar{q}_L \hat{H}^c t_R + h.c.. \end{aligned} \tag{2.2.14}$$

where $\hat{H}$ is defined in eq. (2.2.3) and $\hat{H}^c = i\sigma^2 \hat{H}$ is the charge conjugation of the Higgs doublet, with σ^2 the second Pauli matrix. $\Pi_{0,1}$ and M_1 are the form factors in the kinetic and the mass terms.

The additional Coleman-Weinberg potential from the fermionic loops is

$$\begin{aligned} V(h) =& -2N_c \int \frac{d^4p}{(2\pi)^4} \Bigg\{ 2\log\left(1 + \frac{\Pi_1^q}{\Pi_0^q}\cos\frac{h}{f}\right) + \log\left(1 - \frac{\Pi_1^u}{\Pi_0^u}\cos\frac{h}{f}\right) \\ &+ \log\left(1 - \frac{(M_1^u \sin(h/f))^2}{p^2(\Pi_0^q + \Pi_1^q\cos(h/f))(\Pi_0^u - \Pi_1^u\cos(h/f))}\right)\Bigg\}. \end{aligned} \tag{2.2.15}$$

The form factors $\Pi_1^{u,q}$ and M_1^u decrease fast enough for large Euclidean momentum p^2, the integral is finite and the potential can be approximated with

$$V(h) \simeq \alpha \cos\frac{h}{f} - \beta \sin^2\frac{h}{f}, \tag{2.2.16}$$

where α and β are defined as

$$\alpha = 2N_c \int \frac{d^4p}{(2\pi)^4}\left(\frac{\Pi_1^u}{\Pi_0^u} - 2\frac{\Pi_1^q}{\Pi_0^q}\right), \quad \beta = \int \frac{d^4p}{(2\pi)^4}\left(2N_c \frac{(M_1^u)^2}{(-p^2)(\Pi_0^q + \Pi_1^q)(\Pi_0^u - \Pi_1^u)} - \frac{9}{8}\frac{\Pi_1}{\Pi_0}\right). \tag{2.2.17}$$

Then the Higgs potential has a minimum at

$$\xi = \sin^2\frac{\langle h\rangle}{f} = 1 - \left(\frac{\alpha}{2\beta}\right)^2, \tag{2.2.18}$$

[6]More generally, one can realize this by performing a rotation in the flavor space, which results in a basis where only the third quark generation contributes.

if $\alpha < 2\beta$. I.e. vacuum is misaligned by including the linear coupling between the top quark and the composite fermionic operator.

2.3 An SU(4)/Sp(4) Model

In this section we review a minimal composite Higgs model that is made holographic later in the research part. The original paper is [80][7]. A thorough review including the application of partial compositeness mechanism and lattice results can be found in [62]. Earlier constructions see [97].

2.3.1 Model Setup

The global symmetry in the composite sector is $SU(4)$ realized by two Dirac fermions transforming as the fundamental representation of the $SU(2)$ gauge group. Such a model is first constructed in [98, 99]. The general Lagrangian in terms of Dirac spinors is

$$\mathcal{L} = -\frac{1}{4}F^a_{\mu\nu}F^{a\mu\nu} + \bar{U}(i\gamma^\mu D_\mu - m)U + \bar{D}(i\gamma^\mu D_\mu - m)D, \tag{2.3.1}$$

where U and D are the fermion fields from the new composite sector having the same mass m, D_μ is the covariant derivative contains gauge bosons from the strong sector. In the limit $m \to 0$, the above Lagrangian manifests a $SU(4)$ global symmetry of the fermions

$$U_L = \frac{1}{2}(1-\gamma^5)U, \quad U_R = \frac{1}{2}(1+\gamma^5)U, \quad D_L = \frac{1}{2}(1-\gamma^5)D, \quad D_L = \frac{1}{2}(1+\gamma^5)D. \tag{2.3.2}$$

For a non-vanishing fermion mass $m \neq 0$, the global symmetry $SU(4)$ is broken explicitly. This can be seen by performing an $SU(4)$ transformation on the Lagrangian as follows. Rewriting the Lagrangian as

$$\mathcal{L} = -\frac{1}{4}F^a_{\mu\nu}F^{a\mu\nu} + i\bar{U}\gamma^\mu D_\mu U + i\bar{D}\gamma^\mu D_\mu D + \frac{m}{2}Q^T(-i\sigma^2)CEQ + (\frac{m}{2}Q^T(-i\sigma^2)CEQ)^\dagger, \tag{2.3.3}$$

[7]Here we choose to keep the original notation such that one can compare with the paper immediately. We changed the notation in the research part in chapter 5, but the main idea is the same. The take home message is that a mixing angle θ characterizes the transition between the CH an TC phases in this model.

where Q is defined as

$$Q = \begin{pmatrix} U_L \\ D_L \\ \tilde{U}_L \\ \tilde{D}_L \end{pmatrix}, \quad \tilde{U}_L = -i\sigma^2 C\bar{U}_R^T, \quad \text{same for } \tilde{D}_L. \tag{2.3.4}$$

C is the charge conjugation operator, σ_2 is the Pauli matrix. The matrix E is

$$E = \begin{pmatrix} 0 & 0 & 1 & 0 \\ 0 & 0 & 0 & 1 \\ -1 & 0 & 0 & 0 \\ 0 & -1 & 0 & 0 \end{pmatrix}. \tag{2.3.5}$$

Now performing a general SU(4) transformation

$$Q \to (1 + i\sum_{n=1}^{15} \alpha_n T^n)Q \tag{2.3.6}$$

on the Lagrangian eq. (2.3.3), this will generate an extra term

$$\mathcal{L} \to \mathcal{L} + \frac{im}{2}\sum_{n=1}^{15} \alpha^n Q^T(-i\sigma^2)C(ET^n + T^{nT}E)Q + h.c., \tag{2.3.7}$$

which only vanishes for the generators that fulfill the condition

$$ET^n + T^{nT}E = 0. \tag{2.3.8}$$

This is the defining condition for $Sp(4)$ generators. I.e. for non-vanishing fermion mass from the new sector, the global symmetry $SU(4)$ is explicitly broken down to $Sp(4)$.

The same symmetry breaking can be induced spontaneously when the strong sector fermions condense. The electroweak sector is embedded in the model by organizing the two left handed strong Weyl fermions into a $SU(2)_L$ doublet $Q_L = (U_L, D_L)$ with hypercharge of 0. The two singlets $\tilde{U}_L$ an $\tilde{D}_L$ are assigned with hypercharge $\pm\frac{1}{2}$ respectively.

The spontaneous breaking of the global symmetry is modeled non-perturbatively using the CCWZ construction. The definition of the vacuum Σ in not unique. There are two inequivalent

vacuums

$$\Sigma_A = \begin{pmatrix} i\sigma_2 & 0 \\ 0 & i\sigma_2 \end{pmatrix}, \quad \Sigma_B = \begin{pmatrix} i\sigma_2 & 0 \\ 0 & -i\sigma_2 \end{pmatrix}, \tag{2.3.9}$$

that are not related to each other by any transformation. But the choice is physics independent and both of them preserves the electroweak symmetry. In the following the vacuum is chosen to be Σ_B.

Using eq. (2.3.8) and replacing E with Σ_B, one arrives at the unbroken $SU(4)$ generators

$$S^{1,2,3} = \frac{1}{2}\begin{pmatrix} \sigma_i & 0 \\ 0 & 0 \end{pmatrix}, \quad S^{4,5,6} = \frac{1}{2}\begin{pmatrix} 0 & 0 \\ 0 & -\sigma_i^T \end{pmatrix}, \quad S^{7,8,9} = \frac{1}{2\sqrt{2}}\begin{pmatrix} 0 & i\sigma_i \\ -i\sigma_i & 0 \end{pmatrix}, \quad S^{10} = \frac{1}{2\sqrt{2}}\begin{pmatrix} 0 & 1 \\ 1 & 0 \end{pmatrix}. \tag{2.3.10}$$

The generators $S^{1,2,3,4,5,6}$ form a $SU(2)_L \times SU(2)_R$ subgroup of SO(5). The five broken generators are

$$\begin{aligned} X^1 &= \frac{1}{2\sqrt{2}}\begin{pmatrix} 0 & \sigma_3 \\ \sigma_3 & 0 \end{pmatrix}, \quad X^2 = \frac{1}{2\sqrt{2}}\begin{pmatrix} 0 & i \\ -i & 0 \end{pmatrix}, \quad X^3 = \frac{1}{2\sqrt{2}}\begin{pmatrix} 0 & \sigma_1 \\ \sigma_1 & 0 \end{pmatrix}, \\ X^4 &= \frac{1}{2\sqrt{2}}\begin{pmatrix} 0 & \sigma_2 \\ \sigma_2 & 0 \end{pmatrix}, \quad X^5 = \frac{1}{2\sqrt{2}}\begin{pmatrix} 1 & 0 \\ 0 & -1 \end{pmatrix}. \end{aligned} \tag{2.3.11}$$

Having found the broken generators, we can write the Goldstone matrix to the first order in fluctuations as

$$\Sigma = \epsilon^{i\frac{\phi_i}{f}X^i}\Sigma_B \sim \Sigma_B + \frac{1}{2\sqrt{2}f}\begin{pmatrix} 0 & i\phi_5 & \phi_4 + i\phi_3 & \phi_2 - i\phi_1 \\ -i\phi_5 & 0 & -\phi_2 - i\phi_1 & \phi_4 - i\phi_3 \\ -\phi_4 - i\phi_3 & \phi_2 + i\phi_1 & 0 & i\phi_5 \\ -\phi_2 + i\phi_1 & -\phi_4 + i\phi_3 & -i\phi_5 & 0 \end{pmatrix}. \tag{2.3.12}$$

The interactions of the GBs are encoded in the kinetic term

$$\mathrm{Tr} D_\mu \Sigma^\dagger D^\mu \Sigma, \tag{2.3.13}$$

where D_μ is the covariant derivative that contains the EW gauge bosons. This term doesn't generate mass for the gauge bosons, so introduce the matrix

$$\Sigma_H = E = 2\sqrt{2} i X^4 \Sigma_B, \tag{2.3.14}$$

which breaks the EW symmetry completely. When ϕ_4 acquires a vev, the GBs $\phi_{1,2,3}$ are eaten

by the W and Z bosons and contribute to the gauge bosons' masses. The electric charge is $Q = T^3 + Y = S^3 + S^6$ which is invariant with respect to the vacuum Σ_H.

When ϕ_4 acquires a vev, ϕ_4 is identified with the Higgs. The left scalar ϕ_5 is a singlet and is identified as η. The broken generators associated with Σ_H are $S^1 - S^4$, $S^2 - S^5$, $S^3 - S^6$, S^8 and X^4, where the invariant ones are $S^1 + S^4$, $S^2 + S^5$, $S^3 + S^6$, $S^{7,9,10}$ and $X^{1,2,3,5}$. The generators $S^1 + S^4$, $S^2 + S^5$, $S^3 + S^6$ manifest a invariant $SU(2)_D$.

The full symmetry breaking pattern in this model is organized by the superpositions of the two vacuums

$$\Sigma_0 = \cos\theta\Sigma_B + \sin\theta\Sigma_H, \quad \Sigma_0^\dagger\Sigma_0 = 1. \tag{2.3.15}$$

In this way, the vacuum is actually a mixture of two breaking procedures. The angle parametrizes the type of the model: this setup will describe a technicolor model in the limit $\theta = \pi/2$, and it will become EW unbroken model in the other limit $\theta = 0$, where when $\theta \ll 1$ it describes a realistic composite Higgs model. The broken generator in this case are also parametrized by the mixing angle

$$\begin{aligned} Y^1 =& c_\theta X^1 - s_\theta \frac{S^1 - S^4}{\sqrt{2}}, \quad Y^2 = c_\theta X^2 + s_\theta \frac{S^2 - S^5}{\sqrt{2}}, \quad Y^3 = c_\theta X^3 + s_\theta \frac{S^3 - S^6}{\sqrt{2}}, \\ Y^4 =& X^4, \qquad\qquad Y^5 = c_\theta X^5 - s_\theta S^8, \qquad\qquad c_\theta = \cos\theta, \quad s_\theta = \sin\theta. \end{aligned} \tag{2.3.16}$$

The fluctuations associate to $Y^{1,2,3}$ are eaten by the W and Z bosons, and the fluctuations associate to the Y^4 and Y^5 are the physical Higgs and singlet scalar with respect to $SU(2)_L$ respectively.

2.3.2 Further Aspects of this Model

If one plugs in the above definitions into the kinetic term of the Goldstone matrix, one can read off the masses of W and Z bosons and their coupling strength to the Higgs h and the singlet η. We will not review the exact expressions in this section, but rather summarize further physical interesting implementations in this model.

Introducing the EW gauge interactions into the strong sector will induce a Coleman-Weinberg potential as usual. Also, the vacuum is misaligned by the contribution of the top quarks. This is implemented by inserting a dimension-six four-fermion operator in a technicolor way [100,

101]

$$\frac{y_t}{\Lambda_t^2}(Qt^c)_\alpha^\dagger \psi^T P^\alpha \psi, \tag{2.3.17}$$

where P^α is the projectors that select the part of $\psi^T\psi$ that transforms as a $SU(2)_L$ doublet. ψ is the techni-fermion from the strong sector. If adding only the Coleman-Weinberg potential generated by the top loop, one finds that the minimum is at $\theta = \pi/2$. So adding top contribution will align the vacuum to the technicolor one.

There is an interesting case associated with the dark matter. One can introduce a techni-Higgs σ, like the σ field in QCD. When in the technicolor vacuum, i.e. setting $\theta = \pi/2$, σ becomes the actual Higgs, while (h, η) are degenerated and stable. They make thus good candidates for dark matter in this model.

This model predicts a lightest ρ mass of about 2.5 TeV and the lightest axial-vector mass m_A of 3.3 TeV, both in the technicolor limit. For a composite Higgs model, their masses are generally much higher, and are therefore expected to be challenging to find at the LHC. Later in chapter 5 we predicted the mass ratio between the two, see section 5.4. We predict a ratio of $m_V/m_A \sim 1.26$, which is larger than the ratio shown here ~ 0.76.

2.4 Combining with Holography

One way to perform calculations related to the strong dynamics in CH models is to employ the gauge/gravity duality and construct a holographic CH model by turning on extra dimensions. Such a model was first proposed in [87], the aim was to employ the holography to move the hard calculations to a 5D model where perturbative calculations are viable. The model was inspired by the AdS/CFT correspondence, but the discussions was not based on the explicit conjecture. The extra dimension in this model was merely a tool to provide easy solution on the calculations that a pure 4D theory isn't able to provide.

The basic idea in the early model is to rewrite the 4D composite Higgs model in a 5D form. The symmetry breaking is manifest using two branes, IR and UV branes, located at different positions along the 5th dimension. In the bulk, i.e the space between the two branes, the model is assumed to have a global symmetry $SU(3)_C \times SO(5) \times U(1)_X$. This is the same symmetry as in the 4-dimensional case. On the IR brane, this global symmetry is broken down to $SU(3)_C \times SO(4) \times U(1)_X$, while on the UV brane, the global symmetry is broken down to $SU(3)_C \times SU(2)_L \times U(1)_Y$. These breaking patterns are implemented by imposing correct

boundary conditions for the gauge bosons. The bulk gauge fields A_μ representing the global symmetries have non-vanishing fifth component only for the ones associated with the coset $SO(5)/SO(4)$. It's exactly these components that are later taken to be the composite pNGB Higgs. The 5D theory is then matched with the 4D theory by integrating out the bulk fields on the UV-brane. The form factors are calculated in the 5D theory and plugged in the 4D theory after matching the two theories.

Simply extending the theory to contain an extra dimension is a common way to perform perturbative calculations in the CH models. Usually this doesn't imply that the model has a well defined UV theory that evolves all the way down to the low energy theory like in QCD. Another possibility is to stick to the definitions of the holography and interpret the UV brane as where the UV theory is defined. This idea is realized in the same way as the AdS/QCD model, except that the dual strong theory is more broadly defined. Such models are mostly based on the hard-wall AdS/QCD model, where the UV and IR scales are introduced as cut-offs, see for example [88]. Some of the models are constructed analog to a soft-wall model (for definition and details see section 3.5), but IR scale in the end is not dynamically generated, see for example [49–51, 102]. The reason for that is, the soft-wall models usually adopt an extra warp factor that is a function of the extra dimension into the action without justifying it's origin.

The holographic CH model constructed in this thesis has three main differences comparing to the others. First the IR scale is generated dynamically where it's origin from the top-down model in the string theory is made clear. Second, the composite pNGB Higgs is not just the fifth component of the gauge field, but rather a scalar field that lives in the bulk and evolves dynamically together with the theory. Also, even though the global symmetry group is claimed to be non-abelian in many models, their actual holographic constructions are essentially degenerated abelian theories. In our research, we construct a true non-abelian composite Higgs model by considering multiple flavor branes located at different positions in the transverse directions. The degeneracy is lifted by the separations of the flavor branes.

Chapter 3

Gauge/Gravity Duality

Being initially a theory proposed to explain the strongly coupled quark bound states, string theory has always been deeply related to strongly coupled gauge theory, for instance the QCD. Corresponding researches are boosted by the birth of AdS/CFT correspondence [11]. Such a conjecture went through rapid development and the correspondence is extended to general gauge theories, giving rise to the more general gauge/gravity duality.

One major application of such correspondence is the calculations in SM strongly interacting sector and BSM model building. Giving that QCD is strongly coupled in the low energy regime, perturbation theory is no more applicable as in QED. The correspondence provides an economical tool to perform such calculations in the dual gravity theory. Not only is it useful in QCD, an active research field of the correspondence is to construct BSM models that contains strongly coupled sector(s), such as the composite Higgs models and the technicolor models with the help of the gauge/gravity duality. The major advantage of the correspondence is the potential of linking the low-energy effective BSM field theory to theories at higher energies that can provide a dynamical origin of the model. Such applications is the focus of our research present in this thesis.

This chapter is dedicated to review and summarize the necessary materials of the gauge/gravity duality. The focus of this thesis is the D3/D7 model, it's non-abelian construction of the bottom-up version, and the application of such a bottom-up model on composite Higgs models. Therefore in the following we will only review selective topics that are relevant to our research. Since the whole discussion is based on gravity theory in AdS spaces, we will first review the AdS space in section 3.1. Then in section 3.2 we review the concept of AdS/CFT correspondence

and the holographic dictionary (field-operator map). After establishing the fundamentals, we review a top-down model constructed by D3-stacks and D7-probe in section 3.3. This model utilizes the AdS_5/CFT_4 correspondence to reproduce meson spectrum. Of course such a top-down model cannot reproduce QCD in the dual gauge theory, since the supersymmetry is not completely broken and it doesn't incorporate the confinement and chiral symmetry breaking, which distinguishes QCD from many gauge theories like the electormagentic theory and $\mathcal{N} = 4$ SYM. Therefore, we first review the implementation of confinement in holographic model in section 3.4. Then we introduce the Constable-Myers background which shows confinement for certain parameter space, and introduce the chiral symmetry breaking in this background in section 3.4.1. We review briefly another background that incorporates both of these properties in section 3.4.2, which will be useful in the research part in chapter 4.

We have collected all the essential parts from the top-down model at this stage, so we move on to the bottom-up models. We first review the AdS/QCD model proposed in [39] in section 3.5. This is the foundation of general bottom-up models. Then we review the dynamical AdS/YM model in section 3.6. This model captures the essence of the top-down D3/D7 and the bottom-up AdS/QCD. The dual theory is no more restricted to QCD, but to a general YM theory. The confinement is generated dynamically and is no more inserted by hand as in the AdS/QCD model. This dynamical AdS/YM model is the starting point of our research part. In the end, we review Witten's double-trace prescription and the insertion of NJL interaction in holographic models. These two techniques are useful in constructing the composite Higgs model in chapter 5.

3.1 AdS Spacetime

The **Anti-de Sitter (AdS)** spacetime lies at the heart of the AdS/CFT correspondence. The isometry group of AdS_{d+2} — $SO(2, d+1)$ coincides with the conformal symmetry group of the $d+1$-dimensional Minkowski spacetime. It is this relation that leads to the identification of the physics defined on the two sides. In this section we summarize some basic concepts of the AdS spacetime.

Usually the AdS geometry and related properties can be found in various lecture notes, textbooks or reviews of the AdS/CFT correspondence or gauge/gravity duality. [12] provides a comprehensive introduction to the AdS geometry and the field theory's properties. The discussion in [103] is more thorough and contains more details on the causal structure of the AdS spacetime and it is more physics-related. For a concise introduction see [104]. Various coor-

dinates of the AdS are associated to different physical problems. They are most thoroughly gathered in [105]. For a more mathematical discussion from an abstract differential geometry and group theory point of view, see [106], also [107]. The following review is mainly based on [12].

The AdS spacetime is the solution of Einstein equations associated to the negative cosmological constant, with negative curvature. The "anti" in its name refers to the sign difference comparing to the de Sitter spacetime, since the de Sitter spacetime is the solution with a positive curvature, associated to a positive cosmological constant.

To construct a $d+2$-dimensional AdS spacetime, the easiest way is to embed a $d+2$-dimensional hyperboloid in a $d+3$-dimensional flat spacetime with two timelike directions $\mathbb{R}^{2,d+1}$. Mathematically it is expressed as

$$X_0^2 + X_{d+2}^2 - \sum_{i=1}^{d+1} X_i^2 = R^2, \quad ds^2 = -dX_0^2 - dX_{d+2}^2 + \sum_{i=1}^{d+1} dX_i^2, \tag{3.1.1}$$

where R is the radius of curvature.

There are various solutions (coordinates) that satisfy this definition. We will only discuss the most commonly used ones. There are three of them. The first solution is the **global coordinates of AdS** (τ, ρ, Ω_i)

$$\begin{aligned} &X_0 = R\cosh\rho\cos\tau, \quad X_{d+2} = R\cosh\rho\sin\tau, \\ &X_i = R(\sinh\rho)\Omega_i, \quad (i = 1, ..., d+1; \sum \omega_i^2 = 1), \end{aligned} \tag{3.1.2}$$

ω_i are the coordinates of the S^d sphere. In this coordinate, the AdS_{d+2} metric becomes

$$ds^2 = R^2(-\cosh^2\rho\, d\tau^2 + d\rho^2 + \sinh^2\rho\, d\Omega^2). \tag{3.1.3}$$

Where $\tau \in [0, 2\pi)$ and $\rho \geq 0$ covers the hyperboloid once. The τ direction forms a closed timelike circle, which is disfavored by the causality. To construct a causal AdS spacetime, one simply opens this circle, by letting the time extend from $-\infty$ to ∞.

The second coordinate is the **conformal coordinate**. This coordinate is called "conformal" due to the fact that after a conformal compactification, the AdS_{d+2} boundary coincides with the one of one half Einstein universe. To show this, start with the AdS_{d+2} space

$$ds^2 = -d\tau^2 + d\theta^2 + \sin^2\theta\, d\Omega^2. \tag{3.1.4}$$

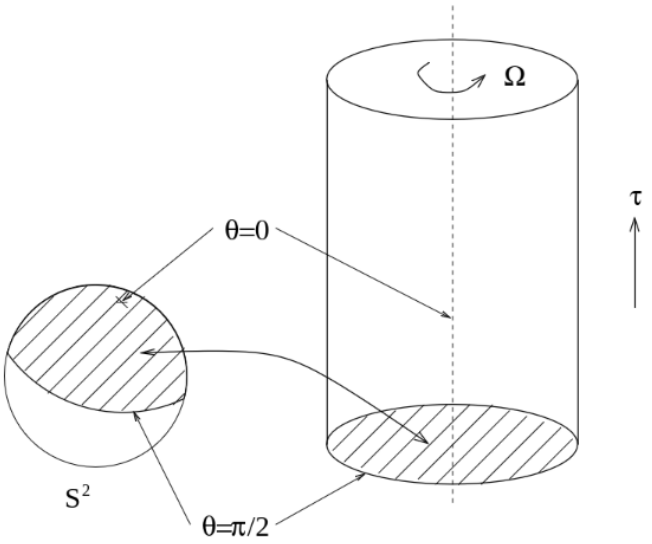

Figure 3.1: The conformal mapping of a constant τ slice of AdS_3 to half of the Einstein universe. Picture taken from [12]

Perform a transformation $\tan\theta = \sinh\rho$, $\theta \in [0, \pi/2)$, this will bring the metric to the form

$$ds^2 = \frac{R^2}{\cos^2\theta}(-d\tau^2 + d\theta^2 + \sin^2\theta\, d\Omega^2). \tag{3.1.5}$$

A conformal rescaling of the above metric arrives at the Einstein universe, while the causal structure is preserved. This shows that the conformal boundary of AdS_{d+2} is a flat $(d+1)$ Minkowski spacetime, or the AdS spacetime is **asymptotically flat**.

Pictorially, this can be viewed as follows. After conformal compactification, for a constant τ slice, the north pole of S^{d+1} is mapped to the center of the disk D^d, the equator is mapped to the boundary and the spaces in between is mapped to the inside of the disk. The equator becomes the boundary of the space with the topology of S^d. For an evolving timelike τ, the AdS spacetime is mapped to a "cylinder", as illustrated in fig. 3.1.

The third coordinate is the **Poincaré coordinates** $(u, t, \vec{x})$

$$\begin{aligned} X_0 &= \frac{1}{2u}\left(1 + u^2(R^2 + \vec{x}^2 - t^2)\right), \quad X^i = Rux^i,\ (i = 1, ..., d), \\ X^{d+1} &= \frac{1}{2u}\left(1 - u^2(R^2 - \vec{x}^2 + t^2)\right), \quad X_{d+2} = Rut, \quad u > 0,\ \vec{x} \in \mathbb{R}^d. \end{aligned} \tag{3.1.6}$$

In this coordinate, the AdS_{d+2} metric is

$$ds^2 = R^2\left(\frac{du^2}{u^2} + u^2(-dt^2 + d\vec{x}^2)\right). \tag{3.1.7}$$

This coordinate covers only half of the hyperboloid. Further define $z = \frac{1}{u}$, this will transform the line element into

$$ds^2 = \frac{R^2}{z^2}\left(dz^2 + (-dt^2 + d\vec{x}^2)\right). \tag{3.1.8}$$

Both of these two definitions are widely used in the AdS/CFT literature, usually u is replaced by r, representing the radial direction.

3.2 AdS/CFT Correspondence

In this section we will review the $\mathrm{AdS}_5/\mathrm{CFT}_4$ correspondence. This conjecture is based on the dynamical object, the so-called D-branes in string theory. D-branes or more explicitly Dp-branes are objects where the open strings can end. "D" stands for Dirichlet, means that the open strings ending on the branes have Dirichlet boundary conditions. It is $p+1$-dimensional, where p represents the number of spatial directions. For N coincident Dp-branes, the massless open strings live on it realize a $U(N)$ gauge symmetry. The action of a single Dp-brane is described by the Dirac-Born-Infeld action (DBI action), it's explicit form will show up in the later sections.

In the following we review the conjecture based on the two limits of the D3-brane. Then we show the field-operator map, or the so-called holographic dictionary. In the end we show the explicit relation that connects the theory on the two sides.

The AdS/CFT correspondence has different versions depends on the dimensionality of the AdS space. For this thesis, we only need the $\mathrm{AdS}_5/\mathrm{CFT}_4$ correspondence. This subject is usually covered in standard string theory textbooks and various lecture notes, with different focuses. The review in this section is based on [12, 108–111].

3.2.1 A Qualitative Explanation

The bridge that connects the two sides of the duality is the D3-branes stack, i.e. N coincident D3-branes. The correspondence can be understood from two aspects. The easier and more elegant aspect is the symmetry. In 10D spacetime, N coincident D3-branes describe $SU(N)$ $\mathcal{N}=4$ SYM theory. The $\mathcal{N}=4$ SYM theory is a theory with conformal symmetry $SO(4,2)$. which contains usual Lorentzian symmetry transformations plus conformal transformations, in total 15 symmetry generators. From the supersymmetric perspective, the $\mathcal{N}=4$ SYM has an

internal global symmetry, which is the $\mathcal{R}$-symmetry, represented by the $SU(4)_{\mathcal{R}}$. The conformal group is isomorphic to $SU(2,2)$, together with the $\mathcal{R}$-symmetry group, they can be written compactly as $SU(2,2|4)$, which describes a $\mathcal{N}=4$ supersymmetric theory.

On the other hand, the near-horizon geometry of a D3-stack is an $\mathrm{AdS}_5 \times \mathrm{S}^5$ spacetime. The S^5 has a $SO(6) \simeq SU(4)$ isometry, where AdS_5 has a isometry group $SO(4,2)$. Since the symmetries of the weakly coupled gravitational theory on AdS space matches with the symmetries of the strongly coupled $\mathcal{N}=4$ SYM theory, it was postulated that the two theories describe the same dynamics in the form of duality.

The other aspect of understanding the duality is using the two limits of the D3-stack in the low-energy limit $\sqrt{\alpha' E} \ll 1$, or equivalently $E \leq E_0$ when $\alpha' \to 0$, E_0 represents an energy bound here. α' is the slope parameter which is related to the string length l_s as $l_s = \hbar c\sqrt{\alpha'}$. The true low-energy limit is the **Maldacena limit** if in addition $U = \frac{r}{\alpha'}$ is fixed given that $E \propto U$. Here r is the u in eq. (3.1.7). Note that one can also understand the r as the distance between a D3-brane sitting at $\vec{r}$ and a D3-stack sitting at $\vec{r}=0$. Then the "W-boson", which is the string stretching between the two D3 sets, has a mass proportional to this distance r. There are two types excitations in the theory: open and closed strings. The coupling between the open and closed strings is g, where one can define the **'t Hooft coupling** $\lambda = 4\pi g N = g_{YM}^2 N$ with N the number of D3-branes. Through out the discussion, the large N limit is kept. In the large N limit, the leading order diagrams are planar diagrams [112], where the higher order contributions are suppressed by powers of $1/N$.

Consider the IIB superstring theory in flat (9+1)D Minkowski space, where the D3-stacks are embedded along the directions (t, x_1, x_2, x_3). In the limit when the string coupling g is small $g \ll 1$, the theory describes open string excitations from the D3-branes interacting with the closed string from the 10D flat Minkowski spacetime. The interactions are weighted by the string length squared α'. When taking the low energy limit $\alpha' \to 0$, the open strings decouple from the closed strings. One finds that the open strings describe a $SU(N)$ $\mathcal{N}=4$ SYM theory while the closed strings describe a free IIB supergravity theory in flat 10D spacetime.

If now dial up the string coupling constant g to the regime $gN \gg 1$, the gravitational effect of the D-branes changes the spacetime geometry, where the D3-branes become solitonic solution of supergrvity. In this case the solution is

$$ds^2 = H(r)^{-1/2} dx^\mu dx_\mu + H(r)^{1/2}(dr^2 + r^2 d\Omega_5^2), \tag{3.2.1}$$

with

$$H(r) = 1 + \left(\frac{R}{r}\right)^4, \tag{3.2.2}$$

where x^μ for $\mu = 0, ...3$ is the 4D spacetime, $r^2 = \sum_{i=4}^{9} x_i^2$ and $R^4 = 4\pi g N \alpha'^2$ is the radius of the horizon. Depending on the relation of R and r, the geometry has different asymptotics. In the **near horizon region** or **throat** where $r \ll R$, one has $H(r) \sim R^4/r^4$, the metric describes an $\mathrm{AdS}_5 \times \mathrm{S}^5$ geometry. At the infinity $r \gg R$, $H(r) \sim 1$, the metric essentially describes a flat spacetime.

An observer at the infinity can observe two kinds of low energy excitations: one is the low energy excitations at the infinity, which are the closed strings in 10D flat spacetime, the other one is the red-shifted high energy excitations from the throat, which are closed strings on the $\mathrm{AdS}_5 \times \mathrm{S}^5$. In this case, the theory is well described by two decoupled systems: low-energy closed strings on the flat space and IIB superstrings on the near-horizon geometry. When looking at the two limits of the same D3-branes, there are two sets of decoupled theory while both of them contain a IIB string theory on 10D flat spacetime. The remaining two theories must describe the same dynamics. Therefore one can identify the $SU(N)$ $\mathcal{N} = 4$ SYM theory with the IIB supergravity on $\mathrm{AdS}_5 \times \mathrm{S}^5$[1]. This is the $\mathrm{AdS}_5/\mathrm{CFT}_4$ correspondence, the coupling constants g, g_{YM}, the horizon radius R and the string length $\sqrt{\alpha'}$ are related by

$$\lambda = 4\pi g N = g_{YM}^2 N = \frac{R^4}{\alpha'^2}. \tag{3.2.3}$$

The AdS/CFT correspondence is still a conjecture. Depends on it's range of validity, there are three versions of the correspondence. The strongest version states that the conjecture is valid for all values of g and N. The weaker version assumes that the correspondence is valid in the large N limit for any finite gN. The weakest version requires that the correspondence is valid only in the 't Hooft limit, i.e. in the large N and large gN limit. For the works reviewed and developed in this thesis, we assumed the weakest version of the correspondence.

The correspondence relates a 10D IIB superstring theory in $\mathrm{AdS}_5 \times \mathrm{S}^5$ with a $SU(N)$ theory in the 4D flat spacetime. Since the asymptotic boundary of AdS_5 is the 4D flat spacetime, after Kaluza-Klein decomposition on the S^5, this correspondence realizes the holographic principle, which states that the informations in a V_{d+1} volume is encoded on it's A_d boundary area [108].

[1]Theoretically, N coincident D-branes manifest a $U(N)$ gauge symmetry. But the duality is only about an $SU(N)$. The reason is that, the $U(1)$ factor corresponds to the center of mass motion of the D-branes, which encodes the topological theory of the Kalb-Ramond B-field on AdS. This $U(1)$ gauge field lives on the AdS boundary, and the corresponding modes are called singletons [12].

3.2.2 Field-Operator Map

Following the discussion in the last part, the correspondence states that the bulk fields in the 5D theory after the Kaluza-Klein decomposition on the S^5 is dual to the operators in the 4D CFT lives on the conformal boundary of the AdS space

$$\mathcal{O} \leftrightarrow \phi|_{\text{AdS boundary}}. \tag{3.2.4}$$

Moreover, the mass of the field is related to the scaling dimension of the dual operator. To see this, one can consider, without loss of generality, a scalar field (also called primary operator) in CFT. Under the dilatation

$$x^\mu \to \lambda x^\mu, \tag{3.2.5}$$

the primary field $\mathcal{O}$ scales as

$$\mathcal{O}(x_\mu) \to \lambda^{-\Delta}\mathcal{O}(\lambda x_\mu), \tag{3.2.6}$$

where Δ is the scaling dimension of the primary operator $\mathcal{O}$[2].

Now consider an AdS_{d+1} spacetime on the Poincaré slice, as defined in eq. (3.1.8)

$$ds^2 = \frac{R^2}{z^2}\left(dz^2 + dx_\mu dx^\mu\right). \tag{3.2.7}$$

The action for a scalar field $\phi(x^\mu, z)$, $\mu = 0, ..., d-1$, with mass m that lives in the $d+1$-dimensional AdS spacetime is

$$\int dz d^d x \left(\partial^M \phi \partial_M \phi + m^2 \phi^2\right), \tag{3.2.8}$$

where M is the spacetime index, runs from $0, ..., d = (x^\mu, z)$. The equation of motion of this scalar field is the Klein-Gordon equation in $(d+1)$D. Solving the equation of motion for ϕ, the solution has a UV ($z \to 0$) asymptotics

$$\phi|_{z\to 0} \to \langle\mathcal{O}\rangle z^{\Delta_+} + \mathcal{J} z^{\Delta_-}, \tag{3.2.9}$$

where

$$\Delta_\pm = \frac{d}{2} \pm \sqrt{\frac{d^2}{4} + m^2 R^2}, \quad \Delta_+ + \Delta_- = d. \tag{3.2.10}$$

[2]The scaling dimension is the eigenvalue of the the scaling operator D in CFT. The primary operators $\mathcal{O}$ are the operators or fields in the CFT with the lowest scaling dimension. Mathematically, in a d-dimensional spacetime, the primary operator will be annihilated by the special conformal transformation K_μ, $\mu = 0, ..., d-1$: $[K_\mu, O(0)] = 0$. Details see for example [12, 108].

operator	relation
scalars	$\Delta_\pm = \frac{1}{2}(d \pm \sqrt{d^2 + 4m^2})$
spinors	$\Delta = \frac{1}{2}(d + 2\|m\|)$
vectors	$\Delta_\pm = \frac{1}{2}(d \pm \sqrt{(d-2)^2 + 4m^2})$
p-forms	$\Delta_\pm = \frac{1}{2}(d \pm \sqrt{(d-2p)^2 + 4m^2})$
firs-order $(d/2)$-forms (d even)	$\Delta = \frac{1}{2}(d + 2\|m\|)$
spin-3/2	$\Delta = \frac{1}{2}(d + 2\|m\|)$
massless spin-2	$\Delta = d$

Table 3.1: The mass-dimension relations for other types of fields when $R = 1$. Table taken from from [114].

The dual operator's scaling dimension $\Delta = \Delta_+$ is related to the bulk field's mass m through the relation

$$m^2 R^2 = \Delta(\Delta - d). \tag{3.2.11}$$

The above condition comes from matching the SUGRA scalar solution with the one from the dual CFT. As indicated by the notation, $\langle \mathcal{O} \rangle$ is the vev of the dual operator $\mathcal{O}$, this term is the normalizable solution, corresponding to physical fluctuations [113]. $\mathcal{J}$ is the source that couples to the operator $\mathcal{O}$ with the dimension Δ_+ in the dual field theory, which is non-normalizable, corresponds to the non-fluctuating background. Normalizable means that when evaluating the action on the solution, the action is finite. The mass-scaling dimension relation in eq. (3.2.11) exists for all other types of fields. These relations are worked out in various papers. A summary for $R = 1$ can be found in [114], we list them in table 3.1.

For massive scalar fields that live in an AdS_{d+1} spacetime, there exists a so-called Breitenloher-Freedman bound (BF bound)[3]

$$m^2 R^2 \geq -d^2/4. \tag{3.2.12}$$

If the squared mass m^2 (when $R = 1$) passes below this bound, the potential of the scalar field doesn't have a minimum anymore, i.e it turns unstable. What is special about this bound is, for scalar field with $m^2 R^2 < 0$, the potential can still be stable above this bound.

The scaling (conformal) dimension of the dual scalar operator is also bounded by the unitarity of the dual gauge theory

$$\Delta \geq (d-2)/2. \tag{3.2.13}$$

[3]The relation of this bound to our model in the research part is reviewed in appendix B.

For operators with scaling dimension $\Delta \in [(d-2)/2, d/2)$, one can switch the role of the vev and the source in the UV asymptotics of the scalar solution. Translate into m^2R^2, if the bulk scalar field's m^2R^2 is in the range [108]

$$-\frac{d^2}{4} < m^2R^2 \leq -\frac{d^2}{4} + 1, \tag{3.2.14}$$

then one has a freedom in defining the vev and the source terms.

Since the two theories are identified at the boundary, their partition functions should be the same at the boundary. As pointed out in [115, 116], quantitatively the duality means the generating functional of the 4D CFT is equal to the SUGRA action evaluated on the AdS boundary[4]

$$e^{W|_{\text{CFT}}} = \left\langle e^{\int d^4x \phi^0(x)\mathcal{O}(x)} \right\rangle_{CFT} \approx e^{\text{extreme } S_{\text{Sugra}}}, \tag{3.2.15}$$

or put it another way

$$\left\langle e^{\int d^4x \phi^0(x)\mathcal{O}(x)} \right\rangle_{CFT} = e^{-S_{\text{Sugra}}}|_{\phi=\phi^0}. \tag{3.2.16}$$

Here ϕ^0 is the boundary value of the field ϕ, which is the source $\mathcal{J}$ mentioned above. From this relation, one can compute the two-point correlation function. In doing this, one needs to first solve the equation of motion (eom) for the bulk field to get the extremum. Then evaluate the action on this solution. Integrating by parts, one finds that the action becomes the form

$$\text{5D action}|_{\text{boundary}} = \int dz d^4x \left(\text{eom} + \partial_z(...)\right), \tag{3.2.17}$$

so the action is determined by a surface term on the AdS boundary. This will give the RHS of eq. (3.2.16). Differentiating this action twice with respect to the boundary fields ϕ^0 one gets the two-point correlation function

$$\langle \mathcal{O}_1(x_1)\mathcal{O}_2(x_2)\rangle_{\text{CFT, connected}} = -\frac{\delta^2 S_{sugra}}{\delta\phi_1^0(x_1)\phi_2^0(x_2)}. \tag{3.2.18}$$

3.3 A Top-Down Model: D3/D7

N D3-branes manifest an $SU(N)$ gauge symmetry in the bulk, where the worldvolume gauge fields transform as the adjoint representation of the $SU(N)$ gauge group. This system however doesn't contain matter fields in the fundamental representation, which is essential if we were to

[4]Notice that this relation is derived in the euclidean space. For a Lorentzian space the factor in front of the action S is i.

construct a realistic QCD(-like) theory. To include the quarks and the flavour symmetry, it's intuitive to add another set of D-branes. These D-branes can not be D3-branes, otherwise the implementation just extends the $SU(N)$ to another $SU(N')$. It was pointed out in [24] that such a set of D-branes must cover the world-volume of the D3-stacks. Also, the new Dp-branes should have extra dimensions extending to the directions transverse to the D3-stack such that scalar fluctuations are present. Within the type-IIB string theory, this means only the Dp-branes with p odd and $3 < p < 9$ can be considered. Since D9-branes are space-filling, they cannot give rise to scalar fields to allow dual meson states. The D5-branes leads to the so-called defect theory [117], which is also ruled out. Therefore, the unique choice of adding flavors with D-branes is using the D3-stacks embedded in the worldvolume of the D7-branes. Usually the D7-branes are called D7-probes, i.e. the number of flavour N_f should be much smaller than the number of color $N_f \ll N_c$. Here N_c is the number of color, it is used interchangeably with N in the following text to refer to the number of D3-branes. This is called the probe limit. In this limit, the back-reaction of the D7-probe on the background D3-stack is negligible. This corresponds to the quenched approximation in lattice QCD, where in calculating the fermion interactions, the gluons are taken into account, but the fermions don't affect the gluons.

D-branes	t	x_1	x_2	x_3	x_4	x_5	x_6	x_7	x_8	x_9
D3	×	×	×	×	–	–	–	–	–	–
D7	×	×	×	×	×	×	×	×	–	–

Table 3.2: World volume of D-branes in 10D spacetime. × marks the longitudinal directions where – marks the transverse directions.

After adding the D7-probe, the open strings between the D7- and D3-branes transform in the fundamental representation of $SU(N_c)$. The open strings between the D7-branes are in the adjoint representation of the $SU(N_f)$. These states have two flavor indices, therefore they are dual to the composite states (like mesons in the QCD). The length of the D3-D7 strings determines the quark masses. This construction is the D3/D7-probe setup [24, 29, 30], which is a relatively simple top-down model that was build on top of the most intensively studied $\mathrm{AdS}_5/\mathrm{CFT}_4$ correspondence. The implementation of D7-probe will break the $\mathcal{N} = 4$ SYM theory in the dual theory to $\mathcal{N} = 2$ SYM. The $\mathcal{N} = 2$ hypermultiplet transform in the fundamental representation of $SU(N)$, contains two complex scalar fields ϕ^m and two Weyl fermions with opposite chirality $\psi^{\pm}$. The spectrum of this model with a displacement between the D3-stack and the D7-brane is first calculated in [30]. In the following we will review the construction of this model in [30], and summarize briefly the results that are relevant to our research. This section will be restricted to the bosonic states. For implementation of fermionic states in D3/D7, see [31].

The model contains N D3-branes and only one D7 flavor brane. If the D7-brane coincides with the D3-stack, the R-symmetry of $\mathcal{N}=4$ SYM is broken to $SU(4)\sim SO(6)\to SU(2)_R\times SU(2)_L\times U(1)_R$. The R-symmetry is $SU(2)_R\times U(1)_R$ in this case. If the D7-brane is separated from the D3-stack in the $8,9$, i.e. the directions transverse to the D7-brane, then this symmetry group is further broken down to $SU(2)_R$. In this case, the induced metric is

$$ds^2=\frac{\rho^2+L^2}{R^2}dx^\mu dx_\mu+\frac{R^2}{\rho^2+L^2}d\rho^2+\frac{R^2\rho^2}{\rho^2+L^2}d\Omega_3^2, \tag{3.3.1}$$

where $\mu=0,...,3$, $r^2=L^2+\rho^2$, $L^2=|\vec{Y}|^2$ and Y^i with $i=1,...,6$ are the coordinates of the 4,..,9 directions. This metric is asymptotically $AdS_5\times S^3$. Note that were the D7-brane coincides with the D3-brane, we will have $|\vec{Y}|=r$. The corresponding dual field theory is conformal invariant.

The dynamics of the open strings on the D7-brane are described by the DBI-action of the D7-brane

$$S_{D7}=-\mu_7\int d^8\xi\sqrt{-\det(P[G]_{ab}+2\pi\alpha' F_{ab})}+\frac{(2\pi\alpha')^2}{2}\mu_7\int P[C^{(4)}]\wedge F\wedge F. \tag{3.3.2}$$

Here G_{ab} is the bulk metric, P is the pullback of the bulk field to the brane's world volume, $\mu_7=[(2\pi)^7 g_s\alpha'^4]^{-1}$ is the D7-brane tension. $C^{(4)}=\frac{r^4}{R^4}dx^0\wedge dx^1\wedge dx^2\wedge dx^3$ is the Ramond-Ramond (RR) potential. For a non-zero separation L, embed the D7-brane as

$$Y^5=0+2\pi\alpha'\chi,\quad Y^6=L+2\pi\alpha'\varphi, \tag{3.3.3}$$

where $Y^{5,6}$ are the two transverse directions 8, 9. χ and φ are the corresponding scalar fluctuations of the open strings in these two directions. The dynamics of the scalar fields are described by the Lagrangian

$$\mathcal{L}\simeq-\mu_7\sqrt{-\det g_{ab}}\left(1+2(R\pi\alpha')^2\frac{g^{cd}}{r^2}\left(\partial_c\chi\partial_d\chi+\partial_c\varphi\partial_d\varphi\right)\right), \tag{3.3.4}$$

g_{ab} is the induced metric. These two scalars are degenerated, represented below with Φ, and have the same equation of motion

$$\begin{aligned}&\partial_a\left(\frac{\rho^3\sqrt{\det\tilde{g}}}{\rho^2+L^2}g^{ab}\partial_b\Phi\right)=0,\\ \to&\frac{R^4}{(\rho^2+L^2)^2}\partial^\mu\partial_\mu\Phi+\frac{1}{\rho^3}\partial_\rho\left(\rho^3\partial_\rho\Phi\right)+\frac{1}{\rho^2}\nabla^i\nabla_i\Phi=0,\end{aligned} \tag{3.3.5}$$

where $\tilde{g}_{ab}$ is the metric of the three sphere S^3, i runs over the directions of the S^3. This equation can be solved using separation of variables, where one writes the solution as

$$\Phi = \phi(\rho)e^{ik\cdot x}\mathcal{Y}^l(S^3), \quad \nabla^i\nabla_i\mathcal{Y}^l = -l(l+2)\mathcal{Y}^l, \tag{3.3.6}$$

with $\mathcal{Y}^l(S^3)$ the spherical harmonics on S^3. Redefine the coordinate and factors to

$$\varrho = \frac{\rho}{L}, \quad \bar{M}^2 = -\frac{k^2R^4}{L^2}, \quad y = -\varrho^2, \tag{3.3.7}$$

one can rewrite the eom in the second line of eq. (3.3.5). Together with the ansatz

$$\phi(\varrho) = \varrho^l(1+\varrho^2)^{-\alpha}P(\alpha), \tag{3.3.8}$$

we arrive at a general solution

$$\begin{aligned} P(y) &= F(a,b;c;y), \\ \rightarrow \phi(\rho) &= \rho^l(\rho^2+L^2)^{-\alpha}F(-\alpha,-\alpha+l+1;l+2;-\rho^2/L^2), \end{aligned} \tag{3.3.9}$$

where $F(a,b;c;y)$ is the standard hypergeometric function (we omit the determination of the coefficients a,b,c here, they are directly given in the solution). Several criterion need to be fulfilled for this general solution to be a physical solution — the regularity at origin, the normalizability [113, 118] in the UV and reality of the solution. These conditions constraint the final solution to be

$$\phi(\rho) = \frac{\rho^l}{(\rho^2+L^2)^{n+l+1}}F(-(n+l+1),-n;l+2;-\rho^2/L^2), \tag{3.3.10}$$

where $-\alpha+l+1=-n$, $n=0,1,2,....$ The 4D spectrum is

$$M_s(n,l) = \frac{2L}{R^2}\sqrt{(n+l+1)(n+l+2)}, \quad l \geq 0. \tag{3.3.11}$$

The gauge fluctuations are analyzed in the same way, but the discussion is more subtle. We omit the detailed derivations of the gauge fields' fluctuations here but to summarize the bosonic field content in table table 3.3. Note that the gauge bosons have three scalar fluctuations $\phi_I^{\pm}$, ϕ_{III} and one vector fluctuation A_{II}^{μ}. Also note that fields are characterized by their representations under $SU(2)_R \times SU(2)_L$, where $j_{1,2}$ are the corresponding spins. Their dual operators must have the same quantum numbers and the corresponding conformal dimension Δ. For derivations see

Type	(j_1, j_2)	$M^2(n,l)$	Δ	$\mathcal{O}$
2 scalars	$(\frac{l}{2}, \frac{l}{2})$	$M_s^2 = \frac{4L^2}{R^4}(n+l+1)(n+l+2)$, $n \geq 0$, $l \geq 0$	$l+3$	$\mathcal{M}_s^{Al}$
1 scalar	$(\frac{l}{2}, \frac{l}{2})$	$M_{III}^2 = \frac{4L^2}{R^4}(n+l+1)(n+l+2)$, $n \geq 0$, $l \geq 1$	$l+3$	$\mathcal{J}^{5l}$
1 scalar	$(\frac{l-1}{2}, \frac{l+1}{2})$	$M_{I,+}^2 = \frac{4L^2}{R^4}(n+l+2)(n+l+3)$, $n \geq 0$, $l \geq 1$	$l+5$	$\mathcal{C}^{Il}$
1 scalar	$(\frac{l+1}{2}, \frac{l-1}{2})$	$M_{I,-}^2 = \frac{4L^2}{R^4}(n+l)(n+l+1)$, $n \geq 0$, $l \geq 1$	$l+1$	$\mathcal{C}^{Il}$
1 vector	$(\frac{l}{2}, \frac{l}{2})$	$M_{II}^2 = \frac{4L^2}{R^4}(n+l)(n+l+2)$, $n \geq 0$, $l \geq 0$	$l+3$	$\mathcal{J}^{\mu l}$
Dual Operators				
$\mathcal{M}_s^{Al} = \bar{\psi}_i \sigma_{ij}^A X^l \psi_j + \bar{q}^m X_V^A X^l q^m$, $i, m = 1, 2$				
$\mathcal{J}^{(\mu,5)l} = \bar{\psi}_i^\alpha \gamma_{\alpha\beta}^{(\mu,5)} X^l \psi_i^\beta + i\bar{q}^m X^l D^{(\mu,5)} q^m - i\bar{D}^{(\mu,5)} \bar{q}^m X^l q^m$, $\mu = 0, 1, 2, 3$				
$C^{Il} = \bar{q}^m \sigma_{mn}^I X^l q^n$				

Table 3.3: The bosonic field content of the D3/D7 top-down model and their dual operators $\mathcal{O}$. (j_1, j_2) are the spins under $SU(2)_R \times SU(2)_L$. Δ is the scaling dimension of the operators in the dual field theory of the D3/D7 model. q^m and ψ_i are the fields in the fundamental hypermultiplet when writing $\mathcal{N} = 2$ SYM theory in terms of $\mathcal{N} = 1$ superspace formalism. σ_{mn}^I, $I = 1, 2, 3$ are the Pauli matrices, X^l is the symmetric traceless operator insertion $X^{\{i_1} ... X^{i_l\}}$ of l adjoint scalars X^i with $i = 4, 5, 6, 7$. Summarized from [30, 119]

[30, 119], we only list the operators in the table.

The fermionic part is analyzed in [31]. This is beyond the scope of this thesis, the fermionic sector isn't summarized in this table. For introducing fermions in AdS/CFT, the relevant discussions see also [120–129].

To complete the discussion, we mention briefly at the end of this section another top-down approach to the QCD model, the D4/D8/$\overline{\text{D8}}$ setup [32, 33]. This model discussed another D-brane structure within the type-IIA string theory. The action is actually non-abelian, but the quark masses are set to be the same. Fermions are also added, in this case they share the same form as the Skymer model, and the fermions, which are dual to the baryons in the field theory are the skymions. Further discussion on the baryons in this model can be found in [34–38] for top-down and [38, 130] for bottom-up.

3.4 Confinement

The D3/D7 model introduced in the last section still has supersymmetric dual field theory. To approach a realistic QCD (-like) theory using the holographic language, the SUSY must be broken. Also, QCD as a strong interacting non-Abelian gauge theory is different from the Abelian theory in two aspects. At low energies, no single quark is observed experimentally.

They always form a colorless bound state bounded by the gluons. This is the color confinement, in that a $q\bar{q}$ potential isn't a Coulomb type as in the QED case, but scales with the separation L of the quark and anti-quark pair — $V(L) \propto L$. The other aspect is that the chiral symmetry is spontaneously broken giving rise to bound states (pNGBs) like the QCD pions. Both of these two aspects are not present in the model introduced before.

In this section we review the introduction of confinement in holographic models by the Constable-Myers background [131] and the spontaneous chiral symmetry breaking realized on top of this model [25]. In the end we will introduce shortly another construction to implement confinement and chiral symmetry breaking by turning on the magnetic field. This is the source of the dilaton flow that is mimicked in the bottom-up model in the research part in chapter 4. For a systematic review on confinement and chiral symmetry breaking in gauge/gravity duality see [108, 119]

In the QCD, to study the quark-antiquark potential, one needs to calculate the expectation value of the Wilson loop $\langle W \rangle$ [132]

$$V(r) = \lim_{T\to\infty} \frac{1}{iT} \ln \langle \Omega | \, \mathrm{Tr} W \, | \Omega \rangle \,, \tag{3.4.1}$$

where Tr traces over color and

$$W = P\left\{ \exp\left[ig_s \oint_{\mathcal{C}} A^a_\mu T^a_{ij} dx^\mu \right] \right\}. \tag{3.4.2}$$

$P\{...\}$ is the path ordering, $\mathcal{C}$ is the integration contour circling a rectangle with edges of Euclidean time T and spatial separation of quarks L. For confining theory, the potential should scale linearly with the separation L, which translates to the criteria that the Wilson loop should follow an area law

$$V \propto L \to \ln\langle W \rangle \sim TL. \tag{3.4.3}$$

Similar area law is also expected in signaling confinement in holographic models. The holographic version of Wilson loop is first calculated in [133]. The idea is to take first a stack of $N+1$ coincident D3-branes. If put one brane of them to be infinitely far away, then the string attaching to the rest N D3 branes and the single D3 brane will acquire a mass. Such a string initially is dual to a "W-boson". But since the single D3-brane is brought infinitely far way, the $U(1)$ essentially decouples from the rest $U(N)$ and the string connecting the two realizes a "quark" that transforms in the fundamental representation of the $U(N)$ gauge group. Two such strings with different orientations realize the quark and antiquark.

The quark-antiquark potential is derived from the renormalized Wilson loop[5], which shows that the energy of the configuration is

$$E = -\frac{4\pi^2(2g_{YM}^2 N)^{1/2}}{\Gamma(\frac{1}{4})^4 L}, \tag{3.4.4}$$

with L the separation of the quark-antiquark pair. It was shown that the quark and anti-quark strings will join to become a single string since in this case the energy is lowered. Moreover, as the quark and anti-quark are separated further apart, the joint string will dip further into the interior of the AdS space.

The simple model in [133] doesn't show confinement, as can be seen from the potential, it is essentially of Coulomb type. This is due to the fact that the dual theory is still conformal invariant. It was then suggested in [129] that a thermal AdS spacetime could lead to a confining theory by compactifying an extra dimension and setting non-supersymmetric boundary conditions (thermal black hole). The criteria in this case is that the glueball spectrum has a mass gap, i.e. the solutions only accepts $k^2 \geq 0$, with k the four-momentum of the bulk field. This construction is then studied in [134–146]. The main issue with this proposal is to decouple the fermions and the scalars in the valid range of supergravity approximation. Another possibility is to modify the interior of the AdS spacetime, by inserting a barrier like a hard wall (definition see section 3.5), a brane etc., such that the quark-antiquark string cannot dip further into the deep interior of the AdS space, but to stretch along the direction of the barrier. This could be done by the so-called GPPZ flow [147, 148] in a 5D $\mathcal{N} = 8$ gauged supergravity, or by a dilaton flow [149] in a non-supersymmetric background in the IIB string theory. Similar constructions see also [26, 150–157]. In the following we will focus on the Constable-Myers background. It was shown that in certain parameter range, the theory defined in the background has confinement.

3.4.1 Constable-Myers Background and Chiral Symmetry Breaking

The Constable-Myers background [131], along the lines of the constructions [149–156], is a family of IIB supergravity solutions that contains two extra scalar fields (comparing to the bulk scalar fields), i.e. the dilaton and an S^5 volume scalar. In the Einstein frame, the solution is

$$ds^2 = H^{-1/2}\left(\frac{w^4+b^4}{w^4-b^4}\right)^{\delta/4}\sum_{j=0}^{3} dx_j^2 + H^{1/2}\left(\frac{w^4+b^4}{w^4-b^4}\right)^{(2-\delta)/4}\frac{w^4-b^4}{w^4}\sum_{i=1}^{6} dw_i^2 \tag{3.4.5}$$

[5]Since the integral contains contributions from the mass of the infinitely heavy "W-boson", the Wilson loop is renormalized with this contribution subtracted. Details see [133].

where

$$H = \left(\frac{w^4+b^4}{w^4-b^4}\right)^{\delta} - 1, \quad w^2 = \sum_{i=1}^{6} w_i^2. \tag{3.4.6}$$

b is a parameter that determines the size of the deformation $\delta = R^4/(2b^4)$, and r is the AdS radius[6]. Here we use the notation in [25] for later convenience. The Constable-Myers' notation is related to this one by redefining the r in Constable-Myers' notation in terms of w

$$\frac{dw}{w} \equiv \frac{r^2 d(r^2)}{2(r^4+b^4)} \to \left(\frac{w}{w_0}\right)^4 = r^4 + b^4. \tag{3.4.7}$$

The integration constant w_0 is set to 1 for $b = 0$. This family of solutions is asymptotically $AdS_5 \times S^5$ and breaks both the supersymmetry and conformal invariance.

The dilaton and the four-form are

$$e^{2\phi} = e^{2\phi_0}\left(\frac{w^4+b^4}{w^4-b^4}\right)^{\Delta}, \quad C_{(4)} = -\frac{1}{4}H^{-1}dt \wedge dx \wedge dy \wedge dz, \tag{3.4.8}$$

where the exponent satisfy $\Delta^2 + \delta^2 = 10$. This family of solutions contains a naked singularity at $w^2 = b^2$. Understanding the physics in this region requires the full string theory. However, the main interesting features can be obtained by studying the parameter space where the supergravity approximation is valid.

For convenience, introduce ρ and define $\sum_{i=1}^{4} dw_i^2 = d\rho^2 + \rho^2 d\Omega_3^2$, the radial coordinate is then $w^2 = \rho^2 + w_5^2 + w_6^2$. Such a deformation is caused by the presence of operators like $\langle \mathrm{Tr}(F^2) \rangle$ in the dual field theory, which breaks the supersymmetry. In this background, the quark-antiquark potential is linear in the length of separation of the quark-antiquark pair L [131]

$$V(L) \simeq \frac{\Sigma^{\frac{\delta-|\Delta|}{4\delta}}}{2\pi\alpha'\sqrt{1-\Sigma}} L, \quad \Sigma = \frac{|\Delta|-\delta}{|\Delta|+\delta}. \tag{3.4.9}$$

The glueball spectrum of the five-sphere fluctuation shows a mass gap. Both of these results signal confinement in the dual field theory.

To realize a chiral symmetry breaking in the Constable-Myers background [25], notice that the R-symmetry $U(1)_R$ from the rotational symmetry in the two transverse directions $w_{5,6}$ (i.e. the $Y_{5,6}$ in the last section) can be taken as the large N limit of the axial $U(1)_A$. In the large N

[6]Here we replace the L in the original notation with R to be consistent with the former notations. The same replacement is also performed for $\Delta x \to L$ such that one can identify the L here with the one in the last section.

limit, $U(1)_A$ is not anomalous. The D7-brane DBI action is

$$S_{D_7} = -\mu_7 \int d^8\xi \epsilon_3 e^{\phi} \mathcal{G}(\rho, w_5, w_6) \left[1 + g^{ab} g_{55} \partial_a w_5 \partial_b w_5 + g^{ab} g_{66} \partial_a w_6 \partial_b w_6\right]^{1/2}, \tag{3.4.10}$$

where μ_7 is the D7-brane tension, ϵ_3 is the determinant factor of S^3, and the determinant of the metric is

$$\mathcal{G}(\rho, w_5, w_6) = \rho^3 \frac{\left((\rho^2 + w_5^2 + w_6^2)^2 + b^4\right)\left((\rho^2 + w_5^2 + w_6^2)^2 - b^4\right)}{(\rho^2 + w_5^2 + w_6^2)^4}. \tag{3.4.11}$$

The ground state is set to $w_6 = w_6(\rho)$ and $w_5 = 0$, and $w_6(\rho)$ satisfies

$$\frac{d}{d\rho}\left[\frac{e^{\phi}\mathcal{G}(\rho, w_6)}{\sqrt{1 + (\partial_\rho w_6)^2}}(\partial_\rho w_6)\right] - \sqrt{1 + (\partial_\rho w_6)^2}\frac{d}{dw_6}\left[e^{\phi}\mathcal{G}(\rho, w_6)\right] = 0. \tag{3.4.12}$$

Looking for a solution where w_6 asymptotes to

$$w_6 \sim m + \frac{c}{\rho^2}. \tag{3.4.13}$$

Rotate $w_{5,6}$ such that the kinetic terms are canonically normalized. This allows one to get the mass dimension of the dual operators. One finds that m has dimension 1, corresponds to the quark (fermion) mass. c has dimension 3, corresponds to the vev $\langle\bar{\psi}\psi\rangle$ of fermion bilinear.

The Constable-Myers background contains a naked singularity, for $m = 0$ there is an exact solution that goes into the singularity. Since this is not in the valid range of the background, this solution is not trustworthy. However, there is a second solution when $m = 0$ with $c = 1.85$, see fig. 3.2(b). The solution lies distance away from the singularity, which shows that the chiral symmetry is broken for all values of m. One subtlety is choosing the correction solution. Given that the radial direction corresponds to the energy scale, the solutions that intersect the semicircle in the $\rho - w_6$ plane with the constant radial distance cannot be interpreted as an RG-flow, therefore only the "good" solution in fig. 3.2(a) is accepted.

If the chiral symmetry is broken, there must be Goldstone bosons associated with the broken symmetry. Here the broken symmetry is $U(1)_R$, therefore one GB is expected. This is achieved by rotating the two transverse directions w_5, w_6 with $\exp(i\epsilon)$ into the basis where the new fluctuations in these two directions correspond to a radial fluctuation w_6 and a phase $w_5 = \epsilon\frac{c}{\rho^2}\sin(k \cdot x)$, with k the four-momentum. Solving their eoms to get the spectrum, the mass of w_5 asymptotes to zero when $m \to 0$ and for small m it's mass scales with $\sqrt{m}$ as expected in QCD. This is the Goldstone boson. The other state w_6, its mass is larger than the m_{w_5}. It

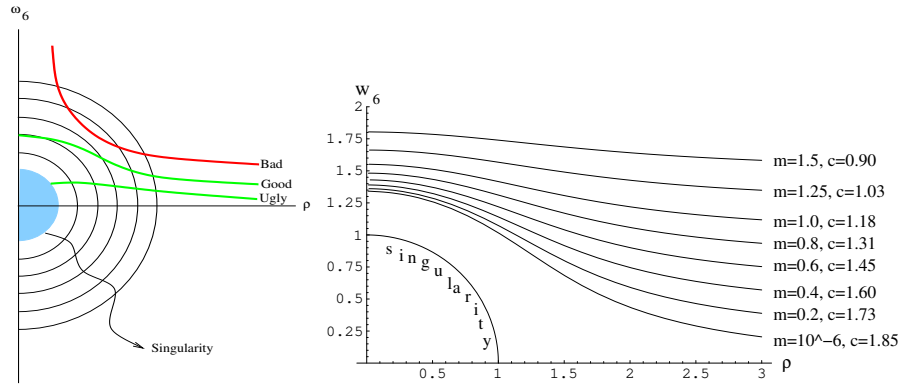

(a) a (b) b

Figure 3.2: Left: three types of solutions. The "bad" solution intersects the semicircle twice thus cannot be an RG-flow. The "ugly" solution goes into the singularity where the supergravity approximation is no more valid. Therefore only the "good" solution is accepted. Right: solutions with varying "quark" mass m, the vev c is read off from the UV asymptotics . There is a non-vanishing vev c when $m = 0$ which demonstrates chiral symmetry breaking for all cases. The solutions are repelled from the singularity due to the chiral symmetry breaking. Both plots are taken from [25].

corresponds to the fluctuation in the radial direction, like a σ meson in QCD.

3.4.2 Turn on a Magnetic Field

Another possibility to introduce chiral symmetry breaking is by turning on a magnetic field, based on a D3/D7 setup [27]. The D3-stack gives rise to the $AdS_5 \times S^5$ geometry with the metric

$$ds^2 = \frac{\rho^2 + L^2}{R^2} dx_\mu dx^\mu + \frac{R^2}{\rho^2 + L^2} \left(d\rho^2 + \rho^2 d\Omega_3^2 + dL^2 + L^2 d\phi^2 \right), \tag{3.4.14}$$

where $\mu = 0, ..., 3$, $d\Omega_3^2$ is the S^3 metric, L and ϕ are the polar coordinates in the transverse $\mathbb{R}^2$ (8,9 directions). The D7-brane is embedded at

$$\phi = \text{const}, \quad L = L(\rho). \tag{3.4.15}$$

Now introduce a magnetic field along some directions of the D3-brane's world volume

$$B^{(2)} = H dx_2 \wedge dx_3. \tag{3.4.16}$$

This will introduce a Chern-Simons term to the D7's DBI action

$$S = -\mu_7 \int d^8\xi e^{-\Phi} \left[-\det(G_{ab} + B_{ab} + 2\pi\alpha' F_{ab}) \right]^{1/2} + 2\pi\alpha' \mu_7 \int F_{(2)} \wedge C_{(6)}, \tag{3.4.17}$$

with μ_7 the D7 brane tension. $a, b = (0, ..., 7)$ are the Lorentz indices on the D7 world volume, G_{ab} is the induced metric and B_{ab} is the induced magnetic field, F_{ab} is the world volume gauge field. To the first order in α', the equations of motion set a constraint for the six-form $C_{(6)}$. The valid ansatz for $C_{(6)}$ is found to be

$$dC_{(6)\,L01\rho\psi\alpha\beta} = \frac{\mu_7\kappa_0^2}{\pi} H \frac{\rho^3 R^4}{L(\rho^2+L^2)^2}\Theta(L - L_0(\rho)) \sin\psi\cos\psi, \tag{3.4.18}$$

where $\kappa_0^2 = 2\pi/\mu_7$ and $0, 1, 2, 3, \rho, \psi, \beta, \gamma$ are the D7 world-volume indices. This contribution breaks the supersymmetry of the probe D7-brane in this model. Since the probe doesn't back-react on the D3, one has essentially a SUSY conserved supergravity background plus a SUSY broken probe theory.

The D7-brane embedding $L_0(\rho)$ is solved from the equation of motion

$$\partial_\rho\left(\rho^3 \frac{L_0'}{\sqrt{1+L_0'^2}}\sqrt{1+\frac{R^4H^2}{(\rho^2+L_0^2)^2}}\right) + \frac{\sqrt{1+L_0'^2}}{\sqrt{1+\frac{R^4H^2}{(\rho^2+L_0^2)^2}}}\frac{2\rho^3 L_0 R^4 H^2}{(\rho^2+L_0^2)^3} = 0, \tag{3.4.19}$$

where $L_0' = \partial_\rho L_0(\rho)$. This equation asymptotes to the equation of $AdS_5\times S^5$ background in the UV in the limit of vanishing H. Thus the UV asymptotics is $L_0(\rho) = m + c/\rho^2$. For a weak magnetic field $H \ll m^2/R^2$, the vev is found to be

$$\langle\bar{\psi}\psi\rangle \propto -c = -\frac{R^4}{4m}H^2, \tag{3.4.20}$$

which shows that the condensate is a function of the magnetic field H. In general, one finds a non-vanishing vev c associated with the mass m even when $m = 0$. This shows that the chiral symmetry is indeed spontaneously broken in this construction.

3.5 AdS/QCD

The models introduced in the last sections are the top-down models, they start with the full string theory, consider the full supersymmetry. The calculations are usually complicated and the model structures are constraint by the symmetry patterns that can be realized by the D-branes. In contrast to the top-down models which starts from the string theory and approaches the QCD-like theory, the bottom-up models are developed [39] which constructs the model in the reversed direction, see also [158–161]. The model considers a single space-filling brane in the AdS space. This single brane is taken effectively as the flavor-brane with a $SU(N_f)$

flavor symmetry. The action is like a holographic version of the chiral perturbation theory, which manifests a $SU(N_f)_L \times SU(N_f)_R$ chiral symmetry. The longitudinal part of the axial vector mixes with the GB where the vector are independent of the other fields. This shows by construction that the $SU(N_f)_L \times SU(N_f)_R$ symmetry is spontaneously broken down to the $SU(N)_V$. Using the AdS/CFT correspondence the meson spectrum and decay constants can be calculated. The results are at 10-15% level comparing to the experimental values [39].

The model inserts an IR and a UV cutoff by hand, thus is called hard-wall model. It is a confining theory given that there's an IR wall that the fluctuations cannot access. It takes essentially an AdS slice, with the metric

$$ds^2 = \frac{1}{z^2}(-dz^2 + dx^\mu dx_\mu), \quad \epsilon < z \leq z_m, \quad \epsilon \to 0, \tag{3.5.1}$$

in Poincaré coordinates. The action considers only a scalar field X, and the gauge fields A_L, A_R dual to the left and right currents in the gauge theory

$$S = \int d^5x\sqrt{g}\,\mathrm{Tr}\{|DX|^2 + 3|X|^2 - \frac{1}{4g_5^2}(F_L^2 + F_R^2)\}, \tag{3.5.2}$$

where g is the determinant of the metric, g_5 is the 5D gauge coupling and $F_{L/R}$ are the field strength tensors. $DX = D^M X = \partial^M X - iA_L^M X + iXA_R^M$ is the covariant derivative. The model manifests a global chiral symmetry $SU(N_f) \times SU(N_f)$ breaking down to $SU(N_f)_V$, thus the fields are matrix valued objects. Consider different fluctuations, one obtains the 5D gravity theory equations of motions. To solve them, one seeks a plane wave solution of the form $f(z, x^\mu) = f(z)e^{ikx}$, for f a general field.

On the boundary, one identifies the generating functionals of the dual theories. The f_0 is the value on the boundary which is sourced by the 5D SUGRA field $f(z, x^\mu)$. Using the relation eqs. (3.2.15) and (3.2.16), one can differentiate the generating functional (obtained by evaluating the action on the solution of each field) with respect to the boundary field twice, to get the corresponding correlator. For example the action, when evaluated on the solution of the vector fluctuation is a boundary term

$$S = -\frac{1}{2g_5^2}\int d^4x \left(\frac{1}{z}V_\mu^a \partial_z V^{\mu a}\right)_{z=\epsilon}. \tag{3.5.3}$$

Differentiating twice with respect to the solution on the boundary, one gets the vector-vector

correlator

$$\Pi_V(-q^2) = -\frac{1}{g_5^2 Q^2}\frac{\partial_z V(q,z)}{z}\Big|_{z=\epsilon}, \tag{3.5.4}$$

where $Q^2 = -q^2$, $V(q,z)$ is the piece in the vector solution that contains the dependence of the 5th dimension. For large Euclidean momentum Q^2, this function has the expansion $V(Q,z) = 1 + \frac{Q^2 z^2}{4}\ln(Q^2 z^2)$. To match the coupling strength of the dual theories, one matches the vector-vector correlator obtained from the gravitational side with the one that is calculated using perturbation theory on the field theory side, i.e.

$$\Pi_V(Q^2)|_{AdS} = -\frac{1}{2g_5^2}\ln Q^2 \equiv \Pi_V(Q^2)|_{QFT} = -\frac{N_c}{24\pi^2}\ln Q^2. \tag{3.5.5}$$

N_c is the number of colors. This gives the 5D gauge coupling

$$g_5^2 = \frac{12\pi^2}{N_c}. \tag{3.5.6}$$

From this expression we see that this coupling is fixed by the number of the colors.

Once the correlator is calculated, one can compute the decay constants of the mesons. This is given by[7]

$$F_\rho^2 = \frac{1}{g_5^2}[\psi_\rho'(\epsilon)/\epsilon]^2 = \frac{1}{g_5^2}[\psi_\rho''(0)]^2, \tag{3.5.7}$$

where $\psi_\rho(z)$ is the solution of the vector equation of motion. F_ρ is the decay constant of the ρ meson in this model.

This model has initially four free parameters: g_5, m_q, the vev of the quark bilinear σ and the IR cutoff z_m. Matching the vector-vector correlator from the gravitational side to the gauge theory one kills g_5, leaving only three free parameters. Matching the ρ meson mass fixes z_m. The π decay constant and the pion mass m_π are matched to give m_q and σ. In the end, with such a simple setup incorporating an extra dimension, this model is able to get a prediction on the other physical quantities at 10-15% level.

However the hard-wall models have some drawbacks, the obvious one is that the confinement is implemented by hand instead of generated dynamically. This justifies the name of the **hard-wall model**. However, the (IR) scales can be generated dynamically. This type of models are called the **soft-wall model**, see [162, 163]. In the next section, we will review a model along this line, where one can see that the vacuum solution has a lower bound that is generated dynamically.

[7] For derivations see the original paper [39].

3.6 AdS/YM

In this work we focus on the bottom-up model from [53], earlier constructions see [164, 165] and [166–171]. Based on the model from [39], this model considers the dual theory to be a general Yang-Mills theory. The warp factor that is usually adopted in the soft-wall models to deform the geometry in this case originates from the top-down D3/D7 model. Thus the confinement is generated dynamically, whose origin can be traced back to the top-down construction.

The gravitational side of this model lives in the AdS_5 spacetime

$$ds^2 = r^2 dx_\mu dx^\mu + \frac{d\rho^2}{r^2}, \tag{3.6.1}$$

where r is the holographic radial direction. It's relation with the ρ is defined to be $r^2 = L^2 + \rho^2$, where L (or later L_0) in the top-down model sets the position of the D7 brane in the transverse directions. It corresponds to the vacuum configuration in this case.

The action is

$$S_{\text{boson}} = \int d\rho\, d^4x\, \rho^3 \text{Tr}\left\{ \frac{1}{r^2} \left(D^M X\right)^\dagger D_M X + \frac{\Delta m^2}{\rho^2}|X|^2 + \frac{1}{2g_5^2}\left(F_L^2 + F_R^2\right)\right\}, \tag{3.6.2}$$

where $X = L(\rho)e^{i\pi}$ is the scalar fluctuation matrix, $L(\rho)$ is the vacuum. $D_M X = \partial_M X - iA_L X + iXA_R$ is the covariant derivative, with the Lorentz index $M = t, x, y, z, \rho$. The field strength tensors F_L and F_R represent the gauge symmetry $SU(N_f)_L \times SU(N_f)_R$ mimicked by the single D-brane. In the actual calculations, the field X and A_M are matrices in the flavor space like in the chiral perturbation theory, i.e. if A_L realizes gauge fields of an $SU(N)$ symmetry, then one needs to write $A_L = A_L^i \tau^i$, with τ^i the $SU(N)$ generators. But the flavors are degenerated here, making the outcome essentially a degenerate abelian theory. The gauge fields for the left and right symmetries are normalized to be

$$A_L = \frac{1}{2}(V + A), \quad A_R = \frac{1}{2}(V - A). \tag{3.6.3}$$

In this way, the gauge symmetry in the bulk is actually the flavor symmetry of the theory. The gauge bosons, which are dual to vector bound states in the dual field theory, are dynamical fields in this model. This is a feature of the hidden local symmetry, and is a common feature shared by the AdS/QCD models [33, 39, 172]. Notice two differences comparing to the original AdS/QCD model. One is that this model has ρ^3 as $\sqrt{-g}$, this comes from the top-down model.

This insures the correct UV behaviour for the vacuum. The other one, which is also the main difference, is the term $\Delta m^2(\rho)$. This term acts like the scalar mass term in a chiral Lagrangian, but in this model it introduces the running of the holographic RG flow[8]. To see how this works, we start with the vacuum L. Turning off all the fields in the action, and apply the Euler-Lagrange equation, one finds the eom of the vacuum is[9]

$$\partial_\rho \left(\rho^3 \partial_\rho L(\rho)\right) - \Delta m^2 L(\rho) = 0. \tag{3.6.4}$$

When setting $\Delta m^2 = 0$, the vacuum has a usual solution of the form

$$L(\rho) \to m + \frac{c}{\rho^2}. \tag{3.6.5}$$

If turn on $\Delta m^2 \neq 0$, then the asymptotic behavior changes to

$$L(\rho) \to m\rho^\gamma + \frac{\langle \mathcal{O} \rangle}{\rho^\gamma}, \tag{3.6.6}$$

where the relation between Δm^2 and γ is

$$\Delta m^2 = \gamma(\gamma - 2). \tag{3.6.7}$$

Related to the scaling dimension of the operator, γ is the anomalous dimension of the quark mass. In QCD this is a running parameter, and in holographic model we introduce the running of the gauge theory through this relation which reproduces the effect of a running dilaton in the top-down model. The two-loop result of running coupling for multi-representational matter is adopted in this case

$$\mu \frac{d\alpha}{d\mu} = -b_o \alpha^2 - b_1 \alpha^3, \tag{3.6.8}$$

where the β-functions $b_{0,1}$ are

$$\begin{aligned} b_0 &= \frac{1}{6\pi}\left(11C_2(G) - 2\sum_R T(R)N_f(R)\right), \\ b_1 &= \frac{1}{24\pi^2}\left(34C_2^2(G) - \sum_R (10C_2(R) + 6C_2(R))T(R)N_f(R)\right). \end{aligned} \tag{3.6.9}$$

In the above equations, R is the representation of the matter field, C_2 is the quadratic Casimir,

[8]The introduction of Δm^2 and the running of strong coupling isn't trivial. There are several discussions needed before arriving at this construction. What we introduced in the following is the final recipe to implement the gauge dynamics. To not digress too much in the main text, we summarize the background ideas in appendix B.

[9]In the following we omit the ρ dependence of Δm^2. As can be seen later, it depends logarithmically on r.

G is the adjoint representation, N_f is the number of Weyl fermion flavors, $d(R)$ is the dimension of quark's representation. For the running of the anomalous dimension γ, the 1-loop result is used

$$\gamma = \frac{3C_2(R)}{2\pi}\alpha. \tag{3.6.10}$$

Since this is a scalar theory defined on the AdS spacetime, there exists a BF bound at $\Delta m^2 = -1$ [164]. Given the relation eq. (3.6.6), one can expand it for γ small

$$\Delta m^2 = -2\gamma. \tag{3.6.11}$$

This means, if γ runs below the value $\frac{1}{2}$, then the BF bound of the scalar fields is violated and the scalars' potential develops an instability. The term Δm^2 represents the effects of a dilaton induced by the deformation of the geometry [165]. Together with the ρ^3 factor from the top-down $\sqrt{-g}$, they function in the same way as the warp factor in the soft-wall AdS/QCD models. But in this model they have a proper origin from the top-down. Note that Δm^2 must depend on r instead of ρ, i.e. it must be a function of L to pass from the chiral symmetry broken phase below the BF bound to the stable phase above the BF bound [165].

To study the dynamics of the fluctuations, we turn on them separately. To get the scalar fluctuation, let $X = L_0(\rho) + S$ for $S(\rho)$ being the scalar fluctuation. Expanding the scalar potential to $\frac{\partial \Delta m^2}{\partial L}$, the eom for scalar is found to be

$$\left(\partial_\rho\left(\rho^3\partial_\rho\right) - \rho\Delta m^2 - \rho\frac{\partial \Delta m^2}{\partial L}|_{L_0} + \frac{M_s^2\rho^3}{r^4}\right)S(\rho) = 0. \tag{3.6.12}$$

The vectors V^i, where i is the component index, are

$$\left(\partial_\rho\left(\rho^3\partial_\rho\right) + \frac{M_V^2\rho^3}{r^4}\right)V(\rho) = 0. \tag{3.6.13}$$

To compute the NGBs and the axial-vector $A^{i,\mu}$, set the scalar fluctuation matrix to $X = L_0(\rho)e^{i\pi}$, with $\pi = \pi^i\tau^i$ the Goldstone matrix and τ^i, $i = 0, 1, .., 3$ are the identity matrix ($i = 0$) and the three Pauli matrices. Writing the axial-vector in transverse and longitudinal

parts $A^\mu = A_\perp^{i,\mu} + \partial^\mu \phi^i$, from the eom of A^μ one gets

$$\begin{aligned}\left(\partial_\rho\left(\rho^3\partial_\rho\right) - g_5^2\frac{\rho^3 L_0^2}{r^4} + \frac{M_A^2\rho^3}{r^4}\right)A^\mu(\rho) = 0\\ \partial_\rho\left(\rho^3\partial_\rho\phi\right) - g_5^2\frac{\rho^3 L_0^2}{r^4}(\pi-\phi) = 0\\ q^2\partial_\rho\phi - g_5^2 L_0^2\partial_\rho\pi = 0.\end{aligned} \tag{3.6.14}$$

The last two equations give rise to the eom for GBs

$$\partial_\rho\left(\rho^2 L_0^2\partial_\rho\pi\right) + \frac{M_\pi^2\rho^3 L_0^2}{r^4}(\pi-\phi) = 0. \tag{3.6.15}$$

This is consistent with the GB eom derived directly from the Lagrangian using the Euler-Lagrange equation.

These equations have non-trivial factors depend on ρ, they can be solved only numerically. One way to solve them is to use the shooting method. The dynamics of the fields are constraint by the boundary conditions. Take the scalar field S as an example, in the IR the regularity condition is imposed, i.e. the first derivative of the field should vanish

$$\text{IR boundary condition 1: } \partial_\rho S(\rho)|_{\text{IR}} = 0. \tag{3.6.16}$$

In the UV, the fluctuations corresponds to the normalisable modes, which asymptote to 0 rapidly, the fluctuation should thus vanish in the UV

$$\text{UV boundary condition: } S(\rho)|_{\rho\to\infty} = 0. \tag{3.6.17}$$

These two conditions forms a boundary value problem. Using the shooting method, one adds and extra IR condition

$$\text{IR boundary condition 2: } S(\rho)|_{\text{IR}} = 1. \tag{3.6.18}$$

This extra boundary condition turns the boundary value problem to an initial value problem associated with each shooting parameter M, i.e the field's mass in the eoms. Since the solution of the initial value problem is always unique, in this way one finds a unique solution associated with the mass M. Applying these boundary conditions, the eoms of the fluctuations can be solved numerically.

The meson decay constant $f_{\pi,V,A}$ are calculated in the similar way as explained in the last section. In the holographic model, the external source is the non-normalizable term in the UV

[53]. In the UV, the $L_0(\rho) \sim 0$ comparing to ρ_{UV}, the function that introduces the running also tends to 0: $\Delta m^2(\rho) \to 0$. So for the V, A and S fluctuations, they have essentially the same asymptotics in the UV

$$\partial_\rho \left(\rho^3 \partial_\rho K\right) - \frac{q^2}{\rho} K = 0. \tag{3.6.19}$$

This equation has the solution [39, 52]

$$K_i = N_i \left(1 + \frac{q^2}{4\rho^2} \ln\left(\frac{q^2}{\rho^2}\right)\right), \; i = V, A, S, \tag{3.6.20}$$

where N_i are the normalization constants to be fixed by matching to the UV gauge theory [39, 165]

$$N_V^2 = N_A^2 = \frac{g_5^2 d(R) N_f(R)}{48\pi^2}, \quad N_S^2 = \frac{d(R) N_f(R)}{48\pi^2}. \tag{3.6.21}$$

The vector decay constant is computed by evaluating the vector-vector correlator Π_{VV}

$$F_V^2 = \int d\rho \frac{1}{g_5^2} \partial_\rho (-\rho^3 \partial_\rho V) K_V(q^2 = 0), \tag{3.6.22}$$

where V is the solution of the vector field. The F_S and F_A are calculated similarly. The pion decay constant is computed from the Π_{AA}

$$f_\pi^2 = \int d\rho \frac{1}{g_5^2} \partial_\rho \left(\rho^3 \partial_\rho K_A(q^2 = 0)\right) K_A(q^2 = 0). \tag{3.6.23}$$

3.7 Double Trace Interaction

By far, the AdS/CFT correspondence covers only the case where the dual theory is of order $\sim \mathrm{Tr} W(\mathcal{O})$, where $\mathcal{O}$ is a function of a single field and its derivatives. Since it involves just a single trace term, the operator $\mathcal{O}$ is called the **single-trace operator**. It is useful in the matter free gauge theories. However, to incorporate a potential for the matter field, a **multi-trace operator** which is nonlinear in $\mathcal{O}$ is needed. Especially in constructing a dynamic holographic composite Higgs model that is relevant to the research in this thesis. As we will see later in section 5.5, the double trace interaction is needed to introduce the EW symmetry breaking on the boundary.

3.7.1 Witten's Double Trace Prescription

The prescription to incorporate the double trace interaction into the AdS/CFT correspondence is work out by Witten in [173]. The method is effectively very simple. One just needs to modify the condition on the AdS boundary according to the double trace interaction term. To see this, consider an action of a scalar field ϕ from a $U(N)$ gauge theory

$$I = \frac{1}{2}\int_{r\geq 0} d^{d+1}x|d\phi|^2 + \int_{r=0} d^d x\, W(\phi, d\phi, ...), \tag{3.7.1}$$

that lives in the AdS_{d+1} spacetime in the Poincaré coordinates

$$ds^2 = \frac{1}{r^2}\left(dr^2 + dx_\mu dx^\mu\right), \quad \mu = 0, ..., d, \quad r \geq 0. \tag{3.7.2}$$

$r = 0$ is the AdS boundary. Then a free scalar ϕ with mass m in the bulk has a solution in the UV that behaves like

$$\phi_{\mathrm{UV}} \to \mathcal{J} r^{d-\Delta} + \langle\phi_0\rangle r^{\Delta}, \tag{3.7.3}$$

where ϕ_0 the boundary value of ϕ, and $\mathcal{J}$ is the source for the dual operator $\mathcal{O}$ of ϕ, Δ is the dimension of the operator $\mathcal{O}$. If we now add a boundary perturbation $N^2 W$ to the Lagrangian, then the variation of the action with respect to ϕ indicates a boundary condition for ϕ

$$\int_{r=0} d^d x \delta\phi \left(\frac{\delta W}{\delta\phi} - \frac{\partial\phi}{\partial r}\right) = 0 \to \frac{\delta W}{\delta\phi} - \frac{\partial\phi}{\partial r} = 0. \tag{3.7.4}$$

Let W first be a single trace interaction on the boundary

$$W = \int d^d x f(x)\mathcal{O}. \tag{3.7.5}$$

In terms of the AdS/CFT correspondence, this boundary condition is equivalent to

$$\mathcal{J} = f(x) = \frac{\delta W}{\delta\langle\phi_0\rangle}, \tag{3.7.6}$$

i.e. the source term is replaced with the derivative of the single trace interaction with respect to the vev of the boundary field. The upshot is, when perturbing the dual field theory with an interaction term $N^2 W$ on the AdS boundary, to calculate physical quantities in the bulk using the AdS/CFT correspondence, the boundary condition eq. (3.7.6) should be applied.

If now W is a multi trace interaction term on the boundary, i.e. it contains nonlinear terms of

the operator, then one simply replace the boundary condition with

$$\mathcal{J}_i = \frac{\delta W(x, \langle\phi_j\rangle, \phi_j)}{\delta\langle\phi_i\rangle}. \tag{3.7.7}$$

3.7.2 NJL

Aside from the standard Higgs mechanism, the Nambu-Jona-Lasino (NJL) model [174, 175] provides another mechanism to reproduce the chiral symmetry breaking. Inspired from the BCS (Bardeen-Cooper-Schrieffer) theory, the NJL model attempts to explain the condensation of quarks in a similar manner (the pions are explained to be a nucleon-antinucleon state). The original model is a toy model, which contains only a kinetic term and a four-fermion interaction term that respects a chiral symmetry at the Lagrangian level

$$\mathcal{L} = -\bar{\psi}\gamma^\mu\partial_\mu\psi + g_0\left[(\bar{\psi}\psi)^2 - (\bar{\psi}\gamma_5\psi)^2\right]. \tag{3.7.8}$$

Then a Coleman-Weinberg potential as a function of the fermion mass m at one-loop breaks the chiral symmetry. The observed fermion (nucleon) mass m, thus the bound states' mass, becomes a function of the bare coupling constant g_0 (NJL coupling), and it grows beyond 0 after the coupling $g_0\Lambda^2$ crosses the critical value 2π

$$\frac{2\pi^2}{g_0\Lambda^2} = 1 - \frac{m}{\Lambda^2}\ln(\frac{\Lambda^2}{m^2} + 1). \tag{3.7.9}$$

Here Λ is the UV cutoff. The typical profile one would expect is that the mass starts to grow drastically after the coupling passes the critical value.

3.7.3 Holographic NJL Interactions

In holographic models, adding an NJL term at the boundary could enhance the chiral symmetry breaking, if such a breaking is already triggered in the theory [176, 177]. Also, it will introduce extra explicit breaking sources into the theory. This is especially useful for incorporating the EW symmetry breaking when constructing holographic composite Higgs models. In the following we will review how the NJL interaction is embedd in the holographic model, restricted to the D3/D7 inspired bottom-up model.

To implement the NJL interaction into holographic bottom-up models originated from the D3/D7 type of models, we follow closely the results in [176, 177]. These results are what we

will use and extend in the later research part.

What we want to achieve is to add a four-fermion interaction term to the boundary field theory, such that the vev in the boundary asymptotics of L

$$L \to m + \frac{c}{\rho^2} \tag{3.7.10}$$

is the vev $c = \langle \bar{q}_L q_R \rangle$. L is the vacuum of the bulk scalar field. This can be done using Witten's prescription by adding an interaction term at the boundary

$$\Delta\mathcal{S} = \frac{g^2}{\Lambda_{UV}^2}(\langle \bar{q}_L q_R \rangle)^2 = \frac{m^2\Lambda_{UV}^2}{g^2}, \tag{3.7.11}$$

where we identified $m = \frac{g^2}{\Lambda_{UV}^2}\langle \bar{q}_L q_R \rangle$ in the last step. g is the NJL coupling, and Λ_{UV} is the cut-off. Adding this term to the Lagrangian of the dual field theory, variation principle requires [177]

$$\delta S = 0 = -\int d\rho(\partial_\rho \frac{\partial\mathcal{L}}{\partial L'} - \frac{\partial\mathcal{L}}{\partial L}) + \frac{\partial\mathcal{L}}{\partial L'}\delta L\Big|_{UV,IR}. \tag{3.7.12}$$

L is allowed to change, so $\delta L \neq 0$. Then this in turn requires that on the boundary

$$\frac{\partial\mathcal{L}}{\partial L'} + \frac{2L\Lambda^2}{g^2} = 0. \tag{3.7.13}$$

Knowing that $L \to m + \frac{c}{\rho^2}$ in the UV, here UV is the cutoff scale Λ_{UV}, the above condition is translated to

$$m \approx \frac{g^2}{\Lambda^2}c. \tag{3.7.14}$$

This is the relation that we want to see in the holographic model in the first place.

Depending on the strength of the coupling, the model experiences a second order phase transition. For $g < g_c$, the minimum lies at $m = 0$, so no symmetry is broken. For $g > g_c$, the minimum is lifted from $m = 0$ which indicates a symmetry breaking.

However, adding an NJL contribution to a holographic theory doesn't guarantee a chiral symmetry breaking (or generally a symmetry breaking) as always. The holographic model must have a chiral symmetry breaking triggered already. As is pointed out in [176, 177], if the holographic model respects SUSY, then adding the NJL contribution won't change the mass m that minimize the potential. Only when the SUSY is broken where a chiral symmetry breaking is manifest does the NJL contribution lift the mass that minimizes the potential above of 0. So the upshot is, the NJL interaction in the holographic model can only enhance but not trigger a

symmetry breaking. For that purpose, one must introduce a symmetry breaking mechanism in advance.

Chapter 4

Non-Abelian AdS/QCD

In this chapter we start constructing a non-abelian AdS/YM model, based on the ingredients we reviewed in the last part. There is a non-abelian top-down model based on the D3/D7 construction in [178], where the authors consider the DBI action for N_f coincident D7-branes, and the non-abelian nature is made obvious by embedding the D7-branes at different positions in the transverse directions. Such an embedding gives rise to heavy-light bound states stretching between the D7-branes that are dual to the meson states with different quark contents. These states are also no more degenerate with the heavy-heavy and light-light states.

By introducing the non-abelian construction, we are able to explain the measured QCD meson spectrum in more details according to the flavor structure of the quark contents. This property is also important in composite Higgs model building to realize different symmetry breaking patterns.

In the following, we will review first the non-abelian D3/D7 top-down model in [178] in section 4.1. We then adopt the essential elements from this model to extend the dynamical AdS/YM model we reviewed in section 3.6 to incorporate the non-abelian gauge structure in the bulk (flavor structure in the dual field theory). This is done in section 4.2, where we also develop the numerical tools that will be used through out our calculations. In section 4.3 we use the non-abelian dynamical AdS/YM model to let it dual to a two flavor QCD on the boundary. We show two spectra, one with degenerate flavors ($m_u = m_d$) and the other with flavors made explicitly different ($m_u \neq m_d$). We then move on to the three flavor case, with the flavor structure $m_u = m_d \neq m_s$. In each step we compute the meson spectrum and compared it with the QCD data. Our results show a good agreement with the QCD meson spectrum. This chapter

is based on the paper we published in [1].

4.1 A Non-Abelian D3/D7 Top-Down Model

The top-down model reviewed in section 3.3 considers essentially only one D7-brane. To realize a non-abelian gauge symmetry, it's intuitive to include more D7 flavor branes. Such a model is constructed in [178], where it describes N_f flavors of $\mathcal{N}=2$ supersymmetric quark hypermultiplet interacting with the gauge sector of the $\mathcal{N}=4$ SYM. The global symmetry of the dual field theory is $U(N_f)\times U(1)_A$. We review in this section the essential elements for constructing the corresponding bottom-up model.

The non-abelian DBI-action for N_f coincident Dp-branes is proposed in [179]

$$S_{N_f}=-\tau_p\int d^{p+1}\xi e^{-\phi}\mathrm{STr}\left(\sqrt{-\det(P[G_{rs}+G_{ra}(Q^{-1}-\delta)^{ab}G_{sb}]+T^{-1}F_{rs})}\sqrt{\det Q^a{}_b}\right), \tag{4.1.1}$$

with

$$Q^a{}_b=\delta^a{}_b+iT[X^a,X^c]G_{cb}, \tag{4.1.2}$$

$T^{-1}=2\pi\alpha'$, τ_p is the D$_p$-brane tension. X^a are the directions transverse to the Dp-branes, for $p=7$, $a,c=8,9$. $P[a_{rs}]$ is the pull-back of a 10D tensor a_{mn} to the world-volume of the branes. When including the fluctuations and taking the diagonal embeddings, $[X^a,X^b]$ is small. Using eq. (4.1.2), the pull-back in eq. (4.1.1) is then approximated as

$$P[G_{rs}+G_{ra}(Q^{-1}-\delta)^{ab}G_{sb}]\approx G_{rs}+D_rX^aD_sX^b(G^{ab}-iT[X^c,X^d]G_{ac}G_{bd}), \tag{4.1.3}$$

where

$$D_rX^a=\partial_rX^a+i[A_r,X^a], \tag{4.1.4}$$

is the covariant derivative, A_r are the non-abelian bulk gauge fields. Expanding the action in $[X^a,X^b]$ and keeping to $\mathcal{O}(X^4)$, the N_f probe Dp-branes' action eq. (4.1.1) is approximated by

$$S_{N_f}=\tau_p\int d^{p+1}\xi e^{-\Phi}\mathrm{STr}\left\{\sqrt{-\det(G_{rs}+G_{ab}D_rX^aD_sX^b+T^{-1}F_{rs})}\times\left(1-\frac{1}{4}\left(TG_{ac}[X^c,X^b]\right)^2\right)\right\}. \tag{4.1.5}$$

In the following we consider D7-probe. It is embedded in the 10D background [180, 181]

$$ds_{10}^2 = e^{\Phi/2}\left(\frac{r^2}{R^2}A^2(r)\eta_{\mu\nu}dx^\mu dx^\nu + \frac{R^2}{r^2}dr^2 + R^2 d\Omega_5^2\right), \tag{4.1.6}$$

where $\Phi(r)$ is the dilaton field and $A(r)$ is a function that takes different values for non- and SUSY cases. The induced metric on the D7 world-volume is

$$ds_8^2 = e^{\Phi/2}\left\{\frac{r^2}{R^2}A^2\eta_{\mu\nu}dx^\mu dx^\nu + \frac{R^2}{r^2}\left((1+(\partial_\rho w)^2)d\rho^2 + \rho^2 d\Omega_3^2\right)\right\}. \tag{4.1.7}$$

For D7-branes, the scalar fluctuations are generated in X^8 and X^9, i.e. the two transverse directions. In the abelian case, they represent the positions of the D7-brane in these two directions. When promoted to the non-abelian case, they have the same geometrical meaning only when the matrices are diagonal. The diagonal ansatz is taken to simplify the computation, where one takes the metric and coordinates to be diagonal matrices

$$X^a = \mathrm{diag}(L_1^a, \dots L_{N_f}^a). \tag{4.1.8}$$

The contents inside the STr in action eq. (4.1.1) are thus extended to $N_f \times N_f$ matrices. There is an ambiguity in defining the order of the matrices. The remedy is to surround the action with a **symmetrized trace STr**, which is an average over all the permutations of fields at the same order as a field strength tensor

$$\mathrm{STr}\left[X_1X_2, ..., X_n\right] \equiv \frac{1}{n!}\left(X_1X_2...X_n + X_2X_1...X_n + \text{all permutations}\right). \tag{4.1.9}$$

The permutation acts on X_i, $D^M X_i$, $[X_i, X_j]$ and F_{MN} [179]. The convention of STr was first introduced by Tseytlin in [182], where it was shown that when expending to $\mathcal{O}(F^4)$, the non-abelian DBI action adopting the STr is consistent with the tree-level open string effective action for the non-abelian vector field. See also [183, 184].

For simplicity, we restrict ourselves in the two-flavor case, i.e. we will have essentially two D7-branes forming a D7-probe, the gauge symmetry is $U(2)$ gives rise to a $U(2)$ flavour symmetry in the dual field theory. The fields (matrices) are expressed in the basis of $U(2)$

$$\tau^0 = \frac{1}{2}\begin{pmatrix}1 & 0\\ 0 & 1\end{pmatrix}, \quad \tau^1 = \frac{1}{2}\begin{pmatrix}0 & 1\\ 1 & 0\end{pmatrix}, \quad \tau^2 = \frac{1}{2}\begin{pmatrix}0 & -i\\ i & 0\end{pmatrix}, \quad \tau^3 = \frac{1}{2}\begin{pmatrix}1 & 0\\ 0 & -1\end{pmatrix}. \tag{4.1.10}$$

Taking the diagonal ansatz for the vacuum and consider general fluctuations, the scalar fields

$X^{8,9}$ and the vector fields are written as

$$X^8 = \tau^i \phi_i^8 \equiv \phi^8, \quad X^9 = \begin{pmatrix} L_1 & 0 \\ 0 & L_2 \end{pmatrix} + \tau^i \phi_i^9, \quad A^M = A_i^M \tau^i. \tag{4.1.11}$$

Note that we don't differentiate between super-/sub-scripts in defining the basis matrices. eq. (4.1.11) is a valid ansatz since due to rotational symmetry, one can align the D7-branes along one direction. Geometrically this vacuum configuration means that the D7-probe is embedded and separated along the 9th-direction at positions L_1 and L_2. Including these fluctuations, the radial direction r becomes a matrix in flavor space

$$r^2 = \rho^2 + (X^8)^2 + (X^9)^2. \tag{4.1.12}$$

This turns the metric — which is a function of r^2 — also into a matrix

$$G_{rs} \to \begin{pmatrix} G_{rs}|_{r=r_{11}} & G_{rs}|_{r=r_{12}} \\ G_{rs}|_{r=r_{21}} & G_{rs}|_{r=r_{22}} \end{pmatrix}, \tag{4.1.13}$$

where r_{ij} denotes the corresponding matrix element of r. Taking the diagonal ansatz, the metric is essentially a diagonal matrix that is not necessarily proportional to the identity matrix.

Expanding the action in eq. (4.1.5) to $\mathcal{O}(X^2)$, we obtain the Lagrangian

$$\begin{aligned} \mathcal{L} = \rho^3 \mathrm{STr}\Bigg(e^{\phi} \Bigg[1 + \frac{1}{2} G_{\rho\rho} D^r X^{9\dagger} D_r X^9 + \frac{1}{2} G_{\rho\rho} \partial^r \phi^8 \partial_r \phi^8 + \frac{1}{4g^2} F^{ab} F_{ab} \\ + \frac{1}{8} G_{\rho\rho}^2 (L_1 - L_2)^2 [(\phi_1^8)^2 + (\phi_2^8)^2] \Bigg] \Bigg). \end{aligned} \tag{4.1.14}$$

The second line is the mass term for the ϕ_8 fluctuations, which is not present for the ϕ_9 fields.

As indicated in eq. (4.1.11), the vacuums L_1 and L_2 are taken differently, this shows that the flavor symmetry $U(2)$ is broken explicitly on the boundary. Such a breaking will cause a Higgs-mechanism happening in the vector sector, where the longitudinal part of the vector is absorbed by the scalar fields. This process happens only between the off-diagonal fields f_1 and f_2, for f being a general field. The diagonal fields (singlet and the third component of the triplet) mix into fields dual to $\bar{u}u$ and $\bar{d}d$ in the diagonal ansatz. This reflects the fact that in the large N limit, the flavor symmetry is broken down to $U(1) \times U(1)$.

There are three kinds of fluctuations in this model. The scalar fluctuations in the 9th and 8th directions are dual to scalar mesons and pseudo-scalar mesons (GBs). The vector fields V^a and

the axial-vector fields A^a are dual to the vector/axial-vector mesons in the 4D field theory. Each of them have four components, which recombines into $f_{u/d} = f_0 \pm f_3$ and $f_{12/21} = f_1 \mp i f_2$. They are dual to the light-light (f_u), heavy-heavy (f_d) and heavy-light ($f_{12/21}$, degenerated) meson excitations. For completeness, and also due to the similarity in the calculations, we derive some of the Lagrangians and the equations of motion from [178] in appendix A. The calculations in the later bottom-up model are based on this.

4.2 $N = 2$ Bottom-Up Non-Abelian Model

In this section we discuss some of essential aspects from the non-abelian top-down model that will be extended to the bottom-up. We start with the kinetic terms of the vacuum

$$\mathcal{L}_{D7} = \rho^3 \mathrm{STr}\left[\frac{1}{2} G_{\rho\rho} G^{ab} \partial_a X^\dagger \partial_b X\right]. \tag{4.2.1}$$

X is the scalar matrix that contains the vacuum and the fluctuations. It combines both the X^8 and X^9 in the previous section, and it is parameterized non-linearly as a $N_f \times N_f$ matrix

$$X = \left(L + \sum_k \xi_k(x) T_k\right) e^{i(\pi_a(x) T_a)}, \tag{4.2.2}$$

where L is the embedding matrix. T^a are the generators of the $U(N_f)$ symmetry group. ξs and πs are the $2N_f^2$ scalar and pseudo-scalar fluctuations around the vacuum. The AdS metric G_{ab} is a matrix also, due to the matrix nature of the coordinate $r^2 = \rho^2 1_{N_f} + L^2$.

In the bottom-up model, the above kinetic term manifests a chiral symmetry. Under the chiral transformation, the scalar matrix and the metric transform as

$$X \to U_L^\dagger X U_R, \qquad G \to U_L^\dagger G U_R, \tag{4.2.3}$$

where U_L and U_R are the left and right transformation matrices respectively. The symmetrized trace deals with the ambiguity of the matrices' positions, the symmetrization is applied to all possible permutations that are invariant under chiral symmetry in the action. Since now the metric is also a matrix in the flavor space, $G^\dagger_{\rho\rho} G^{ab}$ transforms as $U_R U_R^\dagger$ and $G^{ab\dagger} G_{\rho\rho}$ transforms as $U_L U_L^\dagger$. These two combinations show up in the action after bring down the indices. In computing the STr, one inserts the two products in the beginning and in the middle of the kinetic term respectively and average over these two possibilities.

In the following we take the diagonal ansatz, the vacuum matrix L is assumed to be real and diagonal: $L = \text{diag}(L_u(\rho), L_d(\rho))$. Such a configuration leads to two separated equations of motion when X =diag(L_u, L_d)

$$\partial_\rho[\rho^3 \partial_\rho L_{u/d}] = 0, \qquad L_{u/d} = m_{u/d} + \frac{c_{u/d}}{\rho^2}, \tag{4.2.4}$$

where $m_{u/d}$ are the UV quark masses and $c_{u/d}$ are the operators' vevs corresponding to the up and down quark and their condensates in the dual theory respectively.

Deriving these equations require the boundary surface term

$$S_b = \int d^4x \frac{\partial \mathcal{L}}{\partial L} \delta \mathcal{L}_{u/d} = \int d^4x \rho^3 \delta L_{u/d} \partial_\rho L_{u/d} \tag{4.2.5}$$

to vanish, which is made possible when requiring $L'_{u/d}(IR) = 0$ and $L_{u/d}(UV) = 0$.

The kinetic term eq. (4.2.1) has more symmetry than the $\mathcal{N} = 2$ SYM theory in the last section, i.e. we want to break the chiral symmetry down to the diagonal one. This is done by introducing the potential in terms of the commutator $[X^\dagger, X]$

$$V = \frac{1}{2}\text{Tr}[X^\dagger, X]^2 = \text{Tr}(X^\dagger X X^\dagger X) - \text{Tr}(X^\dagger X^\dagger X X), \tag{4.2.6}$$

where the second term breaks $SU(N_f)_L \times SU(N_f)_R$ to $U(N_f)_V \times U(1)_A$.

We need to also include the bulk gauge fields in the holographic model. The action should then contain the terms

$$\mathcal{L}_{kin} = \rho^3 \text{STr}\left[\frac{1}{2} G_{\rho\rho} G^{ab} D_a X^\dagger D_b X + \frac{1}{4g^2} G^{ab} G^{cd} F_{ac} F_{bd}\right], \tag{4.2.7}$$

with the covariant derivative

$$D_a X = \partial_a X + i[T^m, T^n] V_a^m X^n. \tag{4.2.8}$$

Note that the commutator is calculated before applying the STr.

4.2.1 Two-Flavor Example 1: Equal Real Masses

We consider first the above construction with degenerate flavors. Then the vacuum is proportional to an identity matrix and the scalar matrix X is expressed as

$$X_{ij} = m\delta_{ij} + s_{ij} + i\tilde{s}_{ij}, \tag{4.2.9}$$

where δ_{ij} is the Kronecker delta. m represents backgrounds' solution, which is essentially the UV quark mass m. The radial coordinate is also proportional to unit matrix, so is the metric matrix too, which takes the form

$$G^{\rho\rho} = G_{xx} = (\rho^2 + m^2)1_{N_f \times N_f}. \tag{4.2.10}$$

If we derive the equations of motion for the scalar and vectors, we will end up with $2N_f^2$ copies of the abelian equation

$$\partial_\rho[\rho^3 \partial_\rho S] + \frac{M^2}{(\rho^2 + m^2)^2} S = 0, \tag{4.2.11}$$

for the scalars S and N_f^2 copies of the vectors

$$\partial_\rho[\rho^3 \partial_\rho V] + \frac{M^2}{(\rho^2 + m^2)^2} V = 0. \tag{4.2.12}$$

I.e. this is just a degenerate abelian theory we have seen before.

4.2.2 Two-Flavor Example 2: Split Real Masses

We consider now the two flavor case with two embeddings separated, marked by u, d respectively. There will be two classes of fluctuations in this case. In the brane picture, one class corresponds to the open string on a single D7-brane, were it a u- or d-brane. These states will be referred to as diagonal fluctuations/states in the following, since they are the diagonal elements of the fluctuation matrix. The other ones correspond to the open string stretching between the u- and d-brane, they are referred to as the off-diagonal fluctuations.

Diagonal States

If the flavors are made non-degenerate, the eigenstates in of the diagonal component will correspond to the $\bar{u}u$ and $\bar{d}d$ states in the dual field theory, instead of being the singlet and triplet states under the $U(2)_V$. This is the case for both scalar and vector fields. For example, consider the scalar fluctuations around the vacuum $\sigma_{u,d}$. Their holographic action is

$$S_{5d} = \int d^4x d\rho\ \rho^3 \left[(\partial_\rho \sigma_u)^2 + \frac{1}{(\rho^2 + m_u^2)^2} (\partial_\mu \sigma_u)^2 + (\partial_\rho \sigma_d)^2 + \frac{1}{(\rho^2 + m_d^2)^2} (\partial_\mu \sigma_d)^2 \right]. \quad (4.2.13)$$

Their dynamics are described by the equations

$$\partial_\rho (\rho^3 \partial_\rho \sigma_{u/d}) + \rho^3 \frac{M_{u/d}^2}{(\rho^2 + m_{u/d}^2)^2} \sigma_{u/d} = 0, \quad (4.2.14)$$

where they are solved by taking the plane-wave ansatz $\sigma_i(\rho, x) = \sigma_i(\rho) e^{iq.x},\ q^2 = -M_i^2,\ i = u, d$, and requiring the fields to vanish in the UV to solve the mass $M_{u/d}^2$. If we start with another basis that is an admixture of the current basis $(\sigma, \tau) = 1/\sqrt{2}(\sigma_u \pm \sigma_d)$, i.e if we are dealing with coupled equations of motion, the action in this basis is

$$\begin{aligned} S_{5d} = \int d^4x d\rho\ & \left[\rho^3 (\partial_\rho \sigma)^2 + \frac{\rho^3}{2} \left[\frac{1}{(\rho^2 + m_u^2)^2} + \frac{1}{(\rho^2 + m_d^2)^2} \right] (\partial_x \sigma)^2 + \rho^3 (\partial_\rho \tau)^2 \right. \\ & \left. + \frac{\rho^3}{2} \left[\frac{1}{(\rho^2 + m_u^2)^2} + \frac{1}{(\rho^2 + m_d^2)^2} \right] (\partial_x \tau)^2 + \rho^3 \left[\frac{1}{(\rho^2 + m_u^2)^2} - \frac{1}{(\rho^2 + m_d^2)^2} \right] (\partial_x \sigma)(\partial_x \tau). \right. \end{aligned} \quad (4.2.15)$$

As shown in [185], for coupled equations, one should seek the solutions with the common plane-wave ansatz $e^{ikx}, k^2 = -M^2$. Using the usual Euler-Lagrange equation, we arrive at a set of coupled equations of motion in this basis

$$\partial_\rho (\rho^3 \partial_\rho \sigma) + \frac{\rho^3}{2} \left[\frac{1}{(\rho^2 + m_u^2)^2} + \frac{1}{(\rho^2 + m_d^2)^2} \right] M^2 \sigma + \frac{\rho^3}{2} \left[\frac{1}{(\rho^2 + m_u^2)^2} - \frac{1}{(\rho^2 + m_d^2)^2} \right] M^2 \tau = 0, \quad (4.2.16)$$

$$\partial_\rho (\rho^3 \partial_\rho \tau) + \frac{\rho^3}{2} \left[\frac{1}{(\rho^2 + m_u^2)^2} + \frac{1}{(\rho^2 + m_d^2)^2} \right] M^2 \tau + \frac{\rho^3}{2} \left[\frac{1}{(\rho^2 + m_u^2)^2} - \frac{1}{(\rho^2 + m_d^2)^2} \right] M^2 \sigma = 0. \quad (4.2.17)$$

We then impose the boundary conditions for mixed states

$$\sigma(IR) = 1, \quad \sigma'(IR) = 0, \quad \tau(IR) = b, \quad \tau'(IR) = 0, \quad \sigma, \tau(UV) = 0. \quad (4.2.18)$$

The IR value of one of the field, for example $\tau(IR) = b$ is a shooting parameter. By adjusting the values b and M such that both of the fields vanish in the UV simultaneously, one finds the

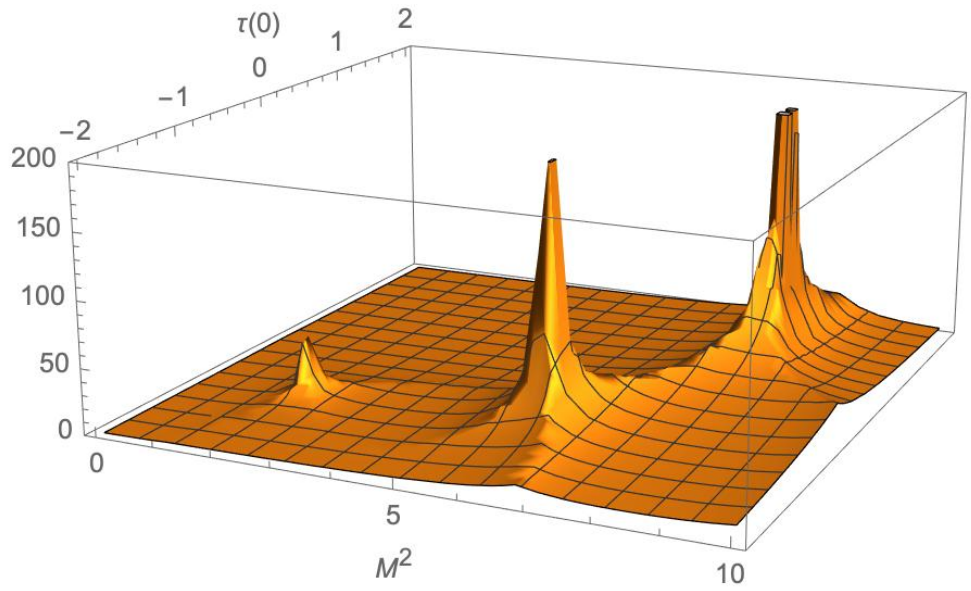

Figure 4.1: We show a numerical method to the solution of the mixed equations, eq. (4.2.16) and eq. (4.2.17). The diagonal basis is known and the solutions in each of the u and d sectors are $M^2 = 4(n+1)(n+2)m_q$. Here, with fixed $\sigma(0) = 1, \sigma'(0) = 0, \tau'(0) = 0$, we vary the mass squared and the value of $\tau(0)$. We plot the quantity $1/(|\sigma(\infty)| + |\tau(\infty)|$, which diverges when both the fields vanish asymptotically. In this case, we have set one quark mass to unity and the other 0.5 — there are clear peaks at $\tau(0) = -1$ and $M^2 = 2, 6$, which are the zeroth and first excited states of the d quark state. The peak at $\tau(0) = 1$ and $M^2 = 8$ is the ground state of the u quark.

unique solution of the set of equations. An example of the solution is shown in fig. 4.1.

The solutions correspond to $\sigma = \tau = \sigma_u$ where $M^2 = M_u^2$ and $\sigma = -\tau = \sigma_d$ where $M^2 = M_d^2$. Plug these solutions back in the action eq. (4.2.15) will return back to the action in $\sigma_{u,d}$. The above discussion is to show that when applying the correct boundary conditions, the solutions from the different bases are equivalent.

Generally for coupled equations of n fields σ_i for $i = 1, ..., n$, one should use the same plane-wave ansatz for all the fields $e^{ikx}, k^2 = -M^2$. Then set the IR boundary conditions as $\sigma_1(0) = 1$, and $\sigma_i'(0) = 0$ for all $i = 1, ..., n$. The mass M and the $n-1$ IR boundary values $\sigma_i(0) = b_i$, $i = 2, ..., n$, are the shooting parameters. Shooting from the IR using these parameters and seek the solution where all n fields vanish simultaneously in the UV will give the unique solutions.

Off-Diagonal States

The off-diagonal states are dual to the bilinear state with different quark flavors — $\bar{u}d$ and $\bar{d}u$. Since the u, d embedding are no more degenerate, the flavor symmetry is broken. This gives rise to additional Higgs mechanism that happens between the off-diagonal vectors and scalars. To illustrate this breaking, we consider for instance the real fluctuations in the following. The

potential in eq. (4.2.6) vanishes. The commutator in the covariant derivative is non-vanishing and mixes thus the scalar with the longitudinal component of the vector field. To illustrate this in detail, we consider the scalar fluctuation along the T^1 direction and the vector field A_2

$$X = \begin{pmatrix} m_u & \delta X_1 \\ \delta X_1 & m_d \end{pmatrix} \qquad \text{and} \qquad A_2 = \begin{pmatrix} 0 & -i \\ i & 0 \end{pmatrix}, \tag{4.2.19}$$

the covariant derivative is then

$$D_a X = (\partial_a \delta X_1 + (m_u - m_d) A_{2a}) \begin{pmatrix} 0 & 1 \\ 1 & 0 \end{pmatrix}. \tag{4.2.20}$$

As shown in [178], one can absorb the scalar fluctuation into the vector longitudinal component by the transformation

$$A_{2a} \to \tilde{A}_{2a} = A_{2a} - \partial_a \frac{\delta X_1}{(m_u - m_d)}. \tag{4.2.21}$$

The vector $\tilde{A}_2$ becomes massive with a mass proportional to the difference of the embeddings $(m_u - m_d)^2$. This Higgs mechanism also happens between the δX_2 and A_1. The equation of motion of the vector field will now be

$$\partial_\rho[\rho^3 \partial_\rho V_a] + \frac{M^2 - (m_u - m_d)^2}{2} \left(\frac{1}{(\rho^2 + m_u^2)^2} + \frac{1}{(\rho^2 + m_d^2)^2} \right) V_a = 0, \tag{4.2.22}$$

for $V_a = A_{1/2,a}$.

If the off-diagonal fluctuations are complex, the contribution from eq. (4.2.6) will set in. This will contribute to the mass term of the (pseudo-)scalars which is again proportional to $(m_u - m_d)^2$. The corresponding dynamics is studied numerically in [178], we will not repeat it here.

4.3 Two-Flavor Non-Abelian AdS/QCD

In the last section we have collected all the essential ingredients, in this section we combine these ingredients to construct a non-abelian bottom-up AdS/QCD model incorporating both dynamical spontaneous symmetry breaking and the explicit symmetry breaking by the UV quark masses. The symmetry breaking pattern is the global chiral symmetry $U(N_f)_L \times U(N_f)_R$ broken down to the $U(N_f)_V$ which is then broken explicitly by separating the flavor branes.

4.3.1 Kinetic Terms

The model lives in the AdS_5 spacetime

$$ds^2 = r^2 dx^2_{(1,3)} + \frac{d\rho^2}{r^2}, \tag{4.3.1}$$

where the radial direction is promoted to a $N_f \times N_f$ matrix as in the last section

$$r^2 = \rho^2 1_{N_f} + X^\dagger X. \tag{4.3.2}$$

X is the scalar matrix, that transforms under the chiral symmetry as $X \to U_L^\dagger X U_R$. This scalar field is needed to construct a QCD-like theory where it describes the chiral condensate in the dual theory. The X matrix is again a combination of the $X^{8,9}$ matrices in the top-down model. The metric becomes matrix too and transforms in the same way as the field X. The chiral symmetric action that contains the kinetic terms is

$$S = \int d^5x \ \rho^3 \mathrm{STr}\left(\frac{1}{r^2}(D^a X)^\dagger (D_a X) + \frac{1}{g_5^2}\left(F_{L,ab}F_L^{ab} + (L \leftrightarrow R)\right)\right). \tag{4.3.3}$$

The covariant derivative in this case is defined as

$$D^a X = \partial^a X - A_L^a X + i X A_R^a, \tag{4.3.4}$$

where $A_{L,R}$ are the gauge fields of the $U(N_f)_{L,R}$ respectively. The gauge fields are the bulk gauge bosons that are dual to the left and right currents associated with the chiral symmetry. The dilaton factor, that introduces the RG-flow that is essential for breaking the chiral symmetry dynamically, is later introduced by Δm^2 term in the potential. The 5D coupling is obtained by matching to the vector-vector correlator in the UV with the field theory one [39, 186], and is determined by

$$g_5^2 = \frac{24\pi^2}{d(R)\ N_f(R)}, \tag{4.3.5}$$

where $d(R)$ is the dimension of the quark's representation R, $N_f(R)$ is the number of flavors in that representation.

4.3.2 Potential

To implement the dynamical chiral symmetry breaking in the model, one must include a scalar potential that is invariant under the chrial symmetry. The simplest form is taken to be an expansion in terms of $X^\dagger X$

$$V = \mathrm{STr}\left(A + BX^\dagger X + C(X^\dagger X)^2 + ...\right), \tag{4.3.6}$$

where the coefficients are ρ dependent and are needed to insure the correct mass dimensions. As the first step, we take the coefficients to be just numbers instead of matrices. A only contributes to the vacuum solutions and is not fixed.

The coefficient of the second term B, which is the Δm^2 in the following context, acts like a scalar mass term in the potential. It represents the effects of the dilaton from the top-down model, and originates from chiral symmetry breaking considerations in the top-down model. In the top-down model, introducing an extra world-volume baryon number magnetic field $\mathcal{B}$ will break the supersymmetry and conformality [27]. Such a construction is reviewed in section 3.4.2. To the leading order in α, the Lagrangian gets effectively a dilaton factor

$$e^{-\phi} = \sqrt{1 + \frac{\mathcal{B}^2}{r^4}}. \tag{4.3.7}$$

The vacuum solution breaks the $U(1)_A$ symmetry. This is due to the fact that the dilaton is divergent in the IR. One can see this if perform the expansion of dilaton around the IR

$$e^{-\phi} = \sqrt{1 + \frac{\mathcal{B}^2}{\rho^4}}(1 - \frac{\mathcal{B}^2}{\sqrt{1 + \frac{\mathcal{B}^2}{\rho^4}}\rho^6}L^2 + \dots), \tag{4.3.8}$$

where in the IR $\rho \to 0$ this expansion is divergent.

The second term in the above expansion is a scalar mass term. The $L = 0$ solution is no more bounded if this term violates the BF-bound. In the duality, this mass is connected with the anomalous dimension γ of the quark mass. In this model, one can show that the relation is $\Delta m^2 = \gamma(\gamma - 2)$ [53]. The violation of BF-bound shows up at $\Delta m^2 = 1$ [164]. Through this relation, the dilaton effect is translated into Δm^2 running in the bottom-up model. Following the discussion in [53], taking the limit $\gamma \ll 1$, the dilaton effect is implemented through

$$\Delta m^2 = -2\gamma, \quad \gamma = \frac{3C_2(R)}{2\pi}\alpha. \tag{4.3.9}$$

For the running coupling α, the two-loop result for multi-representational matter is used[1]

$$\mu\frac{d\alpha}{d\mu} = -b_0\alpha^2 - b_1\alpha^3\,, \tag{4.3.10}$$

where the beta functions are defined as

$$\begin{aligned} b_0 &= \frac{1}{6\pi}\left(11C_2(G) - 2\sum_R T(R)N_f(R)\right)\,, \\ b_1 &= \frac{1}{24\pi^2}\left(34C_2^2(G) - \sum_R \left(10C_2(G) + 6C_2(R)\right)T(R)N_f(R)\right)\,. \end{aligned} \tag{4.3.11}$$

In the above equations, R is the representation of the Weyl fermions, $T(R)$ is the half of the Dynkin index, C_2 is the quadratic Casimir, G is the adjoint representation, N_f is the number of flavors.

The full action is now

$$S = \int d^5x\ \rho^3 \mathrm{STr}\left(\frac{1}{r^2}(D^aX)^\dagger(D_aX) + \Delta m^2 X^\dagger X + \frac{1}{g_5^2}\left(F_{L,ab}F_L^{ab} + (L\leftrightarrow R)\right)\right). \tag{4.3.12}$$

The vacuum eoms are now

$$\partial_\rho(\rho^3\partial_\rho L_i) - \rho\ \Delta m^2(\rho)L_i = 0 \quad (i = 1,\ldots,N_f)\,. \tag{4.3.13}$$

If $\Delta m^2 = 0$, then the solution asymptotes to

$$L_i(\rho) = m_i + c_i\rho^{-2}. \tag{4.3.14}$$

Including Δm^2 will alter this relation to the power law

$$L_i(\rho_{UV}) \sim m\rho^{-\gamma} + c\rho^{\gamma-2}. \tag{4.3.15}$$

The function Δm^2 should depend on $\sqrt{\rho^2 + L_i^2}$, such that the BF bound is not violated at large ρ. This means the function Δm^2 is flavor dependent, and should be included in the STr. If expand Δm^2 in terms of X, the potential eq. (4.3.6) is properly reproduced. This validates the dependence of Δm^2 on $\sqrt{\rho^2 + L_i^2}$.

In the UV, we let $L_i(\rho \to \infty) \sim m_i$, where m_i is the quark masses, which is taken as inputs.

[1]This running is exactly the one reviewed in section 3.6. We repeat it here for the convenience of the reader.

From eq. (4.3.15), the condensate c_i can also contribute, but it is suppressed by the large ρ. One can approximate this quantity by taking the first derivative

$$L_i'(UV) = -\frac{2c}{\rho^3}\Big|_{UV}. \tag{4.3.16}$$

After solving the vacuum eoms numerically with the boundary conditions in the IR and UV, one can read out this quantity and see that it is really different from zero, thus the chiral symmetry is broken. Another way to see the chiral symmetry breaking is the IR quark mass $L(\rho_{IR,i})$. As shown in [25], due to the chiral symmetry breaking, the vacuum profile is lifted away from the singularity in the $L-\rho$ plane, as shown in fig. 3.2(b). Thus the presence of the IR mass indicates the chiral symmetry is broken. This IR mass is flavor dependent. In the numerical calculations, we set the UV quark masses to be $m_u \neq m_d$ or $m_u = m_d \neq m_s$ for the split mass case. Using the shooting method we get different IR masses associated with flavors. These are later the lower bound when searching the solutions for the fluctuations. In the numerics, we set the corresponding IR boundary conditions for the fluctuations at $\rho_{IR} = max(\rho_{IR,i})$.

As for the fluctuations, the scalar fluctuation matrix is parametrized as [187]

$$X = e^{i\pi_a(x)T_a}\left(L + \sum_k \xi_k(x)T_k\right)e^{i\pi_a(x)T_a}\,. \tag{4.3.17}$$

The gauge fields are

$$A = \frac{1}{2}\left(A_L - A_R\right) \quad \text{and} \quad V = \frac{1}{2}\left(A_L + A_R\right), \tag{4.3.18}$$

where V is the vector and A is the axial-vector field in the bulk.

Taking this paramtrization decouples all the fluctuations' eoms. If use the parametrization eq. (4.2.2) as in the abelian case, we will get for example the scalar eom

$$\begin{aligned}
&\partial_\rho(\rho^3\partial_\rho\xi_k(\rho)) - \rho\xi_j\mathrm{STr}\Delta m^2(T^k)(T^j) - \rho\xi_j\mathrm{STr}X_0\tfrac{\partial\Delta m^2}{\partial L}|_{X_0}(T^k)(T^j) + M^2\xi_j\mathrm{STr}\tfrac{\rho^3}{r^4}(T^k)(T^j)\\
&+\partial_\rho\mathrm{STr}\left\{\rho^3 2i\left[\pi^j\left((\partial_\rho X_o^\dagger)T^kT^j + (\partial_\rho X_0^\dagger T^j)(T^k)\right) + \partial_\rho\pi^j(X_0T^j)(T^k)\right] + h.c\right\}\\
&+\rho^3\partial_\rho\pi^b\mathrm{STr}(i(\partial_\rho X_0)T^kT^j + h.c.) + \rho^3M^2\pi_j\mathrm{STr}(i\tfrac{1}{r^4}(X_0T^j)(T^k) + h.c.)\\
&-\rho^3M^2\phi_V^j\mathrm{STr}(i\tfrac{1}{r^4}[T^j, X_0](T^k) + h.c.) - M^2\rho^3\phi_A^j\mathrm{STr}(i\tfrac{1}{r^4}\{T^j, X_0\}(T^k) + h.c.) = 0.
\end{aligned} \tag{4.3.19}$$

For a detailed derivation, see appendix C. This is numerically heavy to solve, and the physics should not depend on the parametrization. Therefore we use eq. (4.3.17) in the following computations. Also we note that our calculations don't include the radial excitations, since to reproduce the Regge M^2 behavior, one needs to include string dynamics in the bulk for excited states. For lowest excited states, the field approximation works well.

4.3.3 The Higgs Mechanism in the Vector Sector

In the usual QCD, the Higgs mechanism for the axial-vectors are known, where the massless GBs can be absorbed into the longitudinal part of the axial-vectors. The reason for this Higgs mechanism to happen is that the axial-vector symmetry, as a gauge symmetry, is spontaneously broken. In our model, setting the quark masses to be different will break the flavor symmetry explicitly on the boundary. This corresponds to breaking the vector gauge symmetry in the bulk. In this case, one should observe a second Higgs mechanism between the vectors and the scalars in addition to the axial-vector-pion one.

To demonstrate this extra Higgs mechanism, consider a $N_f = 2$ theory with a truncated scalar potential

$$\mathcal{L} = \rho^3 \mathrm{STr}\partial_\rho X^\dagger \partial_\rho X + A(\rho)\mathrm{STr}X^\dagger X + B(\rho)\mathrm{STr}X^\dagger X X^\dagger X. \tag{4.3.20}$$

In our model, $A(\rho) = \Delta m^2$ and $B(\rho) = \frac{\partial \Delta m^2}{\partial \rho^2}$. The vacuums are the solutions of

$$\partial_\rho(\rho^3 \partial_\rho L_{u/d}) - A L_{u/d} - 2B L_{u/d}^3 = 0. \tag{4.3.21}$$

Now consider an off-diagonal scalar fluctuation

$$\delta X = \begin{pmatrix} 0 & \xi_2 \\ \xi_2 & 0 \end{pmatrix}, \tag{4.3.22}$$

with an action to the quadratic order

$$\mathcal{L} = \rho^2(\partial_\rho \xi_2)^2 + A\xi_2^2 + B(2L_u^2\xi_2^2 + 2L_u L_d \xi_2^2 + 2L_d^2 \xi_2^2). \tag{4.3.23}$$

Here we seek for the massless solutions, thus drop the space-time kinetic terms in the action (which give rise to the M^2 term) for simplicity. Then one can find that $L_u - L_d$ is a solution of the scalar eom. This is the GB mode in the bulk when $L_u \neq L_d$. This is however not the

physical states in the dual field theory since $L_u - L_d$ doesn't asymtote to 0 in the UV (the normalizable part of the solution should vanish in the UV). To obtain the correct eoms for the scalars, we include these expansions in the action.

Now we turn on the vectors in the action. Then the eoms of the off-diagonal scalar ξ_2 is

$$\begin{aligned}\partial_\rho\left(\rho^3\partial_\rho\xi_2(\rho)\right)+\frac{\rho}{2}\left[-2A-B(4L_u^2+4L_uL_d+4L_d^2)\right]\xi_2\\ +\frac{1}{2}M_{\xi_2}^2\rho^3\left(\frac{1}{r_d^4}+\frac{1}{r_u^4}\right)\Big(\xi_2(\rho)\pm(L_u-L_d)\phi_{V_{2/1}}(\rho)\Big)=0.\end{aligned}\tag{4.3.24}$$

It mixes with the longitudinal part of the vector fields. We can see this if we decompose the vector fields to $V^\mu = V_\perp^\mu + \partial^\mu\phi_V$, $\partial_\mu V_\perp^\mu = 0$, $V_\rho = 0$, where ϕ_V is the longitudinal part. From the eom of the vector field, we find

$$\begin{aligned}\partial_\rho\left(\rho^3\partial_\rho\phi_{V_{1/2}}(\rho)\right)\pm\frac{\rho^3g_5^2}{8}\left(\frac{1}{r_u^4}+\frac{1}{r_d^4}\right)(L_u-L_d)\Big(\xi_2(\rho)\mp(L_u-L_d)\phi_{V_{1/2}}(\rho)\Big)=0\\ 4M^2\partial_\rho\phi_{V_{1/2}}(\rho)\mp g_5^2(L_u-L_d)\partial_\rho\xi_2(\rho)\pm g_5^2\xi_2(\rho)\partial_\rho(L_u-L_d)=0.\end{aligned}\tag{4.3.25}$$

But eq. (4.3.25) is actually a copy of eq. (4.3.24), in the sense that by substituting the second equation into the first one in eq. (4.3.25) one gets eq. (4.3.24). This is stating nothing but the scalar field is the GB of the vector field if the vector symmetry is broken in the bulk. One can furthur show that this property extends to higher order corrections in the expansion. However, in the numerics, the Δm^2 is a running parameter, therefore it will depend on the splitting of the quark mass, thus ruin the consistency. In the following numerical calculations, we ignore the vector field mixing and use the following eom as an approximation

$$\begin{aligned}\partial_\rho\left(\rho^3\partial_\rho\xi_2(\rho)\right)+\frac{\rho}{2}\left[-\Delta m_u^2-\Delta m_d^2-L_u(\rho)\Delta m_u^{2\prime}-L_d(\rho)\Delta m_d^{2\prime}\right]\xi_{1/2}(\rho)\\ +\frac{1}{2}M_{\xi_{1/2}}^2\rho^3\left(\frac{1}{r_d^4}+\frac{1}{r_u^4}\right)\xi_2=0.\end{aligned}\tag{4.3.26}$$

This is the eom one gets if Δm^2 is inserted as flavor-dependent matrix at the level of Lagrangian.

So far we have established the basics for a non-abelian AdS/QCD model, in the following we look further into the details of two scenarios — degenerate and split UV quark masses.

4.3.4 Equal Masses

First we discuss the scenario which corresponds to two coincident D7-branes that are separated from the D3-stack by a distance L_0 in the top-down model. We set therefore $X = L_0$ and

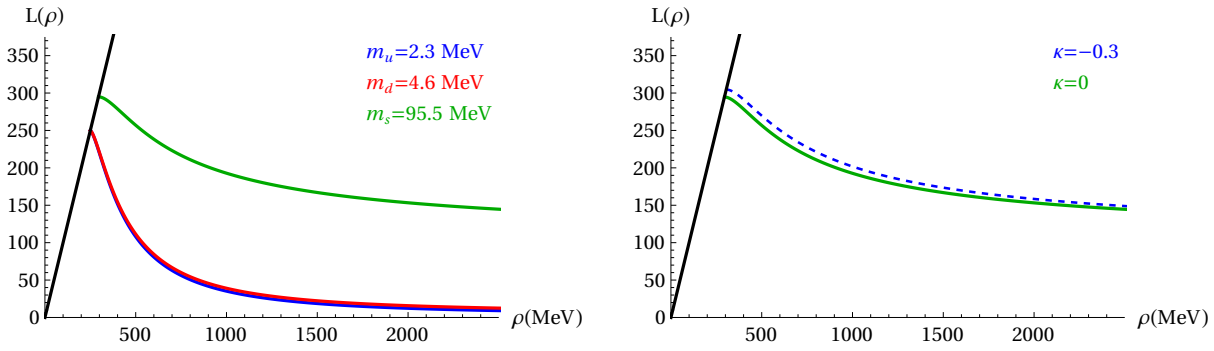

(a) Embedding vs. quark masses.

(b) Embedding with κ.

Figure 4.2: Left plot: different embeddings for various quark masses. We input the boundary quark mass values (2.3, 4.6, 95.5) MeV for L_i, $i = u, d, s$, respectively, in units where $m_\rho = 775$ MeV. The quark condensates can be calculated numerically using eq. (4.3.14) — we find ((65.7 MeV)^3, (67.3 MeV)^3, (180.2 MeV)^3) for the three flavors. Right plot: the dashed line shows the effect of a double trace term with $\kappa = -0.3$ (dashed line) compared to $\kappa = 0$ (full line).

fluctuations to be zero in the action eq. (4.3.12). One obtains the vacuum eom

$$\partial_\rho \left(\rho^3 \partial_\rho L_0\right) - \rho \Delta m^2 L_0 = 0. \tag{4.3.27}$$

Here Δm^2 includes implicitly the running through $\Delta m^2 = \Delta m^2(\log(r)) = \Delta m^2(\log(\sqrt{\rho^2 + L_0^2}))$.

To solve the vacuum eoms, we shoot from the IR using the shooting method. At IR we impose the boundary conditions that the solution should be regular, in the sense that the first derivative should be finite

$$L_0(\rho_{IR}) = \rho_{IR}, \quad \partial_\rho L_0(\rho_{IR}) = 0. \tag{4.3.28}$$

The UV boundary condition is to let the UV vacuum solution extend to the quark mass m, which is an input. After implementing these boundary conditions, the shooting parameter is the ρ-position where the solution ends in the IR. The solutions are shown in fig. 4.2(a).

To get the dynamics of the fluctuations, set

$$X = (L_0 + \sigma\tau^0 + \xi^a\tau^a)e^{2i\pi^i\tau^i} \tag{4.3.29}$$

in the action eq. (4.3.12) where $a = 1, 2, 3$ and $i = 0, ..., 3$. Since the flavor symmetry is kept in this scenario, the factors like the metrics and Δm^2 are proportional to the identity matrix, can be pulled out of the STr. Therefore the above definition of X is equivalent to the definition in eq. (4.3.17).

The singlet and triplet scalar eoms are degenerated, e.g.

$$\partial_\rho(\rho^3\partial_\rho\sigma(\rho)) - \rho\Delta m^2\sigma(\rho) - \rho L_0(\rho)\sigma(\rho)\frac{\partial\Delta m^2}{\partial L}|_{L_0} + M^2\frac{\rho^3}{r^4}\sigma(\rho) = 0. \tag{4.3.30}$$

For the vector fields, we get N_f^2 generated vector fields which share the dynamics

$$\partial_\rho(\rho^3\partial_\rho V(\rho)) + M_V^2\frac{\rho^3}{r^4}V(\rho) = 0. \tag{4.3.31}$$

Due to the spontaneous symmetry breaking of the axial symmetry, there is a Higgs mechanism combines the axial vector and the GBs, as known in [39]. The action of the axial sector is

$$S = \int d^4x d\rho \left[-\frac{\rho^3}{4g_5^2}F_A^a F_A^a + L_0^2\rho^3(\partial\pi - A^a)^2\right]. \tag{4.3.32}$$

Decomposing the axial-vectors into $A^\mu = A_\perp^\mu + \partial^\mu\phi_A$, and use the Lorentz gauge $\partial_\mu A_\perp^\mu = 0$, the axial-vector $A_\perp^\mu$ decouples from the rest. We get again N_f^2 copies of the eom

$$\partial_\rho(\rho^3\partial_\rho A(\rho)) - g_5^2\frac{\rho^3 L_0^2}{r^4}A(\rho) + \frac{\rho^3 M_A^2}{r^4}A(\rho) = 0\,. \tag{4.3.33}$$

The longitudinal parts of the axial-vectors ϕ_A mix with the GBs π which explains the Higgs mechanism

$$\partial_\rho(\rho^3 L_0^2\partial_\rho\pi^a) - \frac{L_0\rho^3 q^2}{(\rho^2 + L_0)^2}(\pi^a - \phi_A^a) = 0 \tag{4.3.34}$$

$$q^2\partial_\rho(\rho^3\partial_\rho\phi_A^a) - \frac{L_0\rho^3 q^2}{(\rho^2 + L_0)^2}(\pi^a - \phi_A^a) = 0. \tag{4.3.35}$$

These eoms are nothing but N_f^2 copies of the abelian theory. The spectrum has been studied in [53]. The N_f massless pions show a Gell-Mann-Oakes-Renner relation.

4.3.5 The 1/N Effect

Apparently, the discussion in the last section shows that, the current potential will not tell the differences between, say, the singlets and triples, which we know from both $N_f = 2$ and $N_f = 3$ QCD their masses are not degenerated. To work around this point one must include extra terms in the scalar potential that is also invariant under the symmetry. Such a term in the lowest order is the double trace term $\kappa\mathrm{Tr}[X^\dagger X]$ that is controlled by the coupling constant κ. Double

trace term in QCD should be suppressed by $1/N^2$, so the range of κ is chosen to be small.

$$\left(\mathrm{Tr}X^\dagger X\right)^2 = \frac{1}{4}\left[(L_0+\sigma)^2 + \sum_k \xi_k^2\right]^2 \simeq 2L_0^2\xi_k^2 + 6L_0^2\sigma^2 + \dots . \tag{4.3.36}$$

Adding this contribution will change the scalar potential and therefore change the eoms of the scalar fields to split the singlet from the triplet. And it will also change the vacuum eoms to include the double trace contribution

$$\partial_\rho\left(\rho^3\partial_\rho L_0(\rho)\right) - \rho\Delta m^2(\rho)L_0(\rho) - \kappa L_0(\rho)^3\rho = 0\,. \tag{4.3.37}$$

Numerically, the extra contribution will lift the vacuum solution a bit above the original one. In fig. 4.2(b) we plot the vacuum solution setting the UV quark mass to be 95.5 MeV (e.g. strange quark mass). As can be seen from the plot, for such a mass, the effect of the double trace term is very limited. One can easily imagine that including the double trace term will only introduce minor effect into the vacuum solutions for the u and d quarks.

The diagonal scalar eoms are changed to

$$\begin{aligned}
&\partial_\rho(\rho^3\partial_\rho\sigma(\rho)) - \rho(\Delta m^2)\sigma(\rho) - \rho L_0(\rho)\sigma(\rho)\frac{\partial\Delta m^2}{\partial L}|_{L_0} + M_\sigma^2\frac{\rho^3}{r^4}\sigma(\rho) - 3\kappa L_0^2\sigma(\rho)\rho = 0\\
&\partial_\rho(\rho^3\partial_\rho\xi_3(\rho)) - \rho(\Delta m^2)\xi_3(\rho) - \rho L_0(\rho)\xi_3(\rho)\frac{\partial\Delta m^2}{\partial L}|_{L_0} + M_{\xi_3}^2\frac{\rho^3}{r^4}\xi_3(\rho) - \kappa L_0^2\xi_3(\rho)\rho = 0.
\end{aligned} \tag{4.3.38}$$

Solving them numerically using the shooting method for coupled equations developed in section 4.2, the results are plotted in fig. 4.3. We find a dependence of the scalar masses on the coupling κ. To have the masses in the observed range [7], the coupling κ can only be varied in a narrow range.

The full spectrum when including the double trace term is listed in table 4.1. We fitted the ρ meson mass to read out other masses as predictions. The double trace term should scale as $1/N^2 \sim 1/9$, therefore we chose $\kappa = -0.3$ as an example to compute the spectrum. As shown in the last column of table 4.1, most of the masses are at 3% level comparing to the data. The π mass is very sensitive to the UV quark mass that we input in solving the vacuum. This explains the larger deviation in the table. This value can decrease to a value very close to the real pion mass if tune down the UV quark mass just a bit. What we find out in this table is the mass splitting in the states $f_0(980)$ and $a_0(980)$, i.e. the scalar singlet and triplet respectively. One sees that including such a term does produce the correct mass splitting in and only in the scalar sector.

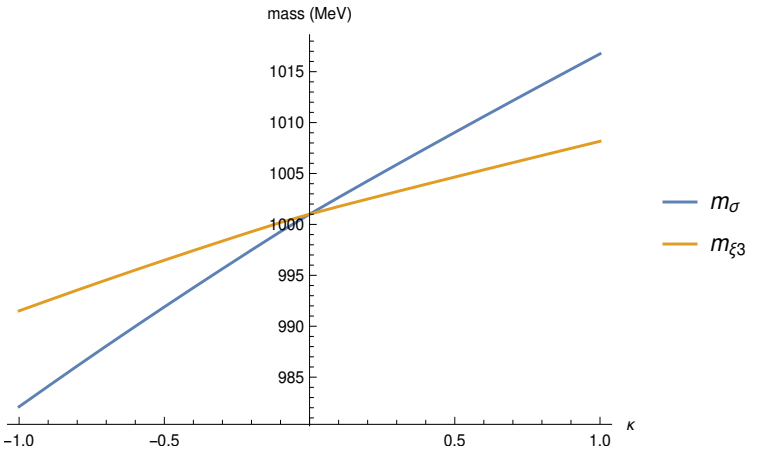

Figure 4.3: Dependence of the scalar masses on κ when quark mass $m_q = 2$ MeV. κ is the coupling of the double trace term introduced in eq. (4.3.38), which gives a small splitting in the singlet and triplet scalar masses m_σ and m_{ξ_3}.

Observables	QCD [MeV]	$U(N_f = 2)$ [MeV]	Deviation
$M_\rho(770)$	775.26 ± 0.23	775*	fitted
$M_{a_1(1260)}$	1230 ± 40	1194	3%
$M_{f_0(980)}$	990 ± 20	994*	$< 1\%$
$M_{a_0(980)}$	980 ± 20	997	2%
π^0	134.9768 ± 0.0005	117	14%

Table 4.1: Meson masses of the lowest lying states in the $U(N_f)$ model with equal quark masses. The ρ meson mass is fixed to 775 MeV and we have set $m_q = m_u = 2.3$ MeV and $\kappa = -0.3$ (therefore the asterisk next to 994.). The QCD masses are taken from the PDG [7]. The mass difference in $f_0(980)$ and $a_0(980)$ is introduced by the double trace term with the coupling κ. The π^0 mass is very sensitive to the quark mass, this explains the large deviation.

4.3.6 Split Masses

We consider in this section a more interesting case. We split the quark masses in UV by separating the branes. This is dual to a 4D QFT with broken $U(2)$ flavour symmetry. We neglect the EM contributions in this discussion.

When separating the D7-branes, additionally, the global flavor symmetry $U(2)$ is broken explicitly on the boundary. This is because we introduce the breaking through inputting different UV quark masses. The vacuum eoms are changed to

$$\partial_\rho \left(\rho^3 \partial_\rho L_i\right) - \Delta m_i^2 \rho L_i = 0, \quad i = u, d. \tag{4.3.39}$$

This refers to two $U(1)$s representing the u and d-branes respectively. The corresponding fluctuation states are $u\bar{u}$ and $d\bar{d}$, i.e. the eigenstates in the large N limit when no multi-trace terms

present.

The off-diagonal fluctuations are now no more degenerated with the diagonal ones due to the mass splitting. The eoms can thus be sorted into two groups, the diagonal ($q\bar{q}$) and the off-diagonal ($u\bar{d}$ and $d\bar{u}$). The off-diagonal ones correspond to two charged components in the triplet. In the following we take the vector state as an example to demonstrate the numerical computations. The other equations can be found in appendix D.

For the vector meson, the off-diagonal states are $V_{1/2}$. Their eoms are

$$V_{1/2}: \quad \partial_\rho \left(\rho^3 \partial_\rho V_{1/2}(\rho)\right) + \frac{\rho^3}{8}\left(\frac{1}{r_u^4}+\frac{1}{r_d^4}\right)\left[4M_{V_{1/2}}^2 - g_5^2\left(L_u(\rho)-L_d(\rho)\right)^2\right] V_{1/2}(\rho) = 0. \tag{4.3.40}$$

Where in the computations, we have defined $V_i^\mu = V_{\perp,i}^\mu + \partial_\mu \phi_{V,i}$, $\partial_\mu V_\perp^\mu = 0$ and taking the $V_\rho = 0$ gauge. The transverse part is the vector fluctuation. The longitudinal part mixes with the scalars, see eq. (D.2). This is a bulk Higgs mechanism that is caused by the spontaneous symmetry breaking of the bulk gauge symmetry (explicit symmetry breaking of the flavor symmetry on the boundary), where the scalars become the GBs of the vector bosons.

To solve these equations numerically, we set the IR boundary conditions to be

$$V_i(\rho_d) = 1, \quad \partial_\rho V_i(\rho_d) = 0, \quad V_i(\rho_{UV}) = 0, \quad i = 1, 2, \tag{4.3.41}$$

where ρ_d is the IR mass we get from solving the embedding L_d. In the UV we required that the fluctuations should vanish. We use the shooting method to shoot from the IR, seek a mass $M_{V_{1/2}}$ such that the field vanishes in the UV. In this way we obtain the physical mass of the charged vector meson.

The scalar fields are mixed with the longitudinal parts of the dual vector fields ϕ_V due to the bulk Higgs mechanism. One can set the IR boundary condition to

$$\phi_{v,i}(\rho_d) = 1, \quad \phi'_{v,i}(\rho_d) = 0, \quad \xi_2(\rho_d) = b. \tag{4.3.42}$$

Here b is a shooting parameter. Now one seeks the parameter pair (b, M_ξ) such that the scalar and the ϕ_V both vanish in the UV. Same boundary conditions can also be used in the pion sector, since they mix with the longitudinal part of the axial vector fields. However, we find out that for $\phi_{V/A}, \partial_\rho \phi_{V/A} \ll f$ where f a general meson field, ignoring the mixing is a good approximation. This corresponding to the decoupling limit of the coupled equations. We take

this limit in computing the spectrum. The results are listed in table 4.2. The values are very close to the ones in table 4.1. But we see that there is a splitting in π^0 and $\pi^\pm$ after introducing the mass splitting. We illustrate this splitting in fig. 4.4(a).

Observables	QCD [MeV]	$U(N_f = 2)$ [MeV]	Deviation
$M_\rho(770)$	775.26 ± 0.23	775*	fitted
$M_{a_1(1260)}$	1230 ± 40	1196	3%
$M_{a_0(980)}$	980 ± 20	998	2%
$\pi^\pm$	139.57039 ± 0.00017	146	2%

Table 4.2: Meson masses of the lowest lying states in the $U(N_f)$ model with unequal quark masses, $m_u = 2.3$ MeV and $m_d = 4.6$ MeV. The ρ meson mass is fixed to 775 MeV. The QCD masses are taken from the PDG [7]. Notice the deviation of pion from the initial π^0 state to the $\pi^\pm$ state.

On splitting the quark masses one ends up with the $u\bar{u}$ and $d\bar{d}$ type of states in the dual field theory. As is known from the QCD, the true physical states are actually admixtures of the two states. For this purpose, we include the 1/N effect to find physical states for the scalar fields. By adding the double trace term, the vacuum dynamics are described by a set of mixed equations

$$\begin{aligned}\partial_\rho\left(\rho^3\partial_\rho L_u(\rho)\right) - \Delta m_u(\rho)\rho L_u(\rho) - 2\kappa L_u(\rho)^3\rho - 2\kappa L_u(\rho)L_d(\rho)^2 = 0,\\ \partial_\rho\left(\rho^3\partial_\rho L_d(\rho)\right) - \Delta m_d(\rho)\rho L_d(\rho) - 2\kappa L_d(\rho)^3\rho - 2\kappa L_d(\rho)L_u(\rho)^2 = 0.\end{aligned} \tag{4.3.43}$$

The diagonal scalar fields now have the dynamics

$$\begin{aligned}\partial_\rho(\rho^3\partial_\rho\sigma_u) + \rho\left(-\Delta m_u(\rho) - L_u(\rho)\Delta m_u'(\rho) - 2\kappa\left(3L_u(\rho)^2 + L_d(\rho)^2\right) + \frac{\rho^2M^2}{r_u^4}\right)\sigma_u(\rho)\\ -4\kappa\rho L_u(\rho)L_d(\rho)\sigma_d(\rho) = 0,\end{aligned} \tag{4.3.44}$$

$$\begin{aligned}\partial_\rho(\rho^3\partial_\rho\sigma_d) + \rho\left(-\Delta m_d(\rho) - L_d(\rho)\Delta m_d'(\rho) - 2\kappa\left(+3L_d(\rho)^2 + L_u(\rho)^2\right) + \frac{\rho^2M^2}{r_d^4}\right)\sigma_u(\rho)\\ -4\kappa\rho L_u(\rho)L_d(\rho)\sigma_u(\rho) = 0.\end{aligned} \tag{4.3.45}$$

These are a set of coupled differential equations. To solve this, we again employ the method developed in section 4.2

$$\sigma_u(\rho)|_{IR} = 1, \quad \sigma_d(\rho)|_{IR} = b, \quad \sigma_{u,d}'(\rho)|_{IR} = 0, \tag{4.3.46}$$

where the IR boundary of σ_d is taken to be a free shooting parameter called b. The IR is taken

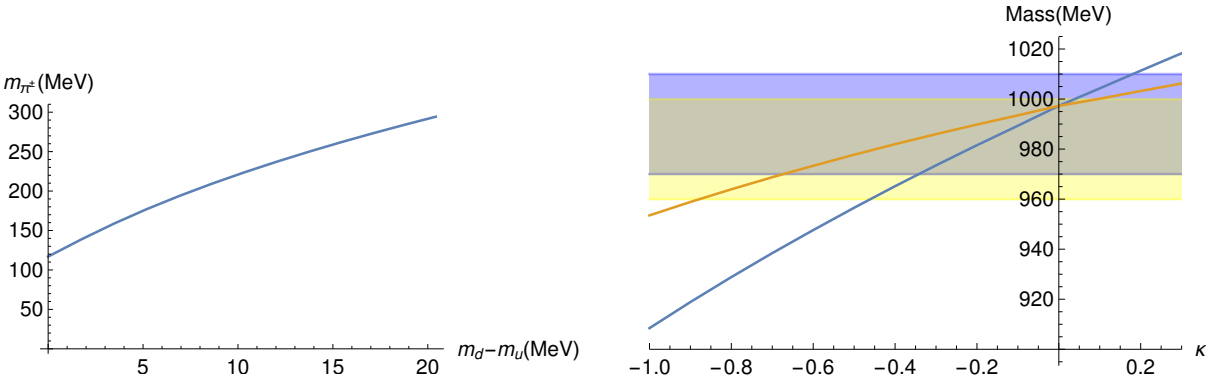

(a) $\pi^\pm$ vs. Δm_q .

(b) The diagonal scalar fields vary with κ.

Figure 4.4: Left plot: The $\pi^\pm$ mass increases with the growing quark mass splitting at fixed m_u and $\kappa = 0$. Right plot: The scalar masses in the presence of $\kappa\rho\mathrm{Tr}(X^\dagger X)^2$ in the split mass case. The shaded blue area marks the valid data range of the $f_0(980)$, and the yellow area marks that of the $a_0(980)$. This indicates a range $\kappa \in [-0.4, 0]$.

to the be IR mass of L_d. This essentially means that the two fields should end at different positions in the IR. Then one can use the `NDSolve` function in `Mathematica` to shoot from the IR, seek for the combinations of the free parameters (b, M) such that both of the fields σ_u and σ_d vanish in the UV.

Since the coupling κ is a free parameter, one can vary it to find the range that the scalar singlet and the third triplet masses lie within the correct range. This is shown in fig. 4.4(b). We note that the η' mass is not discussed in this section, since the $U(1)_A$ is not anomalous in the large N. To obtain a meaningful discussion on this mass, the Wess-Zumino-Witten term must be added to the action to include the chiral anomaly. This term is currently missing in the theory.

4.4 Three-Flavor Non-Abelian AdS/QCD

Using the formalism discussed in the last section, one can compute the three-flavor QCD for the case $m_u = m_d \ll m_s$. The eoms are listed in appendix E. They have the same structure as the two flavor QCD case if we define

$$f_{u+d} := \sqrt{\frac{2}{3}} f_0 + \frac{1}{\sqrt{3}} f_8, \quad f_s := \frac{1}{\sqrt{3}} f_0 - \sqrt{\frac{2}{3}} f_8. \tag{4.4.1}$$

f denotes a general meson field. Requiring $m_u = m_d \ll m_s$ is equivalent to separate the three flavor-branes into two coincident branes (u- and d-branes) and a s-brane. This breaks the $U(3)$ gauge symmetry in the bulk to $U(2) \times U(1)$. The corresponding singlets are $(u\bar{u} + d\bar{d})/\sqrt{2}$ and $s\bar{s}$ states. In this case, the ω and ρ mesons are degenerated (they contain only the u and d

Observables	QCD [MeV]	$N_f = 3$ - split masses [MeV]	Deviation
$M_{\rho(770)}$, $\omega(782)$	775.26 ± 0.23	775*	fitted
$M_{K^*(892)}$	891.67 ± 0.26	1009	12%
$M_{\phi(1020)}$	1019.461 ± 0.016	1048	3%
$M_{a_1(1260)}$, $M_{f_1(1285)}$	1230 ± 40	1104	11%
$M_{K_1(1400)}$	1403 ± 7	1377	2%
$M_{f_1(1420)}$	1426.3 ± 0.9	1713	18%
$M_{a_0(980)}$, $M_{f_0(980)}$	980 ± 20	929	5%
$M_{K_0^*(700)}$	845 ± 17	876	4%
$M_{f_0(1370)}$	1370	970	34%
M_π	139.57039 ± 0.00017	139	1%
M_K	497.611 ± 0.013	584	16%
$M_{\eta'}$	957.78 ± 0.06	791	19%
$M_{\pi(1300)}$	1300 ± 100	1438	10%
$M_{K(1460)}$	1460	1807	21%

Table 4.3: Meson masses in the three flavor case compared with the experimental data [7]. We have fixed the masses for the vector mesons ρ and ω and calculated the masses for the axial vectors, the scalars and the pNGBs. The quark masses used are $m_u = m_d = 3.1$ MeV and $m_s = 95.7$ MeV.

quarks).

In the $q\bar{q}$ hadron model, the singlet and the eighth component of the octet vector mesons are ideally mixed, with a mixing angle of 35.3° [188]. This means that the vector meson $\phi(1020)$ is a $s\bar{s}$ state. The axial vectors are supposed to follow the same structure. The scalar mesons states are not uniquely defined. In the quark model, the lowest states are supposed to be the $f_0(500)$, but it is also suspected to be a tetraquark state [7]. They don't follow an ideal mixing pattern. Therefore the heavy-light scalar state (u/d-s state) is not a $s\bar{s}$ state and the model's prediction is expected to show large deviation.

The pseudo-scalars are the GBs in the massless limit. In the three-flavor QCD, the singlet and octet are only slightly mixed, with a mixing angle of 18°. Also, the singlet state η' receives large contribution from the chiral anomaly. This is implemented by adding a Wess-Zumino-Witten term to the action. Such a term is expected to be nontrivial in the non-abelian DBI, therefore the discussion is postponed for future work. Nevertheless, this state is still included in the spectrum to complete the analysis. Higher radial excitations can also be computed. But the spectrum doesn't show a Regge trajectory. The reason for this is, the states are point

like instead of stringy states. For a better prediction on the physical observables, one need to include the stringy effects. Two radial excitation states $\pi(1300)$ and $K(1460)$ are included to demonstrate this point.

The full spectrum is listed in table 4.3. As already mentioned, the heavy-light scalar state is not well defined. The $f_0(1370)$ state is also modeled as glueball or meson molecule in other models, see section 63 of [7] and references therein. Thus the large deviation of the $f_0(1370)$ mass from the experimental data is understandable. Also the η' state has a deviation of 19%, this is due to the absence of the chiral anomaly. Aside from these two states, the rest part of the spectrum shows a good agreement with the measured data.

Chapter 5

Holographic Sp$(2N_c)$ Gauge Dynamics: from Composite Higgs to Technicolor

In this chapter we realize the final goal of our project. We construct a holographic model showing both composite Higgs and technicolor phases and realizes a phase transition between the two. Such a transition has been considered in the field theory in [62, 80, 97]. The model describes generally a $Sp(2N_c)$ gauge theory, with two Dirac fermion flavors in the fundamental representation. The global symmetry to realize in the dual field theory is $SU(4)$. Holographically, the $U(1)_A$ in the large N limit is not anomalous, thus in the holographic model we construct, the global symmetry is $U(4)$. We consider the global symmetry breaking pattern of $SU(4) \to Sp(4)$ (holographically $U(4) \to Sp(4)$). Such a breaking pattern in the field theory is constructed in [80], and is reviewed in section 2.3. We construct a similar model in this chapter holographically. However our focus is not on embedding the EW gauge group explicitly but rather breaking the symmetry dynamically in the higher energy regime.

The embedding of the CH and TC phases in the holographic model is realized by constructing a non-abelian AdS/YM theory with two different vacuums. This model contains a quadruplet that transforms under a $SU(2) \times SU(2)$ invariant subgroup. If the EW gauge group is incorporated, such this quadruplet will provide a candidate for composite Higgs.

In the following we will construct the model step by step, from a composite Higgs model to a mixed model with the CH and TC phases in the end. In section 5.1 we discuss the gauge theory of the model, where we show the Lagrangian, the generators and the vacuums all on the dual field theory side. Then in section 5.2 we construct the corresponding holographic model. In

section 5.3 we first construct a $U(4) \to Sp(4)$ case with the UV fermion mass all degenerate. Then we separate the flavors in section 5.4 as an intermediate step. Finally in section 5.5 we incorporate two $U(4) \to Sp(4)$ vacuums — one from adding a UV fermion mass and the other from introducing the NJL four-fermion interaction — realizing a transition from the composite Higgs to technicolor. This scenario is the case with split UV fermion masses in section 5.4 modulo a rotation. In each step we calculate the bosonic bound states' spectrum and the decay constants. The work in this chapter is published in [2].

5.1 The Gauge Theory

We will reformulate the construction in [80] which is reviewed in section 2.3 in this section, and set our notations. The need for reformulating the theory is for the extension of this theory to the holographic one in the next section.

The dynamics of an $Sp(2N_c)$ gauge theory with 2 Dirac fermions in the fundamental representation is formulated by [62, 80, 97]

$$\mathcal{L} = -\frac{1}{4}G^{\mu\nu}G_{\mu\nu} + i\bar{\psi}_i \not{D}\psi_i - \bar{\psi}_i M_{ij}\psi_j, \tag{5.1.1}$$

and the Dirac spinor is defined in terms of four two-component right-handed Weyl spinors

$$\psi_i = \begin{pmatrix} U_L^C \\ D_L^C \\ D_R \\ U_R \end{pmatrix}. \tag{5.1.2}$$

By far this is similar to the conventions in section 2.3. Since we want to realized the $SU(4) \to Sp(4)$ theory later holographically using the D-branes, the global symmetry group should be $U(4)$. This is because the global symmetry corresponds to the gauge symmetry realized by the D7 flavor branes and this symmetry is $U(N_f)$. The $U(1)_A$ is not anomalous in the large N limit, therefore the global symmetry is essentially $U(N_f)$. The generators of the $U(4)$ symmetry group is chosen to be

$$T^{1-3} = \frac{1}{2\sqrt{2}}\begin{pmatrix} \tau_i & 0 \\ 0 & \tau_i \end{pmatrix}, \quad T^{4-6} = \frac{1}{2\sqrt{2}}\begin{pmatrix} \tau_i & 0 \\ 0 & -\tau_i \end{pmatrix}, \tag{5.1.3}$$

for $i = 1, 2, 3$, τ_i are the Pauli matrices and

$$T^{7/8} = \frac{1}{2\sqrt{2}} \begin{pmatrix} 0 & 0 & 0 & -i \\ 0 & 0 & \pm i & 0 \\ 0 & \mp i & 0 & 0 \\ i & 0 & 0 & 0 \end{pmatrix}, \quad T^{9/10} = \frac{1}{2\sqrt{2}} \begin{pmatrix} 0 & 0 & -i & 0 \\ 0 & 0 & 0 & \mp i \\ i & 0 & 0 & 0 \\ 0 & \pm i & 0 & 0 \end{pmatrix}, \tag{5.1.4}$$

$$T^{11/12} = \frac{1}{2\sqrt{2}} \begin{pmatrix} 0 & 0 & 1 & 0 \\ 0 & 0 & 0 & \pm 1 \\ 1 & 0 & 0 & 0 \\ 0 & \pm 1 & 0 & 0 \end{pmatrix}, \quad T^{13/14} = \frac{1}{2\sqrt{2}} \begin{pmatrix} 0 & 0 & 0 & 1 \\ 0 & 0 & \pm 1 & 0 \\ 0 & \pm 1 & 0 & 0 \\ 1 & 0 & 0 & 0 \end{pmatrix}, \tag{5.1.5}$$

$$T^{15} = \frac{1}{2\sqrt{2}} \begin{pmatrix} 1_2 & 0 \\ 0 & -1_2 \end{pmatrix}, \quad T^{16} = \frac{-1}{2\sqrt{2}} \begin{pmatrix} 1_2 & 0 \\ 0 & 1_2 \end{pmatrix}. \tag{5.1.6}$$

If we want to incorporate the EW sector, the U and D doublet need to be promoted to be in the fundamental representation of the gauge group $SU(2)_L$. The corresponding generators are then $(T^1 + T^4)/\sqrt{2}$, $(T^2 + T^5)/\sqrt{2}$ and $(T^3 + T^6)/\sqrt{2}$. This is considered as a neglectably weak perturbation on the strong gauge dynamics.

Given that the representation of $U(4)$ is pseudo-real, the bound states, i.e the fluctuations in the later holographic model, are parametrized in the anti-symmetric matrix

$$X_f = \begin{pmatrix} 0 & \sigma - Q_5 + iS - i\pi_5 & Q_2 - \pi_2 + i\pi_1 - iQ_1 & -Q_4 + \pi_4 + iQ_3 - i\pi_3 \\ -\sigma + Q_5 + i\pi_5 - iS & 0 & Q_4 + \pi_4 + iQ_3 + i\pi_3 & Q_2 + \pi_2 + iQ_1 + i\pi_1 \\ \pi_2 - Q_2 + iQ_1 - i\pi_1 & -Q_4 - \pi_4 - iQ_3 - i\pi_3 & 0 & \sigma + Q_5 + iS + i\pi_5 \\ Q_4 - \pi_4 + i\pi_3 - iQ_3 & -Q_2 - \pi_2 - iQ_1 - i\pi_1 & -\sigma - Q_5 - iS - i\pi_5 & 0 \end{pmatrix}. \tag{5.1.7}$$

Under $U(4)$ flavor symmetry Ω, the matrix X transforms as

$$X_{ab} \to X'_{cd} = \Omega_{ca}\Omega_{db}X_{ab} \Leftrightarrow X \to X' = \Omega X \Omega^T. \tag{5.1.8}$$

The gauge theory is expect to behave like a strong interacting theory in a similar way like QCD, thus the fermions are expect to condense. The condensate is assumed to be colorless, anti-symmetric in color indices. For conserved Lorentz invariance, the angular momentum wave function must be antisymmetric. So the condensate must be anti-symmetric in flavor too. When

σ acquires a vev, the vacuum matrix should be anti-symmetric and might be in the form

$$X = \begin{pmatrix} 0 & L_0 & 0 & 0 \\ -L_0 & 0 & 0 & 0 \\ 0 & 0 & 0 & L_0 \\ 0 & 0 & -L_0 & 0 \end{pmatrix}. \tag{5.1.9}$$

This vev corresponds to an invariant $Sp(4)$ subgroup of $U(4)$, the broken generators are T^i, for $i = 8, 10, 11, 14, 15, 16$. Given that $U(4)$ has 16 generators, breaking $U(4)$ down to $Sp(4)$ will give rise to 6 GBs — π_i for $i = 1, ..., 5$ and S, where the S is a singlet. One can also consider an equivalent vacuum when Q_4 acquires a vev, which also breaks the $U(4)$ to $Sp(4)$ with the form

$$X_{Q_0} = \begin{pmatrix} 0 & 0 & 0 & -Q_0 \\ 0 & 0 & Q_0 & 0 \\ 0 & -Q_0 & 0 & 0 \\ Q_0 & 0 & 0 & 0 \end{pmatrix}. \tag{5.1.10}$$

The two vevs are related by the transformation $X = UX_{Q_0}U^T$, where the transformation matrix is

$$U = \frac{1}{\sqrt{2}} \begin{pmatrix} 0 & -1 & 0 & 1 \\ 1 & 0 & -1 & 0 \\ 0 & 1 & 0 & 1 \\ 1 & 0 & 1 & 0 \end{pmatrix}. \tag{5.1.11}$$

The GBs associated with the broken symmetry by this vev are $Q_1 - Q_5$ and S.

The mass terms for the bound states are introduced in the same way as the vevs, especially they are aligned with the vevs taking the following forms respectively

$$M_L = \begin{pmatrix} 0 & m_1 & 0 & 0 \\ -m_1 & 0 & 0 & 0 \\ 0 & 0 & 0 & m_2 \\ 0 & 0 & -m_2 & 0 \end{pmatrix}, \quad M_Q = \begin{pmatrix} 0 & 0 & 0 & -m_1 \\ 0 & 0 & m_2 & 0 \\ 0 & -m_2 & 0 & 0 \\ m_1 & 0 & 0 & 0 \end{pmatrix}. \tag{5.1.12}$$

When $m_1 = m_2 \neq 0$, both cases manifest an explicit flavor symmetry breaking of the form $U(4) \to Sp(4)$, where the associate GBs become massive pNGBs. Splitting the masses $m_1 \neq m_2$, the global flavor symmetry is broken explicitly down to $SU(2)_L \times SU(2)_R$.

If combine the two vevs, then the global symmetry is also broken explicitly to $SU(2)_L \times SU(2)_R$,

the corresponding matrix is

$$X = \begin{pmatrix} 0 & L_0 & 0 & -Q_0 \\ -L_0 & 0 & Q_0 & 0 \\ 0 & -Q_0 & 0 & L_0 \\ Q_0 & 0 & -L_0 & 0 \end{pmatrix}. \tag{5.1.13}$$

Then this vev can be rotated to a similar form as the M_L in eq. (5.1.12) by the transformation $X \to UXU^T$ to the following forms

$$X \to \begin{pmatrix} 0 & L_0+Q_0 & 0 & 0 \\ -L_0-Q_0 & 0 & 0 & 0 \\ 0 & 0 & 0 & L_0-Q_0 \\ 0 & 0 & -L_0+Q_0 & 0 \end{pmatrix}, \quad \text{using} \quad U = \frac{1}{\sqrt{2}} \begin{pmatrix} 0 & -1 & 0 & 1 \\ 1 & 0 & -1 & 0 \\ 0 & 1 & 0 & 1 \\ -1 & 0 & -1 & 0 \end{pmatrix}, \tag{5.1.14}$$

$$X \to \begin{pmatrix} 0 & L_0+Q_0 & 0 & 0 \\ -L_0-Q_0 & 0 & 0 & 0 \\ 0 & 0 & 0 & -L_0+Q_0 \\ 0 & 0 & L_0-Q_0 & 0 \end{pmatrix}, \quad \text{using} \quad U = \frac{1}{\sqrt{2}} \begin{pmatrix} 0 & -1 & 0 & 1 \\ 1 & 0 & -1 & 0 \\ 0 & 1 & 0 & 1 \\ 1 & 0 & 1 & 0 \end{pmatrix}. \tag{5.1.15}$$

We write this out explicitly here. Their applications will become clear when we introduce the NJL interaction in section 5.5.

The two vacuums are equivalent at the gauge theory level. However, when gauging the EW $SU(2)_L$, the vacuum in eq. (5.1.9) is invariant while the one in eq. (5.1.10) isn't. Since the vacuum corresponds to the effective potential tends to align the vacuum in the gauge symmetry preserving direction [100], the vacuum preferred is eq. (5.1.9). This is the vacuum adopted in some composite Higgs models. The associated pNGBs $\pi_{1,\dots,4}$ forms a Higgs doublet.

The other vacuum in eq. (5.1.10) breaks the EW symmetry in the sense of the technicolor model. Such a vacuum is favored if one introduces, for example, the four-fermion NJL interactions. The Lagrangian for such an interaction is

$$\mathcal{L} = \frac{g_s^2}{\Lambda_{UV}^2}(\bar{\Psi}_L U_R \bar{U}_R \Psi_L + \bar{\Psi}_L D_R \bar{D}_R \Psi_L), \tag{5.1.16}$$

where Λ is the UV cut-off, and g_s is the dimensionless NJL coupling.

5.2 Holographic Model

To describe the aforementioned gauge theory holographically, we employ the non-abelian AdS/YM theory developed in chapter 4. The bilinear operators' vev and fluctuations are introduced through the scalar field X. In the bulk, they live in the AdS_5 space

$$ds^2 = (\rho^2 + X^\dagger X)dx_{3+1}^2 + (\rho^2 + X^\dagger X)^{-1}d\rho^2, \tag{5.2.1}$$

where ρ is the holographic radial coordinate as before. The X, like in the non-Abelian AdS/QCD case, is a matrix in flavor space. Generally the action for the X field is

$$\begin{aligned}\mathcal{L} = &\frac{1}{2}\rho^3 \mathrm{Tr}\left(\partial_\rho X^\dagger \partial_\rho X\right) + \frac{1}{2}\rho^3 \mathrm{Tr}\left(\rho^2 + X^\dagger X\right)^{-2}\left(\partial_x X^\dagger \partial_x X\right) \\ &+ \frac{1}{2}\rho\, A\left[\mathrm{Tr}\left(\rho^2 + X^\dagger X\right)\right]\mathrm{Tr}X^\dagger X + \frac{B}{\rho}\left(4\mathrm{Tr}X^\dagger X X^\dagger X - \left(\mathrm{Tr}X^\dagger X\right)^2\right).\end{aligned} \tag{5.2.2}$$

This action is quite similar as the one eq. (4.3.12) in non-Abelian AdS/QCD, but here we change the introduction of running through the Δm^2-matrix with the function A. It works as follows. A is a function of $\mathrm{Tr}(\rho^2 + X^\dagger X)$, for all the fields f in X, their eoms will be

$$\partial_\rho(\rho^3 \partial_\rho f) - \rho A f - \frac{1}{2}\frac{\partial A}{\partial f} f^2 = 0. \tag{5.2.3}$$

To arrive at the same eom for the embedding as seen in eq. (4.3.27), we impose the following relation between A and Δm^2

$$A + \frac{1}{2}\frac{\partial A}{\partial f} f \equiv \Delta m^2\left[\rho^2 + f^2\right]. \tag{5.2.4}$$

Here we let Δm^2 be a function of $r^2 = \rho^2 + f^2$, the explicit dependence will be $\Delta m^2[\log r]$, where r is dual to the running energy scale μ. The function Δm^2 should depend on r instead of ρ is to insure the stability of the potential against the BF-bound in large embedding L [177].

The gauge theory dynamics is then introduced to the model using the AdS/CFT dictionary $M^2 = \Delta(\Delta - 4)$ by relating the gauge theory running with Δm^2

$$\Delta m^2 = -2\gamma. \tag{5.2.5}$$

The running is introduced in the same way as before. We repeat it here for the convenience of

Gauge Group	$C_2(G)$	$C_2(F)$	$d(F)$	$T(F)$	$N_f = N_{\bar{f}}$
$SU(N_c)$	N_c	$\frac{N_c^2-1}{2N_c}$	N_c	$\frac{1}{2}$	2
$Sp(2N)$	$N+1$	$\frac{2N+1}{4}$	$2N$	$\frac{1}{2}$	4

Table 5.1: Factors in eq. (5.2.6) for various gauge groups. The matter fields are in the fundamental representations, which is marked as F.

the reader

$$\begin{aligned}
&\mu\frac{d\alpha}{d\mu} = -b_0\alpha^2 - b_1\alpha^3, \\
&b_0 = \frac{1}{6\pi}\left(11C_2(G) - 2\sum_R T(R)N_f(R)\right), \\
&b_1 = \frac{1}{24\pi^2}\left(34C_2^2(G) - \sum_R \left[10C_2(G) + 6C_2(R)\right]T(R)N_f(R)\right),
\end{aligned} \tag{5.2.6}$$

where R is the representation of the matter field. The expression is again rewritten in terms of the number of Weyl fermions. The one-loop result for anomalous dimension is

$$\gamma = \frac{3C_2(R)}{2\pi}\alpha. \tag{5.2.7}$$

C_2 is the quadratic Casimir, G is the adjoint representation, N_f is the number of flavors, $d(R)$ is the dimension of fermion's representation. We list the relevant definitions for this part in Table 5.1. We have also set $\alpha(1) = 0.65$ in our computations, but the physical scales are normalized in terms of the physical ρ mass. This choice is arbitrary and will not affect the results. Note also that using the perturbative result in the non-perturbative regime is an assumption, the features of IR pole are not expect to affect much of the spectrum.

If only including the contributions from A, then only $(\mathrm{Tr}X^\dagger X)^n$ terms are included. This will lead to an accidental symmetry where the 12 elements of X becomes a 12-plet of $SO(12)$. Therefore we include the B term in eq. (5.2.2), which is the simplest term that breaks the accidental $SO(12)$ symmetry. As can be seen later in the eoms, for a degenerate model, i.e. all fermions have the same mass, only the $Q_{1,..,5}$ fields feel the effect of B. But including B introduces a new free parameter. The mass splitting of the two sets of GBs, the (π_i,S) and (Q_i, σ) are thus introduced by hand rather than predicted by the model via the gauge dynamics.

The mass terms for the operators in X are included in the usual AdS/CFT way. The UV asymptotics of the matrix X is

$$X_{ij} \sim \mathcal{J} + \frac{\mathcal{O}}{\rho^2} = m_{ij} + \bar{\psi}_i\psi_j/\rho^2. \tag{5.2.8}$$

Where the mass terms are introduced from the UV source terms m_{ij}. In the following, we split the scalar matrix X into

$$X = X_0 + X_f, \tag{5.2.9}$$

where X_0 is the vev. It will be later substituted with the ones in eq. (5.1.9), eq. (5.1.10) and eq. (5.1.13). X_f is the scalar fluctuation matrix, as in eq. (5.1.7).

One could include an NJL interaction in the UV

$$\mathcal{L} = \frac{g^2}{\Lambda^2}\bar{\psi}_i\psi_j\bar{\psi}_j\psi_i, \tag{5.2.10}$$

where Λ is the UV cut-off. Such a term is introduced using Witten's double trace prescription reviewed in section 3.7. In this case, we reinterpret the mass term as the source term due to the NJL interaction

$$\frac{g^2}{\Lambda^2} = \frac{\mathcal{J}}{\mathcal{O}}, \tag{5.2.11}$$

where $\mathcal{O}$ the operator vev in eq. (5.2.8).

5.2.1 The U(4) Gauge Theory

The bulk gauge field from the $U(4)$ flavor symmetry that is dual to $\bar{\psi}\gamma^\mu\psi$ are A^b, with $b = 1, ..., 16$, each associated with the generators in eq. (5.1.3). They are dual to the vector bound states. The final action in the bulk describing a holographic $U(4) \to Sp(4)$ model is

$$\begin{aligned} S = \int d^4x d\rho\rho^3 \mathrm{STr}\Big\{ &\frac{1}{r^2}(D^M X)^\dagger D_M X + \frac{1}{\rho^2} A\left[Tr(\rho^2 + X^\dagger X)\right] Tr X^\dagger X \\ &+ \frac{B}{\rho^4}(4\mathrm{Tr}X^\dagger X X^\dagger X - (\mathrm{Tr}X^\dagger X)^2) + \frac{2}{g_5^2}\left(F_{A,ab}F_A^{ab}\right)\Big\}, \end{aligned} \tag{5.2.12}$$

where $M = 1, ..., 5$ is the spacetime index. STr is the symmetrised trace, as defined in [182]. The covariant derivative is defined as

$$D^M X = \partial^M + iA^{bM}(T^b X + X T^{bT}), \tag{5.2.13}$$

which introduces the interaction between the gauge fields and the scalar fields. The 5-dimensional coupling g_5^2 is

$$g_5^2 = \frac{24\pi^2}{d(R)N_f(R)}. \tag{5.2.14}$$

This coupling is identified as reviewed in section 3.6.

We then expand the action in terms of fluctuations f_i to the quadratic order around the vacuum and get the equations of motion, where f_i represents a general fluctuation (field). To solve the equations of motion numerically, we again employ the shooting technique. We look for solution with the space-time dependence $f_i(\rho)e^{ik.x}$, $k^2 = -M_f^2$ that asymptotes to 0 in the UV. We shoot from the IR and impose the following boundary conditions for a generic field f

$$f(\rho_{IR}) = 1, \quad \partial_\rho f(\rho_{IR}) = 0, \quad f(\rho_{UV}) = 0, \tag{5.2.15}$$

where the shooting parameter will be the field's mass M_f. For coupled equations, we use the boundary conditions developed in chapter 4

$$\begin{aligned} f_1(\rho_{IR}) = 1, \quad \partial_\rho f_1(\rho_{IR}) = 0, \quad f_1(\rho_{UV}) = 0, \\ f_2(\rho_{IR}) = b, \quad \partial_\rho f_2(\rho_{IR}) = 0, \quad f_2(\rho_{UV}) = 0, \end{aligned} \tag{5.2.16}$$

where the shooting parameters in this case are the mass M_f and an IR boundary value b.

The boundary conditions when including the NJL interactions need a further discussion. Since the fluctuations should feel the same NJL contribution in the UV as the embedding, then their UV boundary conditions should have the same NJL effect between the source and the vev as the embedding in eq. (5.2.11). We will clarity the details later in the corresponding section.

Aside from the bound states' masses, another physical quantity we can calculate is the decay constant. They are computed exactly as reviewed in section 3.6, we will not repeat it here.

5.3 The Mass Degenerate Case

We start first with the simplest construction, i.e. the flavor symmetry breaking of $U(4) \to Sp(4)$. This is realized when all the fermions have the same mass m in the UV. The corresponding vacuum in the holographic model is

$$L = \begin{pmatrix} 0 & L_0(\rho) & 0 & 0 \\ -L_0(\rho) & 0 & 0 & 0 \\ 0 & 0 & 0 & L_0(\rho) \\ 0 & 0 & -L_0(\rho) & 0 \end{pmatrix}. \tag{5.3.1}$$

I.e. we have taken eq. (5.1.9) setting $\sigma = L_0$ and the corresponding mass matrix in the UV is the M_L in eq. (5.1.12). The scalar fluctuations in eq. (5.1.7) split to: the Higgs-like mode

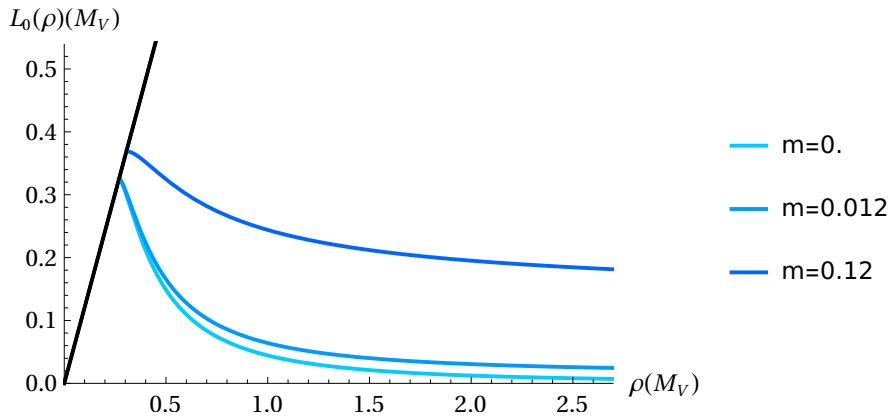

Figure 5.1: Vacuum solutions for L_0 against RG scale ρ for different UV fermion masses in the $SU(2)$ theory. The plot is in units where $M_V = 1$ when $m = 0$. The embeddings corresponds to m=0, 0.012 and 0.12 M_V respectively.

σ which is a singlet under $Sp(4)$, the GBs $\pi_1, ..., 5$ and S which form a 5-plet and a singlet of $Sp(4)$ respectively, and the massive modes $Q_{1,...,5}$ affected by the B-term in eq. (5.2.12), which forms another 5-plet under $Sp(4)$. The broken generators are T^i for $i = 8, 10, 11, 14, 15, 16$ in eq. (5.1.3) – eq. (5.1.6). The vector fields split into a 10-plet of $Sp(4)$ which are dual to the vector bound states, a 5-plet that are dual to axial-vector bound states and a singlet.

5.3.1 The Vacuum

The embedding $L_0(\rho)$ is solved from the equation of motion

$$\partial_\rho(\rho^3 \partial_\rho L_0) - \rho \Delta m^2 L_0 = 0, \tag{5.3.2}$$

shooting from the IR using the boundary condition

$$L_0(\rho_{IR}) = \rho, \quad \partial_\rho L_0(\rho_{IR}) = 0. \tag{5.3.3}$$

Vary the IR value ρ_{IR} and find the solution that asymptotes to different fermion masses m in the UV. Here $\Delta m^2 \equiv \Delta m^2[\log(\rho^2 + L_0^2)]$. We illustrate the profiles associated to three different UV fermion masses in fig. 5.1.

5.3.2 Fluctuations

The scalars contain the σ, the Q_i, π_i and the S, for $i = 1, ..., 5$. The σ is a fluctuation around the vacuum $L_0(\rho)$, it's dynamics is describe by the solution of

$$\partial_\rho \left(\rho^3 \partial_\rho \sigma(\rho)\right) - \rho \Delta m^2 \sigma(\rho) - \rho L_0(\rho)\sigma(\rho) \frac{\partial \Delta m^2}{\partial L}\bigg|_{L_0} + M^2 \frac{\rho^3}{r^4}\sigma(\rho) = 0, \tag{5.3.4}$$

where $r^2 = (\rho^2 + L_0^2)$. In deriving this equation, certain relation between the function A and Δm^2 are needed. This is derived in detail in appendix F.1.

The Q_i fields satisfy

$$\partial_\rho(\rho^3 \partial_\rho Q_i) - \rho \Delta m^2 Q_i - \frac{16B}{\rho} L_0^2 Q_i + M^2 \frac{\rho^3}{r^4} Q_i = 0. \tag{5.3.5}$$

The vectors that are not higgsed have the equations of motion

$$\partial_\rho(\rho^3 \partial_\rho V_i(\rho)) + M_{V_i}^2 \frac{\rho^3}{r^4} V_i(\rho) = 0, \quad i = 1 - 7, 9, 12, 13. \tag{5.3.6}$$

Where the rest 6 higgsed axial vectors have the equations of motion

$$\partial_\rho \left(\rho^3 \partial_\rho A_i(\rho)\right) - g_5^2 \frac{\rho^3 L_0^2}{r^4} A_i(\rho) + \frac{\rho^3 M_{A_i}^2}{r^4} A_i(\rho) = 0, \quad i = 8, 10, 11, 14 - 16. \tag{5.3.7}$$

In arriving at these equations, we have separate the axial-vectors in transverse and longitudinal parts $A_\mu = A_{i,\mu\perp} + \partial_\mu \phi_i$, for $i = 8, 10, 11, 14 - 16$ and adopted the gauge $A_\rho = 0$. The above equations are for the transverse part of the axial-vector states.

The πs and S mix with the longitudinal components of the axial-vectors sharing mixed equations of motion

$$\begin{aligned} \partial_\rho \left(\rho^3 \partial_\rho \phi_j\right) + g_5^2 \frac{L_0 \rho^3}{r^4} \left(\sqrt{2}\pi_i - L_0 \phi_j\right) = 0, \\ \partial_\rho \left(\rho^3 \partial_\rho \pi_i\right) - \rho \Delta m^2 \pi_i + M^2 \frac{\rho^3}{r^4} \left(\pi_i - \frac{L_0}{\sqrt{2}} \phi_j\right) = 0, \\ i = 1 - 5,\ j = 14, 8, 11, 10, 15. \end{aligned} \tag{5.3.8}$$

The ordering of the indices is π_1 mixes with ϕ_{14} etc. The S mixes with the ϕ_{16} and their equations of motion are the same as in eq. (5.3.8).

The masses of the π_i and S need a further discussion. If in the UV the embedding asymptotes

Observables	$SU(2)$	Lattice $SU(2)$	$Sp(4)$	Lattice $Sp(4)$	$Sp(6)$	$Sp(8)$	$Sp(10)$
m_V (10)	1^*	1.00(3)	1^*	1.00(33)	1^*	1^*	1^*
m_A (6)	1.66	1.11(46)	1.26	1.61(17)	1.18	1.14	1.12
m_σ (1)	1.26	1.5(1.1)	1.20		1.22	1.23	1.23
m_Q (5)	1.13		1.13		1.13	1.13	1.13
$m_{\pi,S}$ (6)	0.02		0.01		0.01	0.01	0.01
F_V	0.38		0.53	0.52(10)	0.59	0.64	0.67
F_A	0.48		0.54	0.673(92)	0.59	0.63	0.66
f_π	0.06		0.10	0.122 (99)	0.12	0.12	0.13

Table 5.2: Bound states' masses and decay constants at $m \sim 0$ for gauge groups SU(2) to Sp(10) respectively. The 4 Weyl fermions are in the fundamental representations of each gauge group. We normalized the vector mass to 1 (this is noted by the asterisk). In computing we set $B = 1$ as an example. The lattice result for the SU(2) gauge theory are taken from [189, 190]. The lattice results for the Sp(4) theory are from [191] — the scalar sector has not yet been studied at low mass [192]. A further lattice study at large quark mass is in [193].

to 0, then there exists a solution where $\pi_i, S = L_0$ and $\phi_j = \sqrt{2}$. This corresponds to a massless solution $M^2_{\pi_i,S} = 0$ which reflects that they are the Goldstones of the broken symmetry. Once the embedding asymptotes to a non-zero fermion mass $m \neq 0$, then this solution is no more physical in the dual gauge theory, since it's no more a fluctuation of the operator, but of the mass. In this case in the bulk, these states still sever as the Goldstones that higgses the bulk gauge fields. The GBs becomes pNGBs in that we get massive solutions.

The above equations of motion are solved by imposing the boundary conditions in eq. (5.2.15) and eq. (5.2.16). We list the spectrum for the fields when $m \sim 0$ and $B = 1$ for different gauge groups in table 5.2. The Goldstones $\pi_{1,\ldots,5}, S$ are not exactly massless since m is not exactly 0. We have rescaled the physical quantities in the units of the vector bound states' mass M_{V_0} when $m \sim 0$. This is seen as in table 5.2 the vector bound states' masses are marked with an asterisk. The vector and axial-vector masses are compatible with the lattice QCD results. The hadron masses are stable with respect to different gauge groups, except the axial-vectors are decreasing with growing N_c.

The Qs are also solved in the similar manner, where as mentioned before, their masses depend on the free parameter B. Were this term not present, the model will return back to a theory with 12 degenerated scalars, where such an accidental symmetry is not present in the gauge theory model we are studying. In fig. 5.2(a) we plot the Q mass against the parameter B in the $SU(2)$ gauge theory. As can be seen from the plot, the mass start to stabilze around $B = 1$ and reach the same scale as the other hadrons. Since it's mass is controlled by this free parameter, a precise mass for Qs cannot be predicted from this model.

We have also plotted the masses and decay constants as functions of the UV fermion mass

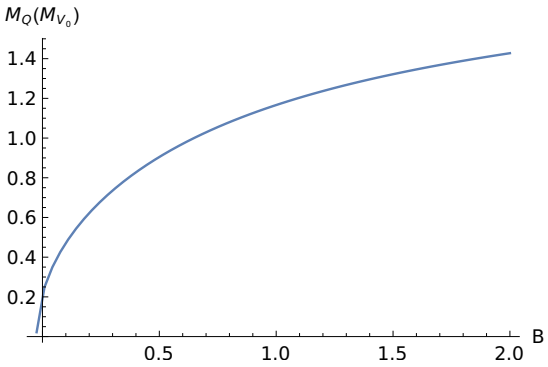

(a) The Q mass increases with B.

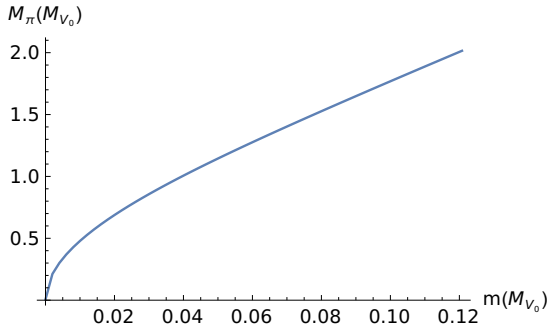

(b) The degenerate π states.

Figure 5.2: Results for the $SU(2)$ gauge theory. On the left: the Q state mass varies with the parameter B, $m = 0.006 M_{V_0}$. Below $B \sim -0.03$ the mass becomes tachyonic, which is not favored by the current discussion. On the right: The π mass as a function of the UV fermion mass. As $m \to 0$ the π mass vanishes, which shows the behavior of a Goldstone boson.

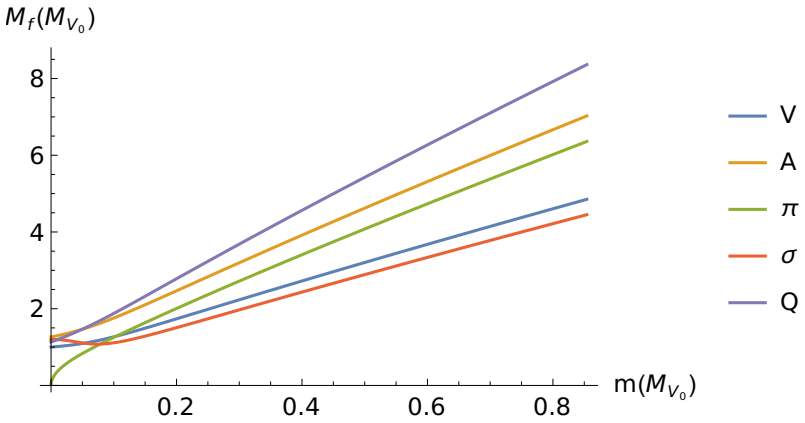

Figure 5.3: The masses of the bound state f against the UV fermion mass in the unit of M_{V_0}. The gauge group is Sp(4) and $B = 1$.

when $B = 1$. As is shown in fig. 5.2(b), the Goldstones' masses show a behavior $M_\pi \sim \sqrt{m}$ as expected from the QCD for small fermion mass. We show the mass behavior against m for $Sp(4)$ gauge group explicitly in fig. 5.3. The masses of other fields increase with m, except the scalar σ shows a slight drop before rise up again with m. The reason for that is the scalar mass M_σ is very sensitive to the running of γ. When m is small, the conformal symmetry breaking is large, resulting in a dominant contribution from the running that causes the mass to drop. We also show the mass dependence of the spectrum and decay constants with different gauge groups in fig. 5.4

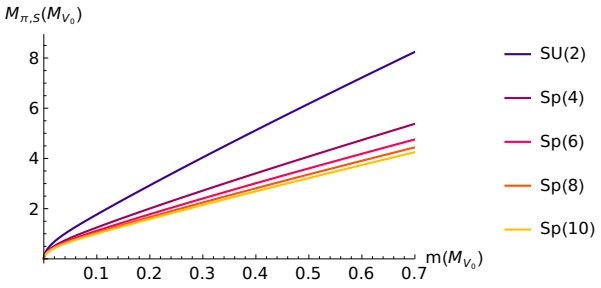

(a) $M_{\pi,S}$

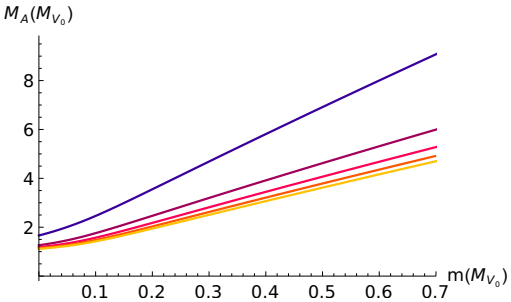

(b) M_A

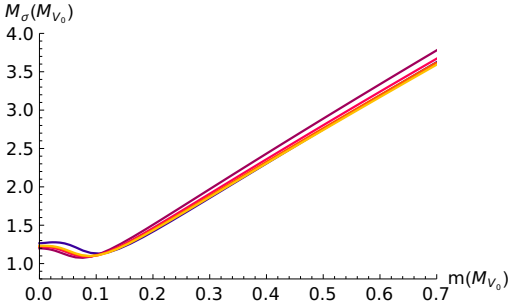

(c) M_σ

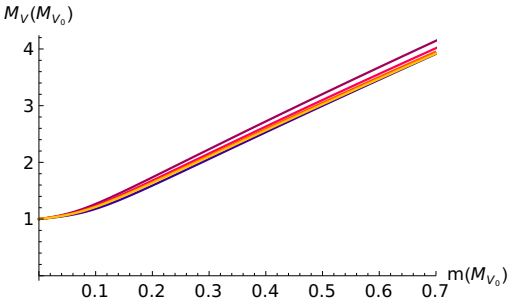

(d) M_V

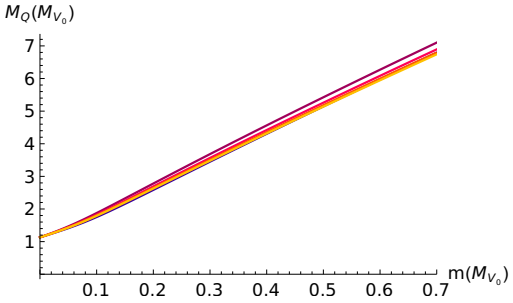

(e) M_Q

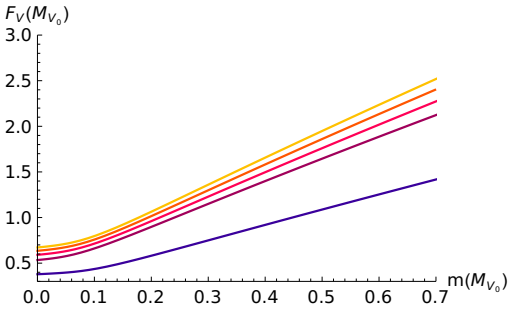

(f) F_V

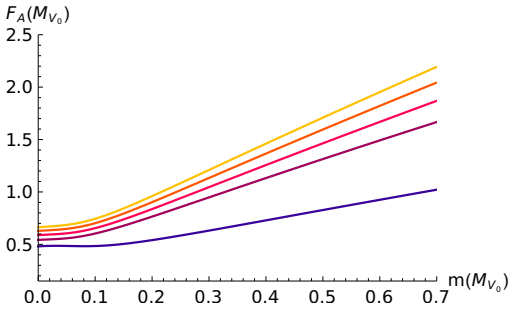

(g) F_A

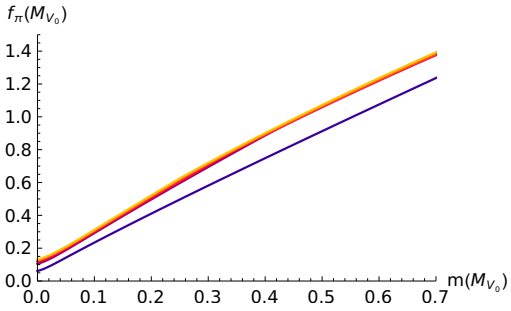

(h) f_π

Figure 5.4: Bound states' masses and decay constants vary with increasing UV fermion mass, with different gauge groups in the degenerate case when $B = 1$. The plots are shown in units of M_{V_0} at zero fermion mass.

5.4 Split The Mass

In this section we consider the scenario where the fermion UV masses are made different $m_1 \neq m_2 \neq 0$. Making this difference brings the model essentially to the non-Abelian holographic model we developed in the last chapter. This scenario is also a prototype for the model where the NJL interactions are included.

5.4.1 The Vacuum

Making the mass different corresponding to the vacuum configuration

$$L = \begin{pmatrix} 0 & L_1(\rho) & 0 & 0 \\ -L_1(\rho) & 0 & 0 & 0 \\ 0 & 0 & 0 & L_6(\rho) \\ 0 & 0 & -L_6(\rho) & 0 \end{pmatrix}. \tag{5.4.1}$$

Here we use $L_1(\rho)$ and $L_6(\rho)$ to represent different embeddings that asymptote to $m_{1,2}$ in the UV respectively. Choosing this embedding will break the $Sp(4)$ to $SU(2)_L \times SU(2)_R$, where the invariant generators are $T^{1,\dots,6}$. This contains an invariant $SU(2)_L$ thus still describes a composite Higgs model.

The equations of motion for the embeddings are coupled

$$\begin{aligned} \partial_\rho\left(\rho^3\partial_\rho L_u\right) - \rho L_u \Delta m^2 - \frac{4B}{\rho} L_u\left(L_u^2 - L_d^2\right) = 0, \\ \partial_\rho\left(\rho^3\partial_\rho L_d\right) - \rho L_d \Delta m^2 - \frac{4B}{\rho} L_d\left(L_d^2 - L_u^2\right) = 0, \end{aligned} \tag{5.4.2}$$

where $\Delta m^2 \equiv \Delta m^2\left[\log\sqrt{\rho^2 + \frac{1}{2}\left(L_u^2 + L_d^2\right)}\right]$. The radial coordinate is $r^2 = \rho^2 1_4 + L^\dagger L = \mathrm{diag}(r_1^2, r_1^2, r_6^2, r_6^2)$, where $r_1^2 = \rho^2 + L_1^2$, $r_6^2 = \rho^2 + L_6^2$. They are solved using the boundary conditions

$$\begin{aligned} &\partial_\rho L_1(\rho_{IR,1}) = 0, \quad L_1(\rho_{IR,1}) = \rho_{IR,1}, \quad L_1(\rho_{UV}) = m_1 \\ &\partial_\rho L_6(\rho_{IR,6}) = 0, \quad L_6(\rho_{IR,6}) = \rho_{IR,6}, \quad L_6(\rho_{UV}) = m_2, \end{aligned} \tag{5.4.3}$$

where the shooting parameters are the IR masses $\rho_{IR,1,6}$. The profiles will look like two curves asymptote to different UV values in fig. 5.1.

5.4.2 Fluctuations

In this case, the fluctuations are parametrized as

$$X_f = \begin{pmatrix} 0 & \sigma_1 + iS_1 & Q_2 - \pi_2 + i\pi_1 - iQ_1 & -Q_4 + \pi_4 + iQ_3 - i\pi_3 \\ -\sigma_1 - iS_1 & 0 & Q_4 + \pi_4 + iQ_3 + i\pi_3 & Q_2 + \pi_2 + iQ_1 + i\pi_1 \\ \pi_2 - Q_2 + iQ_1 - i\pi_1 & -Q_4 - \pi_4 - iQ_3 - i\pi_3 & 0 & \sigma_2 + iS_2 \\ Q_4 - \pi_4 + i\pi_3 - iQ_3 & -Q_2 - \pi_2 - iQ_1 - i\pi_1 & -\sigma_2 - iS_2 & 0 \end{pmatrix}. \tag{5.4.4}$$

The scalars $\pi_{1,2,3,4}$ and $Q_{1,2,3,4}$ each belong to a $(2,2)$ multiplet of $SU(2) \times SU(2)$, and the rest scalars $\sigma_{1,2}$ and $S_{1,2}$ are singlets. The πs are still the Goldstones, they have the equations of motion

$$\begin{aligned} \partial_\rho \left(\rho^3 \partial_\rho \phi_j\right) - \frac{\rho^3 g_5^2}{8} \left(L_u + L_d\right) \left(\frac{1}{r_u^4} + \frac{1}{r_d^4}\right) \left((L_u + L_d)\phi_j - 2\sqrt{2}\pi_i\right) = 0 \\ \partial_\rho \left(\rho^3 \partial_\rho \pi_i\right) - \rho \Delta m^2 \pi_i \\ + \frac{\rho M^2}{2} \left(\frac{1}{r_u^4} + \frac{1}{r_d^4}\right) \left(\pi_i - \frac{1}{2\sqrt{2}}(L_u + L_d)\phi_j\right) - \frac{4B}{\rho}(L_u - L_d)^2 \pi_i = 0 \\ i = 1,2,3,4, j = 14,8,11,10. \end{aligned} \tag{5.4.5}$$

Since the UV masses of the embeddings $L_{1,6}$ are non-vanishing, these states don't have massless solutions. They are massive pNGBs. The Qs also become the Goldstones of the additional broken symmetry of $Sp(4) \to SU(2) \times SU(2)$ in this case. Their dynamics are described by the equations

$$\begin{aligned} \partial_\rho \left(\rho^3 \partial_\rho \phi_j\right) + \frac{\rho^3 g_5^2}{4} \left(L_u - L_d\right) \left(\frac{1}{r_u^4} + \frac{1}{r_d^4}\right) \left(\sqrt{2} Q_i - \frac{L_u - L_d}{2} \phi_j\right) = 0, \\ \partial_\rho \left(\rho^3 \partial_\rho Q_i\right) + \frac{\rho^3 M^2}{2} \left(\frac{1}{r_u^4} + \frac{1}{r_d^4}\right) Q_i - \rho \Delta m^2 Q_i - \frac{4B}{\rho} \left(L_u + L_d\right)^2 Q_i \\ - \frac{\rho^3}{4\sqrt{2}} \left(L_u - L_d\right) M^2 \left(\frac{1}{r_u^4} + \frac{1}{r_d^4}\right) \phi_j = 0, \\ i = 1,2,3,4 \text{ for } j = 13,7,12,9. \end{aligned} \tag{5.4.6}$$

They are the Goldstone states when $Q_i = L_1 - L_6$ and $\phi_j = \sqrt{2}$.

The singlets $S_{1,2}$ are formed by the S and π_5 in the degenerate case as $S_{1,2} = S \pm \pi_5$. They are the GBs associated with the axial-vectors $\frac{1}{2}(A_{15} \pm A_{16})$ which corresponds to the generators $\frac{1}{2\sqrt{2}}\text{diag}(1,1,0,0)$ and $\frac{1}{2\sqrt{2}}\text{diag}(0,0,1,1)$ respectively. Their equations of motion take a similar

form as the others

$$\begin{aligned}\partial_\rho\left(\rho^3\partial_\rho S_1\right)-\rho\Delta m^2 S_1+\frac{\rho^3M^2}{r_1^4}\left(S_1-\frac{L_u}{\sqrt{2}}\phi_{16-15}\right)-\frac{4B}{\rho}\left(L_u^2-L_d^2\right)S_1=0,\\ \partial_\rho\left(\rho^3\partial_\rho\phi_{16-15}\right)+\frac{\rho^3L_1g_5^2}{r_1^4}\left(\sqrt{2}S_1-L_1\phi_{16-15}\right)=0,\end{aligned}\tag{5.4.7}$$

$$\begin{aligned}\partial_\rho\left(\rho^3\partial_\rho S_2\right)-\rho\Delta m^2 S_2+\frac{\rho^3M^2}{r_6^4}\left(S_2-\frac{L_d}{\sqrt{2}}\phi_{15+16}\right)-\frac{4B}{\rho}\left(L_d^2-L_u^2\right)S_2=0,\\ \partial_\rho\left(\rho^3\partial_\rho\phi_{15+16}\right)+\frac{\rho^3L_6g_5^2}{r_6^4}\left(\sqrt{2}S_2-L_6\phi_{15+16}\right)=0.\end{aligned}\tag{5.4.8}$$

They become the massless GBs when $\phi_i=\sqrt{2}$ with $S_1=L_1$ and $S_2=L_6$.

The other two singlets $\sigma_{1,2}$ correspond to the fluctuations around the embeddings $L_{1,6}$ respectively. Their equations of motion are

$$\begin{aligned}\partial_\rho\left(\rho^3\partial_\rho\sigma_1\right)+\left(\frac{\rho^3M^2}{r_1^4}-\frac{4B}{\rho}\left(3L_u^2-L_d^2\right)-\rho\Delta m^2-\frac{\rho L_u^2}{2r_{arg,16}^2}\Delta m^{2\prime}\right)\sigma_1\\ +L_uL_d\left(\frac{8B}{\rho}-\frac{\rho}{2r_{arg,16}^2}\Delta m^{2\prime}\right)\sigma_2=0,\\ \partial_\rho\left(\rho^3\partial_\rho\sigma_2\right)+\left(\frac{\rho^3M^2}{r_6^4}-\frac{4B}{\rho}\left(3L_d^2-L_u^2\right)-\rho\Delta m^2-\frac{\rho L_d^2}{2r_{arg,16}^2}\Delta m^{2\prime}\right)\sigma_2\\ +L_uL_d\left(\frac{8B}{\rho}-\frac{\rho}{2r_{arg,16}^2}\Delta m^{2\prime}\right)\sigma_1=0,\end{aligned}\tag{5.4.9}$$

where $\Delta m^2\equiv\Delta m^2\left(\log r_{arg,16}\right)$, $\Delta m^{2\prime}=\frac{d\Delta m^2}{d\log(r_{arg,16})}$, $r_{arg,16}^2=\rho^2+\frac{1}{2}\left(L_u^2+L_d^2\right)$. As can be seen from the equations, they are not mixed with any longitudinal components of the vectors — they are not eaten by any vectors. In deriving the equations above, we have used the relation

$$\begin{aligned}A+2\left(L_u^2+L_d^2\right)\frac{dA}{d\mathrm{Tr}(\rho^2{}_4+L^\dagger L)}=\Delta m^2\left(\log r_{arg,16}\right)\\ \frac{dA}{d\mathrm{Tr}(\rho^2{}_4+L^\dagger L)}+\left(L_u^2+L_d^2\right)\frac{d^2A}{d\mathrm{Tr}(\rho^2{}_4+L^\dagger L)^2}=\frac{1}{16r_{arg}^2}\Delta m^{2\prime}.\end{aligned}\tag{5.4.10}$$

The derivation of this relation is shown explicitly in appendix F.2.

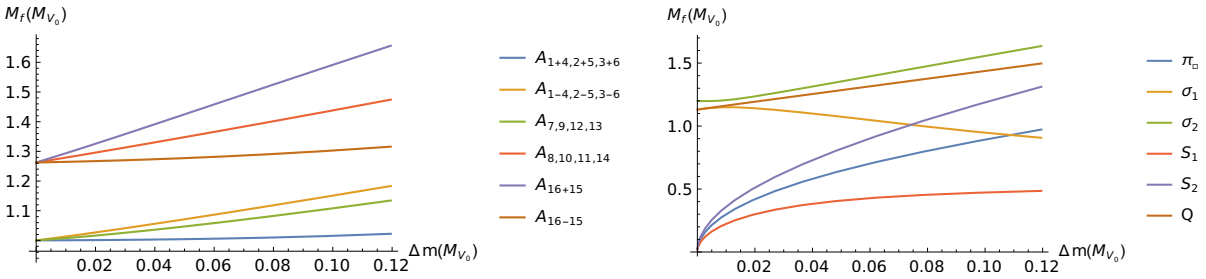

(a) M_f, f = spin 1 state, Sp(4)

(b) M_f, f = spin 0 state, $Sp(4)$

Figure 5.5: Dependence of meson masses on the difference $\Delta m = m_2 - m_1$ of the UV fermion masses for $Sp(4)$ gauge groups in units of M_{V_0}. We have set $B = 1$ and $m_1 = 0.014 M_{V_0}$. The $(1 \pm 4, 2 \pm 5, 3 \pm 6)$ vector states are members of the (3,1) and (1,3); $(7, 9, 12, 13)$ and $(8, 10, 11, 14)$ are members of the two (2,2); 16 ± 15 are singlets.

Finally there are 6 unbroken vectors and 10 axial-vectors, their equations of motion are

$$\begin{gathered}
\partial_\rho \left(\rho^3 \partial_\rho A_i\right) + \frac{\rho^3 M_{A_i}^2}{r_j^4} A_i = 0, \\
i = (1 \pm 4, 2 \pm 5, 3 \pm 6), j = 6, 1, \\
\partial_\rho \left(\rho^3 \partial_\rho A_i\right) + \frac{\rho^3}{8}\left(\frac{1}{r_u^4} + \frac{1}{r_d^4}\right)\left[4M_{A_i}^2 - (L_u - L_d)^2 g_5^2\right] A_i = 0, \; i = 7, 9, 12, 13, \\
\partial_\rho \left(\rho^3 \partial_\rho A_i\right) + \frac{\rho^3}{8}\left(\frac{1}{r_u^4} + \frac{1}{r_d^4}\right)\left[4M_{A_i}^2 - (L_u + L_d)^2 g_5^2\right] A_i = 0, \; i = 8, 10, 11, 14, \\
\partial_\rho \left(\rho^3 \partial_\rho A_i\right) + \frac{\rho^3}{r_j^4}\left[M_{A_i}^2 - L_j^2 g_5^2\right] A_i = 0, \; i = 16 \pm 15, j = 6, 1.
\end{gathered} \tag{5.4.11}$$

We solve the equations using the boundary conditions for the corresponding scenarios as mentioned in eq. (5.2.15) and eq. (5.2.16). The results for the $Sp(4)$ gauge group are shown in fig. 5.5, where we set $B = 1$ and $m_1 = 0.014 M_{V_0}$ and vary m_2. The bound states' masses increase with the growing fermion UV mass as expected. One can also see that, due to the mass splitting, the vectors $A_{7,9,12,13}$ are no more degenerate with the $A_{1\pm4,\ldots}$. Also the $A_{1\pm4,\ldots}$ split into two groups — (3,1) and (1,3) under $SU(2) \times SU(2)$. The pNGBs show a Gell-Mann-Oakes-Renner behavior with the heavier UV fermion mass given that the lowest fermion mass is small. The N_c dependence for the masses and the decay constants are shown in fig. 5.6 and fig. 5.7 respectively.

5.4.3 Phenomenological Considerations

Our results could be compared with two kinds of phenomenological models. The pNGBs could either be considered as providing composite Higgs candidate as suggested in [80, 86, 194–196].

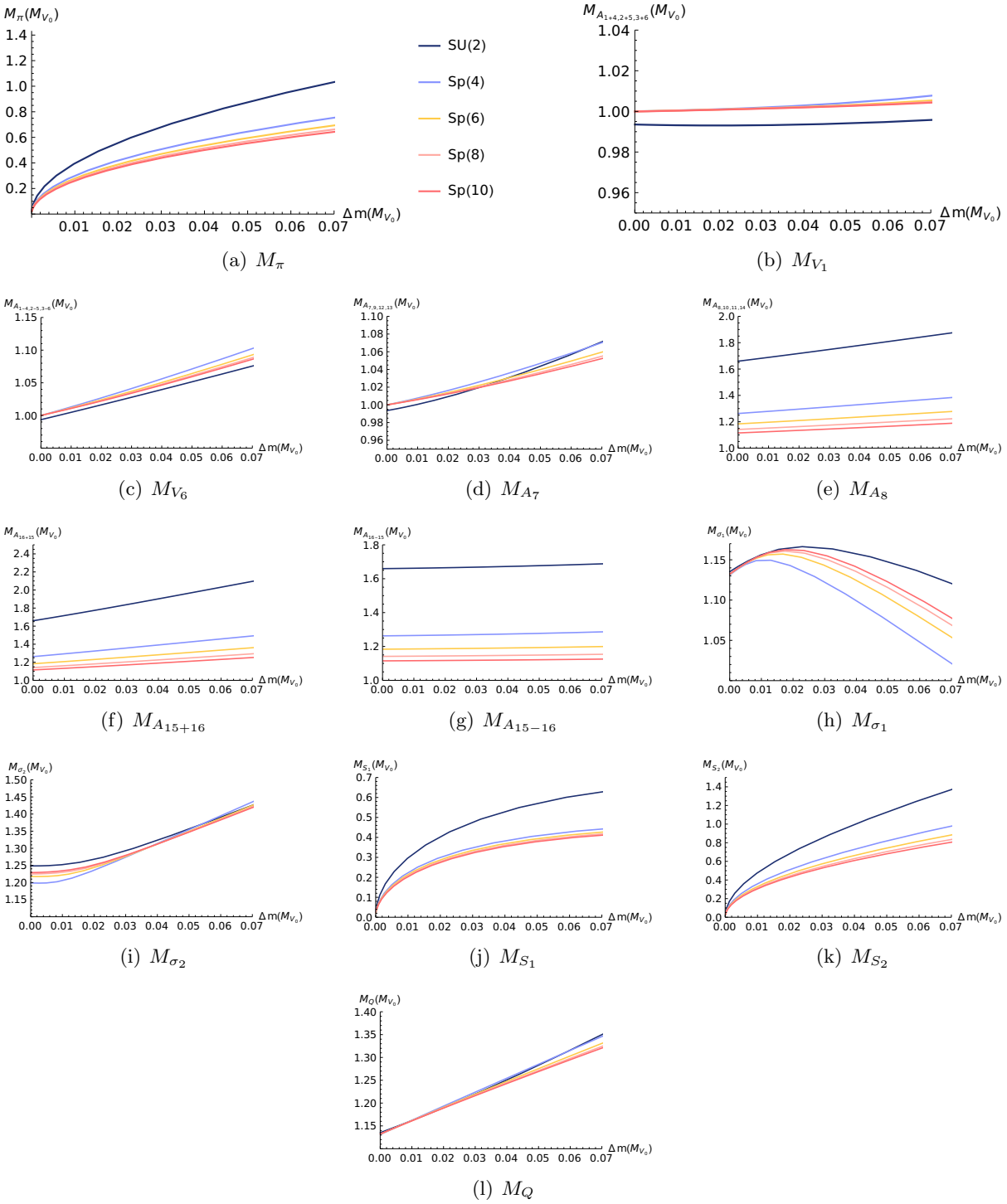

(a) M_π (b) M_{V_1}

(c) M_{V_6} (d) M_{A_7} (e) M_{A_8}

(f) $M_{A_{15+16}}$ (g) $M_{A_{15-16}}$ (h) M_{σ_1}

(i) M_{σ_2} (j) M_{S_1} (k) M_{S_2}

(l) M_Q

Figure 5.6: Dependence of meson masses on the difference of the UV fermion masses $\Delta m = m_2 - m_1$ for different gauge groups in unit M_{V_0}. We have set $B = 1$ and $m_1 = 0.014 M_{V_0}$.

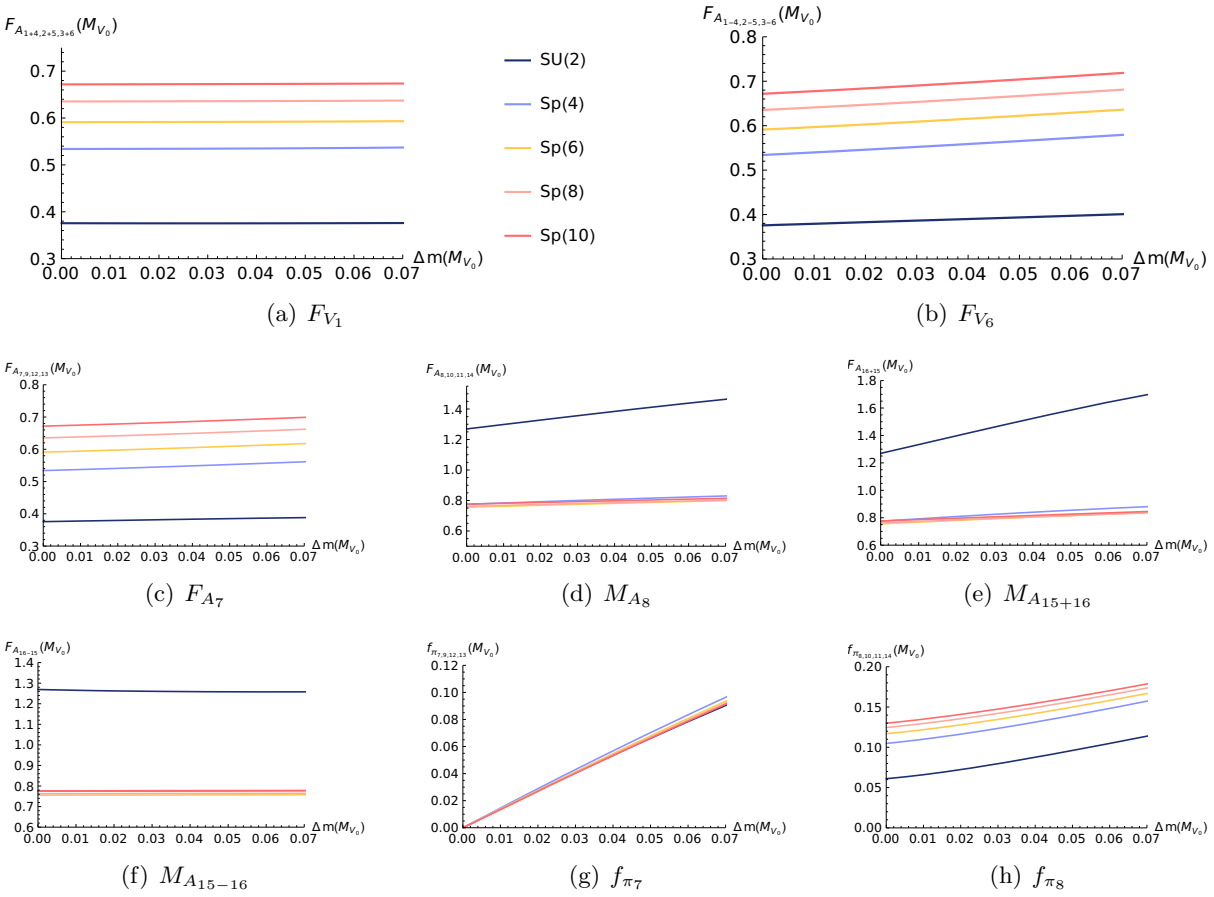

(a) F_{V_1} (b) F_{V_6}

(c) F_{A_7} (d) M_{A_8} (e) $M_{A_{15+16}}$

(f) $M_{A_{15-16}}$ (g) f_{π_7} (h) f_{π_8}

Figure 5.7: Meson decay constants vary with increasing UV fermion mass difference, with different gauge groups in the non-degenerate case. We have set $B = 1$ and $m_1 = 0.014$.

Alternatively, they could be the dark sector considered in [193, 197, 198], become dark matter candidates.

For the scenario that the pNGBs provide composite Higgs candidate, since we didn't include the interaction of the EW gauge gauge couplings and the top Yukawa coupling, we cannot set the Higgs mass to 125 GeV. But we expect our pNGB could be about 100 GeV so as to construct an EW model. The phenomenological aspect of an $SU(4) \to Sp(4)$ model is discussed in [196]. The EW gauge sector and the flavor gauge bosons — which are the later vector bound states — are embedded in two $SU(4)$ groups realized using the hidden local symmetry technique [40]. The spin-1 resonance is bound to be up to 2 TeV. Combining with our results require $M_{V_0}/M_\pi \gtrsim 10$. From fig. 5.6 this indicates that the UV fermion mass is $\lesssim 10^{-3} M_{V_0}$. We list the dictionary between our model and [196] in table 5.3. Note that this model predicts two more gauge singlets with masses around m_H which is still compatible with the present data. The lowest lying bound

$A_{1+4,2+5,3+6}$	$A_{1-4,2-5,3-6}$	$A_{7,9,12,13}$	$A_{8,10,11,14}$
$v^{0,\pm}$	$s^{0,\pm}$	$\tilde{s}^{0,\pm} + \tilde{v}^0$	$a^{0,\pm} + x^0$

Table 5.3: Dictionary between our notation, upper row, and the one of [196] for the spin-1 states. Our states A_{15} and A_{16} correspond to an admixture of $\tilde{x}^0$ of [196] and the additional $U(1)$ axial vector boson.

states have the mass ratios roughly around

$$M_{A_{1+4},A_{1-4},A_7} : M_{Q,S_1} : M_{S_2} : M_{A_8,A_{16+15},A_{16-15}} \simeq 1 : 1.1 : 1.2 : 1.26\,. \tag{5.4.12}$$

Given the mass bound on vector bound states, this indicates that it is challenging to observe the scalars Q and $S_{1,2}$ at the high luminosity LHC given that for masses above 2 TeV, their production cross section is low.

The second possibility is to consider the pNGBs as dark matter candidates in strongly interacting dart sectors [197]. If the pNGB is the only dark matter candidate in such theories, it's mass is strictly bound to be $m_\pi \lesssim 100$ MeV, which in turn is in tension with the observations from the Bullet Cluster [199]. In [199] it was suggested that this tension is relaxed if other dark matter candidates are present, such as a dark ρ-meson. They consider a strong-interacting dark sector, similar to QCD, with an $SU(N_{C_D})$ gauge group. For the dark ρ-meson's mass m_{ρ_D} in the range $1.45 \leq m_{\rho_D}/m_{\pi_D} \leq 2$, they found a dark-pion mass around 100 MeV where the relic density is roughly reproduced. This could be realized in our model when the UV fermion mass is within the range $0.02M_{V_0} \lesssim m \lesssim 0.1M_{V_0}$ for the degenerate case. In our model, the σ state is also a candidate for dark matter, which will contribute to the relic density too. We postpone the discussion on this to the future work. The same feature is expected in the mass-splitting case. The lowest lying pNGB S_1 is a singlet while the vector bound state is a triplet under $SU(2)_D$, the vector will not decay into $2S_1$, thus the πs are still the dark matter candidates.

5.5 From Composite Higgs to Technicolor: Including the NJL Interaction

In this section we construct the model which incorporates both the UV mass term and the NJL interactions. Such a construction is meant to contain the composite Higgs and technicolor and their transitions in a similar way suggested in [80] which is reviewed in section 2.3. In the following, we constraint our discussion in the model with an $SU(2)$ gauge group. For N_c dependence we expect a similar behavior as observed in the former two scenarios.

The starting point is the degenerate case in section 5.3 where all fermions have a common UV mass. In this case the pNGBs are the $\pi_{1,\ldots,5}$ and S. They contain a four-plet that transforms as (2,2) under $SU(2) \times SU(2)$ that is identified as the Higgs doublet in the composite Higgs models. On top of this construction, we add the NJL interaction eq. (5.1.16), which favors the embedding Q_4.

5.5.1 The Vacuum

Combing the mass term and the NJL term, one essentially changed the vacuum configuration to

$$X = \begin{pmatrix} 0 & L_0(\rho) & 0 & -Q(\rho) \\ -L_0(\rho) & 0 & Q(\rho) & 0 \\ 0 & -Q(\rho) & 0 & L_0(\rho) \\ Q(\rho) & 0 & -L_0(\rho) & 0 \end{pmatrix}. \tag{5.5.1}$$

This is previously given in eq. (5.1.13). This vacuum matrix is brought to the form of mass-splitting case as in eq. (5.4.1) by a unitary transformation in (5.1.14) as

$$U^T X U = \begin{pmatrix} 0 & L_0+Q & 0 & 0 \\ -L_0-Q & 0 & 0 & 0 \\ 0 & 0 & 0 & L_0-Q \\ 0 & 0 & -L_0+Q & 0 \end{pmatrix} = \begin{pmatrix} 0 & L_p & 0 & 0 \\ -L_p & 0 & 0 & 0 \\ 0 & 0 & 0 & L_m \\ 0 & 0 & -L_m & 0 \end{pmatrix}, \tag{5.5.2}$$

where $L_{p/m} = L_0 \pm Q$. The NJL interaction is turned on once $Q \neq 0$, i.e. $L_P > L_0$. This is realized by turning on two UV "masses". One is interpreted as the fermion mass m, which is held fixed, corresponding to the embedding L_0. The other one is interpreted as an NJL contribution, which we vary (increase from 0, pass m and beyond), corresponding to the embedding Q. At the point when $L_0 = Q$, there is a subtlety that needs a further discussion. If Q keeps increasing, L_m will become negative and it's profile will lie below the axis in fig. 5.1. We employed a phase rotation to flip the profile of L_m above the axis at this point. This is actually the preferred vacuum, since if consider the string picture, the strings stretching between the L_p and L_m branes have their length (thus the bound states' masses) minimized if L_m is flipped. We apply such a rotation for $L \geq Q$, where to arrive at the correct vacuum, we used the transformation in eq. (5.1.14)

$$U^T X U = \begin{pmatrix} 0 & L_0+Q & 0 & 0 \\ -L_0-Q & 0 & 0 & 0 \\ 0 & 0 & 0 & -L_0+Q \\ 0 & 0 & L_0-Q & 0 \end{pmatrix} = \begin{pmatrix} 0 & L_p & 0 & 0 \\ -L_p & 0 & 0 & 0 \\ 0 & 0 & 0 & -L_m \\ 0 & 0 & L_m & 0 \end{pmatrix}. \tag{5.5.3}$$

Note that at this point $L_m = L - Q$. Later in the calculations, we will rotate this too, to $L_m = Q - L$.

From this transformation we can see that the vacuum eq. (5.5.1) will break the $SU(4)$ to $SU(2) \times SU(2)$. More precisely, L_0 will break the generators T^8 with the associated GB π_2, $T^{10}(\pi_4)$, $T^{11}(\pi_3)$, $T^{14}(\pi_1)$, $T^{15}(\pi_5)$ and $T^{16}(S)$. Q will break $T^4(Q_1)$, $T^5(Q_2)$, $T^6(Q_3)$, $T^9(Q_5)$, $T^{11}(S)$, $T^{16}(\pi_3)$. The $T^{1+7,2+12,3+13}$ are the invariant custodial $SU(2)_D$. $T^{1-7,2-12,3-13}$ form a second $SU(2)$ which is broken explicitly by the NJL interactions through the NJL boundary conditions.

The equations of motion for $L_{p,m}$ are

$$\begin{aligned} \partial_\rho \left(\rho^3 \partial_\rho L_p\right) - \rho \Delta m^2 L_p - \frac{4B(L_p^2 - L_m^2)}{\rho} L_p = 0, \\ \partial_\rho \left(\rho^3 \partial_\rho L_m\right) - \rho \Delta m^2 L_m - \frac{4B(L_m^2 - L_p^2)}{\rho} L_m = 0, \end{aligned} \tag{5.5.4}$$

where $\Delta m^2 = \Delta m^2 \left[\log\left(\sqrt{\rho^2 + \frac{1}{2}(L_p^2 + L_m^2)}\right)\right] \equiv \Delta m^2({}_{njl})$, $r_{njl}^2 = \rho^2 + \frac{1}{2}(L_p^2 + L_m^2)$. The radial direction is now $r^2 = \mathrm{diag}(r_p^2, r_p^2, r_m^2, r_m^2)$, where $r_p^2 = \rho^2 + (L_0 + Q)^2$, $r_m^2 = \rho^2 + (L_0 - Q)^2$. To track the NJL contribution properly, we rotate back to the L_0-Q basis, where the equations are

$$\begin{aligned} \partial_\rho \left(\rho^3 \partial_\rho L_0\right) - \rho \Delta m^2 L_0 - \frac{16BQ^2}{\rho} L_0 = 0, \\ \partial_\rho \left(\rho^3 \partial_\rho Q\right) - \rho \Delta m^2 Q - \frac{16BL_0^2}{\rho} Q = 0. \end{aligned} \tag{5.5.5}$$

In the UV, L_0 should include the fermion mass, i.e. $L_0 \sim m + c_0/\rho^2$ where Q includes the NJL contribution $Q \sim \mathcal{J} + \langle \mathcal{O} \rangle / \rho^2$. Translate to the L_p-L_m basis, their UV behaviors are

$$L_p(\rho_{UV}) \sim \mathcal{J} + m + \frac{\langle \mathcal{O} \rangle}{\rho^2} + \frac{c_0}{\rho^2}, \quad L_m(\rho_{UV}) \sim m - \mathcal{J} + \frac{c_0}{\rho^2} - \frac{\langle \mathcal{O} \rangle}{\rho^2}. \tag{5.5.6}$$

More precisely, the NJL source term is introduced by the higher order operator [53, 176]

$$\mathcal{L}_{UV} = G \mathcal{O}^\dagger \mathcal{O}, \quad \mathcal{J} = G \langle \mathcal{O}^\dagger \rangle, \tag{5.5.7}$$

where

$$G = \frac{g_s^2}{\Lambda_{UV}^2} \quad \text{or} \quad g_s^2 = \frac{\mathcal{J} \Lambda_{UV}^2}{\langle \mathcal{O}^\dagger \rangle}. \tag{5.5.8}$$

Λ_{UV} is the UV cut-off. Below the critical value of g_s^2, the source term is zero $\mathcal{J} = m_{UV} = 0$. Once the source term m_{UV} is switched on by hand, the g_s^2 is above the critical value, i.e. the

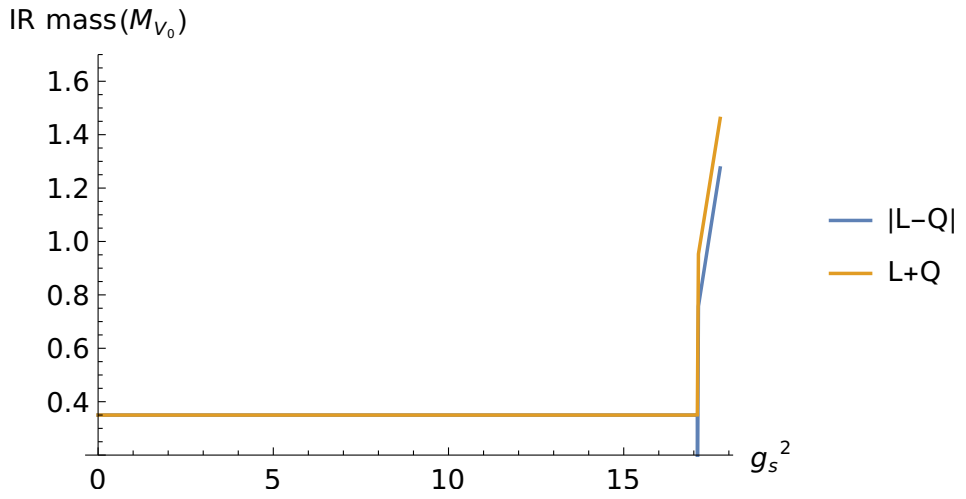

Figure 5.8: The vacuum of the $SU(2)$ gauge theory with NJL interactions. IR masses are plotted against the scalar NJL coupling g^2 in units of the vector mass M_{V_0}, $B = 0.1$, $m_L = 0.12\,M_{V_0}$, $\Lambda_{UV} = 12.1 M_{V_0}$. Initially we plotted the IR masses of $L+Q$ and $L-Q$. As soon as $Q > L$, we flip the $L-Q$ and show the IR mass of $Q-L$.

NJL interaction is present. The vev of the dual operator is read off by

$$\frac{Q'(\Lambda_{UV})}{-2\Lambda_{UV}^{-3}} = \langle \mathcal{O}^\dagger \rangle, \quad \mathcal{J} = m_{UV} - \frac{\langle \mathcal{O}^\dagger \rangle}{\Lambda_{UV}^2}. \tag{5.5.9}$$

Incorporating the discussion above, we set the following boundary conditions in solving the embeddings

$$\begin{aligned} & L_p(\rho_{IR,p}) = \rho_{IR,p}, \quad L_p'(\rho_{IR,p}) = 0, \quad L_p(\Lambda_{UV}) = m_{UV,p} \\ & \begin{cases} L_m(\rho_{IR,m}) = -\rho_{IR,m},\ L_m(\Lambda_{UV}) = m_{UV,m},\ L_m(\rho) \equiv -L_m(\rho), & m_{UV,m} < 0 \\ L_m(\rho_{IR,m}) = \rho_{IR,m},\ L_m(\Lambda_{UV}) = m_{UV,m}, & m_{UV,m} > 0 \end{cases} \\ & L_m'(\rho_{IR,m}) = 0. \end{aligned} \tag{5.5.10}$$

We see that at the point when $L_m = L_0 - Q = 0$, we rotate the solution to $L_m \equiv -L_m = Q - L_0$. We show the profiles for the two embeddings $L_{p,m}$ in fig. 5.8, where $L_0(UV)$ is fixed to $0.12 M_{V_0}$, and $B = 0.1$. This shows an expected second order phase transition at the critical value around $g_s^2 \sim 17$. The profiles increase fast since the NJL interaction is raising the Q vev to the cut-off scale Λ_{UV}. Since the composite Higgs model is realized when the two vacuums are only slightly misaligned, this implies that the transition from the composite Higgs model to the techincolor model is highly fine-tuned in g_s^2.

5.5.2 Fluctuations

Since the vacuums can be rotated to the same form with two split masses, the equations of motion for the fluctuations can be read off from the split-mass scenario with $L_{1,6} \to L_{p,m}$. However, one needs to take care of the mixed states in this case. We show all the equations of motion in appendix G including the corresponding boundary conditions.

The inclusion of the NJL contribution leads to non-trivial UV boundary conditions for some scalar fields. As can be seen from the fluctuation matrix, if we rotate it in the basis of eq. (5.5.1), the fluctuation matrix becomes

$$X_f = \begin{pmatrix} 0 & \sigma + Q_4 + iS + i\pi_3 & -Q_2 - \pi_2 - i\pi_1 - iQ_1 & Q_5 + \pi_4 + iQ_3 + i\pi_5 \\ -\sigma - Q_4 - iS - i\pi_3 & 0 & -Q_5 + \pi_4 + iQ_3 - i\pi_5 & -Q_2 + \pi_2 + iQ_1 - i\pi_1 \\ \pi_2 + Q_2 + iQ_1 + i\pi_1 & Q_5 - \pi_4 - iQ_3 + i\pi_5 & 0 & \sigma - Q_4 + iS - i\pi_3 \\ -Q_5 - \pi_4 - i\pi_5 - iQ_3 & Q_2 - \pi_2 - iQ_1 + i\pi_1 & -\sigma + Q_4 - iS + i\pi_3 & 0 \end{pmatrix}. \tag{5.5.11}$$

The $Q_{1,2,3,4}$ fields feel the NJL. The $\pi_{1,2,3,4}$ are simply phases of Q_i thus they are not affected by the NJL contribution.

Even though $Q_{1,2,3,5}$ have the same set of equations of motion, only the $Q_{1,2,3}$ feel the NJL interaction while the Q_5 doesn't. Therefore we impose the NJL boundary condition to $Q_{1,2,3}$

$$\begin{aligned} f(\Lambda_{UV}) = \frac{(g_s^2+1)c}{\Lambda_{UV}^2}, \quad f'(\Lambda_{UV}) = -2\Lambda_{UV}^{-3}c, \quad f'(IR) = 0, \\ \phi(\Lambda_{UV}) = \pm\sqrt{2} + \frac{\Lambda_{UV} b}{-2}, \quad \phi'(\Lambda_{UV}) = b, \quad \phi'(IR) = 0, \end{aligned} \tag{5.5.12}$$

where f denotes the fields that matches with the NJL coupling in the UV and ϕ denotes the ϕ_js, which asymptotes to $\pm\sqrt{2}$ in the UV before and after the unitary rotation. c is the vev, corresponding to the $\langle\mathcal{O}\rangle$ in the above discussion. g_s^2 is the NJL coupling found in solving the embeddings. For the points below the critical value of g_s^2, i.e. when $Q = 0$, one needs to apply the NJL boundary condition to the fluctuations with g_s^2 values put in by hand. The NJL interaction split the 4-plet of $Q_{1,2,3,5}$ to a triplet $Q_{1,2,3}$ and a singlet Q_5 under $SU(2)_V$.

Q_4 and σ are fluctuations around the corresponding vacuum, their equations of motion are

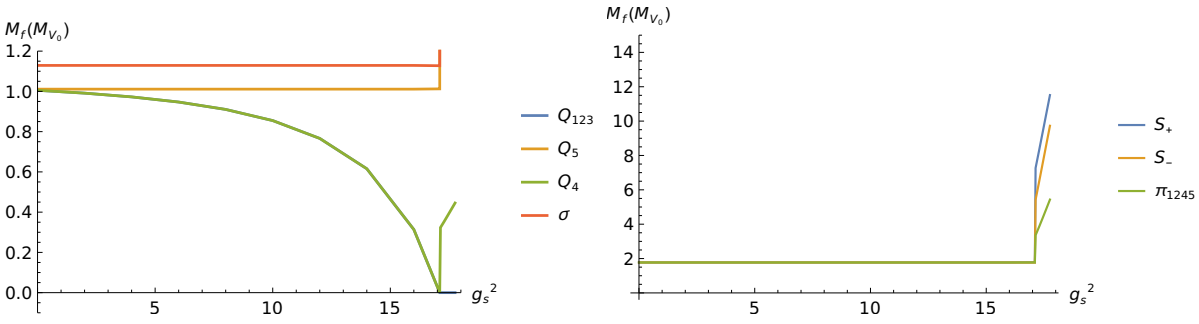

(a) M_f^2, $f = Q_{123}, Q_4, Q_5, \sigma$ (b) M_f^2, $f = \pi_{1245}, S_+, S_-$

Figure 5.9: Scalar bound states' masses vary with increasing scalar NJL coupling g_s^2, with gauge group $SU(2)$, $B = 0.1$, $m_L = 0.12M_{V_0}$, $_{UV} = 12.1M_{V_0}$.

mixed

$$\begin{aligned}
&\partial_\rho\left(\rho^3\partial_\rho\sigma\right) - \rho\Delta m^2\sigma - \frac{\rho L_0^2}{r_{njl}^4}\Delta m^{2\prime}\sigma - \frac{16B}{\rho}Q^2\sigma + \frac{\rho^3M^2}{2}\left(\frac{1}{r_p^4}+\frac{1}{r_m^4}\right)\sigma \\
&\qquad -\frac{32BL_0Q}{\rho}Q_4 - \frac{L_0Q\rho}{r_{njl}^2}\Delta m^{2\prime}Q_4 + \frac{\rho^3M^2}{2}\left(\frac{1}{r_p^4}-\frac{1}{r_m^4}\right)Q_4 = 0, \\
&\partial_\rho\left(\rho^3\partial_\rho Q_4\right) - \rho\Delta m^2 Q_4 - \frac{\rho Q^2}{r_{njl}^4}\Delta m^{2\prime}Q_4 - \frac{16B}{\rho}L_0^2Q_4 + \frac{\rho^3M^2}{2}\left(\frac{1}{r_p^4}+\frac{1}{r_m^4}\right)Q_4 \\
&\qquad -\frac{32BL_0Q}{\rho}\sigma - \frac{L_0Q\rho}{r_{njl}^2}\Delta m^{2\prime}\sigma + \frac{\rho^3M^2}{2}\left(\frac{1}{r_p^4}-\frac{1}{r_m^4}\right)\sigma = 0.
\end{aligned} \tag{5.5.13}$$

In the above equations $\Delta m^{2\prime} = \frac{\partial\Delta m^2}{\partial \arg}$, $\arg = \log(r_{njl})$ is the argument of Δm^2, where $r_{njl} = \rho^2 + \frac{1}{2}(L_p^2 + L_m^2)$. We impose the NJL boundary condition to Q_4 while require the σ asymptotes to 0 in the UV. All the other fields are required to vanish in the UV. We plot the scalar mass against the NJL coupling g_s^2 in fig. 5.9 for $B = 0.1$, $m = 0.12M_{V_0}$ and $\Lambda_{UV} = 12.1M_{V_0}$.

From this plot we can see that, below the critical coupling, only $Q_{1,2,3,4}$ are affected by the NJL interaction. Their masses fall to 0 at the critical coupling and their potential will become unstable if Q increase the NJL coupling across the critial value.

Above the critical coupling, the $Q_{1,2,3}$ have massless Goldstone solutions corresponding to the breaking of an $SU(2)$ axial symmetry. The Q_4 field is like a σ field in the technicolor model, which grows sharply with the NJL vev Q. The other scalar fields are insensitive to the NJL interaction until the Q vev becomes larger than the L_0 vev, where their masses increases together with the ever larger NJL coupling. The $\pi_{1,2,4}$ form a triplet that is degenerate with the π_5 which is a singlet. The other scalars σ, Q_5 $S_\pm = S \pm \pi_3$ are singlets.

In solving the vectors, we require them to vanish in the UV. We plot their spectrum against the

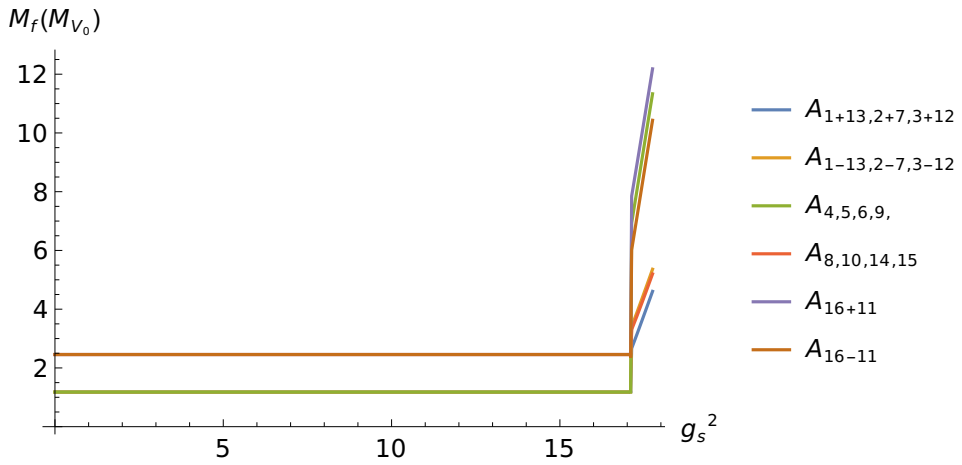

Figure 5.10: Spin-1 bound states' masses. The multiplets are: two triplets associated with generators $1 \pm 13, 2 \pm 7, 3 \pm 12$; two sets of degenerate triplet and singlet associated with generators $4, 5, 6, 9$ and $8, 10, 14, 15$; and two singlets associated with generators 16 ± 11.

NJL coupling g_s^2 in fig. 5.10. The vectors $V_{1+13,2+7,3+12}$ and $V_{1-13,2-7,3-12}$ transform as $\mathbf{3}$ of $SU(2)_V$ ($(\mathbf{1},\mathbf{3})+(\mathbf{3},\mathbf{1})$ of $SU(2)_L \times SU(2)_R$). The axial vectors $A_{4,5,6,9}$ and $A_{8,10,14,15}$ transform both as $\mathbf{3}+\mathbf{1}$ of $SU(2)_V$ ($(\mathbf{2},\mathbf{2})$ of $SU(2)_L \times SU(2)_R$). The rest two axial vectors $A_{16\pm11}$ are both singlets of $SU(2)_V$ ($SU(2)_L \times SU(2)_R$). Below the critical coupling, their masses behave simply as in the degenerate case. Once the NJL interaction sets in, some of the vectors become axial-vectors due to the additional symmetry breaking. All of the masses increase sharply with the NJL coupling.

We also compute the decay constants and plot them against the NJL coupling in fig. 5.11. They increase also with the NJL coupling in the same manner as the spectrum. Especially we show in fig. 5.11(d) the ratio of the EW breaking vev over the global symmetry breaking vev. As shown by the sharp rise after the critical coupling, the transition from the composite Higgs to the technicolor requires a highly fine-tuned g_s^2.

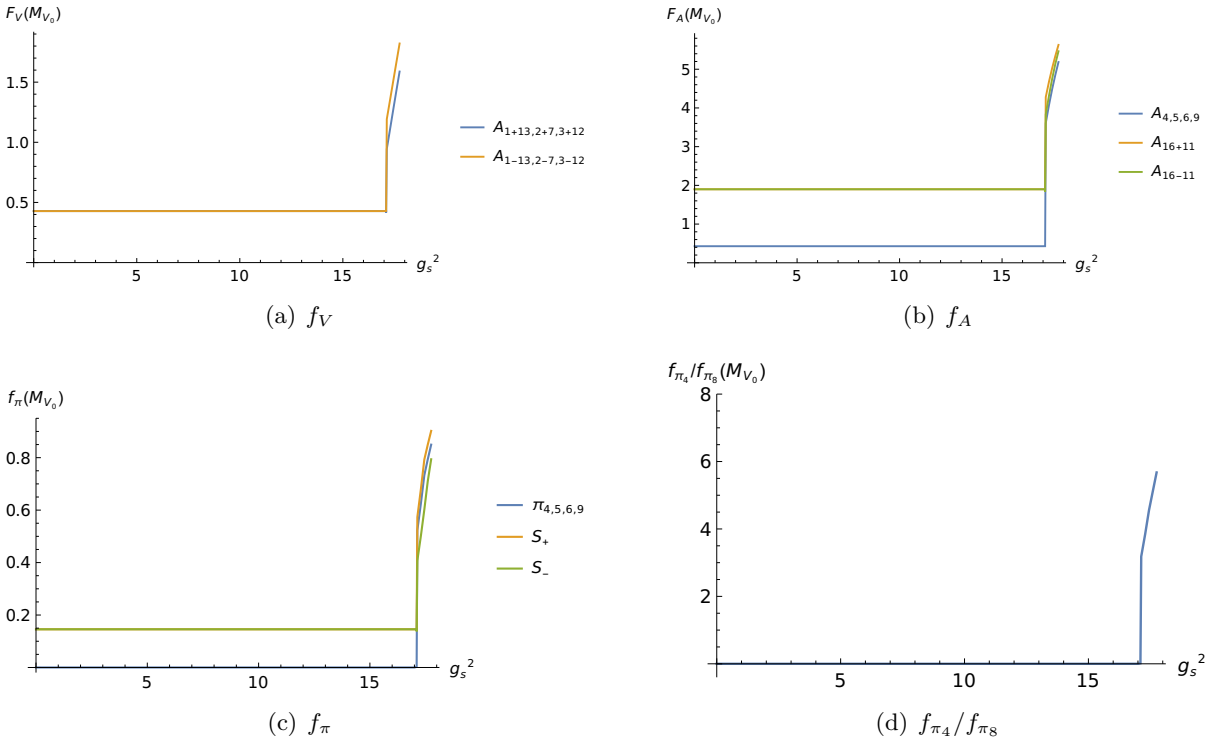

(a) f_V (b) f_A

(c) f_π (d) f_{π_4}/f_{π_8}

Figure 5.11: Meson decay constants vary with increasing scalar NJL coupling g_s^2, with gauge group $SU(2)$, $B = 0.1$.

Chapter 6

Conclusions and Outlook

In this thesis, we show the construction of a holographic model that includes both the composite Higgs and the technicolor models and manifests a transition between the two phases. Our starting point is an abelian dynamical AdS/YM model developed in [52, 53]. This is a bottom-up model, which encodes the essence of the holographic top-down model descend from the string theory and the gauge/gravity duality. Especially, the model utilizes the property that the radial direction of the AdS space is dual to an RG-flow in the field theory, and incorporates the gauge theory running explicitly through the running of the anomalous dimension of the dual quark's mass. In this way, the symmetry breaking in the dual theory is realized dynamically in the holographic model, instead of placing hard cut-offs as an ansatz. We combined this model with a top-down model that shares a non-abelian structure in the bulk gauge theory from [178]. This results in the non-abelian AdS/YM theory developed in chapter 4. While constructing the model, we also developed the corresponding numerical tools to solve the coupled equations in the holographic language. As a proof, we tested our construction against the QCD meson spectrum. Our results are at 20%, most of the cases 10% level of the experimental data. The finer structure of the QCD meson spectrum is predicted, which shows the power of incorporating the non-abelian structure in the holographic model.

Having tested the first principles, we move on to achieve the aim of our project, which is the holographic composite Higgs model. There have been various composite Higgs models' constructions in the field theory, some of them also descend from models containing extra dimensions. The composite Higgs model we realized was initially suggested in [62, 80, 97]. The model realizes a $Sp(2N)$ gauge symmetry with two Dirac fermions in the fundamental. In particular, the mass eigenstates of the pNGBs are admixtures of the pNGBS from two

different symmetry breakings — composite Higgs like and technicolor like (EW). By dialing the mixing angle, one switches from symmetry conserved phase to a composite Higgs phase (when the mixing angle is tiny) and then to the technicolor phase. We construct a holographic model that incorporates these properties in chapter 5. This is realized using the non-abelian holographic model we developed. In that we discussed three scenarios — degenerate and non-degenerate flavor structure and inserting both fermion masses and the NJL interaction term. We looked first into the model with degenerate flavor structure, this corresponds to a pure composite Higgs model when the UV fermion mass is turned on. Then we split the flavor structure by giving different masses to femions that are associated to different flavors. This simply corresponds to a composite Higgs model with non-abelian flavor structure. Then we move on to insert an NJL interaction term holographically on top of the degenerate scenario. Such a construction manifests a superposition of two different symmetry breakings — one is the spontaneous symmetry breaking of the global flavor group, the other is the EW symmetry breaking realized in the technicolor sense. By performing a unitary rotation, one can rotate this scenario back to the non-degenerate flavor structure, which is the second scenario we considered. The phase transition from the composite Higgs model to the technicolor model is controlled by the NJL coupling constant g_s, which is highly fine tuned. At each step we calculated the bound states' spectrum and their decay constants. For the results that have lattice data to compare with, they show a good agreement.

Of course much could be done along this line. First we need to emphasize that our constructions are restricted to the bosonic part of the theory. Incorporating the non-abelian structure will also result in a finer baryon spectrum in the holographic model. One way to include the baryon states is to add bulk fermion fields. In the original top-down language, they are dual to the superpartners of the mesons, the so-called mesinos. One can approximate the baryon states with these mesino states as suggested in [31]. For abelian dynamical AdS/YM model this has already been done in [52, 53]. These baryon states are potential candidates for top-partners, which are essential ingredients when constructing composite Higgs model that explains the large mass hierarchy of the top quark. Aside from the baryons, one can also construct holographic models using the technique we developed to let it dual to different composite Higgs models. The advantage is that such a holographic model provides naturally a UV-completion for the field theory. Possible minimal UV-complete composite Higgs models that can be made holographic are $SU(2N) \to Sp(2N)$ and $SU(N) \times SU(N) \to SU(N)$. The potential of our non-abelian dynamical AdS/YM model is certainly not restrict to composite Higgs models. One can put on the dual theory any non-conformal Yang-Mills field theory with non-abelian structure and

make predictions on the bound states' spectrum and other physical observables. Also, such a holographic model serves as a good alternative of lattice calculations. We hope our work could stimulate more lattice studies on this subject, and potential model building in the BSM physics.

Appendix A

Derivation of Equations of Motion in the Top-Down Model

In this appendix we show the calculations of some of the equations in the top-down non-abelian model in [178]. The calculations in the non-abelian bottom-up model is based on this.

A.1 Notations

We unify the notations for this appendix section. Indices are assigned as follows: m, n= 0,...,9; r, s, p, q, t= 0,...,7; a, b= 5, 6, 7; μ, ν, α, β= 0,...,3; $\rho = 4$.

The metric is

$$ds_{10}^2 = e^{\frac{\Phi(r)}{2}} \left(\frac{r^2}{R^2} A^2(r) \eta_{\mu\nu} dx^\mu dx^\nu + \frac{R^2}{r^2} \left[d\rho^2 + \rho^2 d\Omega_3^2 + (dX^8)^2 + (dX^9)^2 \right] \right), \tag{A.1.1}$$

and therefore

$$G_{88} = e^{\frac{\Phi(r)}{2}} \frac{R^2}{r_i^2} \delta_{88} \qquad G_{88} = e^{\frac{\Phi(r)}{2}} \frac{R^2}{r_i^2} \delta_{99}. \tag{A.1.2}$$

The $\bar{a}^{rs}$:

$$\bar{a}^{rs}\Big|_{w_i} = \begin{pmatrix} \frac{R^2}{A_i^2 r_i^2} e^{-\frac{\Phi(r_i)}{2}} \eta_{\mu\nu} & & \\ & \frac{r_i^2}{R^2} \frac{e^{-\frac{\Phi(r_i)}{2}}}{1+\left(\partial_\rho w_i^2\right)} & \\ & & \frac{r_i^2}{R^2 \rho^2} e^{-\frac{\Phi(r_i)}{2}} g^{ab} \end{pmatrix}, \tag{A.1.3}$$

where $A_i = A(r_i)$.

$$\begin{aligned}
\bar{F} =& e^{-\Phi(r_i)}\sqrt{-\det \bar{a}_{rs}} = e^{-\Phi(r_i)}\left[-\det(G_{rs}+G_{99}\partial_r\bar{X}^9\partial_s\bar{X}^9)\right]^{\frac{1}{2}} \\
=& e^{-\Phi(r_i)}\det\left[-\begin{pmatrix} G_{\mu\nu} & & \\ & G_{\rho\rho}+G_{99}\partial_\rho\bar{X}^9\partial_\rho\bar{X}^9 & \\ & & G_{ab}\end{pmatrix}\right]^{\frac{1}{2}} \\
=& e^{-\Phi(r_i)}\Bigg[-\left(e^{\frac{\Phi(r_i)}{2}}\right)^4\left(\frac{r_i^2}{R^2}A(r_i)^2\right)^4(-1)(1)^3\left(e^{\frac{\Phi(r_i)}{2}}\frac{R^2}{r_i^2}+e^{\frac{\Phi(r_i)}{2}}\frac{R^2}{r_i^2}(\partial_\rho w_i)^2\right) \\
& \times\left(e^{\frac{\Phi(r_i)}{2}}\right)^3\left(\frac{R^2}{r_i^2}\rho^2\right)^3\det(g_{ab})\Bigg]^{\frac{1}{2}} \\
=& e^{-\Phi(r_i)}\left[\left(e^{\frac{\Phi(r_i)}{2}}\right)^8\left(\frac{r_i^2}{R^2}\right)^4A(r_i)^8\left(\frac{R^2}{r_i^2}\right)^4\left(1+(\partial_\rho w_i)^2\right)\rho^6\det(g_{ab})\right]^{\frac{1}{2}} \\
=& e^{\Phi(r_i)}\rho^3A(r_i)^4\sqrt{\det(g_{ab})\left[1+(\partial_\rho w_i)^2\right]},
\end{aligned} \tag{A.1.4}$$

$$F_i = \frac{e^{\Phi(r_i)}A_i^4}{\sqrt{1+(\partial_\rho w_i)^2}}, \qquad K_{r_i} = \partial_{r^2}\log\left(e^{\Phi(r_i)}A_i^4\right). \tag{A.1.5}$$

A.2 Scalar Lagrangian, Only ϕ^8

In this section we compute the ϕ^8 part of the scalar Lagrangian, corresponding to eq.(33) in [178].

Consider only ϕ^8 fluctuations, i.e. set $\phi^9 = A_s = 0$, then the two-flavor D7-brane action [178]

$$\begin{aligned}
S_{N_f=2} = \tau_7\int d^8\xi\,\mathrm{STr}\Bigg\{& e^{-\Phi}\sqrt{-\det(\bar{a}_{rs})}\Bigg(1+\frac{1}{2}\mathrm{Tr}_{rs}(\bar{a}^{-1}a^{(1)})+\frac{1}{8}\left(\mathrm{Tr}_{rs}(\bar{a}^{-1}a^{(1)})\right)^2 \\
& -\frac{1}{4}\mathrm{Tr}_{rs}\left((\bar{a}^{-1}a^{(1)})^2\right)+\frac{1}{2}\mathrm{Tr}_{rs}(\bar{a}^{-1}a^{(2)})-\frac{1}{8}G_{88}G_{99}\left((\phi_1^8)^2+(\phi_2^8)^2\right)v^2+...\Bigg)\Bigg\}
\end{aligned} \tag{A.2.1}$$

reduces to

$$S_{N_f} = \tau_7\int d^8\xi\,\mathrm{STr}\left\{\underbrace{e^{-\Phi}\sqrt{-\det(\bar{a}_{rs})}}_{\bar{F}}\left[1+\frac{1}{2}\mathrm{Tr}_{rs}(\bar{a}^{-1}a^{(2)})+(\frac{1}{8}G_{88}G_{99})\left((\phi_1^8)^2+(\phi_2^8)^2\right)v^2+...\right]\right\}. \tag{A.2.2}$$

So the Lagrangian is

$$\begin{aligned}\mathcal{L}^{(2)}_{\phi^8} =&\mathrm{STr}\left\{e^{-\Phi}\sqrt{-\det(\bar{a}_{rs})}\left[1+\frac{1}{2}\mathrm{Tr}_{rs}(\bar{a}^{-1}a^{(2)})-(\frac{1}{8}G_{88}G_{99})\left((\phi^8_1)^2+(\phi^8_2)^2\right)v^2+...\right]\right\}\\ =&\underbrace{\mathrm{STr}\bar{F}}_{\text{term A}}+\underbrace{\frac{1}{2}\mathrm{STr}\left[\bar{F}\mathrm{Tr}_{rs}(\bar{a}^{-1}a^{(2)})\right]}_{\text{term B}}+\frac{1}{8}\mathrm{STr}\left[(\bar{F}G_{88}G_{99})\left((\phi^8_1)^2+(\phi^8_2)^2\right)v^2+...\right].\end{aligned} \tag{A.2.3}$$

The last term need not to be modified, we only need to calculate the first two terms. In the Lagrangian, term A is

$$\text{term A}=\mathrm{STr}\bar{F}=\mathrm{STr}\left(\frac{\partial\bar{F}}{\partial r^2}dr^2\right)=\frac{\partial\bar{F}}{\partial r^2}dr^2\Big|_{w_1}+\frac{\partial\bar{F}}{\partial r^2}dr^2\Big|_{w_2}, \tag{A.2.4}$$

since $r^2=\rho^2+\left(\omega\tau_0+v\tau_3+(\phi^9)\right)^2+\left(\phi^8\right)^2$, when $\phi^9=0$ we have

$$dr^2=(\phi^8)^2\Big|_{\phi^9=0}=\frac{1}{4}\begin{pmatrix}\phi^8_+ & \phi^8_{12}\\ \phi^8_{21} & \phi^8_-\end{pmatrix}\begin{pmatrix}\phi^8_+ & \phi^8_{12}\\ \phi^8_{21} & \phi^8_-\end{pmatrix}=\frac{1}{4}\begin{pmatrix}(\phi^8_+)^2+\phi^8_{12}\phi^8_{21} & \phi^8_+\phi^8_{12}+\phi^8_{12}\phi^8_-\\ \phi^8_+\phi^8_{21}+\phi^8_{21}\phi^8_- & (\phi^8_-)^2+\phi^8_{12}\phi^8_{21}\end{pmatrix}, \tag{A.2.5}$$

where dr^2 is interpreted as the fluctuations thus the ϕ^8. Therefore when evaluating dr^2 on the branes we have

$$dr^2\Big|_{\substack{w_1\\ \overline{w_2}}}=\frac{1}{4}\left[(\phi^8_\pm)^2+\phi^8_{12}\phi^8_{21}\right]=\frac{1}{4}\left[(\phi^8_\pm)^2+(\phi^8_1-i\phi^8_2)(\phi^8_1+i\phi^8_2)\right]=\frac{1}{4}\left[(\phi^8_\pm)^2+(\phi^8_1)^2+(\phi^8_2)^2\right], \tag{A.2.6}$$

so we get

$$\text{Term A}=\frac{1}{4}\partial_{r^2}\bar{F}\Big|_{w_1}\left[(\phi^8_+)^2+(\phi^8_1)^2+(\phi^8_2)^2\right]+\frac{1}{4}\partial_{r^2}\bar{F}\Big|_{w_2}\left[(\phi^8_-)^2+(\phi^8_1)^2+(\phi^8_2)^2\right]. \tag{A.2.7}$$

We then calculate Term B:

$$\text{Term B}=\frac{1}{2}\mathrm{STr}\left[\bar{F}\mathrm{Tr}_{rs}(\bar{a}^{-1}a^{(2)})\right]=\frac{1}{2}\mathrm{STr}\left[\bar{F}(\bar{a}^{-1})_{sr}(a^{(2)})_{rs}\right]=\frac{1}{2}\mathrm{Tr}\left[\bar{F}(\bar{a})^{rs}G^{88}\partial_r\phi^8\partial_s\phi^8\right], \tag{A.2.8}$$

where

$$\partial_r\phi^8\partial_s\phi^8=\frac{1}{4}\begin{pmatrix}\partial_r\phi^8_+ & \partial_r\phi^8_{12}\\ \partial_r\phi^8_{21} & \partial_r\phi^8_-\end{pmatrix}\begin{pmatrix}\partial_s\phi^8_+ & \partial_s\phi^8_{12}\\ \partial_s\phi^8_{21} & \partial_s\phi^8_-\end{pmatrix}=\frac{1}{4}\begin{pmatrix}\partial_r\phi^8_+\partial_s\phi^8_++\partial_r\phi^8_{12}\partial_s\phi^8_{21} & \partial_r\phi^8_+\partial_s\phi^8_{12}+\partial_r\phi^8_{12}\partial_s\phi^8_-\\ \partial_r\phi^8_{21}\partial_s\phi^8_++\partial_r\phi^8_-\partial_s\phi^8_{21} & \partial_r\phi^8_{21}\partial_s\phi^8_{12}+\partial_r\phi^8_-\partial_s\phi^8_-\end{pmatrix}. \tag{A.2.9}$$

And

$$\bar{F}\bar{a}^{rs}G_{88} = \begin{pmatrix} \bar{F}\bar{a}^{rs}G_{88}\Big|_{w_1} & 0 \\ 0 & \bar{F}\bar{a}^{rs}G_{88}\Big|_{w_2} \end{pmatrix}. \tag{A.2.10}$$

Then multiply the matrices $\bar{F}\bar{a}^{rs}G_{88}$ and $\partial_r\phi^8\partial_s\phi^8$ and take the trace in the flavor space, we find the Term B is:

$$\begin{aligned}
\text{Term B} =& \frac{1}{8}\left[\bar{F}\bar{a}^{rs}G_{88}\Big|_{w_1}(\partial_r\phi^8_+\partial_s\phi^8_+ + \partial_r\phi^8_{12}\partial_s\phi^8_{21}) + \bar{F}\bar{a}^{rs}G_{88}\Big|_{w_2}(\partial_r\phi^8_-\partial_s\phi^8_- + \partial_r\phi^8_{12}\partial_s\phi^8_{21})\right] \\
=& \frac{1}{8}\Bigg[\bar{F}\bar{a}^{rs}G_{88}\Big|_{w_1}(\partial_r\phi^8_+\partial_s\phi^8_+ + \partial_r\phi^8_1\partial_s\phi^8_1 + \partial_r\phi^8_2\partial_s\phi^8_2 - i\underbrace{(\partial_r\phi^8_2\partial_s\phi^8_1 - \partial_r\phi^8_1\partial_s\phi^8_2)}_{=0,\text{ we can only have r=s}} \\
& + \bar{F}\bar{a}^{rs}G_{88}\Big|_{w_2}(+\to -)\Bigg] \\
=& \frac{1}{8}\left[\bar{F}\bar{a}^{rs}G_{88}\Big|_{w_1}\partial_r\phi^8_+\partial_s\phi^8_+ + \bar{F}\bar{a}^{rs}G_{88}\Big|_{w_2}\partial_r\phi^8_-\partial_s\phi^8_-\right] \\
& + \frac{1}{8}\left(\bar{F}\bar{a}^{rs}G_{88}\Big|_{w_1} + \bar{F}\bar{a}^{rs}G_{88}\Big|_{w_2}\right)\left(\partial_r\phi^8_1\partial_s\phi^8_1 + \partial_r\phi^8_2\partial_s\phi^8_2\right),
\end{aligned} \tag{A.2.11}$$

where as noted in the second step, we can only have diagonal terms ($r = s$) since $\bar{a}^{rs}$ is diagonal. Finally add the three terms together we arrive at the equation

$$\begin{aligned}
\mathcal{L}^{(2)}_{\phi^8} =& \frac{1}{4}\partial_{r^2}\bar{F}\Big|_{w_1}\left[(\phi^8_+)^2 + (\phi^8_1)^2 + (\phi^8_2)^2\right] + \frac{1}{4}\partial_{r^2}\bar{F}\Big|_{w_2}\left[(\phi^8_-)^2 + (\phi^8_1)^2 + (\phi^8_2)^2\right] \\
& + \frac{1}{8}\left[\bar{F}\bar{a}^{rs}G_{88}\Big|_{w_1}\partial_r\phi^8_+\partial_s\phi^8_+ + \bar{F}\bar{a}^{rs}G_{88}\Big|_{w_2}\partial_r\phi^8_-\partial_s\phi^8_-\right] \\
& + \frac{1}{8}\left(\bar{F}\bar{a}^{rs}G_{88}\Big|_{w_1} + \bar{F}\bar{a}^{rs}G_{88}\Big|_{w_2}\right)\left(\partial_r\phi^8_1\partial_s\phi^8_1 + \partial_r\phi^8_2\partial_s\phi^8_2\right) \\
& + \frac{1}{8}\left[\left(\bar{F}G_{88}G_{99}\Big|_{w_1} + \bar{F}G_{88}G_{99}\Big|_{w_2}\right)\left((\phi^8_1)^2 + (\phi^8_2)^2\right)v^2 + ...\right].
\end{aligned} \tag{A.2.12}$$

The equation of motion of $\phi^8_{1,2\pm}$ can be easily derived using Euler-Lagrange equation.

A.3 Equation of Motion of $\phi^8_{1,2}$ Fields, Non-SUSY Case

Use the Lagrangian eq. (A.2.12), we get the eom of ϕ^8_i $(i = 1, 2)$ are:

$$\begin{aligned}
&\frac{\partial \mathcal{L}^{(2)}_{\phi^8}}{\partial \phi^8_i} - \partial_p \frac{\partial \mathcal{L}^{(2)}_{\phi^8}}{\partial(\partial_p \phi^8_i)} = 0 \\
&= \underbrace{\frac{1}{4}\left(\partial_{r^2}\bar{F}\Big|_{w_1} + \partial_{r^2}\bar{F}\Big|_{w_2}\right)\cdot 2\phi^8_i}_{\text{term A}} \underbrace{-\frac{v^2}{8}\left[\left(\bar{F}G_{88}G_{99}\right)\Big|_{w_1} + \left(\bar{F}G_{88}G_{99}\right)\Big|_{w_2}\right]\cdot 2\phi^8_i}_{\text{term B}} \\
&\underbrace{-\partial_p\left\{\frac{1}{8}\left[\left(\bar{F}G_{88}\bar{a}^{rs}\right)\Big|_{w_1} + \left(\bar{F}G_{88}\bar{a}^{rs}\right)\Big|_{w_2}\right]\cdot \partial_r \phi^8_i \delta^p_s \cdot 2\right\}}_{\text{term C}}.
\end{aligned} \tag{A.3.1}$$

In the following we calculate the three terms separately:

term A:

$$\begin{aligned}
\partial_{r^2}\bar{F}\Big|_{w_i} &= \partial_{r^2}\left(e^{\Phi(r_i)}\rho^3 A_i^4 \sqrt{\det(g_{ab})\left[1+(\partial_\rho w_i)^2\right]}\right) \\
&= e^{\Phi(r_i)}A_i^4 \partial_{r^2}\log\left(e^{\Phi(r_i)}A_i^4\right)\rho^3\sqrt{\det g_{ab}}\sqrt{1+(\partial_\rho w_i)^2} \\
&= F_i\rho^3\left[1+(\partial_\rho w_i)^2\right]\partial_{r^2}\log\left(e^{\Phi(r_i)}A_i^4\right)\sqrt{\det g_{ab}} \\
&= F_i\rho^3\left[1+(\partial_\rho w_i)^2\right]K_{r_i}\sqrt{\det g_{ab}},
\end{aligned} \tag{A.3.2}$$

where F_i and K_{r_i} are defined in eq. (A.1.5). So we get

$$\text{term A} = \frac{1}{2}\rho^3\sqrt{\det g_{ab}}\left\{F_1\left[1+(\partial_\rho w_1)^2\right]K_{r_1} + 1 \to 2\right\}\phi^8_i. \tag{A.3.3}$$

term B:

$$\begin{aligned}
&-\frac{v^2}{8}\left[\left(\bar{F}G_{88}G_{99}\right)\Big|_{w_1} + \left(\bar{F}G_{88}G_{99}\right)\Big|_{w_2}\right]\cdot 2\phi^8_i \\
&= -\frac{v^2}{4}\rho^3\sqrt{\det g_{ab}}\left[\underbrace{e^{2\Phi(r_1)}A_1^4\left(\frac{R}{r_1}\right)^4\sqrt{1+(\partial_\rho w_1)^2}}_{\equiv G_1} + 1 \to 2\right]\phi^8_i \\
&= -\frac{v^2}{4}\rho^3\sqrt{\det g_{ab}}(G_1+G_2)\phi^8_i.
\end{aligned} \tag{A.3.4}$$

term C:

$$
\begin{aligned}
&\partial_p\left[\left(\bar{F}G_{88}\bar{a}^{rs}\right)\Big|_{w_1}\cdot\partial_r\phi_i^8\right]\\
=&\partial_\mu\left[\left(\bar{F}G_{88}\bar{a}^{\nu\mu}\right)\Big|_{w_1}\cdot\partial_\nu\phi_i^8\right]+\partial_\rho\left[\left(\bar{F}G_{88}\bar{a}^{\rho\rho}\right)\Big|_{w_1}\cdot\partial_\rho\phi_i^8\right]+\partial_a\left[\left(\bar{F}G_{88}\bar{a}^{ba}\right)\Big|_{w_1}\cdot\partial_b\phi_i^8\right]\\
=&\left(e^{\Phi(r_1)}A_i^4\rho^3\sqrt{\det g_{ab}[1+(\partial_\rho w_1)^2]}e^{\frac{\Phi(r_1)}{2}}\frac{R^2}{r_1^2}e^{-\frac{\Phi(r_1)}{2}}\frac{R^2}{A_1^2r_1^2}\right)_{w_1}\underbrace{\partial^\mu\partial_\mu\phi_i^8}_{-k^2\phi_i^8=M^2\phi_i^8}\\
+&\partial_\rho\left[e^{\Phi(r_1)}A_i^4\rho^3\sqrt{\det g_{ab}[1+(\partial_\rho w_1)^2]}e^{\frac{\Phi(r_1)}{2}}\frac{R^2}{r_1^2}\frac{r_1^2}{R^2}\frac{e^{-\frac{\Phi(r_1)}{2}}}{1+(\partial_\rho w_1)^2}\right]_{w_1}\partial_\rho\phi_i^8+[...]\partial_\rho^2\phi_i^8\\
+&\left(e^{\Phi(r_1)}A_i^4\rho^3\sqrt{\det g_{ab}[1+(\partial_\rho w_1)^2]}e^{\frac{\Phi(r_1)}{2}}\frac{R^2}{r_1^2}e^{-\frac{\Phi(r_1)}{2}}\frac{r_1^2}{\rho^2R^2}\right)_{w_1}\underbrace{\partial^a\partial_a\phi_i^8}_{-l(l+2)\phi_i^8}\\
=&F_1\rho^3\left[1+(\partial_\rho w_1)^2\right]\sqrt{\det g_{ab}}\frac{1}{A_1^2}\left(\frac{R}{r_1}\right)^4M^2\phi_i^8+\left[(\partial_\rho F_1)\rho^3\sqrt{\det g_{ab}}+3\frac{\rho^3}{\rho}F_1\sqrt{\det g_{ab}}\right]\partial_\rho\phi_i^8\\
+&F_1\rho^3\sqrt{\det g_{ab}}\partial_\rho^2\phi_i^8-F_1\rho^3\sqrt{\det g_{ab}}\left[1+(\partial_\rho w_1)^2\right]\frac{l(l+2)}{\rho^2}\phi_i^8.
\end{aligned}
\tag{A.3.5}
$$

So term C is

$$
\begin{aligned}
\text{term C}=&-\frac{1}{4}F_1\rho^3\sqrt{\det g_{ab}}\left\{\left[1+(\partial_\rho w_1)^2\right]\left[\frac{1}{A_1^2}\left(\frac{R}{r_1}\right)^4M^2-\frac{l(l+2)}{\rho^2}\right]+\partial_\rho\left(\log F_1\right)\partial_\rho\right\}\phi_i^8\\
&-\frac{1}{4}F_1\rho^3\sqrt{\det g_{ab}}\frac{3}{\rho}\partial_\rho\phi_i^8-\frac{1}{4}F_1\rho^3\sqrt{\det g_{ab}}\partial_\rho^2\phi_i^8+1\to2.
\end{aligned}
\tag{A.3.6}
$$

Combine eq. (A.3.3), eq. (A.3.4) and eq. (A.3.6) we get the eom of ϕ_i^8:

$$
\begin{aligned}
&\frac{1}{2}\rho^3\sqrt{\det g_{ab}}\left\{F_1\left[1+(\partial_\rho w_1)^2\right]K_{r_1}+1\to2\right\}\phi_i^8-\frac{v^2}{4}\rho^3\sqrt{\det g_{ab}}(G_1+G_2)\phi_i^8\\
&-\frac{1}{4}F_1\rho^3\sqrt{\det g_{ab}}\left\{\left[1+(\partial_\rho w_1)^2\right]\left[\frac{1}{A_1^2}\left(\frac{R}{r_1}\right)^4M^2-\frac{l(l+2)}{\rho^2}\right]+\partial_\rho\left(\log F_1\right)\partial_\rho\right\}\phi_1^8\\
&-\frac{1}{4}F_1\rho^3\sqrt{\det g_{ab}}\frac{3}{\rho}\partial_\rho\phi_i^8-\frac{1}{4}F_1\rho^3\sqrt{\det g_{ab}}\partial_\rho^2\phi_i^8+1\to2,
\end{aligned}
\tag{A.3.7}
$$

$$
\begin{aligned}
&\to (F_1+F_2)\partial_\rho^2\phi_i^8+(F_1+F_2)\frac{3}{\rho}\partial_\rho\phi_i^8 \\
&\quad+\underbrace{\left[F_1\left\{\underbrace{\left[1+(\partial_\rho w_1)^2\right]\left[\frac{1}{A_1^2}\left(\frac{R}{r_1}\right)^4M^2-\frac{l(l+2)}{\rho^2}-2K_{r_1}\right]}_{\equiv K_1}+\partial_\rho\left(\log F_1\right)\partial_\rho\right\}+v^2G_1\right]}_{\equiv N_1}\phi_i^8. \\
&\quad+[1\to 2]\phi_i^8=0 \\
&\Rightarrow (F_1+F_2)\partial_\rho^2\phi_i^8+(F_1+F_2)\frac{3}{\rho}\partial_\rho\phi_i^8+(N_1+N_2)\phi_i^8=0.
\end{aligned}
\tag{A.3.8}
$$

So the eom of $\phi_{1,2}^8$ is:

$$
\left(\partial_\rho^2+\frac{3}{\rho}+\frac{N_1+N_2}{K_1+K_2}\right)\phi_i^8=0. \tag{A.3.9}
$$

A.4 Vector Part (A_s and ϕ^9), eq.(40)

From the full Lagrangian eq. (A.2.1), the terms contributing to the Lagrangian $\mathcal{L}^{(2)}_{A,\phi^9}$ are:

$$
\begin{aligned}
a_{rs}^{(1)}&=T^{-1}F_{rs} \\
a_{rs}^{(2)}&=G_{99}\left(-i[A_r,\bar{X}^9]\partial_s\phi^9-i\partial_r\phi^9[A_s,\bar{X}^9]-[A_r,\bar{X}^9][A_s,\bar{X}^9]+\partial_r\phi^9\partial_s\phi^9\right).
\end{aligned}
\tag{A.4.1}
$$

Calculate first $a_{rs}^{(2)}$, start from the commutators, we have:

$$
\begin{aligned}
[A_r,\bar{X}^9]&=[A_r^0\tau^0+A_r^1\tau^1+A_r^2\tau^2+A_r^3\tau^3,w\tau^0+v\tau^3] \\
&=A_r^1v[\tau^1,\tau^3]+A_r^2v[\tau^2,\tau^3] \\
&=-iA_r^1v\tau^2+iA_r^2v\tau^1,
\end{aligned}
\tag{A.4.2}
$$

where the last step follows from $[\tau^a,\tau^b]=\frac{1}{4}[\sigma^a,\sigma^b]=\frac{1}{4}\cdot 2i\epsilon_{abc}\sigma^c=\frac{1}{2}i\epsilon_{abc}\sigma^c=i\epsilon_{abc}\tau^c$, the σ^a are Pauli matrices. Therefore we have

$$
\begin{aligned}
&-i[A_r,\bar{X}^9]\partial_s\phi^9-i\partial_r\phi^9[A_s,\bar{X}^9] \\
=&(-v\tilde{A}_R^1\tau^1+v\tilde{A}_r^2\tau^1-\partial_r\phi_2^9\tau^2-\partial_r\phi_1^9\tau^1)(\partial_s\phi_0^9\tau^0+\partial_s\phi_1^9\tau^1+\partial_s\phi_2^9\tau^2+\partial_s\phi_3^9\tau^3) \\
&+\partial_s\phi^9(1^{\text{st}}\text{ braket from last line}) \\
=&-\tilde{A}_r^1\partial_s\phi_0^9\{\tau^2,\tau^0\}+...(\text{only }\{\tau^a,\tau^a\}\text{ terms}\neq 0) \\
=&\frac{v}{2}\left(-\tilde{A}_r^1\partial_s\phi_2^9+\tilde{A}_r^2\partial_s\phi_1^9\right)-\frac{1}{2}\left(\partial_r\phi_2^9\partial_s\phi_2^9+\partial_r\phi_1^9\partial_s\phi_1^9\right).
\end{aligned}
\tag{A.4.3}
$$

The term $\partial_r\phi^9\partial_s\phi^9$ has already been calculated before in the ϕ^8 part, then the last term to be considered is

$$-[A_r,\bar{X}^9][A_s,\bar{X}^9]=\frac{v^2}{4}\left(\tilde{A}^1_r\tilde{A}^1_s+\tilde{A}^2_r\tilde{A}^2_s\right)+\frac{1}{4}\left(\partial_r\phi^9_2\partial_s\phi^9_2+\partial_r\phi^9_1\partial_s\phi^9_1\right)+\frac{v}{2}\partial_r\phi^9_2\tilde{A}^1_s-\frac{v}{2}\partial_r\phi^9_1\tilde{A}^2_s. \tag{A.4.4}$$

Combining all these pieces together we have

$$\bar{a}^{(2)}_{rs}=\frac{1}{4}\left[\begin{pmatrix}\partial_r\phi^9_+\partial_s\phi^9_+ & \\ & \partial_r\phi^9_-\partial_s\phi^9_-\end{pmatrix}+v^2\begin{pmatrix}\tilde{A}^1_r\tilde{A}^1_s+\tilde{A}^2_r\tilde{A}^2_s & \\ & \tilde{A}^1_r\tilde{A}^1_s+\tilde{A}^2_r\tilde{A}^2_s\end{pmatrix}\right]. \tag{A.4.5}$$

For constant w_i, $\phi^8_i=0$, $\bar{a}^{(2)}_{rs}=T^{-1}F_{rs}$. $\bar{a}^{(2)}_{rs}\propto F_{rs}$, which is anti-symmetric. Since $\bar{a}^{-1}$ is a symmetric metric, so

$$\begin{aligned}&\mathrm{Tr}_{rs}(\bar{a}^{-1}a^{(1)})=\left[\mathrm{Tr}_{rs}(\bar{a}^{-1}a^{(1)})\right]^2=0\\&\mathrm{Tr}_{rs}\left[(\bar{a}^{-1}a^{(1)})^2\right]=\bar{a}^{rp}a^{(1)}_{pt}\bar{a}^{tq}a^{(1)}_{qr}=\bar{a}^{rp}\bar{a}^{sq}\tilde{F}_{ps}\tilde{F}_{qr}\\&\text{where}\quad\tilde{F}_{ps}\tilde{F}_{qr}=\frac{1}{4}\begin{pmatrix}\tilde{F}^+_{ps}\tilde{F}^+_{qr}+\tilde{F}^{12}_{ps}\tilde{F}^{21}_{qr} & \dots\\ \dots & \tilde{F}^-_{ps}\tilde{F}^-_{qr}+\tilde{F}^{21}_{ps}\tilde{F}^{12}_{qr}\end{pmatrix}.\end{aligned} \tag{A.4.6}$$

Therefore

$$\begin{aligned}\mathcal{L}^{(2)}_{\tilde{A}}&=\mathrm{STr}\left\{e^{-\Phi}\sqrt{-\det\bar{a}_{rs}}\left(-\frac{1}{4}\mathrm{Tr}_{rs}\left[\left(\bar{a}^{-1}a^{(1)}_{\tilde{A}}\right)^2\right]+\frac{1}{2}\mathrm{Tr}_{rs}\left(\bar{a}^{-1}a^{(2)}_{\tilde{A}}\right)\right)\right\}\\&=-\frac{1}{4}\mathrm{STr}\left[\bar{F}\bar{a}^{rp}\bar{a}^{sq}\tilde{F}_{ps}\tilde{F}_{qr}\right]+\frac{1}{2}\mathrm{STr}\left[\bar{F}\bar{a}^{rs}\bar{a}^{(2)}_{sr}\right]\\&=\frac{1}{4}\Bigg\{\frac{1}{4}\left(\bar{F}\bar{a}^{rp}\bar{a}^{sq}\right)_{w_1}\tilde{F}^+_{rs}\tilde{F}^+_{pq}+\frac{1}{4}\left(\bar{F}\bar{a}^{rp}\bar{a}^{sq}\right)_{w_2}\tilde{F}^-_{rs}\tilde{F}^-_{pq}\\&+\frac{1}{4}\left[\left(\bar{F}\bar{a}^{rp}\bar{a}^{sq}\right)_{w_1}+\left(\bar{F}\bar{a}^{rp}\bar{a}^{sq}\right)_{w_2}\right]\left(\tilde{F}^1_{rs}\tilde{F}^1_{pq}+\tilde{F}^2_{rs}\tilde{F}^2_{pq}\right)\\&+\frac{v^2}{2}\left[\left(\bar{F}\bar{a}^{rs}G_{99}\right)_{w_1}+\left(\bar{F}\bar{a}^{rs}G_{99}\right)_{w_2}\right]\left(\tilde{A}^1_s\tilde{A}^1_r+\tilde{A}^2_s\tilde{A}^2_r\right)\Bigg\}.\end{aligned} \tag{A.4.7}$$

Equations of motion follow straightforwardly.

Appendix B

A Brief Summary of the Implementation of Δm^2 and the Running

In this section we summarize some backgrounds of inserting the gauge theory running into holographic models that is first introduced in section 3.6.

Initially the idea is inspired by the papers of Jarvinen and Kiritsis [166] where a two-loop running coupling is generated by imposing potential for the tachyon field that is dual to the chiral condensate. The authors in [164] then extend this idea, matching directly the running dilaton e^{ϕ} in the D3/D7 construction to be the two-loop running QCD gauge coupling λ (which we called α in the text.). Then the vacuum action is

$$S = \int d\rho \lambda(r)^3 \sqrt{1+L'^2} = \int d\rho \left(\frac{1}{2}\lambda(r)\Big|_{L=0} \rho^3 L'^2 + \rho^3 \frac{d\lambda}{dL^2}\Big|_{L=0} L^2 \right), \tag{B.1}$$

where $r^2 = \rho^2 + L^2$ is as defined in the main text. By a redefinition of $\rho \to \tilde{\rho}$ and $L = \tilde{\rho}\phi$, where ϕ is a scalar field, one finds that the action can be rewritten as a canonical scalar action of ϕ with $m^2 = -3$ in AdS_5. The running then show up as a modification of the scalar mass

$$S = \frac{1}{2} \int d\tilde{\rho} \tilde{\rho}^3 \left(\tilde{\rho}^2 \phi'^2 + m^2 \phi^2 \right), \tag{B.2}$$

where

$$m^2 = -3 - \delta m^2, \quad \delta m^2 = -\lambda \frac{\rho^5}{\tilde{\rho}^4} \frac{d\lambda}{d\rho}. \tag{B.3}$$

By the holographic dictionary, $m^2 = \Delta(\Delta - 4)$, this scalar is dual to a dimension $\Delta = 3$ operator with a dimension 1 source in the UV. Since this scalar lives in the AdS_{4+1} space, it

has a BF bound determined by $m^2R^2 \geq -\frac{d^2}{4}$. R is the AdS curvature that is set to 1, d is the spatial dimensionality of the AdS, which is 4. This gives a BF bound at $m^2 = -4$. If naively implementing only the running through the gauge coupling, then one finds the BF bound is only violated for certain range of the ρ, in the IR it returns back to a conformal theory. To have a QCD-like running, it is crucial to implement the running of anomalous dimension of the quark mass: $\gamma_m = 3 - \Delta$ where Δ is the scaling dimension of the dual operator of ϕ, with $m^2 = \Delta(\Delta - 4)$. Then the BF bound appears when $\gamma_m = 1$. Note that identifying the dilaton factor with the running coupling already gives up matching to the explicit value of QCD running coupling. But the chiral symmetry is guaranteed to happen when $\gamma = 1$.

In [41] the authors introduced the term Δm^2 that appears in the main text. The action considered for the vacuum is

$$S \sim \int d\rho \frac{1}{2} \left(\rho^3 (\partial_\rho L)^2 + \rho \Delta m^2(\rho, L) L^2 \right). \tag{B.4}$$

Adding this term changes the mass term for ϕ from $m^2 = -3 - \delta m^2$ to $-3 + \Delta m^2(\rho)$. The dual operators' dimension is still determined by $m^2 = \Delta(\Delta - 4)$, this means when $\Delta m^2 = -1$, the BF bound is violated. This simply shift the running dilaton contribution $\delta m^2 \sim \frac{d\lambda}{d\rho}$ in eq. (B.3) to the term Δm^2, so Δm^2 encodes the effect of a dilaton that can deform the D7-probe's geometry which causes a chiral symmetry breaking. The form of Δm^2 becomes a choice. The simplest choice is to use the duality [165], as shown in eq. (3.6.7). The running is implemented through γ as in eq. (3.6.8) – eq. (3.6.10). Of course these are perturbative results, they are however assumed to be valid in the low-energy regime as an approximation. Note that Δm^2 must depend on L, i.e. it should be a function of r instead of ρ. This is to remove the instability from BF bound violation when L grows large [165].

Appendix C

Derivation of an Equation of Motion Using the General Parametrization

In this part we use the general parametrization $X = (L + \sigma)e^{i\alpha\pi}$ to show that it leads to a complicated, fully mixed eom.

First we rewrite the action eq. (4.3.12) as

$$\mathcal{S} = \frac{1}{2}\mathrm{Tr}\left(O\{A, B\}\right), \quad O = \frac{\rho^3 G^{MM}}{r^2}, \quad A = B^\dagger = (D_M X)^\dagger. \tag{C.1}$$

We have simplified the indices knowing that the metric G_{MN} is diagonal. Then given an arbitrary field f, the derivative acting on the action is[1]

$$\begin{aligned} \partial_f \mathcal{S} &= \frac{1}{2}\partial_f \mathrm{Tr}\left[O\{A, B\}\right] = \frac{1}{2}\mathrm{Tr}\left[O\partial_f\{A, B\}\right] = \frac{1}{2}\mathrm{Tr}\left[O\left(\{\partial_f A, B\} + \{A, \partial_f B\}\right)\right] \\ &= \frac{1}{2}\mathrm{Tr}\left[O\left(\{A^0, (\partial_f A^1)^\dagger + \{A^0, (\partial_f A^2)^\dagger\} + \{A^1, (\partial_f A^1)^\dagger\} + h.c.\}\right)\right], \end{aligned} \tag{C.2}$$

where

$$A = A^0 + A^1 + A^2 = \mathcal{O}(f^0) + \mathcal{O}(f^1) + \mathcal{O}(f^2) = B^\dagger, \tag{C.3}$$

[1] ∂_{df} follows the same logic.

and written in components

$$\begin{aligned}
A^0 &= \partial_M L^\dagger, \\
A^1 &= -i\alpha\pi^\dagger\partial_M L^\dagger + \partial_M\sigma^\dagger - i\alpha\partial_M\pi^\dagger L^\dagger + iL^\dagger A^\dagger_{L,M} - iA^\dagger_{R,M}L^\dagger, \\
A^2 &= -\frac{\alpha^2}{2}\pi^{\dagger 2}\partial_M L^\dagger - i\alpha\pi^\dagger\partial_M\sigma^\dagger + (i\alpha)^2\{\pi^\dagger,\partial_M\pi^\dagger\}L^\dagger - i\alpha\partial_M\pi^\dagger\sigma^\dagger, \\
&\quad + i(-i\alpha)\pi^\dagger L^\dagger A^\dagger_{L,M} + i\sigma^\dagger A^\dagger_{L,M} - iA^\dagger_{R,M}(-i\alpha\pi^\dagger)L^\dagger - iA^\dagger_{R,M}\sigma^\dagger.
\end{aligned} \tag{C.4}$$

If $f = \sigma^c$, the derivatives are

$$\begin{aligned}
&\partial_f A^1 = 0, \quad \partial_{df} A^1 = T^c\delta^M_N, \\
&\partial_f A^2 = -i\alpha\partial_M\pi^b T^b T^c + iT^c A^b_{L,M}T^b - iA^b_{R,M}T^b T^c, \\
&\partial_{df} A^2 = -i\alpha\pi^b T^b T^c\delta^M_N.
\end{aligned} \tag{C.5}$$

The equation of motion will be

$$\begin{aligned}
&\frac{1}{2}\partial_N\frac{\partial}{\partial(\sigma^c)} - \frac{\partial}{\partial\sigma^c} \\
=&\partial_N\mathrm{Tr}\left[O\left(\{A^0,(\partial_{df}A^1)^\dagger\} + \{A^0,(\partial_{df}A^2)^\dagger\} + \{A^1,(\partial_{df}A^1)^\dagger\} + h.c.\right)\right] \\
&- \frac{1}{2}\mathrm{Tr}\left[O\left(\{A^0,(\partial_f A^1)^\dagger\} + \{A^0,(\partial_f A^2)^\dagger\} + \{A^1,(\partial_f A^1)^\dagger\} + h.c.\right)\right] \\
=&\partial_N\mathrm{STr}\Big\{O\Big[(\partial_M L^\dagger)(T^c\delta^M_N) + (\partial_M L^\dagger)(i\alpha\pi^b T^c T^b)\delta^M_N \\
&+ (i\alpha\pi^b\partial_M L^\dagger T^b + \partial_M\sigma^b T^b + i\alpha\partial\pi^b L T^b - iA^b_{L,M}T^b L + iA^b_{R,M}LT^b)(T^c\delta^M_N) + h.c.\Big]\Big\} \\
&- \mathrm{STr}\left[O\left((\partial_M L^\dagger)(i\alpha\partial_M\pi^b T^c T^b - iA^b_{L,M} + iA^b_{R,M}T^c T^b) + h.c.\right)\right].
\end{aligned} \tag{C.6}$$

We use the notation $\mathrm{STr}[(A...)(B...)] = \frac{1}{2}\mathrm{Tr}[\{A..., B...\}]$, and the commutators and anti-commutators are seen at the same level as $(...)$ under permutation. The contributions from the scalar fields are

$$\partial_N\mathrm{STr}\left(O\partial_N\sigma^b(T^b)(T^c) + h.c.\right) = \frac{1}{2}\partial_\rho(\rho^3\partial_\rho\sigma^b)\mathrm{Tr}\{T^b,T^c\} + \rho^3\partial^2_M\sigma^b\frac{1}{2}\mathrm{Tr}\left[\frac{1}{r^4}\{T^b,T^c\}\right]. \tag{C.7}$$

From π we get

$$\begin{aligned}
&\partial_N \mathrm{STr}\left[O\left(i\alpha\pi^b(\partial_N L^\dagger)T^cT^b + i\alpha\pi^b(\partial_N L^\dagger T^b)(T^c) + i\alpha\partial_N\pi^b(LT^b)(T^c) + h.c.\right)\right] \\
&- \mathrm{STr}\left(i\alpha O\partial_N\pi^b(\partial_N L^\dagger)T^cT^b + h.c.\right) \\
=&\partial_\rho \mathrm{STr}\left[i\alpha\rho^3\pi^b\left((\partial_\rho L^\dagger) + (\partial_\rho L^\dagger T^b)(T^c)\right) + i\alpha\rho^3\partial_\rho\pi^b(LT^b)(T^c)\right] \\
&+ \mathrm{STr}\left(i\alpha\partial_\mu^2\pi^b\frac{1}{r^4}(LT^b)(T^c)\right) - \mathrm{STr}\left(i\alpha\partial_\rho\pi^b\rho^3(\partial_\rho L^\dagger)T^cT^b\right) + h.c.,
\end{aligned} \tag{C.8}$$

and from the gauge fields

$$\begin{aligned}
&\partial_N \mathrm{STr}\left[O\left(-iA^b_{L,N}(T^bL)(T^c) + iA^b_{R,N}(LT^b)(T^c)\right)\right] \\
&- \mathrm{STr}\left[O\left(-iA_{L,M^b}(\partial_M L^\dagger)(T^bT^c) + iA^b_{R,M}\right)(\partial_M L^\dagger)(T^cT^b)\right] + h.c. \\
=&-i\mathrm{STr}\left[\frac{\rho^3}{r^4}\left(\partial_\mu^2\phi^b_V[T^b,L](T^c) + \partial_\mu^2\phi^b_A\{T^b,L\}(T^c)\right)\right] + h.c..
\end{aligned} \tag{C.9}$$

Combining all the contributions, together with the scalar potential

$$\mathrm{STr}[\Delta m^2|X|^2] = \mathrm{STr}[\Delta m^2\{L+\sigma, L+\sigma\}] \tag{C.10}$$

we get the scalar eom

$$\begin{aligned}
&\partial_\rho(\rho^3\partial_\rho\sigma^c) + \frac{1}{2}\rho^3\partial_M^2\sigma^b\mathrm{Tr}\left[\frac{1}{r^4}\{T^b,T^c\}\right] - \mathrm{STr}\left(\Delta m^2(T^b)(T^c)\right)\sigma^c - \rho\sigma^b\mathrm{STr}\left(L\frac{\partial\Delta m^2}{\partial L}|_L(T^b)(T^c)\right) \\
&+ \partial_\rho\mathrm{STr}\left[i\alpha\rho^3\pi^b\left((\partial_\rho L^\dagger)T^cT^b + (\partial_\rho L^\dagger T^b)(T^c)\right) + i\alpha\rho^3\partial_\rho\pi^b(LT^b)(T^c)\right] \\
&+ \mathrm{STr}\left(i\alpha\partial_\mu^2\pi^b\frac{1}{r^4}(LT^b)(T^c)\right) - \mathrm{STr}\left(i\alpha\partial_\rho\pi^b\rho^3(\partial_\rho L^\dagger)T^cT^b\right) \\
&i\mathrm{STr}\left[\frac{\rho^3}{r^4}\left(\partial_\mu^2\phi^b_V[T^b,L](T^c) + \partial_\mu^2\phi^b_A\{T^b,L\}(T^c)\right)\right] + h.c. = 0.
\end{aligned} \tag{C.11}$$

As shown above, using a general parametrization leads to complicated also mixed equations of motion, which is numerically intensive to compute.

In the new parametrization, we have $L\pi \to \{L,\pi\}$. This will kill for example the $\partial_\mu\pi^b$, when $L^\dagger = L$

$$\mathrm{STr}\left(i\{LT^b,T^c\} + h.c.\right) \to \mathrm{STr}\left(i\{LT^b,T^c\} - i\{T^bL,T^c\} + i\{T^bL,T^c\} - i\{LT^b,T^c\}\right) = 0. \tag{C.12}$$

Appendix D

Equations of Motion, $N_f = 2$ Split Masses

We use $r_i^2 = r_i^2(\rho) = L_i^2(\rho) + \rho^2$ $(i = d, u)$ in the following. In calculating the masses, we took the limit of vanishing longitudinal ϕ_{v_i} and ϕ_{a_i}.

Scalars

$$\xi_{u,d}: \qquad \partial_\rho\left(\rho^3\partial_\rho\xi_{u/d}(\rho)\right) + \rho\left(-\Delta m_{u/d}^2 - L_{u/d}(\rho)\Delta m_{u/d}^{2\prime} + \frac{\rho^2 M_{\xi_{u/d}}^2}{r_{u/d}^4}\right)\xi_{u/d}(\rho) = 0 \quad \text{(D.1)}$$

$$\begin{aligned}\xi_{1/2}: \qquad & \partial_\rho\left(\rho^3\partial_\rho\xi_{1/2}(\rho)\right) + \frac{\rho}{2}\left[-\Delta m_u^2 - \Delta m_d^2 - L_u(\rho)\Delta m_u^{2\prime} - L_d(\rho)\Delta m_d^{2\prime}\right]\xi_{1/2}(\rho) \\ & + \frac{1}{2}M_{\xi_{1/2}}^2\rho^3\left(\frac{1}{r_d^4} + \frac{1}{r_u^4}\right)\Big(\xi_{1/2}(\rho) \pm (L_u(\rho) - L_d(\rho))\phi_{V_{2/1}}(\rho)\Big) = 0 \quad \text{(D.2)}\end{aligned}$$

Pseudo-Scalars

$$\pi_{u,d}: \qquad \partial_\rho\left(L_{u/d}^2(\rho)\rho^3\partial_\rho\pi_{u/d}(\rho)\right) + \frac{L_{u/d}^2(\rho)M_{\pi_{u/d}}^2\rho^3}{r_{u/d}^4}\Big(\pi_{u/d}(\rho) - \phi_{A_{u/d}}(\rho)\Big) = 0 \quad \text{(D.3)}$$

$$\begin{aligned}\pi_{1/2}: \qquad & \partial_\rho\left((L_u(\rho) + L_d(\rho))^2\rho^3\partial_\rho\pi_{1/2}(\rho)\right) + \frac{M_{\pi_{1/2}}^2\rho^3}{2}\left(\frac{1}{r_u^4} + \frac{1}{r_d^4}\right)(L_u(\rho) + L_d(\rho))^2 \\ & \times\Big(\pi_{1/2}(\rho) - \phi_{A_{1/2}}(\rho)\Big) = 0 \quad \text{(D.4)}\end{aligned}$$

Vectors

$$V_{u,d}: \qquad \partial_\rho\left(\rho^3\partial_\rho V_{u/d}(\rho)\right)+\frac{\rho^3 M^2_{V_{u/d}}}{r^4_{u/d}}V_{u/d}(\rho)=0 \tag{D.5}$$

$$V_{1/2}: \quad \partial_\rho\left(\rho^3\partial_\rho V_{1/2}(\rho)\right)+\frac{\rho^3}{8}\left(\frac{1}{r_u^4}+\frac{1}{r_d^4}\right)\left[4M^2_{V_{1/2}}-g_5^2\left(L_u(\rho)-L_d(\rho)\right)^2\right]V_{1/2}(\rho)=0 \tag{D.6}$$

$$\phi_{v_{1/2}}: \qquad \partial_\rho\left(\rho^3\partial_\rho\phi_{V_{1/2}}(\rho)\right)\pm\frac{\rho^3 g_5^2}{8}\left(\frac{1}{r_u^4}+\frac{1}{r_d^4}\right)\left(L_u(\rho)-L_d(\rho)\right) \times\left(\xi_{2/1}(\rho)\mp\left(L_u(\rho)-L_d(\rho)\right)\phi_{V_{1/2}}(\rho)\right)=0 \tag{D.7}$$

$$4M^2_{\phi_{V_{1/2}}}\partial_\rho\phi_{V_{1/2}}(\rho)\mp g_5^2(L_u(\rho)-L_d(\rho))\partial_\rho\xi_{2/1}(\rho)\pm g_5^2\xi_{2/1}(\rho)\partial_\rho(L_u(\rho)-L_d(\rho))=0 \tag{D.8}$$

Axial-Vectors

$$A_{u,d}: \quad \partial_\rho\left(\rho^3\partial_\rho A_{u/d}(\rho)\right)+\frac{\rho^3}{r^4_{u/d}}\left(M^2_{A_{u/d}}-g_5^2L_{u/d}(\rho)^2\right)A_{u/d}(\rho)=0 \tag{D.9}$$

$$\phi_{A_{u/d}}: \quad \partial_\rho\left(\rho^3\partial_\rho\phi_{A_{u/d}}(\rho)\right)+\frac{\rho^3 g_5^2}{r^4_{u/d}}L_{u/d}(\rho)^2(\pi_{u/d}(\rho)-\phi_{A_{u/d}}(\rho))=0 \tag{D.10}$$

$$M^2_{\phi_{A_{u/d}}}\partial_\rho\phi_{A_{u/d}}(\rho)-g_5^2L_{u/d}(\rho)^2\partial_\rho\pi_{u/d}(\rho)=0 \tag{D.11}$$

$$A_{1/2}: \quad \partial_\rho\left(\rho^3\partial_\rho A_{1/2}(\rho)\right)+\frac{\rho^3}{8}\left(\frac{1}{r_u^4}+\frac{1}{r_d^4}\right)\left[4M^2_{A_{1/2}}-g_5^2\left(L_u(\rho)+L_d(\rho)\right)^2\right]A_{1/2}(\rho)=0 \tag{D.12}$$

$$\phi_{A_{1/2}}: \quad \partial_\rho\left(\rho^3\partial_\rho\phi_{A_{1/2}}(\rho)\right)+\frac{\rho^3 g_5^2}{8}\left(\frac{1}{r_u^4}+\frac{1}{r_d^4}\right)(L_u(\rho)+L_d(\rho))^2(\pi_{1/2}(\rho)-\phi_{A_{1/2}}(\rho))=0 \tag{D.13}$$

$$M^2_{\phi_{A_{u/d}}}\partial_\rho\phi_{A_{1/2}}(\rho)-\frac{g_5^2}{4}(L_u(\rho)+L_d(\rho))^2\partial_\rho\pi_{1/2}(\rho)=0 \tag{D.14}$$

From eq. (D.10) and eq. (D.13) one recovers eq. (D.4).

Appendix E

Equations of Motion, $N_f = 3$

As mentioned in section 4.4, the equations of motion are sorted in groups $(u, 1, 2, 3)$, $(4, 5, 6, 7)$ and s. The groups $(u, 1, 2, 3)$ and s take the abelian form, but with (L_u, r_u) and (L_s, r_s) for $(u, 1, 2, 3)$ and s respectively. The group $(4, 5, 6, 7)$ have mixed equations as the off-diagonal ones (1,2) in the two-flavor case, where (4,5) and (6,7) mixed in the same way as $N_f = 2$ (1,2). We demonstrate this pattern with the scalars as an example.

The scalar fluctuations are

$$\left[\partial_\rho\left(\rho^3\partial_\rho\right) - \Delta m_u^2(\rho)\rho - L_u(\rho)\frac{\partial\Delta m_u^2(\rho)}{\partial L_u}\rho + \rho^3\frac{M_{\sigma_i}^2}{r_u^2}\right]\sigma_i(\rho) = 0, \quad i = u, 1, ..., 3 \tag{E.1}$$

$$\left[\partial_\rho\left(\rho^3\partial_\rho\right) - \Delta m_s^2(\rho)\rho - L_s(\rho)\frac{\partial\Delta m_s^2(\rho)}{\partial L_s}\rho + \rho^3\frac{M_{\sigma_i}^2}{r_s^2}\right]\sigma_i(\rho) = 0, \quad i = s \tag{E.2}$$

where σ_u and σ_s are defined in eq. (4.4.1). To get the equations for off-diagonal ones (4,5,6,7), one can simply take eq. (D.2) and change the pairs

$$\begin{aligned}(1,2) &\to (4,5),\ (6,7)\\ (L_u, L_d) &\to (L_u, L_s).\end{aligned} \tag{E.3}$$

The other fluctuations' equations follow the same logic.

Appendix F

Relating Δm^2 and A

In this appendix, we show how Δm^2 is related to the function A in chapter 5 first for a simple degenerated case and then for a mass splitting/NJL case.

F.1 Degenerate Flavors

The vacuum Lagrangian is

$$\mathcal{L} = 4\rho^3(\partial_\rho L^\dagger)(\partial_\rho L) + \rho A\left[\mathrm{Tr}\left(\rho^2 1_4 + L^\dagger L\right)\right]\mathrm{Tr}L^\dagger L, \tag{F.1.1}$$

here we have omitted other terms for simplicity. This will not change the conclusion. L is the vacuum matrix. A is a function of $\mathrm{Tr}\left(\rho^2 1_4 + L^\dagger L\right)$. Expanding in the fluctuations, substitute L with X we have

$$\mathcal{L} = 4\rho^3(\partial_\rho(L_0+\delta L_0))^2 + \rho\left(A\Big|_{L_0} + \frac{\partial A}{\partial L_0}\Big|_{L_0}\delta L_0 + \frac{1}{2}\frac{\partial^2 A}{\partial L_0^2}\Big|_{L_0}\delta L_0^2\right)\mathrm{Tr}X^\dagger X, \tag{F.1.2}$$

where

$$A = A\left[\mathrm{Tr}\left(\rho^2 1_4 + L^\dagger L\right)\right] = A\left[4\rho^2 + 4\left(L_0+\sigma\right)^2 + 4\sum_i f_i^2\right], \tag{F.1.3}$$

f_i are other fluctuation (fields). The eom of $\sigma = \delta L$ is then

$$\begin{aligned}\partial_\rho\left(\rho^3\partial_\rho L_0\right) - \rho A\Big|_{L_0} - \frac{\rho}{2}\frac{\partial A}{\partial L}\Big|_{L_0}L_0^2 + \partial_\rho\left(\rho^3\partial_\rho\delta L\right) - \rho A\Big|_{L_0}\delta L - 2\rho\frac{\partial A}{\partial L}\Big|_{L_0}L_0\delta L \\ -\frac{\rho}{2}\frac{\partial^2 A}{\partial L^2}\Big|_{L_0}L_0^2\delta L = 0.\end{aligned} \tag{F.1.4}$$

Define

$$A\Big|_{L_0} + \frac{1}{2}\frac{\partial A}{\partial L}\Big|_{L_0} L_0 \equiv \Delta m^2 \left[\log\sqrt{\rho^2 + \frac{1}{4}\mathrm{Tr}L^\dagger L}\right] \tag{F.1.5}$$

we get the vacuum eom as in eq. (5.3.2). Expand the relation eq. (F.1.5) further to first order in δL

$$\begin{aligned} LHS &= A\Big|_{L_0} + \frac{\partial A}{\partial L}\Big|_{L_0}\delta L + \frac{1}{2}\left(\frac{\partial A}{\partial L}\Big|_{L_0} + \frac{\partial^2 A}{\partial L^2}\Big|_{L_0}\delta L\right)(L_0+\delta L) \\ &= A\Big|_{L_0} + \frac{1}{2}\frac{\partial A}{\partial L}\Big|_{L_0} + \left(\frac{3}{2}\frac{\partial A}{\partial L}\Big|_{L_0} + \frac{1}{2}L_0\frac{\partial^2 A}{\partial L^2}\Big|_{L_0}\right)\delta L \\ &\overset{\text{RHS}}{=} \Delta m^2\Big|_{L_0} + \frac{\partial \Delta m^2}{\partial L}\Big|_{L_0}\delta L, \end{aligned} \tag{F.1.6}$$

this leads to

$$\frac{3}{2}\frac{\partial A}{\partial L}\Big|_{L_0} + \frac{1}{2}L_0\frac{\partial^2 A}{\partial L^2}\Big|_{L_0} = \frac{\partial \Delta m^2}{\partial L}\Big|_{L_0}. \tag{F.1.7}$$

Using the above relations, we get the eoms as in section section 5.3.

F.2 Split Masses

The Lagrangian is

$$\begin{aligned} \mathcal{L} &= \mathrm{Tr}\left[\rho^3(\partial_\rho L)^\dagger\partial_\rho L + \rho A L^\dagger L\right] \\ &= 2\left(\rho^3(\partial_\rho L_1)^2 + \rho^3(\partial_\rho L_6)^2 + \rho A L_1^2 + \rho A L_6^2\right). \end{aligned} \tag{F.2.1}$$

Expanding in the fluctuations

$$\begin{aligned} \frac{1}{2}\mathcal{L} &= \rho^3\left(\partial_\rho(L_1+\delta L_1)\right)^2 + \left(\partial_\rho(L_6+\delta L_6)\right)^2 \\ &\quad + \rho\left(A\Big|_{L_0} + \frac{\partial A}{\partial L_1}\Big|_{L_0}\delta L_1 + \frac{\partial A}{\partial L_6}\Big|_{L_0}\delta L_6 + \frac{1}{2}\frac{\partial^2 A}{\partial L_1^2}\Big|_{L_0}\delta L_1^2 + \frac{1}{2}\frac{\partial^2 A}{\partial L_6^2}\Big|_{L_0}\delta L_6^2 + \frac{\partial^2 A}{\partial L_1\partial L_6}\Big|_{L_0}\delta L_1\delta L_6\right) \\ &\quad \times\left[(L_1+\delta L_1)^2 + (L_6+\delta L_6)^2\right], \end{aligned} \tag{F.2.2}$$

where $\Big|_{L_0}$ means evaluate the function at the vacuum. The equation of motion of δL_1 is

$$\begin{aligned} &\partial_\rho\left(\rho^3\partial_\rho L_1\right) - \rho A\Big|_{L_0} L_1 - \frac{\rho}{2}\left(L_1^2+L_6^2\right)\frac{\partial A}{\partial L_1}\Big|_{L_0} \\ &+\partial_\rho\left(\rho^3\partial_\rho\delta L_1\right) - \rho\left[A\Big|_{L_0} + 2\frac{\partial A}{\partial L_1}\Big|_{L_0} L_1 + \frac{1}{2}\frac{\partial^2 A}{\partial L_1^2}\Big|_{L_0}\left(L_1^2+L_6^2\right)\right]\delta L_1 \\ &-\rho\left[\frac{\partial A}{\partial L_6}\Big|_{L_0} L_1 + 2\frac{\partial A}{\partial L_1}\Big|_{L_0} L_6 + \frac{1}{2}\frac{\partial^2 A}{\partial L_1\partial L_6}\Big|_{L_0}\left(L_1^2+L_6^2\right)\right]\delta L_6 = 0. \end{aligned} \tag{F.2.3}$$

The equation of motion for δL_6 is similar, one just needs to exchange 1 with 6. From the two equations of motion, we define

$$\begin{aligned} A\Big|_{L_0} L_1 + \frac{1}{2}\left(L_1^2+L_6^2\right)\frac{\partial A}{\partial L_1}\Big|_{L_0} &\equiv \Delta m^2\left[\log\sqrt{\frac{1}{4}\mathrm{Tr}\left(\rho^2+L^\dagger L\right)}\right]L_1, \\ A\Big|_{L_0} L_6 + \frac{1}{2}\left(L_1^2+L_6^2\right)\frac{\partial A}{\partial L_6}\Big|_{L_0} &\equiv \Delta m^2\left[\log\sqrt{\frac{1}{4}\mathrm{Tr}\left(\rho^2+L^\dagger L\right)}\right]L_6. \end{aligned} \tag{F.2.4}$$

Multiply both equations by L_1 and L_6, respectively, and adding them together, this is nothing but

$$A\Big|_{L_0} + 2\left(L_1^2+L_6^2\right)\frac{dA}{d\mathrm{Arg}}\Big|_{L_0} \equiv \Delta m^2\left[\log\sqrt{\frac{1}{4}\mathrm{Tr}\left(\rho^2+L^\dagger L\right)}\right], \tag{F.2.5}$$

where $\mathrm{Arg} = \mathrm{Tr}(\rho^2 1_4 + X^\dagger X)$, $\frac{dA}{d\mathrm{Arg}} \equiv A'$, and

$$\frac{1}{4}\mathrm{Tr}(\rho^2 1_4 + L^\dagger L) = \rho^2 + \frac{1}{2}(L_1^2+L_6^2) \equiv r_{arg,16}^2. \tag{F.2.6}$$

Expanding the above equation in fluctuations to first order

$$\begin{aligned} &A\Big|_{L_0} + \frac{\partial A}{\partial L_1}\Big|_{L_0}\delta L_1 + \frac{\partial A}{\partial L_6}\Big|_{L_0}\delta L_6 + 2\left[(L_1+\delta L_1)^2+(L_6+\delta L_6)^2\right]\left(A'\Big|_{L_0} + \frac{\partial A'}{\partial L_1}\Big|_{L_0}\delta L_1 + \frac{\partial A'}{\partial L_6}\Big|_{L_0}\delta L_6\right) \\ =&A\Big|_{L_0} + 2(L_1^2+L_6^2)A'\Big|_{L_0} \to \Delta m^2\Big|_{L_0} \\ &+\left(\frac{\partial A}{\partial L_1}\Big|_{L_0} + 4L_1A'\Big|_{L_0} + 2\left(L_1^2+L_6^2\right)\frac{\partial A'}{\partial L_1}\Big|_{L_0}\right)\delta L_1 \to \frac{\partial \Delta m^2}{\partial L_1}\delta L_1 \\ &+\left(\frac{\partial A}{\partial L_6}\Big|_{L_0} + 4L_6A'\Big|_{L_0} + 2\left(L_1^2+L_6^2\right)\frac{\partial A'}{\partial L_6}\Big|_{L_0}\right)\delta L_6 \to \frac{\partial \Delta m^2}{\partial L_6}\delta L_6. \end{aligned} \tag{F.2.7}$$

Notice that

$$\begin{aligned} \frac{\partial \Delta m^2}{\partial L_1} &= \frac{1}{2}\frac{L_1}{\rho^2+\frac{1}{2}(L_1^2+L_6^2)}\frac{d\Delta m^2}{d(\log r_{arg,16})} \equiv \frac{1}{2}\frac{L_1}{\rho^2+\frac{1}{2}(L_1^2+L_6^2)}\Delta m^{2\prime}, \\ \frac{\partial \Delta m^2}{\partial L_6} &= \frac{1}{2}\frac{L_6}{\rho^2+\frac{1}{2}(L_1^2+L_6^2)}\Delta m^{2\prime}, \end{aligned} \tag{F.2.8}$$

we find

$$8A' + 8\left(L_1^2+L_6^2\right)A'' = \frac{1}{2}\frac{1}{\rho^2+\frac{1}{2}\left(L_1^2+L_6^2\right)}\Delta m^{2\prime}, \quad A'' = \frac{d^2A}{d\mathrm{Arg}^2}. \tag{F.2.9}$$

Using the above relations, we get the equations of motion as in section 5.4.

The same computation is done for the NJL case. Without repeating the details, we only list the result here

$$16\left(A' + \left(L_p^2+L_m^2\right)A''\right) = \frac{1}{\rho^2+\frac{1}{2}\left(L_p^2+L_m^2\right)}\Delta m^{2\prime}. \tag{F.2.10}$$

One can get this relation from eq. (F.2.9) by substituting $L_{6,1}$ with $L_{p,m}$.

Appendix G

Equations of Motion, With NJL

In this section we collect the equations of motion when the NJL interactions are incorporated.

The equations of motion for $Q_{1,2,3,5}$ are

$$\begin{aligned}\partial_\rho\left(\rho^3\partial_\rho\phi_j\right)+\frac{g_5^2\rho^3 Q}{2}\left(\frac{1}{r_p^4}+\frac{1}{r_m^4}\right)(\sqrt{2}Q_i-Q\phi_j)=0\\ \partial_\rho\left(\rho^3\partial_\rho Q_i\right)-\rho\Delta m^2 Q_i-\frac{16B}{\rho}L_0^2Q_i+\frac{\rho^3M_{Q_i}^2}{2}\left(\frac{1}{r_p^4}+\frac{1}{r_m^4}\right)(Q_i-\frac{Q}{\sqrt{2}}\phi_j)=0,\end{aligned} \tag{G.1}$$

where $i=1,2,3,5,\ j=4,5,6,9.$

Those for π_is are

$$\begin{aligned}\partial_\rho\left(\rho^3\partial_\rho\phi_j\right)+\frac{g_5^2\rho^3 L_0}{2}\left(\frac{1}{r_p^4}+\frac{1}{r_m^4}\right)(\sqrt{2}\pi_i-L_0\phi_j)=0\\ \partial_\rho\left(\rho^3\partial_\rho\pi_i\right)-\rho\Delta m^2\pi_i-\frac{16B}{\rho}Q^2\pi_i+\frac{\rho^3M_{\pi_i}^2}{2}\left(\frac{1}{r_p^4}+\frac{1}{r_m^4}\right)(\pi_i-\frac{L_0}{\sqrt{2}}\phi_j)=0,\end{aligned} \tag{G.2}$$

for $i=1,2,4,5,\ j=14,8,10,15.$

To solve the Q_is and π_is, we match only $Q_{1,2,3}$ and $\pi_{1,2,4}$ with the NJL coupling g_s^2 in the UV. This is done using the following boundary conditions

$$\begin{aligned}f(\Lambda_{UV})=\frac{(g_s^2+1)c}{\Lambda_{UV}^2},\ f'(\Lambda_{UV})=-2\Lambda_{UV}^{-3}c,\ f'(IR)=0,\\ \phi(\Lambda_{UV})=(0,\pm\sqrt{2})+\frac{\Lambda_{UV}b}{-2},\ \phi'(\Lambda_{UV})=b,\ \phi'(IR)=0,\end{aligned} \tag{G.3}$$

where f denotes the fields that match with the NJL coupling in the UV and ϕ denotes the ϕ_js,

which asymptote to 0 in the UV when solving the πs and to $\pm\sqrt{2}$ when solving the Qs. $\pm$ corresponding to the case before and after the unitary rotation. c is the vev term, which is a free input. b and the mass eigenvalues of f are the shooting parameters. As for the fields Q_5 and π_5, they are not affected by the NJL term, so we use the boundary condition eq. (5.2.16) to solve them.

If we define $S \pm \pi_3 = S_\pm$, we find two sets of coupled equations

$$\begin{aligned}
\partial_\rho\left(\rho^3\partial_\rho\phi_{16+11}\right) + \frac{\rho^3 g_5^2 L_p}{r_p^4}(\sqrt{2}S_+ - L_p\phi_{16+11}) &= 0\\
\partial_\rho\left(\rho^3\partial_\rho S_+\right) - \rho\Delta m^2 S_+ - \frac{16B}{\rho}L_0 Q S_+ + \frac{\rho^3 M^2}{r_p^4}(S_+ - \frac{L_p}{\sqrt{2}}\phi_{16+11}) &= 0\\
\partial_\rho\left(\rho^3\partial_\rho\phi_{16-11}\right) + \frac{\rho^3 g_5^2 L_m}{r_m^4}(\sqrt{2}S_- - L_m\phi_{16-11}) &= 0\\
\partial_\rho\left(\rho^3\partial_\rho S_-\right) - \rho\Delta m^2 S_- + \frac{16B}{\rho}L_0 Q S_- + \frac{\rho^3 M^2}{r_m^4}(S_- - \frac{L_m}{\sqrt{2}}\phi_{16-11}) &= 0.
\end{aligned} \tag{G.4}$$

The scalars σ and Q_4 are mixed, since we only match Q_4 with the NJL coupling in the UV, we work then in the (σ, Q_4) basis.

$$\begin{aligned}
\partial_\rho\left(\rho^3\partial_\rho\sigma\right) - \rho\Delta m^2\sigma - \frac{\rho L_0^2}{r_{njl}^4}\Delta m^{2\prime}\sigma - \frac{16B}{\rho}Q^2\sigma + \frac{\rho^3 M^2}{2}\left(\frac{1}{r_p^4}+\frac{1}{r_m^4}\right)\sigma\\
-\frac{32BL_0Q}{\rho}Q_4 - \frac{L_0 Q\rho}{r_{njl}^2}\Delta m^{2\prime}Q_4 + \frac{\rho^3 M^2}{2}\left(\frac{1}{r_p^4}-\frac{1}{r_m^4}\right)Q_4 = 0,\\
\partial_\rho\left(\rho^3\partial_\rho Q_4\right) - \rho\Delta m^2 Q_4 - \frac{\rho Q^2}{r_{njl}^4}\Delta m^{2\prime}Q_4 - \frac{16B}{\rho}L_0^2 Q_4 + \frac{\rho^3 M^2}{2}\left(\frac{1}{r_p^4}+\frac{1}{r_m^4}\right)Q_4\\
-\frac{32BL_0Q}{\rho}\sigma - \frac{L_0 Q\rho}{r_{njl}^2}\Delta m^{2\prime}\sigma + \frac{\rho^3 M^2}{2}\left(\frac{1}{r_p^4}-\frac{1}{r_m^4}\right)\sigma = 0.
\end{aligned} \tag{G.5}$$

The gauge bosons are

$$\begin{aligned}
\partial_\rho\left(\rho^3\partial_\rho A_i\right) + \frac{\rho^3 M_{A_i}^2}{r_m^4}A_i = 0, i = (1+13, 2+7, 3+12)\\
\partial_\rho\left(\rho^3\partial_\rho A_i\right) + \frac{\rho^3 M_{A_i}^2}{r_p^4}A_i = 0, i = (1-13, 2-7, 3-12)\\
\partial_\rho\left(\rho^3\partial_\rho A_i\right) + \frac{\rho^3}{r_p^4}\left[M_{A_i}^2 - L_p^2 g_5^2\right]A_i = 0, i = 11+16;\\
\partial_\rho\left(\rho^3\partial_\rho A_i\right) + \frac{\rho^3}{r_m^5}\left[M_{A_i}^2 - L_m^2 g_5^2\right]A_i = 0, i = 16-11;\\
\partial_\rho\left(\rho^3\partial_\rho A_i\right) + \frac{\rho^3}{2}\left(\frac{1}{r_p^4}+\frac{1}{r_m^4}\right)\left[M_{A_i}^2 - \frac{(L_p \pm L_m)^2}{4}g_5^2\right]A_i = 0,\\
i = (4,5,6,9)(+), i = (8,10,14,15)(-).
\end{aligned} \tag{G.6}$$

All these fields are solved by shooting from the IR, using the boundary conditions eq. (5.2.15) and eq. (5.2.16) for the decoupled and coupled equations respectively.

Bibliography

[1] Johanna Erdmenger et al. "Holographic Non-Abelian Flavour Symmetry Breaking". In: *Universe* 9.6 (2023), p. 289. DOI: 10.3390/universe9060289. arXiv: 2304.09190 [hep-th].

[2] Johanna Erdmenger et al. "Holography for Sp($2N_c$) Gauge Dynamics: from Composite Higgs to Technicolour". In: (Apr. 2024). arXiv: 2404.14480 [hep-ph].

[3] Serguei Chatrchyan et al. "Observation of a New Boson at a Mass of 125 GeV with the CMS Experiment at the LHC". In: *Phys. Lett. B* 716 (2012), pp. 30–61. DOI: 10.1016/j.physletb.2012.08.021. arXiv: 1207.7235 [hep-ex].

[4] Georges Aad et al. "Observation of a new particle in the search for the Standard Model Higgs boson with the ATLAS detector at the LHC". In: *Phys. Lett. B* 716 (2012), pp. 1–29. DOI: 10.1016/j.physletb.2012.08.020. arXiv: 1207.7214 [hep-ex].

[5] Raymond Davis Jr., Don S. Harmer, and Kenneth C. Hoffman. "Search for neutrinos from the sun". In: *Phys. Rev. Lett.* 20 (1968), pp. 1205–1209. DOI: 10.1103/PhysRevLett.20.1205.

[6] K. S. Hirata et al. "Real time, directional measurement of B-8 solar neutrinos in the Kamiokande-II detector". In: *Phys. Rev. D* 44 (1991). [Erratum: Phys.Rev.D 45, 2170 (1992)], p. 2241. DOI: 10.1103/PhysRevD.44.2241.

[7] R. L. Workman. "Review of Particle Physics". In: *PTEP* 2022 (2022), p. 083C01.

[8] Roberto Contino et al. "Warped/composite phenomenology simplified". In: *JHEP* 05 (2007), p. 074. DOI: 10.1088/1126-6708/2007/05/074. arXiv: hep-ph/0612180.

[9] Steven Weinberg. "Implications of Dynamical Symmetry Breaking". In: *Phys. Rev. D* 13 (1976). [Addendum: Phys.Rev.D 19, 1277–1280 (1979)], pp. 974–996. DOI: 10.1103/PhysRevD.19.1277.

[10] Leonard Susskind. "Dynamics of Spontaneous Symmetry Breaking in the Weinberg-Salam Theory". In: *Phys. Rev. D* 20 (1979), pp. 2619–2625. DOI: 10.1103/PhysRevD.20.2619.

[11] Juan Martin Maldacena. "The Large N limit of superconformal field theories and supergravity". In: *Adv. Theor. Math. Phys.* 2 (1998), pp. 231–252. DOI: 10.1023/A:1026654312961. arXiv: hep-th/9711200.

[12] Ofer Aharony et al. "Large N field theories, string theory and gravity". In: *Phys. Rept.* 323 (2000), pp. 183–386. DOI: 10.1016/S0370-1573(99)00083-6. arXiv: hep-th/9905111.

[13] Sean A. Hartnoll, Christopher P. Herzog, and Gary T. Horowitz. "Building a Holographic Superconductor". In: *Phys. Rev. Lett.* 101 (3 2008), p. 031601. DOI: 10.1103/PhysRevLett.101.031601. URL: https://link.aps.org/doi/10.1103/PhysRevLett.101.031601.

[14] Sean A. Hartnoll, Christopher P. Herzog, and Gary T. Horowitz. "Holographic Superconductors". In: *JHEP* 12 (2008), p. 015. DOI: 10.1088/1126-6708/2008/12/015. arXiv: 0810.1563 [hep-th].

[15] Sean A. Hartnoll et al. "Towards strange metallic holography". In: *JHEP* 04 (2010), p. 120. DOI: 10.1007/JHEP04(2010)120. arXiv: 0912.1061 [hep-th].

[16] C. P. Herzog, P. K. Kovtun, and D. T. Son. "Holographic model of superfluidity". In: *Phys. Rev. D* 79 (2009), p. 066002. DOI: 10.1103/PhysRevD.79.066002. arXiv: 0809.4870 [hep-th].

[17] Christopher P. Herzog. "Lectures on Holographic Superfluidity and Superconductivity". In: *J. Phys. A* 42 (2009), p. 343001. DOI: 10.1088/1751-8113/42/34/343001. arXiv: 0904.1975 [hep-th].

[18] Sean A. Hartnoll. "Lectures on holographic methods for condensed matter physics". In: *Class. Quant. Grav.* 26 (2009). Ed. by A. M. Uranga, p. 224002. DOI: 10.1088/0264-9381/26/22/224002. arXiv: 0903.3246 [hep-th].

[19] Subir Sachdev and Jinwu Ye. "Gapless spin fluid ground state in a random, quantum Heisenberg magnet". In: *Phys. Rev. Lett.* 70 (1993), p. 3339. DOI: 10.1103/PhysRevLett.70.3339. arXiv: cond-mat/9212030.

[20] Alexei Kitaev. "A simple model of quantum holography". In: *KITP strings seminar and Entanglement 2015 program* (2015). URL: http://online.kitp.ucsb.edu/online/entangled15/.

[21] Vladimir Rosenhaus. "An introduction to the SYK model". In: *J. Phys. A* 52 (2019), p. 323001. DOI: 10.1088/1751-8121/ab2ce1. arXiv: 1807.03334 [hep-th].

[22] Juan Maldacena, Douglas Stanford, and Zhenbin Yang. "Diving into traversable wormholes". In: *Fortsch. Phys.* 65.5 (2017), p. 1700034. DOI: 10.1002/prop.201700034. arXiv: 1704.05333 [hep-th].

[23] Daniel Jafferis et al. "Traversable wormhole dynamics on a quantum processor". In: *Nature* 612.7938 (2022), pp. 51–55. DOI: 10.1038/s41586-022-05424-3.

[24] Andreas Karch and Emanuel Katz. "Adding flavor to AdS / CFT". In: *JHEP* 06 (2002), p. 043. DOI: 10.1088/1126-6708/2002/06/043. arXiv: hep-th/0205236.

[25] J. Babington et al. "Chiral symmetry breaking and pions in nonsupersymmetric gauge / gravity duals". In: *Phys. Rev. D* 69 (2004), p. 066007. DOI: 10.1103/PhysRevD.69.066007. arXiv: hep-th/0306018.

[26] James Babington, David E. Crooks, and Nick J. Evans. "A Nonsupersymmetric deformation of the AdS / CFT correspondence". In: *JHEP* 02 (2003), p. 024. DOI: 10.1088/1126-6708/2003/02/024. arXiv: hep-th/0207076.

[27] Veselin G. Filev et al. "Flavoured large N gauge theory in an external magnetic field". In: *JHEP* 10 (2007), p. 019. DOI: 10.1088/1126-6708/2007/10/019. arXiv: hep-th/0701001.

[28] J. Babington et al. "A Gravity dual of chiral symmetry breaking". In: *Fortsch. Phys.* 52 (2004). Ed. by Harald Dorn and D. Lust, pp. 578–582. DOI: 10.1002/prop.200310147. arXiv: hep-th/0312263.

[29] M. Bertolini et al. "N=2 gauge theories on systems of fractional D3/D7 branes". In: *Nucl. Phys. B* 621 (2002), pp. 157–178. DOI: 10.1016/S0550-3213(01)00568-5. arXiv: hep-th/0107057.

[30] Martin Kruczenski et al. "Meson spectroscopy in AdS / CFT with flavor". In: *JHEP* 07 (2003), p. 049. DOI: 10.1088/1126-6708/2003/07/049. arXiv: hep-th/0304032.

[31] Ingo Kirsch. "Spectroscopy of fermionic operators in AdS/CFT". In: *JHEP* 09 (2006), p. 052. DOI: 10.1088/1126-6708/2006/09/052. arXiv: hep-th/0607205.

[32] Tadakatsu Sakai and Shigeki Sugimoto. "Low energy hadron physics in holographic QCD". In: *Prog. Theor. Phys.* 113 (2005), pp. 843–882. DOI: 10.1143/PTP.113.843. arXiv: hep-th/0412141.

[33] Tadakatsu Sakai and Shigeki Sugimoto. "More on a holographic dual of QCD". In: *Prog. Theor. Phys.* 114 (2005), pp. 1083–1118. DOI: 10.1143/PTP.114.1083. arXiv: hep-th/0507073.

[34] Hiroyuki Hata et al. "Baryons from instantons in holographic QCD". In: *Prog. Theor. Phys.* 117 (2007), p. 1157. DOI: 10.1143/PTP.117.1157. arXiv: hep-th/0701280.

[35] Deog Ki Hong et al. "Dynamics of baryons from string theory and vector dominance". In: *JHEP* 09 (2007), p. 063. DOI: 10.1088/1126-6708/2007/09/063. arXiv: 0705.2632 [hep-th].

[36] Deog Ki Hong et al. "Chiral Dynamics of Baryons from String Theory". In: *Phys. Rev. D* 76 (2007), p. 061901. DOI: 10.1103/PhysRevD.76.061901. arXiv: hep-th/0701276.

[37] Kanabu Nawa, Hideo Suganuma, and Toru Kojo. "Baryons in holographic QCD". In: *Phys. Rev. D* 75 (2007), p. 086003. DOI: 10.1103/PhysRevD.75.086003. arXiv: hep-th/0612187.

[38] Kanabu Nawa, Hideo Suganuma, and Toru Kojo. "Brane-induced skyrmions: Baryons in holographic QCD". In: *Prog. Theor. Phys. Suppl.* 168 (2007). Ed. by Teiji Kunihiro et al., pp. 231–236. DOI: 10.1143/PTPS.168.231. arXiv: hep-th/0701007.

[39] Joshua Erlich et al. "QCD and a holographic model of hadrons". In: *Phys. Rev. Lett.* 95 (2005), p. 261602. DOI: 10.1103/PhysRevLett.95.261602. arXiv: hep-ph/0501128.

[40] Masako Bando, Taichiro Kugo, and Koichi Yamawaki. "Nonlinear Realization and Hidden Local Symmetries". In: *Phys. Rept.* 164 (1988), pp. 217–314. DOI: 10.1016/0370-1573(88)90019-1.

[41] Nick Evans and Kimmo Tuominen. "Holographic modelling of a light technidilaton". In: *Phys. Rev. D* 87.8 (2013), p. 086003. DOI: 10.1103/PhysRevD.87.086003. arXiv: 1302.4553 [hep-ph].

[42] Alexander Belyaev et al. "Any room left for technicolor? Holographic studies of NJL assisted technicolor". In: *Phys. Rev. D* 101.8 (2020), p. 086013. DOI: 10.1103/PhysRevD.101.086013. arXiv: 1910.10928 [hep-ph].

[43] Shinya Matsuzaki and Koichi Yamawaki. "Holographic techni-dilaton at 125 GeV". In: *Phys. Rev. D* 86 (2012), p. 115004. DOI: 10.1103/PhysRevD.86.115004. arXiv: 1209.2017 [hep-ph].

[44] Deog Ki Hong and Ho-Ung Yee. "Holographic estimate of oblique corrections for technicolor". In: *Phys. Rev. D* 74 (2006), p. 015011. DOI: 10.1103/PhysRevD.74.015011. arXiv: hep-ph/0602177.

[45] Christopher D. Carone, Joshua Erlich, and Jong Anly Tan. "Holographic Bosonic Technicolor". In: *Phys. Rev. D* 75 (2007), p. 075005. DOI: 10.1103/PhysRevD.75.075005. arXiv: hep-ph/0612242.

[46] Kaustubh Agashe et al. "The S-parameter in holographic technicolor models". In: *JHEP* 12 (2007), p. 003. DOI: 10.1088/1126-6708/2007/12/003. arXiv: 0704.1821 [hep-ph].

[47] Will Clemens, Nick Evans, and Marc Scott. "Holograms of a Dynamical Top Quark". In: *Phys. Rev. D* 96.5 (2017), p. 055016. DOI: 10.1103/PhysRevD.96.055016. arXiv: 1703.08330 [hep-ph].

[48] Daniel Elander, Ali Fatemiabhari, and Maurizio Piai. "Towards composite Higgs: minimal coset from a regular bottom-up holographic model". In: (Mar. 2023). arXiv: 2303.00541 [hep-th].

[49] Daniel Elander et al. "Holographic models of composite Higgs in the Veneziano limit. Part I. Bosonic sector". In: *JHEP* 03 (2021), p. 182. DOI: 10.1007/JHEP03(2021)182. arXiv: 2011.03003 [hep-ph].

[50] Daniel Elander et al. "Holographic models of composite Higgs in the Veneziano limit. Part II. Fermionic sector". In: *JHEP* 05 (2022), p. 066. DOI: 10.1007/JHEP05(2022)066. arXiv: 2112.14740 [hep-ph].

[51] Domènec Espriu and Alisa Katanaeva. "Soft wall holographic model for the minimal composite Higgs boson". In: *Phys. Rev. D* 103.5 (2021), p. 055006. DOI: 10.1103/PhysRevD.103.055006. arXiv: 2008.06207 [hep-ph].

[52] Johanna Erdmenger et al. "Gauge/gravity dynamics for composite Higgs models and the top mass". In: *Phys. Rev. Lett.* 126.7 (2021), p. 071602. DOI: 10.1103/PhysRevLett.126.071602. arXiv: 2009.10737 [hep-ph].

[53] Johanna Erdmenger et al. "Gauge/gravity dual dynamics for the strongly coupled sector of composite Higgs models". In: *JHEP* 02 (2021), p. 058. DOI: 10.1007/JHEP02(2021)058. arXiv: 2010.10279 [hep-ph].

[54] Francisco del Aguila, Adrian Carmona, and Jose Santiago. "Neutrino Masses from an A4 Symmetry in Holographic Composite Higgs Models". In: *JHEP* 08 (2010), p. 127. DOI: 10.1007/JHEP08(2010)127. arXiv: 1001.5151 [hep-ph].

[55] Claudia Hagedorn and Marco Serone. "Leptons in Holographic Composite Higgs Models with Non-Abelian Discrete Symmetries". In: *JHEP* 10 (2011), p. 083. DOI: 10.1007/JHEP10(2011)083. arXiv: 1106.4021 [hep-ph].

[56] Miao Li. "A Model of holographic dark energy". In: *Phys. Lett. B* 603 (2004), p. 1. DOI: 10.1016/j.physletb.2004.10.014. arXiv: hep-th/0403127.

[57] Shuang Wang, Yi Wang, and Miao Li. "Holographic Dark Energy". In: *Phys. Rept.* 696 (2017), pp. 1–57. DOI: 10.1016/j.physrep.2017.06.003. arXiv: 1612.00345 [astro-ph.CO].

[58] Sidney R. Coleman, J. Wess, and Bruno Zumino. "Structure of phenomenological Lagrangians. 1." In: *Phys. Rev.* 177 (1969), pp. 2239–2247. DOI: 10.1103/PhysRev.177.2239.

[59] Curtis G. Callan Jr. et al. "Structure of phenomenological Lagrangians. 2." In: *Phys. Rev.* 177 (1969), pp. 2247–2250. DOI: 10.1103/PhysRev.177.2247.

[60] Roberto Contino. "The Higgs as a Composite Nambu-Goldstone Boson". In: *Theoretical Advanced Study Institute in Elementary Particle Physics: Physics of the Large and the Small*. 2011, pp. 235–306. DOI: 10.1142/9789814327183_0005. arXiv: 1005.4269 [hep-ph].

[61] Giuliano Panico and Andrea Wulzer. *The Composite Nambu-Goldstone Higgs*. Vol. 913. Springer, 2016. DOI: 10.1007/978-3-319-22617-0. arXiv: 1506.01961 [hep-ph].

[62] Giacomo Cacciapaglia, Claudio Pica, and Francesco Sannino. "Fundamental Composite Dynamics: A Review". In: *Phys. Rept.* 877 (2020), pp. 1–70. DOI: 10.1016/j.physrep.2020.07.002. arXiv: 2002.04914 [hep-ph].

[63] Brando Bellazzini, Csaba Csáki, and Javi Serra. "Composite Higgses". In: *Eur. Phys. J. C* 74.5 (2014), p. 2766. DOI: 10.1140/epjc/s10052-014-2766-x. arXiv: 1401.2457 [hep-ph].

[64] Edward Farhi and Leonard Susskind. "Technicolor". In: *Phys. Rept.* 74 (1981), p. 277. DOI: 10.1016/0370-1573(81)90173-3.

[65] R. Sekhar Chivukula. "Lectures on technicolor and compositeness". In: *Theoretical Advanced Study Institute in Elementary Particle Physics (TASI 2000): Flavor Physics for the Millennium*. June 2000, pp. 731–772. arXiv: hep-ph/0011264.

[66] Kenneth D. Lane. "An Introduction to technicolor". In: *Theoretical Advanced Study Institute (TASI 93) in Elementary Particle Physics: The Building Blocks of Creation - From Microfermius to Megaparsecs*. June 1993. DOI: 10.1142/9789814503785_0010. arXiv: hep-ph/9401324.

[67] Michael E. Peskin and Tatsu Takeuchi. "A New constraint on a strongly interacting Higgs sector". In: *Phys. Rev. Lett.* 65 (1990), pp. 964–967. DOI: 10.1103/PhysRevLett.65.964.

[68] Michael E. Peskin and Tatsu Takeuchi. "Estimation of oblique electroweak corrections". In: *Phys. Rev. D* 46 (1992), pp. 381–409. DOI: 10.1103/PhysRevD.46.381.

[69] E. Farhi and Leonard Susskind. "A Technicolored G.U.T." In: *Phys. Rev. D* 20 (1979), pp. 3404–3411. DOI: 10.1103/PhysRevD.20.3404.

[70] Estia Eichten and Kenneth D. Lane. "Dynamical Breaking of Weak Interaction Symmetries". In: *Phys. Lett. B* 90 (1980), pp. 125–130. DOI: 10.1016/0370-2693(80)90065-9.

[71] Francesco Sannino. "Technicolor and Beyond: Unification in Theory Space". In: *J. Phys. Conf. Ser.* 259 (2010). Ed. by Susana Cabrera et al., p. 012003. DOI: 10.1088/1742-6596/259/1/012003. arXiv: 1010.3461 [hep-ph].

[72] Bob Holdom. "Raising the Sideways Scale". In: *Phys. Rev. D* 24 (1981), p. 1441. DOI: 10.1103/PhysRevD.24.1441.

[73] William A. Bardeen, Chung Ngoc Leung, and S. T. Love. "The Dilaton and Chiral Symmetry Breaking". In: *Phys. Rev. Lett.* 56 (1986), p. 1230. DOI: 10.1103/PhysRevLett.56.1230.

[74] Koichi Yamawaki, Masako Bando, and Ken-iti Matumoto. "Scale Invariant Technicolor Model and a Technidilaton". In: *Phys. Rev. Lett.* 56 (1986), p. 1335. DOI: 10.1103/PhysRevLett.56.1335.

[75] Brando Bellazzini et al. "A Higgslike Dilaton". In: *Eur. Phys. J. C* 73.2 (2013), p. 2333. DOI: 10.1140/epjc/s10052-013-2333-x. arXiv: 1209.3299 [hep-ph].

[76] David B. Kaplan and Howard Georgi. "SU(2) x U(1) Breaking by Vacuum Misalignment". In: *Phys. Lett. B* 136 (1984), pp. 183–186. DOI: 10.1016/0370-2693(84)91177-8.

[77] David B. Kaplan, Howard Georgi, and Savas Dimopoulos. "Composite Higgs Scalars". In: *Phys. Lett. B* 136 (1984), pp. 187–190. DOI: 10.1016/0370-2693(84)91178-X.

[78] Michael J. Dugan, Howard Georgi, and David B. Kaplan. "Anatomy of a Composite Higgs Model". In: *Nucl. Phys. B* 254 (1985), pp. 299–326. DOI: 10.1016/0550-3213(85)90221-4.

[79] P. Sikivie et al. "Isospin Breaking in Technicolor Models". In: *Nucl. Phys. B* 173 (1980), pp. 189–207. DOI: 10.1016/0550-3213(80)90214-X.

[80] Giacomo Cacciapaglia and Francesco Sannino. "Fundamental Composite (Goldstone) Higgs Dynamics". In: *JHEP* 04 (2014), p. 111. DOI: 10.1007/JHEP04(2014)111. arXiv: 1402.0233 [hep-ph].

[81] D. A. Kosower. "SYMMETRY BREAKING PATTERNS IN PSEUDOREAL AND REAL GAUGE THEORIES". In: *Phys. Lett. B* 144 (1984), pp. 215–216. DOI: 10.1016/0370-2693(84)91806-9.

[82] Howard Georgi and David B. Kaplan. "Composite Higgs and Custodial SU(2)". In: *Phys. Lett. B* 145 (1984), pp. 216–220. DOI: 10.1016/0370-2693(84)90341-1.

[83] N. Arkani-Hamed et al. "The Littlest Higgs". In: *JHEP* 07 (2002), p. 034. DOI: 10.1088/1126-6708/2002/07/034. arXiv: hep-ph/0206021.

[84] Emanuel Katz, Ann E. Nelson, and Devin G. E. Walker. "The Intermediate Higgs". In: *JHEP* 08 (2005), p. 074. DOI: 10.1088/1126-6708/2005/08/074. arXiv: hep-ph/0504252.

[85] Luca Vecchi. "The Natural Composite Higgs". In: (Apr. 2013). arXiv: 1304.4579 [hep-ph].

[86] Alexander Belyaev et al. "Di-boson signatures as Standard Candles for Partial Compositeness". In: *JHEP* 01 (2017). [Erratum: JHEP 12, 088 (2017)], p. 094. DOI: 10.1007/JHEP01(2017)094. arXiv: 1610.06591 [hep-ph].

[87] Kaustubh Agashe, Roberto Contino, and Alex Pomarol. "The Minimal composite Higgs model". In: *Nucl. Phys. B* 719 (2005), pp. 165–187. DOI: 10.1016/j.nuclphysb.2005.04.035. arXiv: hep-ph/0412089.

[88] Roberto Contino, Leandro Da Rold, and Alex Pomarol. "Light custodians in natural composite Higgs models". In: *Phys. Rev. D* 75 (2007), p. 055014. DOI: 10.1103/PhysRevD.75.055014. arXiv: hep-ph/0612048.

[89] Giuliano Panico and Andrea Wulzer. "The Discrete Composite Higgs Model". In: *JHEP* 09 (2011), p. 135. DOI: 10.1007/JHEP09(2011)135. arXiv: 1106.2719 [hep-ph].

[90] G. F. Giudice et al. "The Strongly-Interacting Light Higgs". In: *JHEP* 06 (2007), p. 045. DOI: 10.1088/1126-6708/2007/06/045. arXiv: hep-ph/0703164.

[91] Riccardo Barbieri et al. "The Higgs boson from an extended symmetry". In: *Phys. Rev. D* 76 (2007), p. 115008. DOI: 10.1103/PhysRevD.76.115008. arXiv: 0706.0432 [hep-ph].

[92] Adrian Carmona and Florian Goertz. "A naturally light Higgs without light Top Partners". In: *JHEP* 05 (2015), p. 002. DOI: 10.1007/JHEP05(2015)002. arXiv: 1410.8555 [hep-ph].

[93] Edward Witten. "Some Inequalities Among Hadron Masses". In: *Phys. Rev. Lett.* 51 (1983), p. 2351. DOI: 10.1103/PhysRevLett.51.2351.

[94] Tom Banks. "CONSTRAINTS ON SU(2) x U(1) BREAKING BY VACUUM MISALIGNMENT". In: *Nucl. Phys. B* 243 (1984), pp. 125–130. DOI: 10.1016/0550-3213(84)90389-4.

[95] Howard Georgi, David B. Kaplan, and Peter Galison. "Calculation of the Composite Higgs Mass". In: *Phys. Lett. B* 143 (1984), pp. 152–154. DOI: 10.1016/0370-2693(84)90823-2.

[96] David B. Kaplan. "Flavor at SSC energies: A New mechanism for dynamically generated fermion masses". In: *Nucl. Phys. B* 365 (1991), pp. 259–278. DOI: 10.1016/S0550-3213(05)80021-5.

[97] Thomas A. Ryttov and Francesco Sannino. "Ultra Minimal Technicolor and its Dark Matter TIMP". In: *Phys. Rev. D* 78 (2008), p. 115010. DOI: 10.1103/PhysRevD.78.115010. arXiv: 0809.0713 [hep-ph].

[98] Thomas Appelquist, P. S. Rodrigues da Silva, and Francesco Sannino. "Enhanced global symmetries and the chiral phase transition". In: *Phys. Rev. D* 60 (1999), p. 116007. DOI: 10.1103/PhysRevD.60.116007. arXiv: hep-ph/9906555.

[99] Randy Lewis, Claudio Pica, and Francesco Sannino. "Light Asymmetric Dark Matter on the Lattice: SU(2) Technicolor with Two Fundamental Flavors". In: *Phys. Rev. D* 85 (2012), p. 014504. DOI: 10.1103/PhysRevD.85.014504. arXiv: 1109.3513 [hep-ph].

[100] Michael E. Peskin. "The Alignment of the Vacuum in Theories of Technicolor". In: *Nucl. Phys. B* 175 (1980), pp. 197–233. DOI: 10.1016/0550-3213(80)90051-6.

[101] John Preskill. "Subgroup Alignment in Hypercolor Theories". In: *Nucl. Phys. B* 177 (1981), pp. 21–59. DOI: 10.1016/0550-3213(81)90265-0.

[102] Adam Falkowski and Manuel Perez-Victoria. "Electroweak Breaking on a Soft Wall". In: *JHEP* 12 (2008), p. 107. DOI: 10.1088/1126-6708/2008/12/107. arXiv: 0806.1737 [hep-ph].

[103] Leszek M. Sokołowski. "The bizarre anti-de Sitter spacetime". In: *Int. J. Geom. Meth. Mod. Phys.* 13.09 (2016), p. 1630016. DOI: 10.1142/S0219887816300166. arXiv: 1611.01118 [gr-qc].

[104] Makoto Natsuume. *AdS/CFT Duality User Guide*. Vol. 903. 2015. ISBN: 978-4-431-55441-7, 978-4-431-55440-0. DOI: 10.1007/978-4-431-55441-7. arXiv: 1409.3575 [hep-th].

[105] Matthias Blau. *Lecture Notes on General Relativity*. 2022. URL: http://www.blau.itp.unibe.ch/GRLecturenotes.html.

[106] G. W. Gibbons. "Anti-de-Sitter spacetime and its uses". In: *2nd Samos Meeting on Cosmology, Geometry and Relativity: Mathematical and Quantum Aspects of Relativity and Cosmology*. Oct. 2011, pp. 102–142. arXiv: 1110.1206 [hep-th].

[107] Ingemar Bengtsson. *Anti-de Sitter Space*. 1998. URL: https://ncatlab.org/nlab/files/Bengtsson98.pdf.

[108] Martin Ammon and Johanna Erdmenger. *Gauge/Gravity Duality: Foundations and Applications*. Cambridge University Press, 2015.

[109] Barton Zwiebach. *A First Course in String Theory*. 2nd ed. Cambridge University Press, 2009.

[110] Elias Kiritsis. *String theory in a nutshell*. USA: Princeton University Press, 2019. ISBN: 978-0-691-15579-1, 978-0-691-18896-6.

[111] K. Becker, M. Becker, and J. H. Schwarz. *String theory and M-theory: A modern introduction*. Cambridge University Press, Dec. 2006. ISBN: 978-0-511-25486-4, 978-0-521-86069-7, 978-0-511-81608-6. DOI: 10.1017/CBO9780511816086.

[112] Gerard 't Hooft. "A Planar Diagram Theory for Strong Interactions". In: *Nucl. Phys. B* 72 (1974). Ed. by J. C. Taylor, p. 461. DOI: 10.1016/0550-3213(74)90154-0.

[113] Vijay Balasubramanian, Per Kraus, and Albion E. Lawrence. "Bulk versus boundary dynamics in anti-de Sitter space-time". In: *Phys. Rev. D* 59 (1999), p. 046003. DOI: 10.1103/PhysRevD.59.046003. arXiv: hep-th/9805171.

[114] D. Z. Freedman et al. "Renormalization group flows from holography supersymmetry and a c theorem". In: *Adv. Theor. Math. Phys.* 3 (1999), pp. 363–417. DOI: 10.4310/ATMP.1999.v3.n2.a7. arXiv: hep-th/9904017.

[115] Edward Witten. "Anti-de Sitter space and holography". In: *Adv. Theor. Math. Phys.* 2 (1998), pp. 253–291. DOI: 10.4310/ATMP.1998.v2.n2.a2. arXiv: hep-th/9802150.

[116] S. S. Gubser, Igor R. Klebanov, and Alexander M. Polyakov. "Gauge theory correlators from noncritical string theory". In: *Phys. Lett. B* 428 (1998), pp. 105–114. DOI: 10.1016/S0370-2693(98)00377-3. arXiv: hep-th/9802109.

[117] Oliver DeWolfe, Daniel Z. Freedman, and Hirosi Ooguri. "Holography and defect conformal field theories". In: *Phys. Rev. D* 66 (2002), p. 025009. DOI: 10.1103/PhysRevD.66.025009. arXiv: hep-th/0111135.

[118] Vijay Balasubramanian et al. "Holographic probes of anti-de Sitter space-times". In: *Phys. Rev. D* 59 (1999), p. 104021. DOI: 10.1103/PhysRevD.59.104021. arXiv: hep-th/9808017.

[119] Johanna Erdmenger et al. "Mesons in Gauge/Gravity Duals - A Review". In: *Eur. Phys. J. A* 35 (2008), pp. 81–133. DOI: 10.1140/epja/i2007-10540-1. arXiv: 0711.4467 [hep-th].

[120] Luca Martucci et al. "Dirac actions for D-branes on backgrounds with fluxes". In: *Class. Quant. Grav.* 22 (2005), pp. 2745–2764. DOI: 10.1088/0264-9381/22/13/014. arXiv: hep-th/0504041.

[121] Donald Marolf, Luca Martucci, and Pedro J. Silva. "Actions and Fermionic symmetries for D-branes in bosonic backgrounds". In: *JHEP* 07 (2003), p. 019. DOI: 10.1088/1126-6708/2003/07/019. arXiv: hep-th/0306066.

[122] Donald Marolf, Luca Martucci, and Pedro J. Silva. "Fermions, T duality and effective actions for D-branes in bosonic backgrounds". In: *JHEP* 04 (2003), p. 051. DOI: 10.1088/1126-6708/2003/04/051. arXiv: hep-th/0303209.

[123] Mans Henningson and Konstadinos Sfetsos. "Spinors and the AdS / CFT correspondence". In: *Phys. Lett. B* 431 (1998), pp. 63–68. DOI: 10.1016/S0370-2693(98)00559-0. arXiv: hep-th/9803251.

[124] Wolfgang Mueck and K. S. Viswanathan. "Conformal field theory correlators from classical field theory on anti-de Sitter space. 2. Vector and spinor fields". In: *Phys. Rev. D* 58 (1998), p. 106006. DOI: 10.1103/PhysRevD.58.106006. arXiv: hep-th/9805145.

[125] Roberto Camporesi and Atsushi Higuchi. "On the Eigen functions of the Dirac operator on spheres and real hyperbolic spaces". In: *J. Geom. Phys.* 20 (1996), pp. 1–18. DOI: 10.1016/0393-0440(95)00042-9. arXiv: gr-qc/9505009.

[126] Raman Sundrum. "Effective field theory for a three-brane universe". In: *Phys. Rev. D* 59 (1999), p. 085009. DOI: 10.1103/PhysRevD.59.085009. arXiv: hep-ph/9805471.

[127] Edward Witten. "Baryons in the 1/n Expansion". In: *Nucl. Phys. B* 160 (1979), pp. 57–115. DOI: 10.1016/0550-3213(79)90232-3.

[128] Edward Witten. "Baryons and branes in anti-de Sitter space". In: *JHEP* 07 (1998), p. 006. DOI: 10.1088/1126-6708/1998/07/006. arXiv: hep-th/9805112.

[129] Edward Witten. "Anti-de Sitter space, thermal phase transition, and confinement in gauge theories". In: *Adv. Theor. Math. Phys.* 2 (1998). Ed. by L. Bergstrom and U. Lindstrom, pp. 505–532. DOI: 10.4310/ATMP.1998.v2.n3.a3. arXiv: hep-th/9803131.

[130] Muneto Nitta and Noriko Shiiki. "Skyrme Strings". In: *Prog. Theor. Phys.* 119 (2008), pp. 829–838. DOI: 10.1143/PTP.119.829. arXiv: 0706.0316 [hep-ph].

[131] Neil R. Constable and Robert C. Myers. "Exotic scalar states in the AdS / CFT correspondence". In: *JHEP* 11 (1999), p. 020. DOI: 10.1088/1126-6708/1999/11/020. arXiv: hep-th/9905081.

[132] Matthew D. Schwartz. *Quantum Field Theory and the Standard Model*. Cambridge University Press, 2013.

[133] Juan Martin Maldacena. "Wilson loops in large N field theories". In: *Phys. Rev. Lett.* 80 (1998), pp. 4859–4862. DOI: 10.1103/PhysRevLett.80.4859. arXiv: hep-th/9803002.

[134] Csaba Csaki et al. "Glueball mass spectrum from supergravity". In: *JHEP* 01 (1999), p. 017. DOI: 10.1088/1126-6708/1999/01/017. arXiv: hep-th/9806021.

[135] Hirosi Ooguri, Harlan Robins, and Jonathan Tannenhauser. "Glueballs and their Kaluza-Klein cousins". In: *Phys. Lett. B* 437 (1998), pp. 77–81. DOI: 10.1016/S0370-2693(98)00877-6. arXiv: hep-th/9806171.

[136] Robert de Mello Koch et al. "Evaluation of glueball masses from supergravity". In: *Phys. Rev. D* 58 (1998), p. 105009. DOI: 10.1103/PhysRevD.58.105009. arXiv: hep-th/9806125.

[137] M. Zyskin. "A Note on the glueball mass spectrum". In: *Phys. Lett. B* 439 (1998), pp. 373–381. DOI: 10.1016/S0370-2693(98)01067-3. arXiv: hep-th/9806128.

[138] Joseph A. Minahan. "Glueball mass spectra and other issues for supergravity duals of QCD models". In: *JHEP* 01 (1999), p. 020. DOI: 10.1088/1126-6708/1999/01/020. arXiv: hep-th/9811156.

[139] Jorge G. Russo and Konstadinos Sfetsos. "Rotating D3-branes and QCD in three-dimensions". In: *Adv. Theor. Math. Phys.* 3 (1999), pp. 131–146. DOI: 10.4310/ATMP.1999.v3.n1.a5. arXiv: hep-th/9901056.

[140] Csaba Csaki et al. "Supergravity models for (3+1)-dimensional QCD". In: *Phys. Rev. D* 60 (1999), p. 044001. DOI: 10.1103/PhysRevD.60.044001. arXiv: hep-th/9902067.

[141] Jorge G. Russo. "New compactifications of supergravities and large N QCD". In: *Nucl. Phys. B* 543 (1999), pp. 183–197. DOI: 10.1016/S0550-3213(98)00828-1. arXiv: hep-th/9808117.

[142] Csaba Csaki et al. "Large N QCD from rotating branes". In: *Phys. Rev. D* 59 (1999), p. 065012. DOI: 10.1103/PhysRevD.59.065012. arXiv: hep-th/9810186.

[143] Akikazu Hashimoto and Yaron Oz. "Aspects of QCD dynamics from string theory". In: *Nucl. Phys. B* 548 (1999), pp. 167–179. DOI: 10.1016/S0550-3213(99)00120-0. arXiv: hep-th/9809106.

[144] Miao Li. "'t Hooft vortices and phases of large N gauge theory". In: *JHEP* 08 (1998), p. 014. DOI: 10.1088/1126-6708/1998/08/014. arXiv: hep-th/9804175.

[145] Miao Li. "'t Hooft vortices on D-branes". In: *JHEP* 07 (1998), p. 003. DOI: 10.1088/1126-6708/1998/07/003. arXiv: hep-th/9803252.

[146] David J. Gross and Hirosi Ooguri. "Aspects of large N gauge theory dynamics as seen by string theory". In: *Phys. Rev. D* 58 (1998), p. 106002. DOI: 10.1103/PhysRevD.58.106002. arXiv: hep-th/9805129.

[147] L. Girardello et al. "Novel local CFT and exact results on perturbations of N=4 superYang Mills from AdS dynamics". In: *JHEP* 12 (1998), p. 022. DOI: 10.1088/1126-6708/1998/12/022. arXiv: hep-th/9810126.

[148] L. Girardello et al. "The Supergravity dual of N=1 superYang-Mills theory". In: *Nucl. Phys. B* 569 (2000), pp. 451–469. DOI: 10.1016/S0550-3213(99)00764-6. arXiv: hep-th/9909047.

[149] Steven S. Gubser. "Dilaton driven confinement". In: (Feb. 1999). arXiv: hep-th/9902155.

[150] A. Kehagias and K. Sfetsos. "On Running couplings in gauge theories from type IIB supergravity". In: *Phys. Lett. B* 454 (1999), pp. 270–276. DOI: 10.1016/S0370-2693(99)00393-7. arXiv: hep-th/9902125.

[151] A. Kehagias and K. Sfetsos. "On asymptotic freedom and confinement from type IIB supergravity". In: *Phys. Lett. B* 456 (1999), pp. 22–27. DOI: 10.1016/S0370-2693(99)00431-1. arXiv: hep-th/9903109.

[152] Shinichi Nojiri and Sergei D. Odintsov. "Running gauge coupling and quark - anti-quark potential from dilatonic gravity". In: *Phys. Lett. B* 458 (1999), pp. 226–230. DOI: 10.1016/S0370-2693(99)00580-8. arXiv: hep-th/9904036.

[153] Shin'ichi Nojiri and Sergei D. Odintsov. "Curvature dependence of running gauge coupling and confinement in AdS / CFT correspondence". In: *Phys. Rev. D* 61 (2000), p. 044014. DOI: 10.1103/PhysRevD.61.044014. arXiv: hep-th/9905200.

[154] Shin'ichi Nojiri and Sergei D. Odintsov. "Running gauge coupling and quark - anti-quark potential in nonSUSY gauge theory at finite temperature from IIB SG / CFT correspondence". In: *Phys. Rev. D* 61 (2000), p. 024027. DOI: 10.1103/PhysRevD.61.024027. arXiv: hep-th/9906216.

[155] Robert de Mello Koch, Alastair Paulin-Campbell, and Joao P. Rodrigues. "Nonholomorphic corrections from three-branes in F theory". In: *Phys. Rev. D* 60 (1999), p. 106008. DOI: 10.1103/PhysRevD.60.106008. arXiv: hep-th/9903029.

[156] Shin'ichi Nojiri and Sergei D. Odintsov. "Two boundaries AdS / CFT correspondence in dilatonic gravity". In: *Phys. Lett. B* 449 (1999), pp. 39–47. DOI: 10.1016/S0370-2693(99)00048-9. arXiv: hep-th/9812017.

[157] James Babington, David E. Crooks, and Nick J. Evans. "A Stable supergravity dual of nonsupersymmetric glue". In: *Phys. Rev. D* 67 (2003), p. 066007. DOI: 10.1103/PhysRevD.67.066007. arXiv: hep-th/0210068.

[158] Leandro Da Rold and Alex Pomarol. "The Scalar and pseudoscalar sector in a five-dimensional approach to chiral symmetry breaking". In: *JHEP* 01 (2006), p. 157. DOI: 10.1088/1126-6708/2006/01/157. arXiv: hep-ph/0510268.

[159] Guy F. de Teramond and Stanley J. Brodsky. "Hadronic spectrum of a holographic dual of QCD". In: *Phys. Rev. Lett.* 94 (2005), p. 201601. DOI: 10.1103/PhysRevLett.94.201601. arXiv: hep-th/0501022.

[160] Guy F. de Teramond. "Mapping String States into Partons: Form Factors and the Hadron Spectrum in AdS/QCD". In: *7th Workshop on Continuous Advances in QCD*. June 2006, pp. 110–116. DOI: 10.1142/9789812708267_0011. arXiv: hep-ph/0606143.

[161] Guy F. de Teramond and Stanley J. Brodsky. "Baryonic states in QCD from gauge/string duality at large N(c)". In: *ECT* Workshop on Large Nc QCD 2004*. Sept. 2004, pp. 290–301. arXiv: hep-th/0409074.

[162] Andreas Karch et al. "Linear confinement and AdS/QCD". In: *Phys. Rev. D* 74 (2006), p. 015005. DOI: 10.1103/PhysRevD.74.015005. arXiv: hep-ph/0602229.

[163] Brian Batell and Tony Gherghetta. "Dynamical Soft-Wall AdS/QCD". In: *Phys. Rev. D* 78 (2008), p. 026002. DOI: 10.1103/PhysRevD.78.026002. arXiv: 0801.4383 [hep-ph].

[164] Raul Alvares, Nick Evans, and Keun-Young Kim. "Holography of the Conformal Window". In: *Phys. Rev. D* 86 (2012), p. 026008. DOI: 10.1103/PhysRevD.86.026008. arXiv: 1204.2474 [hep-ph].

[165] Timo Alho, Nick Evans, and Kimmo Tuominen. "Dynamic AdS/QCD and the Spectrum of Walking Gauge Theories". In: *Phys. Rev. D* 88 (2013), p. 105016. DOI: 10.1103/PhysRevD.88.105016. arXiv: 1307.4896 [hep-ph].

[166] Matti Jarvinen and Elias Kiritsis. "Holographic Models for QCD in the Veneziano Limit". In: *JHEP* 03 (2012), p. 002. DOI: 10.1007/JHEP03(2012)002. arXiv: 1112.1261 [hep-ph].

[167] Daniel Arean et al. "V-QCD: Spectra, the dilaton and the S-parameter". In: *Phys. Lett. B* 720 (2013), pp. 219–223. DOI: 10.1016/j.physletb.2013.01.070. arXiv: 1211.6125 [hep-ph].

[168] Daniel Areán et al. "The discontinuities of conformal transitions and mass spectra of V-QCD". In: *JHEP* 11 (2013), p. 068. DOI: 10.1007/JHEP11(2013)068. arXiv: 1309.2286 [hep-ph].

[169] Matti Jarvinen. "Massive holographic QCD in the Veneziano limit". In: *JHEP* 07 (2015), p. 033. DOI: 10.1007/JHEP07(2015)033. arXiv: 1501.07272 [hep-ph].

[170] David Kutasov, Jennifer Lin, and Andrei Parnachev. "Conformal Phase Transitions at Weak and Strong Coupling". In: *Nucl. Phys. B* 858 (2012), pp. 155–195. DOI: 10.1016/j.nuclphysb.2012.01.004. arXiv: 1107.2324 [hep-th].

[171] Matti Jarvinen and Francesco Sannino. "Holographic Conformal Window - A Bottom Up Approach". In: *JHEP* 05 (2010), p. 041. DOI: 10.1007/JHEP05(2010)041. arXiv: 0911.2462 [hep-ph].

[172] Joshua Erlich. "How Well Does AdS/QCD Describe QCD?" In: *Int. J. Mod. Phys. A* 25 (2010). Ed. by Marco Peloso and Arkady Vainshtein, pp. 411–421. DOI: 10.1142/S0217751X10048718. arXiv: 0908.0312 [hep-ph].

[173] Edward Witten. "Multitrace operators, boundary conditions, and AdS / CFT correspondence". In: (Dec. 2001). arXiv: hep-th/0112258.

[174] Yoichiro Nambu and G. Jona-Lasinio. "Dynamical Model of Elementary Particles Based on an Analogy with Superconductivity. 1." In: *Phys. Rev.* 122 (1961). Ed. by T. Eguchi, pp. 345–358. DOI: 10.1103/PhysRev.122.345.

[175] Yoichiro Nambu and G. Jona-Lasinio. "Dynamical model of elementary particles based on an analogy with superconductivity. II." In: *Phys. Rev.* 124 (1961). Ed. by T. Eguchi, pp. 246–254. DOI: 10.1103/PhysRev.124.246.

[176] Nick Evans and Keun-Young Kim. "Holographic Nambu–Jona-Lasinio interactions". In: *Phys. Rev. D* 93.6 (2016), p. 066002. DOI: 10.1103/PhysRevD.93.066002. arXiv: 1601.02824 [hep-th].

[177] Will Clemens and Nick Evans. "A Holographic Study of the Gauged NJL Model". In: *Phys. Lett. B* 771 (2017), pp. 1–4. DOI: 10.1016/j.physletb.2017.05.027. arXiv: 1702.08693 [hep-th].

[178] Johanna Erdmenger, Kazuo Ghoroku, and Ingo Kirsch. "Holographic heavy-light mesons from non-Abelian DBI". In: *JHEP* 09 (2007), p. 111. DOI: 10.1088/1126-6708/2007/09/111. arXiv: 0706.3978 [hep-th].

[179] Robert C. Myers. "Dielectric branes". In: *JHEP* 12 (1999), p. 022. DOI: 10.1088/1126-6708/1999/12/022. arXiv: hep-th/9910053.

[180] Hong Liu and A. A. Tseytlin. "D3-brane-D-instanton configuration and = 4 super YM theory in constant self-dual background". In: *Nuclear Physics B* 553 (1-2 July 1999), pp. 231–249. ISSN: 05503213. DOI: 10.1016/S0550-3213(99)00259-X.

[181] Kazuo Ghoroku and Masanobu Yahiro. "Chiral symmetry breaking driven by dilaton". In: *Physics Letters, Section B: Nuclear, Elementary Particle and High-Energy Physics* 604 (3-4 Dec. 2004), pp. 235–241. ISSN: 03702693. DOI: 10.1016/J.PHYSLETB.2004.10.048.

[182] A.A. Tseytlin. "On non-abelian generalisation of the Born-Infeld action in string theory". In: *Nuclear Physics B* 501.1 (1997), pp. 41–52. DOI: 10.1016/s0550-3213(97)00354-4. URL: https://doi.org/10.1016%2Fs0550-3213%2897%2900354-4.

[183] Arkady A. Tseytlin. "Born-Infeld action, supersymmetry and string theory". In: (Aug. 1999). Ed. by Mikhail A. Shifman, pp. 417–452. DOI: 10.1142/9789812793850_0025. arXiv: hep-th/9908105.

[184] Frederik Denef, Alexander Sevrin, and Jan Troost. "NonAbelian Born-Infeld versus string theory". In: *Nucl. Phys. B* 581 (2000), pp. 135–155. DOI: 10.1016/S0550-3213(00)00278-9. arXiv: hep-th/0002180.

[185] Matthias Kaminski et al. "Holographic Operator Mixing and Quasinormal Modes on the Brane". In: *JHEP* 02 (2010), p. 021. DOI: 10.1007/JHEP02(2010)021. arXiv: 0911.3610 [hep-th].

[186] Leandro Da Rold and Alex Pomarol. "Chiral symmetry breaking from five dimensional spaces". In: *Nucl. Phys. B* 721 (2005), pp. 79–97. DOI: 10.1016/j.nuclphysb.2005.05.009. arXiv: hep-ph/0501218.

[187] Ed Bennett et al. "Sp(4) gauge theory on the lattice: towards SU(4)/Sp(4) composite Higgs (and beyond)". In: *JHEP* 03 (2018), p. 185. DOI: 10.1007/JHEP03(2018)185. arXiv: 1712.04220 [hep-lat].

[188] Claude Amsler. *The Quark Structure of Hadrons: An Introduction to the Phenomenology and Spectroscopy*. Vol. 949. Cham: Springer, 2018. ISBN: 978-3-319-98526-8, 978-3-319-98527-5. DOI: 10.1007/978-3-319-98527-5.

[189] Rudy Arthur et al. "SU(2) gauge theory with two fundamental flavors: A minimal template for model building". In: *Phys. Rev. D* 94.9 (2016), p. 094507. DOI: 10.1103/PhysRevD.94.094507. arXiv: 1602.06559 [hep-lat].

[190] Rudy Arthur et al. "$SU(2)$ Gauge Theory with Two Fundamental Flavours: Scalar and Pseudoscalar Spectrum". In: (July 2016). arXiv: 1607.06654 [hep-lat].

[191] Ed Bennett et al. "Sp(4) gauge theories on the lattice: $N_f = 2$ dynamical fundamental fermions". In: *JHEP* 12 (2019), p. 053. DOI: 10.1007/JHEP12(2019)053. arXiv: 1909.12662 [hep-lat].

[192] Ed Bennett et al. "Singlets in gauge theories with fundamental matter". In: *Phys. Rev. D* 109.3 (2024), p. 034504. DOI: 10.1103/PhysRevD.109.034504. arXiv: 2304.07191 [hep-lat].

[193] Suchita Kulkarni et al. "Low-energy effective description of dark $Sp(4)$ theories". In: *SciPost Phys.* 14.3 (2023), p. 044. DOI: 10.21468/SciPostPhys.14.3.044. arXiv: 2202.05191 [hep-ph].

[194] Gabriele Ferretti and Denis Karateev. "Fermionic UV completions of Composite Higgs models". In: *JHEP* 03 (2014), p. 077. DOI: 10.1007/JHEP03(2014)077. arXiv: 1312.5330 [hep-ph].

[195] Gabriele Ferretti. "Gauge theories of Partial Compositeness: Scenarios for Run-II of the LHC". In: *JHEP* 06 (2016), p. 107. DOI: 10.1007/JHEP06(2016)107. arXiv: 1604.06467 [hep-ph].

[196] Diogo Buarque Franzosi et al. "Vector and Axial-vector resonances in composite models of the Higgs boson". In: *JHEP* 11 (2016), p. 076. DOI: 10.1007/JHEP11(2016)076. arXiv: 1605.01363 [hep-ph].

[197] Yonit Hochberg et al. "Model for Thermal Relic Dark Matter of Strongly Interacting Massive Particles". In: *Phys. Rev. Lett.* 115.2 (2015), p. 021301. DOI: 10.1103/PhysRevLett.115.021301. arXiv: 1411.3727 [hep-ph].

[198] Fabian Zierler et al. "Strongly Interacting Dark Matter from Sp(4) Gauge Theory". In: *EPJ Web Conf.* 274 (2022), p. 08014. DOI: 10.1051/epjconf/202227408014. arXiv: 2211.11272 [hep-ph].

[199] Elias Bernreuther et al. "Dark matter relic density in strongly interacting dark sectors with light vector mesons". In: (Nov. 2023). arXiv: 2311.17157 [hep-ph].